RNA aptamers as selective protein kinase inhibitors

New molecular tools for the elucidation of signal transduction pathways

Dissertation
zur
Erlangung des Doktorgrades (Dr. rer. nat.)
der
Mathematisch-Naturwissenschaftlichen Fakultät
der
Rheinischen Friedrich-Wilhelms-Universität Bonn

vorgelegt von

Sabine Michaela Irmgard Lennarz

aus

Bonn

Bonn 2014

Angefertigt mit Genehmigung der Mathematisch-Naturwissenschaftlichen Fakultät der
Rheinischen Friedrich-Wilhelms-Universität Bonn

1. Gutachter: Prof. Dr. Günter Mayer

2. Gutachter: Prof. Dr. Michael Hoch

Tag der Promotion: 7.11.2014

Erscheinungsjahr: 2015

Parts of this thesis are published in:

V. M. Tesmer, **S. Lennarz**, G. Mayer, and J. J. G. Tesmer, "Molecular mechanism for inhibition of G protein-coupled receptor kinase 2 by a selective RNA aptamer.," Structure, vol. 20, pp. 1300–1309, Aug 2012.

Contents

List of Tables

List of Figures

1 Abstract

Elucidating the precise function of individual protein kinases within complex signal transduction cascades represents one of the greatest challenges in molecular biology. Protein kinases are enzymes that catalyze the transfer of a phosphate group from ATP to proteins. In doing so, they promote alterations within the intricate network of intracellular signal transduction pathways. Deregulated signal transduction pathways caused by aberrant kinase activity drives a multitude of diseases. Because of this, protein kinases have become one of the most intensively pursued classes of drug targets. A comprehensive functional analysis of individual kinases involved in the biology of health and disease is challenging and requires the development of specific inhibitors that can discriminate between highly homologous proteins. Most available protein kinase inhibitors are low molecular weight compounds that address the kinases active site and, thus, block kinase activity. These inhibitors have been proven useful for therapeutic applications but their use as research tools is often hampered by their lack of specificity.

Herein, it was investigated if aptamers represent a promising new class of kinase inhibitors for chemical biology research that might overcome this limitation. Aptamers are single-stranded nucleic acids that adopt complex three-dimensional strucures. More importantly, aptamers are often able to modulate the function of their target protein in a highly specific manner. In this thesis, the potential of aptamers as selective protein kinase inhibitors was studied for two important kinases: G protein-coupled receptor kinase 2 (GRK2) and extracellular signal-regulated kinase 2 (Erk2). GRK2 is a key regulator of G protein-coupled transmembrane receptors and Erk2 is crucial for the regulation of proliferation and differentiation in cells.

The ATP-competitive aptamer C13 and GRK2 were used to unravel the molecular determinants which contribute to the aptamer´s highly specific interaction with its target. Crystallographic structures and biochemical assays revealed that the ATP-competitive aptamer forms extensive interactions both within and outside of the active site which contribute to its specificity and ability to block kinase activity.

The two novel Erk2-binding aptamers C3 and C5 revealed that aptamers can bind distinct sites on one target and are able to employ ATP-competitive or allosteric modes of action in respect to kinase activity perturbation. This demonstrates their potential as domain-specific inhibitors. Aptamer C5 was shown to interfere with Erk2 activity in an ATP-competitive manner. Aptamer C3, on the other hand, recognized the MAP kinase (MAPK) insert region of Erk2. The intriguing ability of C3 to target MAPK insert specific functions was monitored in an activation cascade assay. In this assay, the aptamer was able to inhibit the activation of Erk2 by its upstream kinase Mek1 and to prevent subsequent substrate phosphorylation.

Most importantly, this study implies that RNA aptamers can provide a new class of potent tools to manipulate intracellular kinase activity in neurons. Using aptamer C5, it was shown for first time that the application of an aptamer during whole-cell patch-clamp recordings offers a unique and generally applicable strategy to monitor spatio-temporal effects on individual protein kinases during neuronal functions.

In summary, this thesis demonstrates the versatile potential of RNA aptamer as specific protein kinase inhibitors for chemical biology research and opens the avenue towards their application as tools to specifically interfere with kinase activity during neuronal signaling.

2 Zusammenfassung

Die präzise Charakterisierung individueller Proteinkinasen in intrazellulärenr Signaltransduktionskaskaden ist eine der größten Herausforderungen der Molekularbiologie. Proteinkinasen sind Enzyme, die den Transfer der terminalen Phosphatgruppen von ATP auf Substratproteine katalysieren. Dadurch können Kinasen weitreichende Veränderungen innerhalb der komplexen Signaltransduktionskaskaden bewirken. Fehlregulationen innerhalb von Signaltransduktionskaskaden, die durch anormale Proteinkinaseaktivität hervorgerufen wird, spielen eine entscheidende Rolle bei verschiedenen Krankheiten. Aufgrund dieser Implikation sind Proteinkinasen eine der wichtigsten Ankerpunkte für die Entwicklung von Arzneimitteln.

Eine umfassende funktionale Analyse von individuellen Proteinkinasen ist schwierig und erfordert die Entwicklung von Inhibitoren, die zwischen fast homologen Proteinen unterscheiden können. Die meisten Proteinkinaseinhibitoren sind niedermolekulare Wirkstoffe, die an an das aktive Zentrum binden und dadurch die Enzymaktivität inhibieren können. Diese ATP-kompetitiven Substenzen sind wichtig für therapeutische Anwendungen. Für Forschungszwecke sind sie allerdings nur sehr bedingt geeignet, da sie oft nicht spezifisch genug sind.

Innerhalb dieser Dissertation sollte untersucht werden, ob Aptamere die Probleme anderen Inhibitoren umgehen und dadurch als eine neuartige Klasse von Kinaseinhibitoren für Forschungszwecke eingesetzt werden können. Aptamere sind kurze, einzelsträngige Nukleinsäuren, die sich in dreidimensionale Strukturen falten können. Zudem sind Aptamere sind oft in der Lage, die Funktion ihres Zielpproteins zu modulieren.

Im Rahmen der vorliegenden Arbeit sollte der Einsatz und die Funktionsweise von Aptameren untersucht werden, die die Proteinkinasen Erk2 und GRK2 adressieren. GRK2 spielt eine wichtige Rolle in der Regulation von G-Protein gekoppelten Rezeptoren. Die Kinase Erk2 ist unerlässlich für die Proliferation und Differenzierung von eukaryontischen Zellen.

Anhand des ATP-kompetitiven Aptamers C13 und der Kinase GRK2 wurde untersucht, welche molekularen Interaktionen das Aptamer mit seiner Zielkinase eingeht. Durch kristallographische und biochemische Untersuchungen konnte gezeigt werden, dass das ATP - kompetitive Aptamer weitläufige Interaktionen sowohl innerhalb als auch außerhalb des aktiven Zentrums eingeht. Diese Interaktionen tragen zu einem hohen Maße zu der hoch affinen und spezifischen Bindung bei.

Der Einsatz der neuen Aptamere C3 und C5, die an die Kinase Erk2 binden, zeigt, dass Aptamere an verschiedene Epitope an einem Protein binden und dadurch die Kinaseaktivität in ATP kompetitiver oder nicht ATP kompetitiver Weise beinträchtigen können. Dies veranschaulicht das Potential von Aptameren als domänenspezifische Inhibitoren. Es konnte nachgewiesen werden, dass Aptamer C5 mit ATP um die Bindung an Erk2 konkurriert und die Aktivität inhibiert. Aptamer C3 bindet an das sogenannte MAP kinase (MAPK) Insert. Die Fähigkeit von C3 als domänenspezifischer Inhibitor konnte experimentell nachgewiesen werden. In diesem Versuch konnte gezeigt werden, dass C3 die Aktivierung von Erk2 durch Mek1 bewirkt. Die Wirkung von C3 setzt sich auch auf die Aktivierung von Substratproteinen fort.

In dieser Dissertation wurde erstmals gegen Kinasen gerichtete Aptamere als Intramere zur Analyse zellulärer Signaltransduktionswege in Neuronen eingesetzt. Der Einsatz von Aptameren währen Patch Clamp Messungen ist eine neuartige Methode, um den Effekte von Aptameren auf die Funktion von Kinasen mit hoher zeitlicher und räumlicher Auflösung zu messen. Diese Messungen

legen nahe, dass Aptamer C5 eine neuronale Funktion von Erk2 inhibiert.

Die Ergebnisse dieser Arbeit unterstreichen die Bedeutung von Aptameren als Werkzeuge für die Erforschung von Proteinkinasen innerhalb neuronaler Signaltransduktionskaskaden.

3 Introduction

3.1 Signal transduction pathways

Cells receive and respond to a variety of extracellular stimuli, such as growth factors [1] or neurotransmitters [2]. In order to process these stimuli, cells have to employ a sophisticated system of molecular receptors and intracellular signaling pathways, also called signal transduction cascades [3]. Most receptors are transmembrane proteins, which bind to molecules outside the cell and subsequently transmit the signal to cytosolic signaling pathways [4, 5]. These intracellular signaling pathways typically branch and intersect via diverse protein effector and second messenger cascades, enabling cells to coordinate information from multiple receptors and to regulate multiple effector systems at the same time [3].

3.1.1 Protein kinases

Protein kinases are key regulators of signaling pathways and, thus, control virtually all aspects of cellular life, including metabolism, transcription, cell-cycle progression, and neuronal and immunological functions [6].

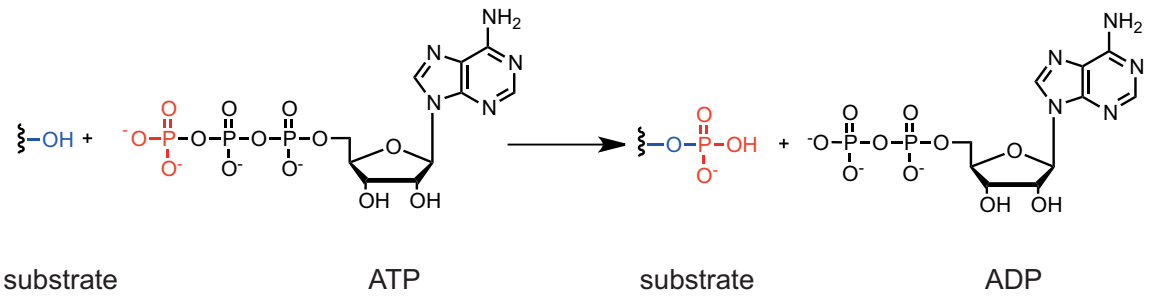

Figure 3.1: Protein kinase reaction. Eukaryotic protein kinases catalyze the transfer of the γ-phosphate group from ATP (red) to hydroxyl groups on serine/threonine or tyrosine residues (blue). ATP: adenosine triphosphate, ADP: adenosine diphosphate.

Protein kinases are enzymes that catalyze the transfer of the terminal phosphate group from adenosine triphosphate (ATP) to amino acid residues on proteins (Figure 3.1). In eukaryotes, protein kinases phosphorylate the hydroxyl groups of serine/threonine or tyrosine residues. More than 86% of protein phosphorylation occurs on serine residues, 12% on threonine residues, and 2% on tyrosine residues [7]. Prokaryotes generally employ histidine kinases for signaling [8–10]. Even though this modification exists in eukaryotes, little is known about its function in humans [11].

3.1.2 Protein phosphorylation as a regulatory mechanism

The phosphate group transferred by kinases acts as a molecular "switch" that is able to control extremely complex signal transduction cascades by formation and reorganization of dynamic protein interaction networks (Figure 3.2) [12, 13].

The unique size and charge properties of covalently attached phosphates can activate or inhibit proteins through allosteric conformational changes or by interfering with substrate recognition [14–16]. Moreover, it allows for specific and inducible recognition of phosphoproteins by phosphospecific-binding domains in other proteins [17]. This, in turn, can promote alterations in protein–protein interactions.

The phosphate group is predominantly dianionic at a physiological pH, which allows it to participate in the formation of hydrogen bonds and electrostatic interactions [17]. The phosphate group is particularly suited for interacting with the guanidinium group of arginine residues. Arginines contain a planar structure that can form direct hydrogen bonds to the negatively charged phosphate groups [12, 17].

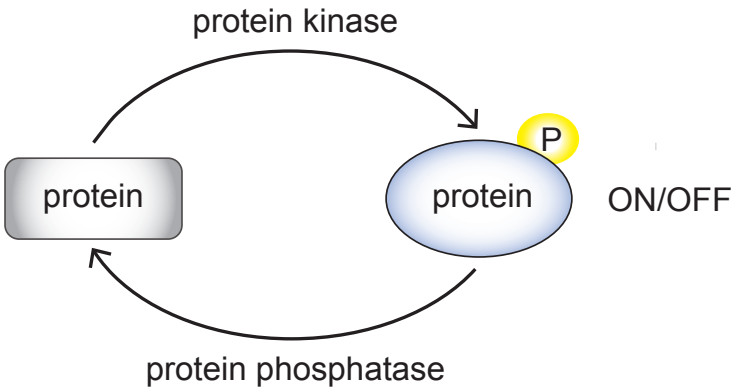

Figure 3.2: Schematic representation of the molecular switch induced by protein kinases. Phosphorylation alters the activity of target proteins and turns them on or off. The reaction is reversible and the phosphate group can easily removed by protein phosphatases. P: phosphate group.

More importantly, however, is the feature that protein phosphorylation is a reversible process, which sets the protein switches back to its original state [13]. At a physiological pH, phosphate esters are chemically stable in aqueous solution but the original hydroxyl group and free phosphate can easily be regenerated by hydrolysis of the phosphate easter via protein phosphatases [17, 18].

3.1.3 The human kinome

Serine/threonine-directed protein kinases were first discovered in 1955 by Fischer and Krebs who demonstrated that the activation of glycogen phosphorylase b to glycogen phosphorylase a was dependent on a protein kinase action together with ATP [19–21]. In 1979, Hunter and colleagues identified phosphotyrosine as the product of a protein kinase activity of a viral oncoprotein which was later identified as the tyrosine kinase vSrc [22, 23]. From then on, the number of identified kinases increased.

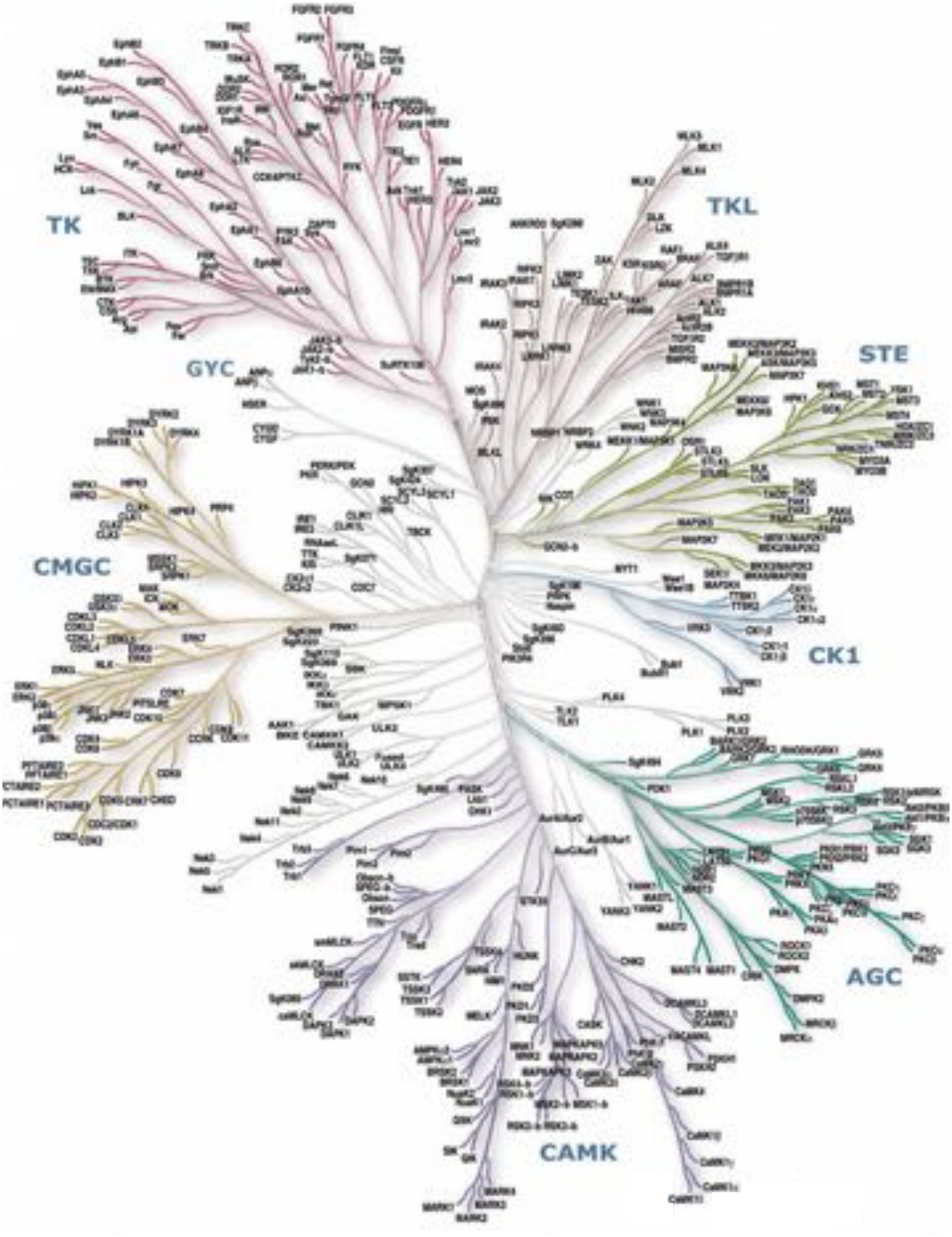

Figure 3.3: The human kinome. Based on sequence and functional homology, eukaryotic protein kinases can be grouped into nine families: AGC (including PKA [protein kinase A], PKG [protein kinase G] and PKC [protein kinase C] families), CAMK (Ca^{2+} /calmodulin-regulated kinases), CK1 (casein kinase 1 family), CMGC (including CDKs [cyclin-dependent kinases], MAPKs [mitogen-activated protein kinases], GSK [glycogen synthase kinases] and CDK-like kinases), STE (related to yeast sterile kinases), tyrosine kinases and TKL (tyrosine kinase-like). RGC (receptor guanylate cyclase kinases) and an additional group labelled as "other" are omitted from this figure. Figure taken from [7].

In 2002, the landmark study of Manning and colleagues revealed that the human genome codes for 518 putative protein kinases [7]. Most kinases have a common evolutionary origin and share highly conserved catalytic residues and mechanisms [24]. Based on sequence homology of the kinase domain and in comparison to other species, the human kinome could be assigned to nine major groups (Figure 3.3). Within most groups, the kinases also share related functions [7]. In total, the so-called "human kinome" is so important for cellular functions that it represents almost 2% of the human genome [7, 24, 25].

The majority of protein kinases are serine/threonine-directed and 90 kinases are tyrosine kinases (58 receptor tyrosine kinases). In addition, there is a small number of dual-specificity kinases that can act as both tyrosine and serine/threonine kinases (such as Mek´s) [12, 26].

Besides active kinases, 48 human proteins are currently known to have kinase-like domains but lack one or more of the conserved catalytic site residues in the kinase domain [27]. Thus, they are coined "pseudokinases". In addition to active protein kinases and pseudokinases, the kinase superfamily contains lipid kinases, carbohydrate and/or small molecule-targeting kinases (e.g. nucleotide kinases) [28]. In some cases, these kinases can also phosphorylate proteins [29].

3.1.4 Structural overview of the catalytic domain

Most eukaryotic protein kinases share similar bi-lobed catalytic domains (or "kinase domains") with conserved residues at critical positions required for catalysis (Figure 3.4A, B) [30]. A deep cleft between the large and small lobe forms the active site where ATP is bound and the phosphotransfer reaction occurs [31].

Within the active site (Figure 3.4B), the adenine ring of ATP forms hydrogen bonds between N1 and N6 and the peptide backbone of the hinge region which connects the two lobes. Nonpolar aliphatic groups line the pocket and provide van der Waals forces to the purine moiety of ATP [32]. The ribose and triphosphate moieties of ATP bind in a hydrophilic channel which extends to the substrate binding site. One important characteristic of this channel is the conserved glycine-rich loop that interacts with the α- and β- phosphate groups of ATP (Figure 3.4 [33–35]).

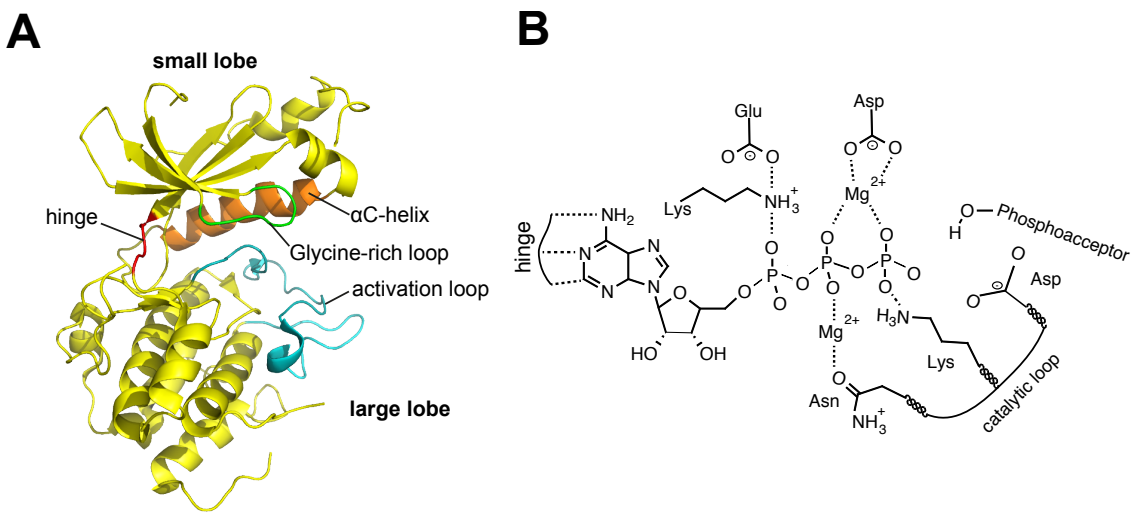

Figure 3.4: Catalytic domain and molecular interactions with ATP. A) Ribbon representation of the kinase domain of G protein coupled receptor kinase 2 (GRK2) (Protein Data Bank ID code 3UZT). Structural features are annotated. The activation loop is marked in cyan and the glycine-rich loop in green. The αC-helix and the hinge region are marked in orange and red, respectively. The PH and RH domains of GRK2 are omitted for clarity. B) Simplified illustration of the molecular contacts between the ATP and conserved active site residues and cofactors. Figure B taken from [12].

The kinase activation segment influences both substrate binding and catalytic efficiency [31]. It contains several structural features (Figure 3.4A). A conserved Asp–Phe–Gly motif (DFG) is located at the start. Next to it lies the activation loop, which differs in length and sequence, and a loop that recognizes phoshorylatable residues on substrate proteins [36, 37]. The activation loop is the most flexible part of the activation segment. For many kinases, phosphorylation of regulatory sites within the loop is required for kinase activation. The phosphorylation usually promotes a rearrangement of the loop which leads to the organization of catalytic active site residues and the phosphoacceptor binding-site [12, 36]. Phosphorylation of the activation loop can also regulate substrate- or ATP-binding [37, 38]. Other kinases are not activated by phosphorylation. Instead, they can be activated or inhibited by accessory peptides, proteins, or lipid cofactors [39, 40]

Activation of kinases usually involves changes in the orientation of the αC-helix in the small lobe and the activation segment in the large lobe [41]. The active kinase then switches between open and closed conformations in the course of the catalytic cycle [42]. In inactive kinase conformations, the αC-helix of the small lobe is rotated away from the ATP- binding site. This prevents the interaction of a glutamate residue of the αC-helix with a conserved lysine residue. In active kinase conformations, this lysine residue helps in the positioning of ATP and participates in the catalytic reaction [43, 44].

The DFG motif of the activation loop is also crucial for catalysis. In active conformations, the negatively charged aspartate residue binds to ATP either directly or through coordinating magnesium ions [41]. The phenylalanine residue interacts with the αC-helix and the nearby catalytic loop via hydrophobic contacts and thereby plays a key role for their correct positioning. In inactive kinase conformations, this residue is often turned in toward the ATP-binding site [32, 41]. The glycine residue is the last amino acid of the DFG motif and is highly conserved among the kinome, but its role remains unclear [41].

The catalytic loop of most eukaryotic protein kinases consists of a conserved His–Arg–Asp (HRD) motif. The HRD aspartate positions the hydroxyl acceptor group in the peptide substrate [37]. The HRD histidine provides a link which interacts with the DFG aspartate and the DFG phenylalanine [45]. The HRD arginine stabilizes the conformation of the activation loop by serving as a scaffold for the catalytic loop, phosphorylation site, and the DFG motif [46].

3.1.5 Substrate specificity and interactions

Phosphorylation is among the most abundant of post-translational modifications made to proteins [47]. Since the initial discovery of phosphorylated proteins by Levene and Alsberg in 1906, 500,000 potential phosphorylation sites in the human proteome and 25,000 phosphorylation events were described for 7,000 human proteins [12].

Because of the high homology of their active sites, protein kinases use many different mechanisms to maintain specificity in signaling pathways. The specificity for tyrosine- over serine-/threonine-directed phosphorylation often results from the depth, charge, or hydrophobicity of the kinase domain [48]. The phosphorylation site of substrate proteins is recognized and positioned by a consensus amino acid sequence that is located immediately N-terminal and C-terminal to the hydroxyl acceptor group in the peptide substrate. The consensus amino acid sequence of the substrate proteins have a complementary sequence epitope on the kinases, which interact based on charge, hydrogen bonding, or hydrophobic interactions [49].

In addition to these interactions, protein kinases contain other consensus amino acid sequences (so - called docking domains) which enhance their fidelity and the efficiency of their action. These epitopes are located located distal or in proximity to the active site and have been found in a variety of kinases and their activators, substrates, scaffolds, or adaptor proteins [50, 51]. Again, the interaction of kinases with other proteins is mediated by charge, hydrogen bonding, or hydrophobic interactions. Docking domains create binding sites for other proteins, and thus, increase local concentrations or enable the orientation of substrates in the active site [52–54]. Docking domains facilitate the localization of protein kinases to distinct subcellular compartments or structures and,

thereby, add another additional layer of specificity [55, 56]. Moreover, docking domains can also participate through allosteric mechanisms in positive or negative regulation of kinase activity [57–59].

3.2 Elucidating the human kinome

Aberrant signaling from over 180 kinases has been shown to contribute to the onset or progression of human pathologies, including inflammatory, cardiovascular, metabolic, and neurodegenerative diseases or cancer, making kinases one of the most heavily investigated drug targets for the pharmaceutical industry [29, 60, 61].

Elucidating the function of individual kinases during health and disease might open new opportunities to address unmet medical needs [62]. Since the approval of the first protein kinase inhibitor drug Imatinib for the treatment of chronic myelogenous leukemia (CML) in 2001 [63, 64], more than 20 kinase inhibitors have been approved in the USA [62, 65].

A comprehensive analysis of the kinome is challenging because signal transduction pathways are a highly dynamic network with multiple cascades diverging and converging in response to diverse stimuli [66]. Moreover, signal transduction pathways are controlled by complex regulatory feedback loops or have compensatory mechanisms, which hamper the evaluation of individual components at a certain time-point [67–69]. Hence, it is not surprising that the detailed functions of many human kinases during development, cellular homeostasis, or disease biology remain to be solved. A recent survey by Fedorov and colleagues found that only a minor fraction (50 kinases) has been studied in detail by both academia and pharmaceutical industries. More than 100 kinases have completely unknown function, and about 50% of all kinases are largely uncharacterized [64].

Over the last century, classical genetic approaches employed mutagenesis strategies to elucidate the function of particular kinases by investigating the relationship between genes and phenotypes [70]. However, this strategy is very time consuming and might be prone to off-target effects, such as lethality or functional compensation by related genes [71]. An alternative approach to the investigation of kinases with classical genetic strategies is represented by RNA interference (RNAi) technologies [72–75]. Potential drawbacks of these methods include incomplete target depletion, off-target effects, and toxicity [76, 77].

3.2.1 Protein kinase inhibitors

Exogenous control over protein kinase activity with kinase inhibitors has emerged as a complementary approach to investigate cellular signaling pathways and, of course, as a therapeutic strategy for the treatment of diseases [70]. In contrast to genetic or RNAi-based approaches, protein kinase inhibitors do not affect kinases at the gene expression level but on the protein level [78, 79].

3.2.1.1 Small molecules

Most currently used inhibitors or modulators of protein function are low molecular weight compounds, so-called small molecules [79]. These inhibitors have a molecular weight below 700 Dalton and can be identified by *in vitro* testing, cell-based high-throughput screenings, or rational design approaches [80–84].

Small molecules are often cell permeable, rather stable, and can be applied in a conditional fashion at any time point of interest [71]. Small molecules offer additional advantages: they can easily be chemically synthesized and modified, offering low-production costs and low batch-to-batch variability [85].

The vast majority of small molecules were identified by their ability to inhibit protein kinase activity, often resulting in inhibitors that target the ATP-binding site in its inactive or active conformation [86]. By preventing ATP from binding, ATP-competitive inhibitors are capable of inhibiting phosphorylation of substrates and downstream signaling in cells. Since the ATP-binding site is highly conserved among the kinome, ATP-competitive inhibitors are often promiscuous and have off-target effects [87–91].

Synergistic effects on multiple kinases are not only acceptable but are also often desirable for therapeutic applications. For example, most cancer therapy-approved ATP-competitive inhibitors are known to target multiple kinases [92, 93]. However, the inhibition of multiple kinases can also induce adverse side effects, such as cardiac toxicity [94].

The use of protein kinase inhibitors for research applications requires high affinity and specificity. Thus, the interpretation of functional data from ATP-competitive inhibitors is limited, making it difficult to draw conclusions about functions specific to one kinase as opposed to several kinases. Furthermore, ATP-competitive inhibitors often do not allow for the investigation of distinct, kinase activity-independent functions, including scaffolding activity, or the blockage of protein-protein interactions [70, 95].

Given these limitations, a general need for alternative approaches to kinase inhibition has emerged in order to better control specificity. Significant effort is spent on the design of inhibitors that target alternative sites, for example an allosteric site [96]. Some allosteric small molecule kinase inhibitors induce conformational changes to modulate activity whereas other allosteric inhibitors directly compete with protein-protein interactions [97–99]. These inhibitors tend to exhibit the highest degree of specificity because they utilize binding sites and regulatory mechanisms that are unique to a kinase [33, 100]. Allosteric inhibitors might provide approaches to differentially regulate the subtypes of a kinase within a subfamily which may have similar or the same substrates and high overall sequence similarity [100].

The identification of allosteric small molecule kinase modulators, in particular those that interfere with protein-protein interactions, is difficult to achieve and requires precise knowledge of the structural features of the putative allosteric site and sophisticated proteomic approaches (pharmacophore modeling, three-dimensional database and virtual high-throughput screening as well as low throughput functional screening) [100]. Moreover, interfaces that are involved in protein-protein interactions are difficult to target with small molecules because they are typically hydrophobic, relatively flat and often lack deep grooves where small molecules can bind [101].

3.2.1.2 Biologics

Biologics, such as monoclonal antibodies, antibody-derived fragments or peptides, can also be employed as allosteric kinase modulators. Because of their large size, they can dock to a large surface on the kinase which offers a greater opportunity to block protein function with higher specificity [102].

Antibodies recognize epitopes on target proteins that are usually made up of 5-8 amino acids with high affinity and specificity [103]. Antibodies against antigens can be derived by hybridoma technology, DNA-based immunization, phage display libraries, and transgenic animals [104–106]. In clinical settings, monoclonal antibodies or antibody-derived fragments are often utilized to address extracellular targets, such as cell surface receptors with intracellular tyrosine kinase activity, and thereby block intracellular signaling cascades [107]. However, the identification and production of these antibodies is laborious and could become very expensive [108]. Moreover, the performance of the same antibody tends to suffer from batch to batch variations.

Antibodies and antibody-derived fragments typically cannot pass the plasma membrane, but can be delivered into or expressed inside cells [109, 110]. The lack of cell permeability limits the application of antibodies as intracellular protein kinase inhibitors. To date, only few antibody-derived inhibitors were used in eukaryotic cells to inactivate oncogenic kinases [110, 111].

Peptide inhibitors are often identified based on specific recognition sequences or docking domains found in binding partners. Alternatively, peptide-based inhibitors can be identified by screening assays [112]. Peptides that copy the motif surrounding the phosphoacceptor site have the potential to act as substrate competitive inhibitors. Peptides that are derived from the docking domains of cognate binding partners prevent phosphorylation without grossly affecting the kinase activity [113].

Peptides have been successfully used as kinase inhibitors inside eukaryotic cells [113, 114]. However, the application of peptides as kinase inhibitors is not always successful. This likely results from large surface areas that are covered by protein-protein-interactions (approximately 1600 $\pm$ 400 A^2), whereas smaller surface area can be covered by a peptide sequence [115]. Furthermore, the intracellular application of peptides is challenging because peptides do not cross cell membranes readily and require the addition of hydrophobic entities, such as fatty acids, or the use of protein transduction domains, such as the nuclear localization signal sequence of NF-kappaB p50 [114, 116, 117].

3.3 Aptamers

An extremely promising alternative class of molecules that might overcome the limitations of small molecule- or biological-based approaches are aptamers. Aptamers are short, single-stranded oligonucleotides (ssRNA and ssDNA) that can bind to target molecules specifically by adopting complex two and three-dimensional structures [118].

Aptamers can recognize a broad variety of target molecules, such as organic dyes [119], amino acids [120], peptides [121], proteins [122], and viruses [123] to whole cells [124]. The dissociation constants of aptamer-target interactions are comparable to those of antibodies and can reach the picomolar range [125]. Similar to small molecule inhibitors, aptamers are produced by chemical synthesis with extreme accuracy and reproducibility [108].

Aptamers often reveal remarkable specificity in discriminating between structurally similar molecules, such as theophylline and caffeine [126], or homologous proteins isoforms [127]. The often highly specific interaction between aptamers and their targets results from structure compatibility and non-covalent interactions, including stacking of aromatic rings, electrostatic forces, van der Waals forces, and hydrogen bonds [128].

High-affinity aptamers have been identified against a broad variety of protein families, including cytokines, kinases, proteases, kinases, cell-surface receptors and cell-adhesion molecules [129]. Because of their size, aptamers are often capable of modulating the function of their target protein by blocking a single domain of a protein while leaving the remainder of the protein functional [130]. Thus, aptamers represent an attractive opportunity to elucidate the function of kinase targets that are otherwise not accessible through specific small molecules.

3.3.1 SELEX

Most aptamers derive from an iterative *in vitro* selection process, termed "**S**ystematic **E**volution of **L**igands by **EX**ponential enrichment" (SELEX) [131, 132]. During a classical SELEX experiment (Figure 3.5), a random sequence library (or pool) of 10^{14}-10^{15} ssDNA or ssRNA molecules of up to 100 nucleotides in length, is employed. The random sequence region is flanked by constant sequences required for primer annealing and enzymatic amplification [133, 134].

In the case of RNA SELEX, a library of ssRNA molecules is prepared by *in vitro* transcription of double-stranded DNA (dsDNA) templates, usually using recombinant T7 RNA polymerase. The initial ssRNA library is then exposed to target molecules. By removing unbound molecules, sequences that bind with high affinity to the target molecule can be recovered. After RT-PCR and *in vitro* transcription, the SELEX library is subjected to the next selection round [135].

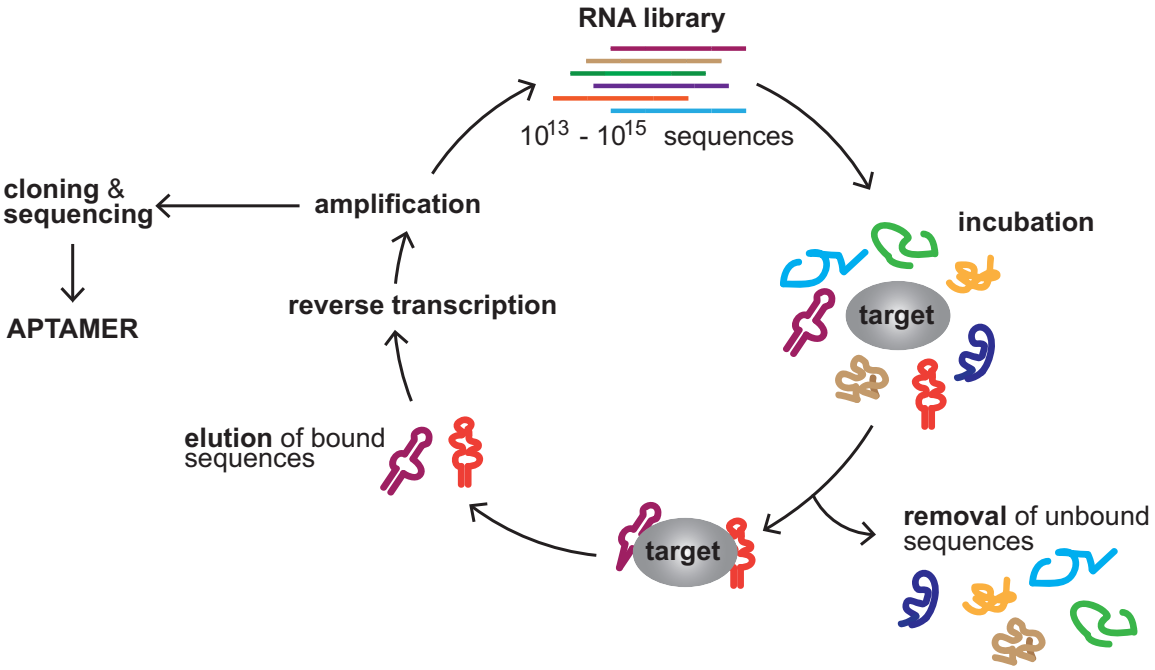

Figure 3.5: SELEX. Schematic representation of the SELEX process.

After additional rounds of selection with increasing selection pressure, the diversity of the SELEX library decreases and candidate aptamers are enriched. As a consequence, the affinity of the enriched library increases during successful SELEX experiments. A typical SELEX is conducted until no further change in affinity can be observed. The final SELEX round is then cloned and sequenced. Monoclones are then grouped into families according to homology in their random region. Lastly, putative aptamers are tested for binding affinity and specificity [134].

Notably, SELEX against proteins is not limited to full length proteins but can also be applied to peptides and protein domains [136]. While traditional SELEX techniques require a soluble, pure form of the target protein [137], newer methods have been developed to identify aptamers in a complex mixture, such as whole-cells [138] or living animals [139, 140]. Nowadays, automated platforms and massive sequencing techniques enable high-throughput parallel selections of aptamers to several protein targets at once [141, 142]. Hence, aptamers can be easily obtained and used to elucidate the function of a defined protein or protein domain.

3.3.2 Chemical modification of aptamers

While the activity of unmodified RNA (and DNA) aptamers is often suitable for *in vitro* experiments, aptamer use for cellular applications requires higher stability to prevent nuclease-mediated degradation [129]. Therefore, a key factor in developing nucleic acids aptamers has been the introduction of chemical modification to individual nucleosides.

Chemical modifications are accessible by enzymatic incorporation or chemical synthesis during [143] or after the SELEX process [144–146]. The most widely used and commercially available modifications involve the substitution of the ribose ring with 2´- desoxy - amino pyrimidines [147–149], 2´- desoxy - fluoro pyrimidines [150, 151] and 2´- O - methyl ribose purines and pyrimidines [152] (Figure 3.6). A study demonstrated that these types of modification can increase serum stability from less than one second for a completely unmodified RNA aptamer to more than 81 hours [145].

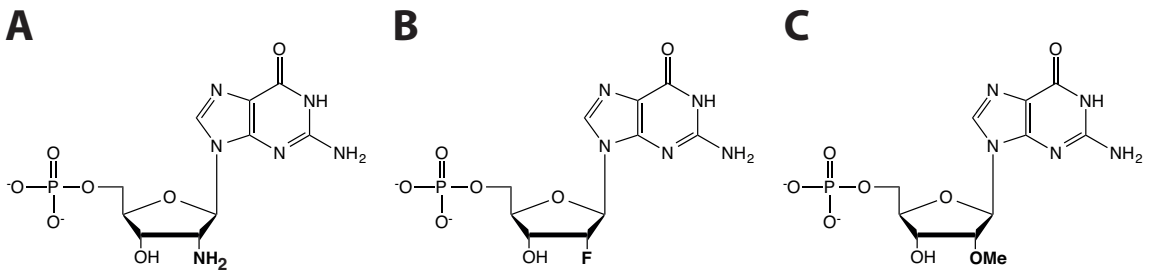

Figure 3.6: Chemical ribonucleotide modifications. Chemical structure of a guanine ribonucleotide with A) 2´-amino, B) 2´-fluoro, or C) 2´-O-methyl modifications.

Chemical modifications are not only utilized to increase the serum stability of aptamers, they also allow for the site-specific introduction of chemical functionalities which can be used for conjugation, such as primary amines, thiol precursors, and aldehyde precursors [129, 153, 154]. For example, so-called starter nucleotides can be utilized to facilitate the incorporation of chemical modifications at the 5‘-end. By employing the starter nucleotide guanosine-monophosphorothioate (GMPS), RNA aptamers can easily be modified with fluorescent dyes, biotin, or other functional entities [155].

The wealth of available chemical modifications enables the application of aptamers as reporters for diagnostic applications, such as *in vivo* and *in vitro* imaging [156], or histochemical staining [157]. Moreover, chemical modifications support the capability of aptamers for many different cell-targeting approaches [158–163]. Among them, one elegant application demonstrated the generation of phototoxic aptamers for the targeted photodynamic therapy of specific cancer cells [164–166]. Aptamers that are selected against cell surface proteins specifically expressed only on the surface of cancer cells can be modified at their 5´-ends with chlorin e6, a photodynamic agent. Upon internalization into the tumor cells, light-activated cytotoxicity then induces cancer cell-specific killing.

3.3.3 Intramers

Aptamers do not only have the potential to target proteins for *in vitro* or extracellular applications. It has become increasingly evident that aptamers can retain their ability to modulate the biological function of their targeted protein inside cells [167, 168].

In 1990, a pioneering study by Sullenger and colleagues reported the use of small structural RNAs as a new approach for inhibiting proteins and enzymes within cells [169]. Sullenger and co-workers could demonstrate that decoys of a small HIV RNA region, called TAR, could be used to inhibit HIV virus replication in cellular models. This study paved the way for the use of aptamers as so-called intramers to interrupt, modulate, or define the functions of a wide range of target proteins within cells [167].

Aptamers cannot readily cross cell membranes. Nevertheless, the introduction of aptamers into cells can easily be facilitated. To this end, the transfer of the genetic information required to synthesize an RNA aptamer within the target cell itself can be achieved, for example, by employing expression plasmids [170–179], or by utilizing virus-based approaches (adeno- [180, 181], vaccinia [182, 183], or lenti virus [184]).

For intracellular expression, the aptamer sequences are often expressed between flanking regions or as multivalent constructs to stabilize the aptamers within the cytoplasm [185]. To achieve this, the aptamers are fused to self-cleaving ribozymes, aberrantly spliced mRNAs, tRNAs, or embedded into U6 small nucleolar RNA [175, 184, 185].

Furthermore, several studies have shown that DNA or RNA aptamers can directly be delivered into the cytosol by microinjection [186], in the context of liposomes [187–190], or by employing nanoparticles [191] (Figure 3.7).

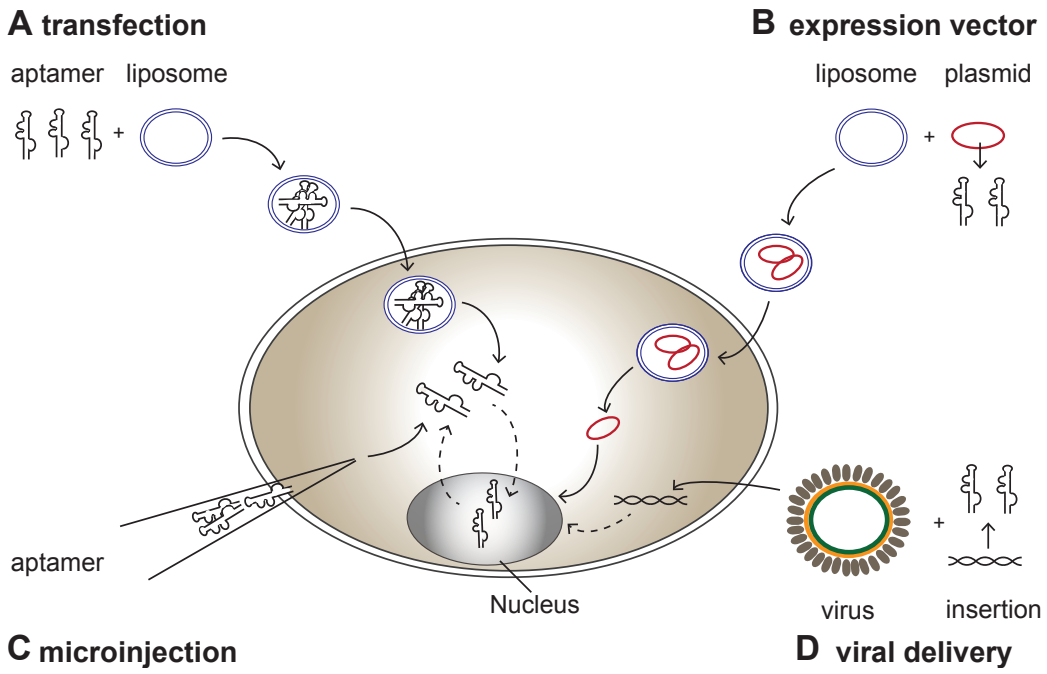

Figure 3.7: Introduction of aptamers into cells. For intracellular applications, aptamers can be introduced into cells with a variety of methods, including A) lipofection, B) expression vectors, C) microinjection, or D) viral delivery vectors.

3.3.3.1 Intramers against nuclear targets

Many examples have shown that aptamers can inhibit endogenous protein targets in the nucleus and, thus, can act as antagonists for nucleic acid binding proteins [168]. Among these aptamers, Ishizaki *et al.* identified an unmodified-RNA aptamer that blocked the DNA-binding activity of the transcription factor E2F with high affinity and inhibited fibroblast proliferation when microinjected into cells [186]. Subsequently, Martell and co-workers selected for a high affinity chimeric tRNA-E2F1 aptamer construct that would facilitate gene therapy approaches. The newly selected aptamer inhibited E2F1-mediated transactivation by up to 80% in human HEK 293 cells [171].

Another interesting example described the effect of intramer expression in an animal model [192]. The target is *Drosophila melanogaster* B52 protein, a factor which is essential for pre-mRNA splicing [193]. The expression of B52 below or above certain levels induces developmental defects or lethal phenotypes [194]. Developmental effects caused by overexpression of B52 could be rescued by expression of a pentameric variant of the aptamer [192].

One of the best examples of the intracellular ability of aptamers as a tool to study biological functions of proteins or protein domains was demonstrated with an aptamer that targets the p50 subunit of the transcription factor NF-kappa B [195]. NF-kappa B plays an essential role in inflammation, innate immunity, and cancer [196]. The RNA aptamer was shown to compete with DNA for binding to the transcription factor [195]. Intracellular expression of the NF-kappa B aptamer under the control of the RNA polymerase III U6 promoter resulted in the inhibition of constitutive

NF-kappa B-mediated gene transcription in mammalian cells and cell growth defects in xenografts which were not observed with a non-binding negative control RNA [181]. Moreover, the inhibitory effect of the aptamer could be reversed by the addition of a complementary RNA sequence (antidote). On the basis of these results, Mi and co-workers used the aptamer as a research tool to determine whether the tumor suppressor protein p53 is required for the resistance to doxorubicin in non-small cell lung cancer [180].

3.3.3.2 Intramers against targets in the cytoplasm

A number of studies further demonstrated that intramers can be used inside the cytoplasm to elucidate biological activities of target proteins or protein domains [168].

Blind *et al.* selected RNA aptamers against the intracellular domain of the $\beta 2$ integrin LFA-1, a transmembrane protein that is important to the regulation of cell adhesion to intercellular adhesion molecule-1 (ICAM-1) [182]. Employing a T7 polymerase-controlled expression system enabled the transcription of the intramers in the cytoplasm. More importantly, intramer expression translated into a biological effect, as measured by reduction of cell adhesion to immobilized ICAM-1.

Mayer *et al.* applied the same T7 polymerase-controlled expression system to investigate the function of the Sec7 domain of cytohesin1 [183], a small guanine nucleotide exchange factor (GEF) for ARF GTPases [197]. Cytohesin1 inhibition *in vitro* by the RNA aptamer M69 correlated with the modulation of cell adhesion and cytoskeletal rearrangement in Jurkat T-cells, revealing the important role of cytohesins in T-cell movement [183].

Because aptamer M69 interacted with both cytohesin1 and cytohesin2 [183], Theis *et al.* selected a new RNA aptamer, termed K61, which specifically targets cytohesin2 [188]. Their work revealed that intramers have the capacity to inhibit protein function without utilizing expression vectors. Transfection of the unmodified RNA aptamers K61 and M69 into human HeLa cells inhibited transcriptional activation through the serum-response element (SRE) promotor. Moreover, Theis and co-workers demonstrated that aptamers M69 and K61 induced specific down-regulation of the Erk1/2 MAP kinase pathway by investigating the phosphorylation status of Elk-1. Elk-1 is a transcription factor which promotes survival, cell division, and motility through regulation of immediate-early genes, such as c-Fos and c-Myc [198].

Taken together, these examples clearly show that intramers are potent and specific tools to study the function of closely related proteins or individual domains within distinct cellular compartments. Furthermore, intramers can also be adapted as biosensors to analytical applications in order to monitor cellular metabolites [199, 200], proteins [201], or RNA [202–205].

3.3.4 Aptamer-displacement assay

Even though aptamers can be applied as modulators of protein function in cell-based assays and even *in vivo* studies [167, 168], they can also be used to facilitate the identification of putative small molecule drug candidates in aptamer-displacement assays [206]. Aptamer-displacement assays are based on the competition of an aptamer by a small molecule. Since aptamers that bind to proteins are often specific and are capable of modulating protein function, small molecules identified by aptamer-displacement screening often exhibit similar inhibitory properties on the same target proteins [206]. Hence, aptamer-displacement assays offer a promising alternative to inhibitor identification by functional assays because binding partner-dependent interactions are not required.

A displacement assay of aptamer M69 enabled the identification of the small molecule SecinH3 as a novel inhibitor for cytohesins [206]. SecinH3 inhibited both insulin receptor [207] and EGF receptor signaling [189], and inhibited the proliferation of cancer cell lines [189].

3.4 Aptamers as protein kinase inhibitors

Aptamers that target receptor tyrosine kinases can be utilized to prevent subsequent intracellular downstream signaling in a similar way to monoclonal antibodies. Recently, Li and colleagues [208] described an aptamer which binds to cells expressing the epidermal growth-factor receptor (EGFR). By outcompeting EGF from binding to the receptor, the aptamer blocked receptor autophosphorylation, and prevented proliferation of tumor cells.

Until now, no intramer has been reported to target kinase activity within cells. Nevertheless, several very promising aptamers that recognize and inhibit protein kinase C (PKC) [127], G protein-coupled receptor kinase 2 (GRK2) [209], and extracellular signal-regulated kinase 2 (Erk2) [210] have been described. Remarkably, most of these aptamers recognize the ATP-site, but nevertheless, exhibit high specificity. Since RNA aptamers against GRK2 and Erk2 play a fundamental role during this thesis, special emphasis is put both on their identification and the physiological role of the kinases in the following sections.

3.4.1 G protein-coupled receptor kinase 2 (GRK2)

G protein-coupled receptor kinases (GRKs) and arrestins participate in the regulation of G protein-coupled receptor (GPCRs), a large family of membrane receptors of key physiological and pharmacological importance [211, 212].

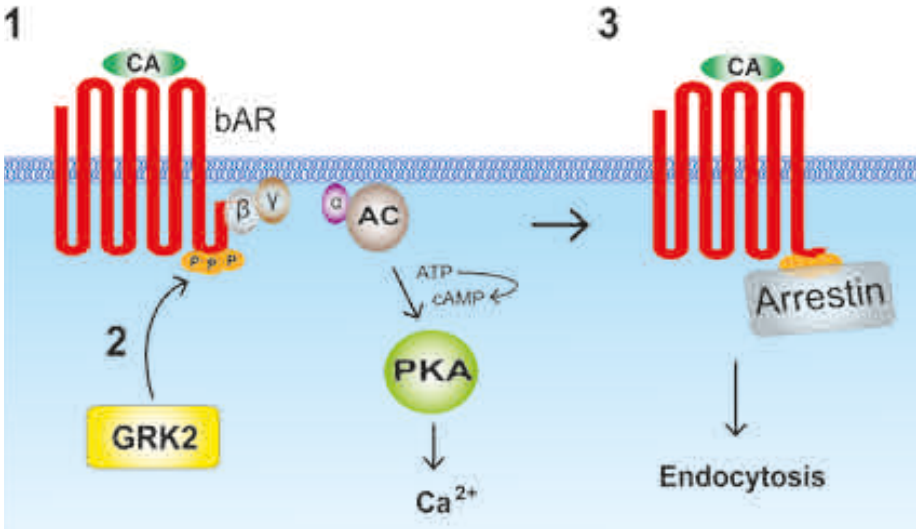

Figure 3.8: Simplified model of β-adrenergic receptor and GRK2 signaling in the myocardium. 1) Upon agonist binding, β-adrenergic receptors activate adenylyl cyclase (AC) and cyclic adenosine monophosphate (cAMP) production through coupling to heterotrimeric G proteins to enhance cardiac inotrophy and chronotrophy. 2) G protein-coupled receptor kinase 2 (GRK2) phosphorylates the activated receptor to attenuate signaling. 3) Once phosphorylated, the receptor binds to β-arrestin. β-arrestins modulate intracellular GPCR signaling and promote the endocytosis of the receptor, leading to its dephosphorylation and degradation or recycling back to the plasma membrane. CA = catecholamines, bAR = β-adrenergic receptor, p = phosphate group, GRK2 = G protein coupled-receptor kinase 2, $\beta\gamma$ = G$\beta\gamma$-subunits, AC = adenylyl cyclase, PKA = protein kinase A, ATP = adenosine triphosphate, cAMP = cyclic adenosine monophosphate. Taken from [211].

GRK2 and the β-adrenergic receptor (β-ARs) family of GPCRs are crucial to the regulation of heart rate and myocardial contraction in response to catecholamines (epinephrine and nore-

pinephrine) [213, 214]. Upon activation, β-ARs undergo a conformational change, which enables the activation of effector proteins (e.g. adenylyl cyclase, phospholipases) via heterotrimeric G proteins. In turn, cAMP accumulates within the cells, which leads to the activation of protein kinase A (PKA). PKA phosphorylates calcium-recognizing proteins and some myofilament components. Thereby, it promotes positive changes in cellular metabolism as well as inotropic and chronotrophic responses [212, 215].

GRK2 is recruited to the agonist-occupied, activated β-AR through interaction with subunits of heterotrimeric G-proteins ($G\beta\gamma$ subunit) and phosphatidylinositol (4,5)-bisphosphate (PIP_2) [216, 217]. Subsequently, GRK2 phosphorylates several residues inside the cytosolic component of the receptor [218]. The phosphorylation enhances the receptor´s affinity for β-arrestin adaptor proteins. β-arrestin binding leads to the receptor´s uncoupling from G proteins and attenuates the receptor´s surface signaling [219]. Furthermore, arrestin binding promotes receptor internalization via clathrin-mediated endocytosis and elicits G protein-independent signaling pathways [220, 221]. Inside the endosomal compartment, β-ARs are dephosphorylated and then either recycled back to the plasma membrane or degraded [220].

In addition to its classical role in mediating GPCR phosphorylation and arrestin binding, GRK2 has emerged as a key regulator of diverse signaling pathways and displays a very complex interactome. GRK2 has been associated with the modulation of signal transduction pathways by interacting with $G\alpha$ and $G\beta$-subunits and non-GPCR substrates, including receptor tyrosine kinases, cytoskeletal proteins, and transcription factors [211].

3.4.1.1 GRK2 as a drug target

Over the last two decades, GRK2 has emerged as a promising target for heart failure therapy [222]. Heart failure is the leading cause of mortality in Western countries [212]. It is associated with a loss of β-AR density which results in impaired cardiac function, rendering the heart incapable to pump enough blood to meet the requirements of the body [214, 223]. At early stages of heart disease, GRK2 activity is often found to be up-regulated [224–227]. The postulated therapeutic potential of cardiac-specific GRK2 inhibition was demonstrated with various transgenic approaches in a variety of animal models [228–231]. Deregulated GRK2 signaling has also been linked to other human pathologies, such as Alzheimer's disease [232], granulose cell tumors [233], and inflammation [234].

Elucidating the complex GRK2 interactome could contribute significantly to the development of novel therapies for all these diseases. Serine/threonine kinase inhibitors that are known to inhibit GRK2 activity include the natural products staurosporine [235], sangivamycin [236], and balanol [237]. However, their application as research tools is difficult because these inhibitors are known to target multiple kinases. Recently, several lead inhibitory compounds for the GRK2/GRK3 family were developed by Takeda Pharmaceuticals (Figure 3.9), [238]. These compounds target the active site and inhibit GRK2/GRK3 activity [239].

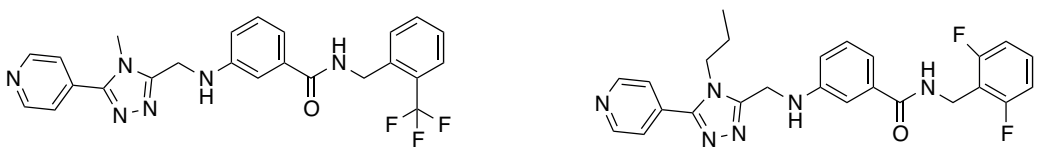

Figure 3.9: Inhibitors of GRK2. Chemical structures of two small molecule GRK2 inhibitors that were discovered by Takeda Pharmaceutical Company LTD [238].

3.4.1.2 RNA aptamers as inhibitors of GRK2

Specific and potent inhibitors for GRK2 were not available for a long time. Several decades ago, natural products (see above), peptides, and the synthetic compound suramin were the only available inhibitors of GRK2 activity [240–243]. Due to low specificity, low potency, or cytotoxic effects, these substances revealed limited usefulness as tools for the characterization of GRK2 activity [209, 244].

The lack of specific inhibitors led to the development of a novel molecular class of GRK2 inhibitors for the functional characterization of GRK2 activity. In 2008, Mayer and colleagues described the identification and characterization of the RNA aptamer C13 [209]. C13 was observed to bind to GRK2 with an affinity of 78.2 ± 2.6 nM.

Aptamer C13 was isolated from an automated *in vitro* selection procedure. For their selection, Mayer *et al.* applied a RNA library consisting of a structurally predefined stem region of 13 nucleotides that flanked a 20 nucleotide random region (Figure 3.10A). Additional sequences were included at the 5´- and 3´-ends to facilitate reverse transcription and PCR amplification. C13 was shown to reflect most of the structural constrains of this library (Figure 3.10B). In accordance with the library design, C13 could easily be truncated by excluding the primer binding sites (Figure 3.10C). The resulting aptamer, termed C13.51, revealed similar affinity for GRK2 as C13 (101.2 ± 7.2 nM).

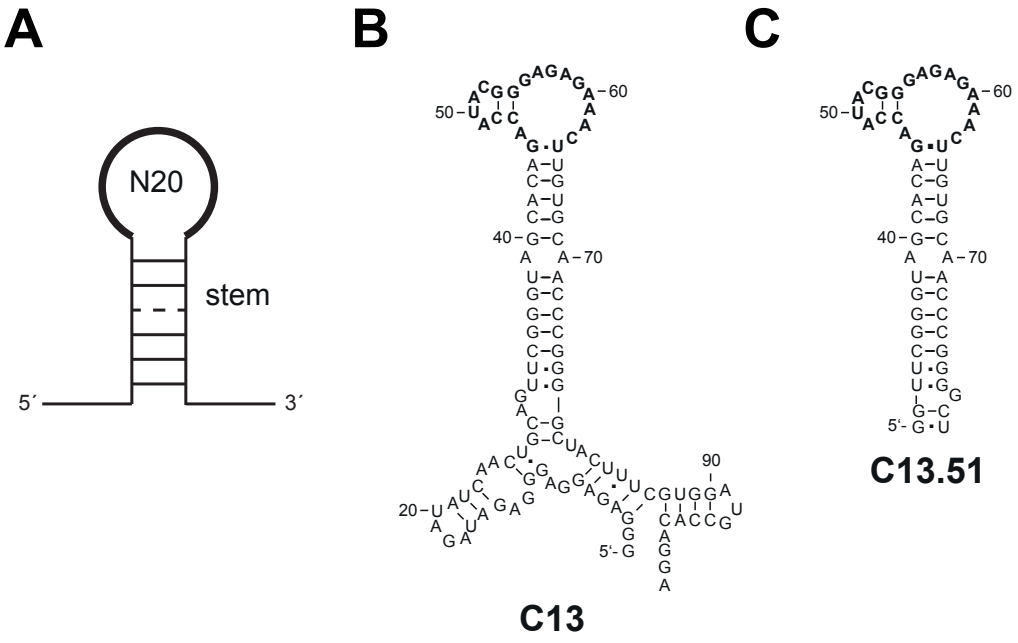

Figure 3.10: *In vitro* selection of aptamer C13. A) Design of the constrained RNA library comprising a 13-nt stem structure with a central A-A mismatch and a 20-nt random region (N20, bold). Additional sequences were included at the 5´- and 3´-ends to facilitate reverse transcription and PCR amplification. B) Sequence of the selected aptamer C13 and C) its truncated variant C13.51. The nucleotide numbers of C13.51 were adapted from C13. Nucleotides in bold represent the selected sequence. Modified from [209].

Aptamer C13 had been the most potent inhibitor of GRK2 kinase function reported so far. It inhibited GRK2 activity *in vitro* with an IC_{50} value of 4 nM. Binding studies with the kinase domain of GRK2 and ATP-competition assays suggest that the aptamer acts as an ATP-competitive inhibitor.

More importantly, however, was the finding that this ATP-competitive aptamer revealed high specificity and thus, represents a promising research tool. C13 demonstrated no or only insignificant

activity towards ten tested protein kinases from distinct kinase groups according to Manning *et al.* (Section 3.1.3 [7]). The aptamer was also capable of discriminating between kinases from the GRK superfamily, as inhibition of GRK5 activity was observed at a 20-fold higher IC_{50} value [209].

3.4.2 Extracellular signal-regulated kinase 2 (Erk2)

Extracellular signal-regulated kinase 2 (Erk2) and the highly homologous kinase Erk1 belong to the mitogen-activated protein kinase (MAPK) superfamily [245]. The MAP kinase superfamiliy includes the Erk family, the p38 MAP kinase family, and the c-Jun N-terminal kinase (JNK) MAP kinase family [245].

The Erk1/2 MAP kinase pathway promotes cell growth, proliferation, survival, differentiation, motility, and angiogenesis [246, 247]. The pathway becomes activated in a variety of cell types by mitogenic and other stimuli, including growth factors [248], Ca^{2+} influx [249], cytokines, osmotic stress, and activated G-protein coupled receptors [250].

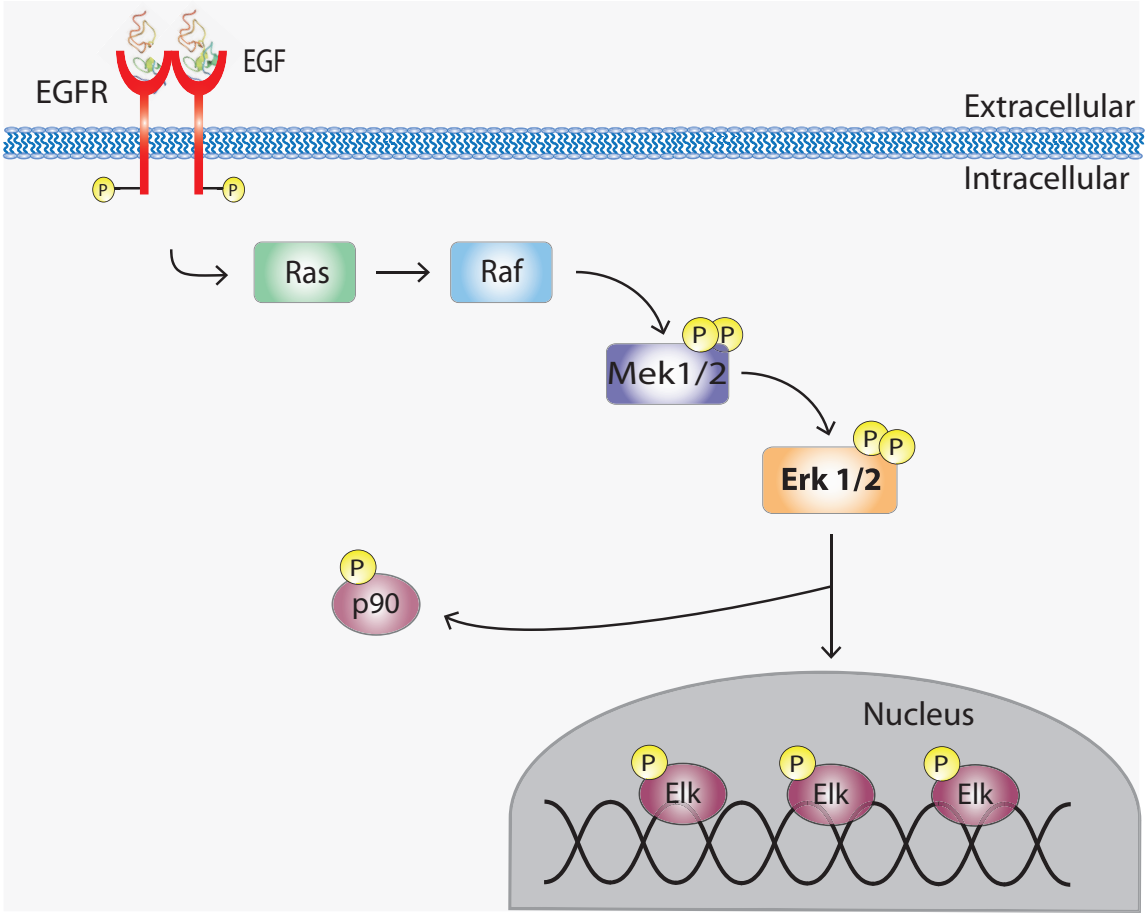

Figure 3.11: Simplified model of the Erk1/2 signaling cascade. Upon binding of EGF (Protein Data Bank ID code 1EGF) or other growth factors, receptor tyrosine kinases (e.g. EGF receptors) activate the Erk1/2 MAP kinase signaling cascade via the GTPase Ras. Ras activates the first MAP kinase Raf. Raf activates the second MAP kinase Mek1/2. Mek1/2 are the activating kinases for Erk1/2. Activated Erk1/2 catalyze the phosphorylation of targets in the cytosol or in the nucleus. EGF: epidermal growth factor, EGFR: epidermal growth factor receptor, Mek: Mitogen-activated protein kinase kinase, Erk: extracellular signal-regulated kinase, p90: p90 ribosomal S6 kinase, p: phosphorylated residue.

Erk1/2 activation in response to growth factors is induced by receptor tyrosine kinases, such as the epidermal growth factor receptor (EGFR, Figure 3.11) [251]. Typically, epidermal growth factor (EGF) binding to the EGF receptor induces dimerization of two receptor monomers and autophosphorylation of specific tyrosine residues within the C-terminal domain [252]. These phosphorylated residues generate binding sites for adaptor proteins, such as growth factor receptor-bound protein 2 (GRB2) [253]. GRB2 then recruits the guanine nucleotide exchange factor SOS to the plasma membrane. SOS, in turn activates the membrane-bound GTPase Ras by catalyzing the exchange of GDP to GTP [254]. In its GTP-bound state, Ras recruits inactive Raf kinases from the cytoplasm to the plasma membrane and activates their serine/threonine kinase function [255]. Upon activation, Raf activates the mitogen-activated protein kinase kinases 1 and 2 (Mek1/2). Mek1/2, in turn, catalyze the activation of their sole effectors Erk1 and Erk2 by phosphorylating the activation loop residues Thr202 and Thr204 of Erk1, and Thr185 and Tyr187 of Erk2 [247].

Erk1 and Erk2 share 84% sequence identity and only little is known about their functional differences [256, 257]. They are activated in parallel [258] and were found to target the same substrates [259]. Activated Erk1/2 catalyze the phosphorylation of serine and threonine residues on over 160 substrate proteins [260, 261]. Most activated Erk1/2 molecules translocate into the nucleus and only a smaller portion of Erk1/2 as well as Mek1/2 and Raf molecules migrate into distinct subcellular compartments, including mitochondria, endosomes, plasma membrane, cytoskeleton, and Golgi apparatus, where they control specific functions [262, 263].

Inside the nucleus, Erk1/2 phosphorylate and regulate various transcription factors, including Elk-1, c-Myc, and c-Fos [261, 264], and promote changes in gene expression [265, 266]. In addition, Erk1/2 can directly regulate transcriptional repression and chromatin remodeling [267]. Erk1/2 substrates in the cytoplasm include phosphatases, kinases, cAMP phosphodiesterase 4 (PDE4), cytosolic phospholipase A2 ($cPLA_2$), cytoskeletal proteins, apoptotic proteins, ion channels, and regulatory and signaling molecules [245, 261].

3.4.2.1 Erk1/2 signaling in neurons

In the central nervous system (CNS), Erk1/2 play an important role in normal proliferation and differentiation [245]. Moreover, accumulating evidence has shown that the Erk1/2 signaling pathway is associated with learning and memory storage in the mammalian brain [268].

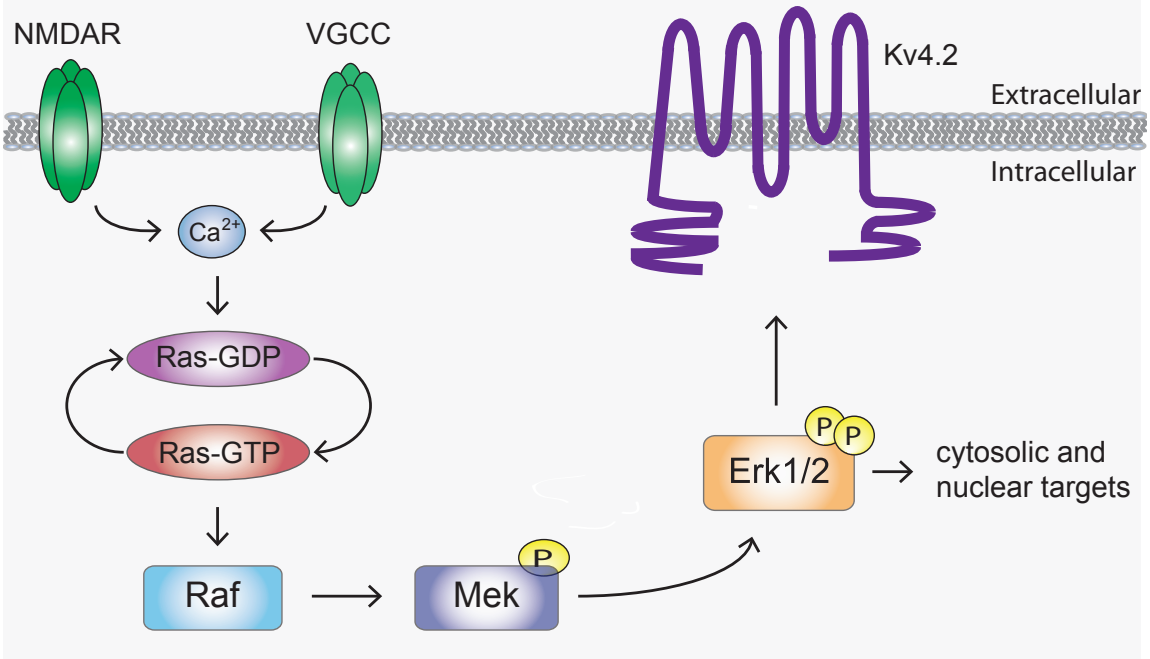

Figure 3.12: Activation of Erk1/2 signaling in response to synaptic signaling. Calcium influx, either through NMDA (N-methyl-D- aspartate) - type glutamate receptors (NMDARs) or voltage-gated calcium channels (VGCCs) triggers the activation of Erk1/2 signaling. Erk1/2 phosphorylates extranuclear targets such as the voltage-dependent potassium channel $K_V4.2$. Mek: Mitogen-activated protein kinase kinase, Erk: extracellular signal-regulated kinase, p: phosphorylated residue. Modified from [269].

Activation of the Erk1/2 signal transduction cascade in response to synaptic signaling is initiated by calcium influx into the postsynapse through synaptic N-methyl-d-aspartate receptors (NMDARs) [270, 271] or voltage-gated calcium channels (VGCCs, Figure 3.12) [272, 273]. In neurons, Erk1/2 control postsynaptic 5 - methyl - 4 -isoxazolepropionic acid (AMPA) receptor trafficking and insertion [274–276], outgrowth and stabilization of postsynaptic spines [277, 278], and activity-dependent translation and targeting of mRNAs [278–280]. Furthermore, Erk1/2 catalyze the phosphorylation of voltage-dependent potassium channel $K_V4.2$ subunits (Figure 3.12) [281]. Phosphorylation by Erk1/2 was described to inhibit the channels activity [282] and to decrease the potassium current [283].

In addition to the regulation of cytosolic targets, Erk1/2 propagate signals into the nucleus. Erk1/2, or kinases activated by Erk1/2, regulate gene expression by phosphorylating transcription factors, such as c-Jun and c-Fos [284–288] or CREB [289].

3.4.2.2 Structure and functional domains of Erk2

Erk1/2 have a bi-lobed kinase structure with conserved residues for ATP-binding and catalysis as described for a typical protein kinase in Section 3.1.3 and shown in Figure 3.4.

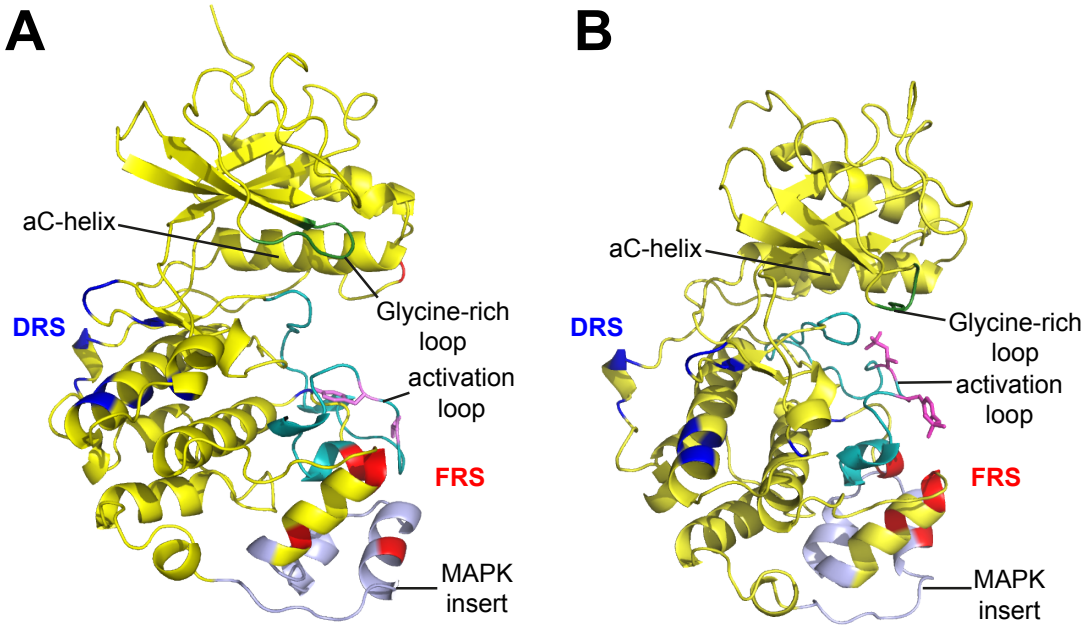

Figure 3.13: Extracellular signal regulated kinase 2 (Erk2). Ribbon representation of the A) inactive or B) active conformation of Erk2 (Protein Data Bank ID codes 1ERK, 2ERK). Structural features are annotated. The glycine-rich loop and the activation loop residues are marked in green and cyan, and D-site recruitment site (DRS) and F-site recruitment site (FRS) residues are annotated in blue and red, respectively. The activation loop phosphorylation site residues Thr185 and Tyr187 are labeled in pink. In inactive Erk2 (A), the two lobes of the kinase domain are rotated away from each other. Once Erk2 becomes phosphorylated (B), the two lobes of the kinase domain rotate 5.4° closer. The activation segment refolds and the conserved aspartate side chain of the DFG sequence faces into the ATP-binding pocket and coordinates Mg^{2+} [290]. In addition, the aC-helix of the small kinase lobe rotates and becomes a part of the active site by positioning a conserved lysine residue required for ATP-binding and catalysis [290, 291]. Conformational changes also include the docking domains and MAP kinase insert region.

Erk1/2 possess two independent docking domains to interact with substrate proteins, activating kinases, or inactivating phosphatases (Figure 3.12) [245]. The so-called D-site recruitment site (DRS) is located opposite of the catalytic cleft and is comprised of negatively charged and hydrophobic components. The F-site recruitment site (FRS) is located near the activation segment and catalytic cleft.

The docking sites of interacting proteins are interspersed. Some binding partners contain either a D-docking site or F-docking site, both sites or none of these sites [292]. For example, phosphorylation of the transcription factor Elk-1 requires binding of Erk2 to both D- and F-docking sites [293] whereas p90-RSKs and Erk1/2 interact via a D-docking site motif [294].

Another functional domain of Erk2, the MAP kinase insert, is located at the C-terminus (Figure 3.12). The MAP kinase insert is a sequence insertion that distinguishes the MAP kinase superfamiliy from other kinases [245]. In Erk2, this domain has been associated with diverse kinase activity - dependent and - independent functions, including the interaction of Erk2 with regulatory proteins [295, 296] or effectors [297, 298], nuclear translocation [299, 300], or DNA-binding activity [301].

A study from Robinson *et al.* demonstrated that the MAP kinase insert is also involved in the activation of Erk2 by Mek1 [295]. They demonstrated that point mutations within the MAP kinase insert of Erk2 abolished the interaction of Erk2 with Mek1 in a yeast-two-hybrid screen and resulted in reduced activation after over-expression of constitutive Mek1 inside cells.

3.4.2.3 The Erk1/2 pathway as a drug target

Erk1/2 are versatile protein kinases that regulate many cellular functions: They are crucial for the regulation of proliferation, differentiation and survival [246, 247] and some forms of neuronal plasticity in the central nervous system [302, 303]. However, aberrant Erk1/2 activation is also associated with many human pathologies, such as cancer [246, 247] or neurodegerative diseases [302]. Erk1/2 activity is upregulated in all of these cases, suggesting that direct inhibition of Erk1/2 might be beneficial for therapeutic applications.

Accordingly, the Erk1/2 MAP kinase pathway is considered an important therapeutic target, in particular for cancer therapy. In more than 30% of all human malignancies, amplification or gain-of-function mutations in genes that encode for receptor tyrosine kinases, Ras and/or Raf are potent drivers of oncogenesis [304]. Surprisingly, amplifications or gain-of-function mutations in genes encoding for Erk1/2 are absent in cancer [305].

In recent years, several successful therapeutic strategies have been identified for cancer therapy. Thereby, Erk1/2 signaling is inhibited either by targeting cell surface receptors or proteins upstream of Erk1/2 [306]. In contrast, the development of direct inhibitors of Erk1/2 has been less successful. Most available Erk1/2 inhibitors are ATP-competitive small molecule inhibitors with various degrees of specificity [307].

In addition, non ATP-competitive Erk1/2 inhibitors that target the a specific part of the DRS - docking site on either active Erk2 or inactive Erk2 have been described [308, 309]. These inhibitors revealed the intriguing potential of Erk1/2 domain-specific inhibition in cellular studies [307] and model organisms [308, 309].

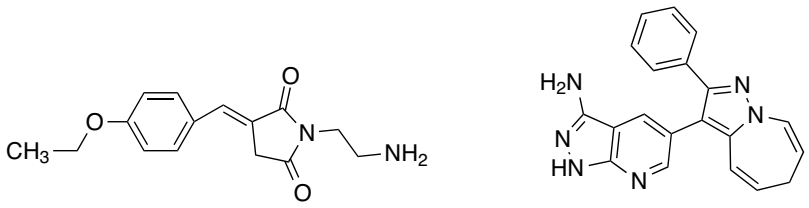

76 FR180204

Figure 3.14: Small molecule Erk1/2 inhibitors. Chemical structures of the DRS - docking domain inhibitor 76 [307] and the ATP-competitive inhibitor FR180204 [310].

3.4.2.4 RNA-based Erk1/2 inhibitors

In 2001, Seiwert and colleagues identified the first RNA aptamers that recognize Erk1/2 [210]. They performed a nitrocellulose membrane-based *in vitro* selection experiment to identify RNA aptamers that discriminate between the active, diphosphorylated and inactive, non-phosphorylated conformation of Erk2. In order to remove RNA molecules that recognize epitopes unique to both conformational states of Erk2, they included additional negative selection steps using inactive Erk2 in the SELEX process. Their SELEX approach yielded two different families of RNA aptamers, coined "family I" and "family II" aptamers. The family II aptamer bound with a K_D of 10 nM to the active conformation of Erk2 and with 10-fold lower affinity to the inactive variant. Moreover, the familiy II aptamer was shown to potently inhibit Erk2 activity and to recognize Erk2 in an ATP-

dependent manner. Seiwert and colleagues were able to truncate this aptamer from 135 nucleotides down to 63 nucleotides. The truncated aptamer, termed "TRA", retained its functionality [210].

In contrast, the simultaneously enriched family I aptamers revealed similar affinity (K_D values of approximately 2 nM) towards inactive and active Erk2 and inhibited Erk2 activity in a substrate-dependent manner. A truncated version could not be generated for this aptamer. Most remarkably, both family I and II aptamers exhibited high specificity for Erk2 and the closely related MAP kinase Erk1 and did not inhibit the activity of other MAP kinases of the p38 and JNK superfamilies.

Vaish and colleagues utilized these Erk2-targeting aptamers for the design of allosteric ribozymes [311]. Allosteric ribozymes are RNA enzymes whose activity is modulated by the binding of an effector molecule to an aptamer domain, which is located apart from the ribozymes active site. Thus, they act as precise molecular switches which are controlled by the presence or absence of a specific effector [312, 313]. By utilizing the described Erk2-binding aptamers, Vaish and colleagues designed allosteric ribozymes that were controlled by the active or inactive conformation of Erk2 [311]. These allosteric ribozymes enabled the detection of active or inactive Erk2 *in vitro* and in mammalian cell lysate. The latter, however, was only described for recombinant, inactive Erk2 and not for endogenous Erk2. Notably, the allosteric ribozyme for active Erk2, whose Erk2-recognizing domain is based on the sequence of the TRA aptamer, was not employed within cell lysate.

3.4.2.5 *In vitro* selection of novel Erk2-binding aptamers

The Erk2-inhibiting aptamer TRA (Figure 3.15A) was supposed to be used as an Erk2 inhibitor in cell-based assays [314]. However, TRA was selected in Hepes buffer in the absence of any monovalent cations [210]. Binding studies performed by Mayer and co-workers implicated that the binding of TRA was affected in a high salt containing phosphate buffer (PBS, supplemented with 3 mM $MgCl_2$) [314]. Since monovalent cations, such as potassium ions, are highly abundant within the cell, this sensitivity to ionic conditions would likely impair the intracellular application of TRA.

In order to identify an Erk2-binding aptamer that stills shares the same favorable properties as the TRA aptamer, but would be less susceptible to different ion concentrations, a re-selection with a partially randomized library based on the sequence of TRA was performed prior to this thesis [314]. In 85% of all cases (Figure 3.15A), the library had the original nucleotide at a defined position as in TRA, but the remaining three nucleotides were at 5% probability each [314]. This library was subjected to an automated *in vitro* selection protocol targeting active, diphosphorylated Erk2. To optimize the binding to Erk2 under high ionic conditions, PBS buffer supplemented with 3 mM $MgCl_2$ was chosen as the selection buffer. This buffer has been shown in previous experiments to give rise to aptamers that are adaptable to intracellular applications [182, 183].

The most promising aptamer derived from this selection was aptamer C5 [314]. Compared to TRA, C5 bears twelve mutations located mainly in the central stem and upper bulged region (Figure 3.15B). Based on secondary structure predictions and TRA-homology modeling, these mutations are supposed to lead to a stabilization of the central stem and allow building in additional base pairs in the upper bulged region.

An additional selection was performed in order to obtain an aptamer that recognizes epitopes present of both the active and inactive conformation of Erk2 [314]. In contrast to the previous SELEX which yielded aptamer C5, a completely randomized library was utilized and inactive Erk2 was employed as the target. The selection was again performed in PBS buffer, supplemented with 3 mM $MgCl_2$, and yielded aptamer C3 (Figure 3.15C).

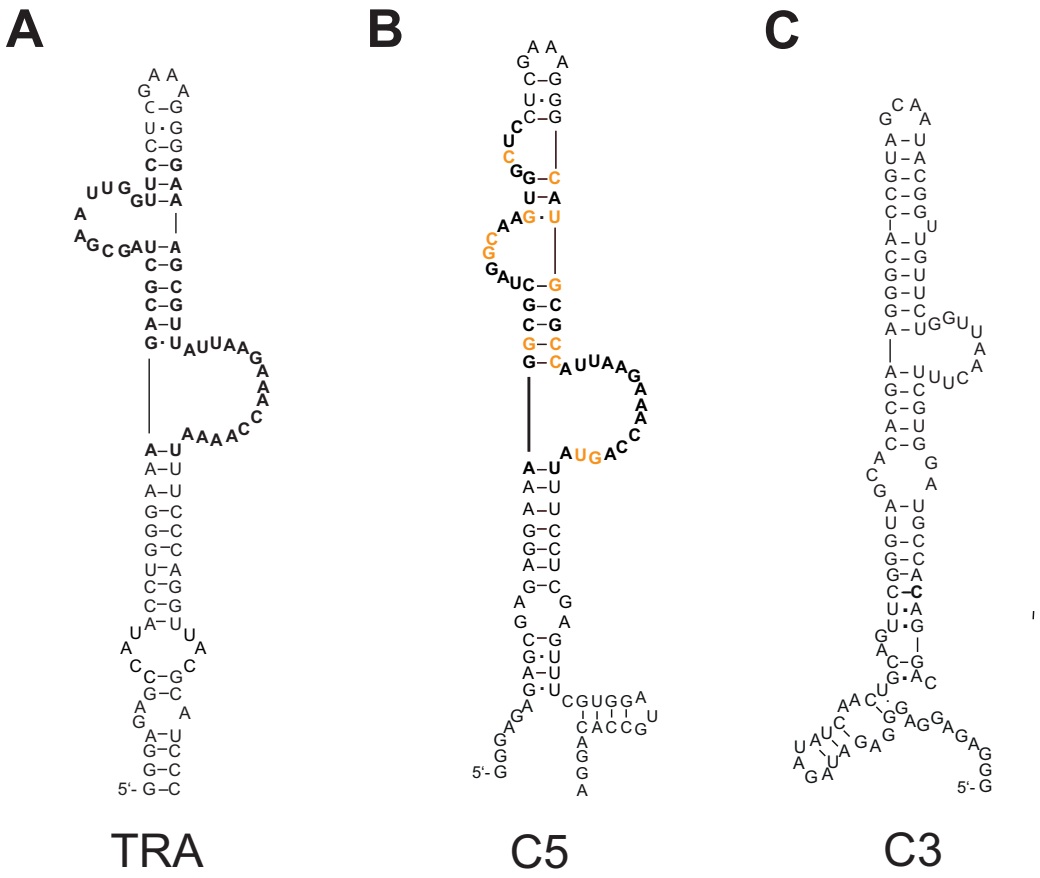

Figure 3.15: RNA aptamers targeting Erk2. Proposed secondary structure of the RNA aptamers A) TRA, B) C5, and C) C3. A) The sequence of TRA was adapted according to [210]. Nucleotides that were randomized and utilized in a doped library for reselection are highlighted in bold letters. B) Reselection of the doped library against active Erk2 yielded the RNA aptamer C5. Secondary structure prediction of the aptamer C5 shown is based on the structure of TRA. Nucleotides initially randomized are depicted in bold letters. Nucleotides that differ from TRA are highlighted in green. C) Secondary structure prediction of C3.

4 Aim of this study

The aim of this study was to investigate the potential of RNA aptamers as a novel class of selective protein kinase inhibitors for chemical biology research.

Within the past decades, low molecular weight compounds have often been used as protein kinase inhibitors. Most of these inhibitors block kinase activity by interfering with ATP-binding. However, the evolutionary relatedness and structural conservation of the ATP-binding site often lead to unforeseen cross reactivity, which limits their application as research tools.

Several very promising aptamers that recognize and inhibit protein kinase C (PKC) [127], G protein-coupled receptor kinase 2 (GRK2) [209], and extracellular signal-regulated kinase 2 (Erk2) [210] were described. In contrast to many low molecular weight inhibitors, these RNA aptamers have been shown to inhibit the activity of their respective kinases with high specificity. Competitive binding experiments with ATP, kinase activity assays, or binding studies with isolated kinase domains provide strong evidence that these aptamers act by addressing the active site and thus sterically prevent ATP from binding.

The residues that ATP-competitive inhibitors can interact with in the active site are highly conserved among the kinome and the precise aspects of how ATP-competitive aptamers derive their high specificity are yet unknown. Thus, the first part of this project sets out to examine the molecular interaction of aptamer C13 and GRK2. Aptamer C13 is the most potent inhibitor of GRK2 activity *in vitro*. GRK2 is involved in the regulation of G protein-coupled transmembrane receptors and is associated with heart failure. Elucidating the precise determinants which contribute to the high specificity of the aptamers may aid in the development of novel inhibitors.

The Erk1/2 MAP kinase pathway promotes cell growth and proliferation and has often been found to be deregulated in human malignancies. Unfortunately, specific inhibitors for Erk1/2 are still rare. An ATP-competitive RNA aptamer, coined TRA, represented one of the most promising Erk2 inhibitors. It blocked the activity of the MAP kinase Erk2 with high affinity and specificity *in vitro*. However, the binding of TRA to Erk2 was also affected by ionic strength, which hampers its application in cell-based studies. Therefore, two novel Erk2-recognizing aptamers, termed C3 and C5, were selected prior to this thesis.

In the second part of this thesis, the novel Erk2-recognizing aptamers C3 and C5 will be explored to gain a refined biochemical understanding for their potential as specific protein kinase inhibitors. In order to investigate the assessments of C3 and C5 in a more complex cellular system, their sensitivity to ionic strength and specificity, will be investigated.

By recognizing different sites on the same protein kinase, aptamers can provide fundamental insight into domain-specific protein functions. To analyze if the aptamers C3 and C5 can be utilized as domain specific inhibitors, their putative binding sites and modes of actions will be identified.

Aptamers that interfere with protein kinase activity inside cells might aid in unravelling the complex interplay between kinase signaling in health and disease. In the final piece of the project, distinct cellular assays will be utilized to elucidate the ability of aptamers C3 and C5 to interfere with Erk1/2 signaling within cells and to answer the question if aptamers can be employed as a new class of molecular tools for chemical biology research.

5 Results

This chapter describes the investigation of the potential of RNA aptamers as selective inhibitors for the protein kinases G protein-coupled receptor kinase 2 (GRK2) and extracellular signal-regulated kinase 2 (Erk2).
In the first part, the molecular determinants of the C13-GRK2 complex are investigated to elucidate how ATP-competitive aptamers derive their high specificity (Section 5.1).
The second part of this chapter extends the concept of RNA aptamers as selective protein kinase inhibitors towards the MAP kinase Erk2 and describes the characterization and validation of novel Erk2-binding RNA aptamers C3 and C5 (Section 5.2).
Lastly, the ability of aptamers C3 and C5 to control intracellular kinase activity is evaluated (Section 5.3).

5.1 The co-crystal structure of aptamer C13 and GRK2

Specific GRK2 inhibitors are essential for therapeutic applications and chemical biology research. At the moment, such inhibitors are rare (Section 3.4.1.1). An ATP-competitive RNA aptamer, termed C13, represents one of the most potent and specific inhibitors of GRK2 [209].

In order to understand how this aptamer can derive its high specificity, the molecular determinants of the C13-GRK2 complex were investigated. GRK2 participates together with arrestins in the regulation of G protein-coupled receptors [211, 212]. Since aberrant GRK2 signaling has been shown to contribute to the onset or progression of human pathologies, such as cardiovascular diseases [214, 223], unraveling the molecular interaction can aid in the development of novel drug candidates.

In order to elucidate the molecular determinants contributing to the specificity of aptamer C13, co-crystal structures of the C13-GRK2 complex were obtained in collaboration with the lab of Prof. Dr. John Tesmer, University of Michigan. Valerie Tesmer determined all crystal structures that are shown for the C13-GRK2 complex in this chapter. This structural data was supported by biochemical binding assays that were performed in parallel during this thesis.
Additional information about the C13-GRK2 complex was published in [315].

5.1.1 Structural determinants of GRK2 binding and selectivity in the C13 aptamer

Full-length aptamer C13 and the truncated variant C13.51 revealed an affinity of 78.2 ± 2.6 nM and 101.2 ± 7.2 nM for GRK2 in filter retention assays, respectively [209]. The K_D values represents the equilibrium binding constant of the aptamer-protein complex. All filter retention assays were performed at 37°C in selection buffer (PBS, 3mM $MgCl_2$).

To determine the regions of C13 that are important for GRK2 binding and to shorten the RNA sequence for crystallographic experiments, truncated versions based on the C13.51 variant of the aptamer were synthesized and tested for their ability to bind to GRK2 or other GRK family members (Figure 5.1).

The interaction of GRK2 with truncated C13 variants was measured with flow cytometry using a bead protein-RNA interaction assay. In this assay, GRK2 was biotinylated, coupled to streptavidin-coated beads and incubated with increasing concentrations of 5´- Alexa 488-labeleld RNA at 4°C. The beads were then passed through a flow cytometry and the amount of fluorescence bound to the beads was quantified to calculate a K_D value.

The half maximal inhibitory concentration (IC_{50}) values for C13 variants were determined by measuring the transfer of γ-^{32}P from ATP to rhodopsin at room-temerapture. Rhodopsin is a natural substrate for GRK family members [316]. These experiments were kindly performed by V. Tesmer (Tesmer lab, University of Michigan).

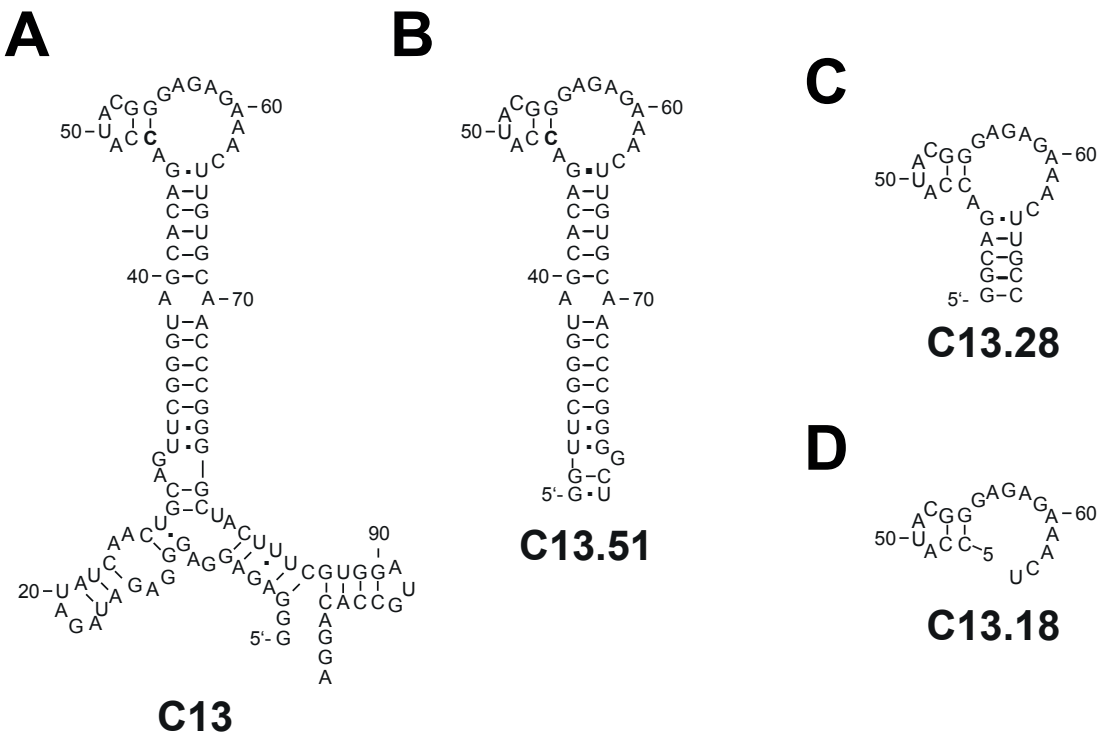

Figure 5.1: RNA aptamer C13 and truncated variants. Proposed secondary structure model of RNA aptamer C13 (A) and its truncated variant C13.51 (B) as described in [209]. Truncated variants of C13.51, namely C13.28 (C) and C13.18 (D) were employed for structural assays. Nucleotde numbers were taken from full-length C13.

Table 5.1: Binding and inhibitory properties of C13 variants.

Variants	**K_D [nM]**	**Temperature [°C]**	**Activity/ IC_{50} [nM]**	**Temperature [°C]**
C13*	78.2 ± 2.6	37	4.1 nM ± 1.2	23
C13.51*	101.2 ± 7.2	37	n.d.	23
C13.28	1.2 ± 0.6	4	11 ± 4	23
C13.18	35 ± 5	4	220 ± 40	23

* Taken from Mayer *et al.* [209], n.d.: not described

One truncated variant of C13.51, C13.28, was designed by shortening the stem of the original aptamer to only four Watson-Crick base pairs (Figure 5.1C). C13.28 had 60-fold higher affinity for GRK2 than C13 (Table 5.1). This can be explained by differences in the assay setups, in particular the lower temperature which was used during the bead-based flow cytometry assays.
In addition, C13.28 inhibited GRK2 activity with identical potency as C13 (IC_{50} value 11 ± 4 nM, Table 5.1). C13.28 also exhibited similar specificity properties as C13. It inhibited GRK6 activity (IC_{50} 210 ± 10 nM) and GRK1 activity (IC_{50} 590± 160 nM) with more than 60 times lower potency than C13.

C13.28 was further truncated down to 18 nucleotides (Figure 5.1D). The resulting aptamer, C13.18, lacked a terminal stem and two residues from the 5´end of the nucleotide variable region. C13.18 revealed a 35-fold lower affinity for GRK2 binding than C13.28 (Table 5.1).

In summary, these data indicate that these 18 nucleotides within the selected sequence of C13 are key for binding and inhibiting GRK2. The aptamers terminal stem seems to be required to maintain its high potency.

5.1.2 C13 variants target the active site of GRK2

The structural models of the C13-GRK2 complexes were determined with C13.28 and C13.18. The co-crystal structure of the C13.18-GRK2 complex was determined at a 3.5 Angstrom resolution (Figure 5.2A):

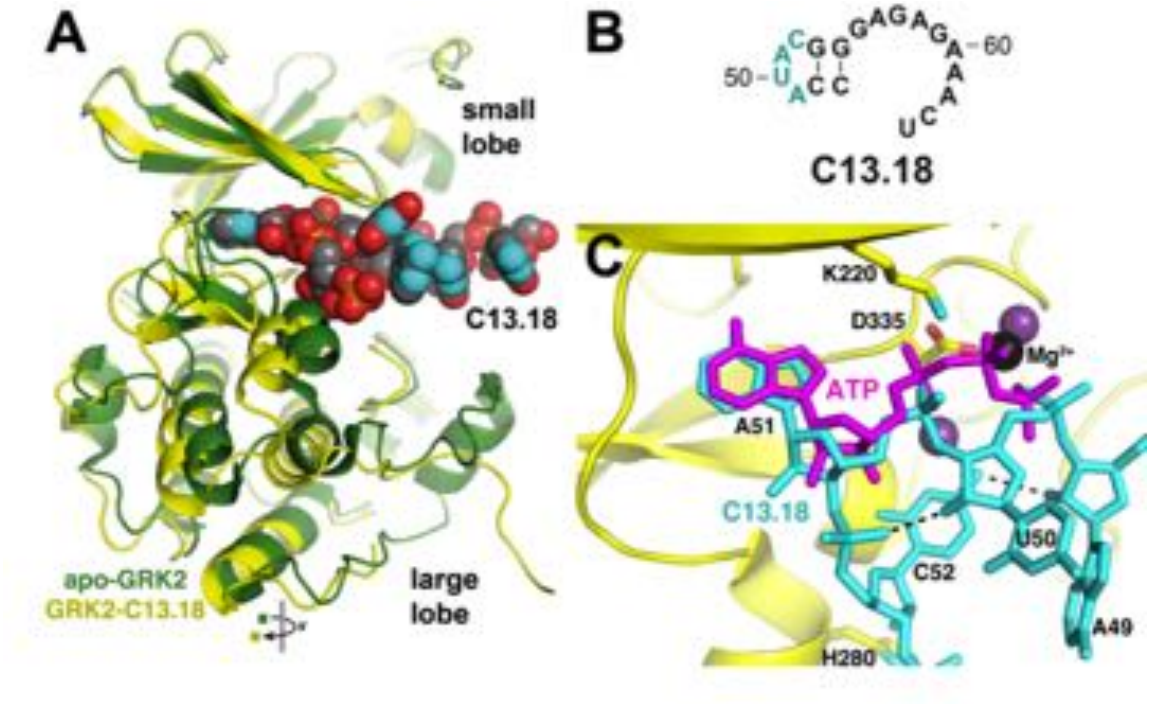

Figure 5.2: C13.18 targets the active site of GRK2. A) C13.18 stabilizes a unique conformation of the GRK2 kinase domain. The small lobe of the kinase domain in structures of apo-GRK2 (green; PDB entry 2BCJ5) and C13.18-bound GRK2 (yellow) were superimposed to show the 8° rotation of the large lobe. B) Proposed secondary structure of C13.18 based on the C13 aptamer. Nucleotides A49-C52 were modeled into the active site of GRK2 as described in [315] and are marked in cyan. C) C13.18 mimics ATP-binding within the kinase domain of GRK2. Nucleotides A49-C52 of C13 are marked in cyan. ATP is shown in magenta.

The RNA aptamer forms extensive interactions with the kinase domain which bury about 1,140 Angstrom^2 of accessible surface area. The C13-GRK2 structure revealed that C13.18 binds into a cleft formed between the large and small lobe of the kinase domain where the aptamer stabilizes a unique conformation. In this conformation, the lobes of the kinase domain differ by 8° relative to those in previously described structures of GRK2 and ATP [317, 318].

Electron density was obtained for nucleotides 47 to 52 of the C13.18 aptamer within the active site of GRK2. As can be seen in Figures 5.2B,C, adenine 51 (A51) of C13.18 binds deep into the active site of GRK2 where it overlaps with the AMP moiety of ATP. Moreover, the aptamer seems to recapitulate specific contacts made by ATP within the active site, including hydrophobic contacts to the base and hydrogen bonds to the ribose and adenine ring. Furthermore, the 5´-phosphate of uracil 50 (U50) was shown to replace the γ-phosphate group of ATP. A bridging magnesium ion was modeled between the 5´-phosphate of U50 and Asp335 of GRK2. This magnesium ion might help in neutralizing negative charges.

The overall structure of the nucleotides interacting within the active site of GRK2 seems to be stabilized by hydrogen bonds between N4 of C52 and the 2´-OH of A49 and between the 5´-phosphate of C52 and the 2´-OH of U50.

5.1.3 Nucleotides A49-G53 of C13 are essential for GRK2 binding

The importance of nucleotides A49 - C52 for GRK2 binding was validated with additional assays. Therefore, point mutations at positions A49, U50, A51, C52 and G53 were introduced into full-length C13 by site-directed mutagenesis (Figure 5.3A). These point mutations were verified by sequencing and analyzed for binding to GRK2 in filter retention assays. In this assay, α-^{32}P labeled RNA is incubated with increasing GRK2 concentrations in binding buffer (PBS, 3 mM $MgCl_2$, 1 mg/ml Heparin). The amount of radioactively labeled RNA retained on GRK2 was detected and quantified for K_D value determination by assuming a 1:1 binding model.

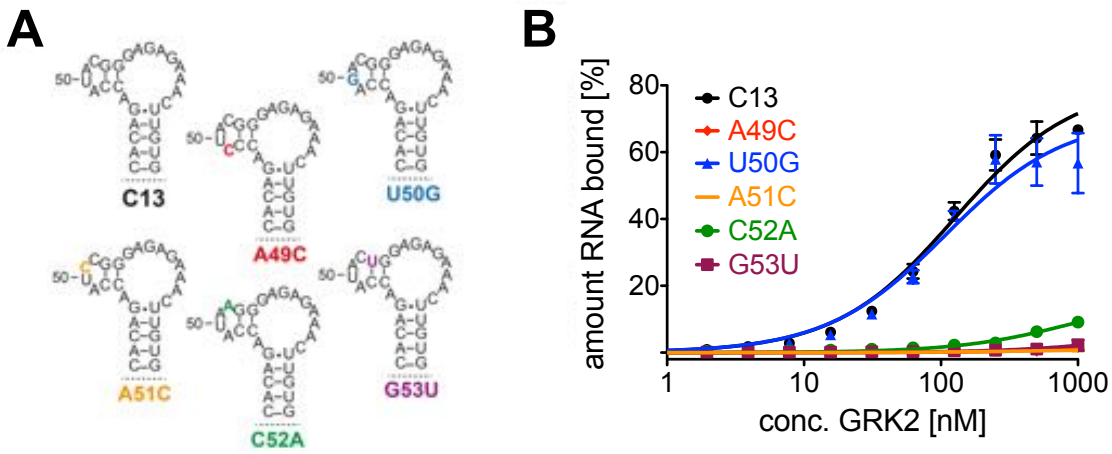

Figure 5.3: Nucleotides A49-G53 are essential for GRK2 binding. A) In accordance with Figure 5.2C, point mutations in C13 nucleotides A49-G53 were generated by site-directed mutagenesis. Nucleotides 1-40 and 69-101 of aptamer C13 are omitted for clarity in this picture. B) Filter retention assay of C13 and point mutants binding to GRK2. The amount of radioactively labeled RNA bound to GRK2 is plotted against the protein concentration. K_D values are listed in Table 5.2. Experiments were performed at least twice (mean ± SEM).

Table 5.2: K_D values [nM] of C13 variants for GRK2 as determined from Figure 5.3B.

Variant	**K_D [nM]**
C13	126.3 ± 15.3
C13 U50G	108.2 ± 20.7
all others	n.d.

n.d.: no binding detectable

As can be seen in Figure 5.3B and Table 5.2, the full-length aptamer C13 revealed an affinity of 126 ± 15.3 nM for GRK2 in filter retention assays, consistent with previous data [209]. Most strikingly, the C13 point mutant U50G bound with similar affinity to GRK2 as C13 itself (Figure 5.3B, Table 5.2).
As shown in Figure 5.2C, the nucleotide at position 50 contributes its 5´-phosphate to GRK2 binding and does not form specific interaction to GRK2 or within the C13.18 structure, explaining why the uracil base could be exchanged easily with a guanine without a loss of affinity.

In contrast to U50G, point mutation at adenine 51 to cytosine completely diminished the binding to GRK2 in filter retention assays. According to the structural model (Figure 5.2C), the adenine base occupies the adenine-binding site within the kinase domain. A smaller cytosine base does not seem to allow for structural substitution.

Mutations of A49, C52 and G53 completely abolished aptamer binding in filter retention assays, most likely by changes in the aptamer fold or loss of hydrogen interaction within the nucleotide sequence.

This data further support that nucleotides interacting within the active site are essential for GRK2 binding.

5.1.4 Aptamer C13 forms extensive interactions both within and outside of the active site of GRK2

The co-crystal structure of the C13.18-GRK2 complex (Figure 5.4A) implicated that the C13 nucleotides A49 - C52 could engage in electrostatic interactions with the active site residues His280 and Asp335 (Section 5.1.2). To further delineate the interaction of C13 with the active site residues His280 (H280) and Asp335 (D335), the residues were individually mutated to alanine and analyzed for C13 binding (Figure 5.4B).

The binding data are summarized in Figure 5.4B and Table 5.3. Mutating His280 to alanine droped the affinity of C13 for GRK2. H280 likely interacts electrostatically with the aptamer. A less polar amino acid does not seem to able to replace this interaction.
In contrast, the interaction of C13 with active site mutant GRK2-D335A was barely detectable, highlighting the necessity of Aps335 for the coordination of the bridging magnesium ion. This magnesium ion might be crucial for neutralizing negative charges.
These data further support the important role of active site residues His280 and Asp335 for the interaction with aptamer C13 within the active site, consistent with the structural model in Section 5.1.2.

The 12 unresolved residues of C13.18 were projected into a cavity outside of the active site, where they likely interact electrostatically with positively charged residues that line the cavity (Figure 5.4A). Inside this cavity, the basic residues of the αF-αG-loop region might interact with the phosphodiester backbone of nucleotides 56-63 of GRK2.
In order to refine this model, the basic residues in the αF-αG-loop region (Arg392, His394, Lys395, Lys397, Lys399, and His400) were simultaneously mutated to alanine (GRK2 FG-6A) and analyzed for C13 binding.

These binding experiments are summarized in Figure 5.4B and Table 5.3 and show that C13

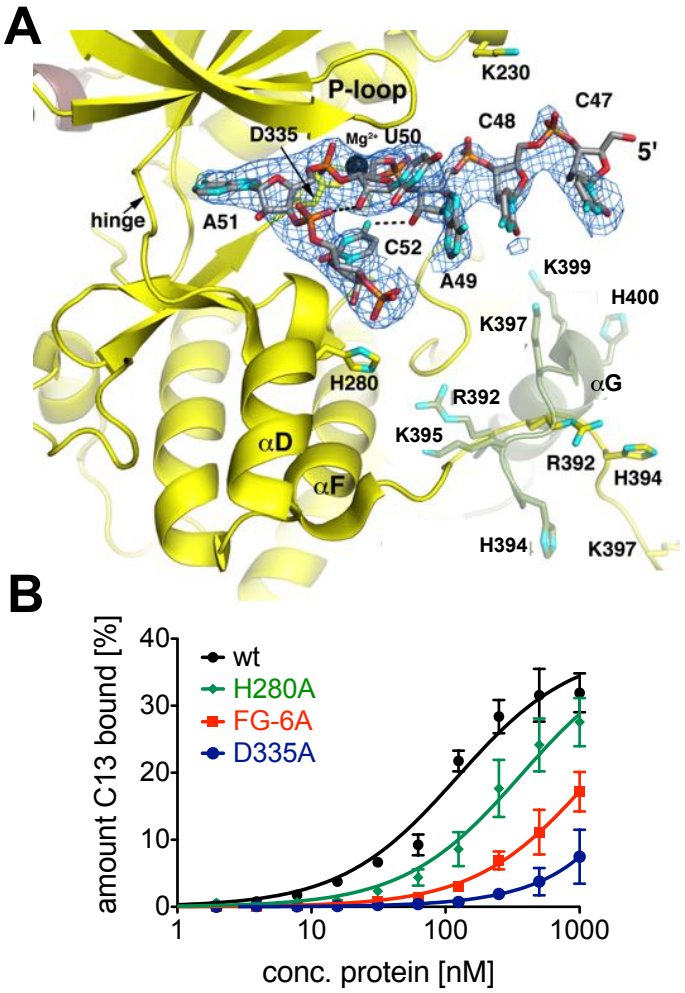

Figure 5.4: Structural determinants of GRK2 involved in mediating the binding to C13. A) Interactions of the C13.18 aptamer within the active site of GRK2. The position of the αF-αG-loop and αG-helix in apo-GRK2 (amino acids 391–410; PDB entry 2BCJ) is shown in green at half transparency. The blue wire cage shown corresponds to an electron density map around residues 47-CCAUAC-52 of C13.18. Carbons atoms are gray for C13.18, and yellow for the kinase domain. Nitrogens are in cyan, oxygens are red, phosphates are orange and magnesium ions are black. Intramolecular hydrogen bonds in the RNA are dashed lines. The 12 C-terminal nucleotides of the aptamer are disordered, but extend into a crystal contact lined with positively charged amino acids. B) GRK2 active site residues H280 or D335 as well as 6 residues of the basic αF-αG-loop (FG-6A) were mutated to alanine. The affinity of C13 to GRK2 wildtype ("wt") or the GRK2 mutants was analyzed by filter retention assay. Experiments were performed at least twice (mean ± SEM). K_D values are listed in Table 5.3.

Table 5.3: K_D values of C13 and GRK2 variants [nM] as determined from Figure 5.3B.

Variant	K_D [nM]
GRK2	126.3 ± 15.3
H280	> 1000
D335	> 1000
FG-6A	> 1000

forms interactions outside of the active site. Mutations in the basic αF-αG-loop of GRK2 (GRK2-FG-6A) outside of the active site showed a strong drop in affinity for C13. This further supports the notion that the basic αF-αG-loop interacts with the phosphodiester backbone of unmodeled nucleotides 56 – 63 of C13.

Taken together, the binding data and co-crystal structures presented in this chapter indicate that C13 stabilizes a unique inactive conformation of GRK2 through multiple interactions, both within and outside of the kinase domain.

5.2 *In vitro* characterization of novel Erk2 - recognizing aptamers C3 and C5

This section extends the concept of aptamers as selective protein kinase inhibitors to the MAP kinase Erk2. Erk1/2 are versatile protein kinases that are associated with many human pathologies, such as cancer [246, 247] and neurodegerative diseases [302].

The ATP-competitive RNA aptamer TRA represented one of the most promising Erk2 inhibitors. *In vitro*, it blocks the activity of the MAP kinase Erk2 with high affinity and specificity. However, the binding of TRA to Erk2 was shown to be affected in a PBS buffer supplemented with 3 mM $MgCl_2$ [314]. Since this sensitivity to ionic strength will likely hamper the application of TRA in cell-based studies, two novel Erk2-recognizing aptamers, C3 and C5, were selected in a high salt containing buffer prior to this thesis (Sections 3.4.2.5, 5.2.1.3).

In order to evaluate the aptamers dependency on cations for future applications, the interaction of TRA as well as the novel Erk2-recognizing aptamers C3 and C5 are tested under distinct ionic buffer conditions (Sections 5.2.1.1, 5.2.1.3).

Furthermore, to assess the potential of C3 and C5 as research tools, their specificity is characterized (Section 5.2.3).

The last part of this section identifies the modes of actions and putative binding sites of C3 and C5 (Section 5.2.4).

5.2.1 Binding studies

5.2.1.1 Characterization of the ionic strength dependence of TRA binding

Insensitivity to cationic strength could play an important role for the successful intracellular application of aptamers. Previous experiments implicated that the binding of the Erk2- recognizing aptamer TRA was affected in a high salt buffer. The buffer used for these experiments was PBS, pH 7.4, supplemented with 3 mM $MgCl_2$ [314]. PBS is a phosphate buffer which contains 2.7 mM KCl and 130 mM NaCl.

TRA was selected in the absence of monovalent cations in 10 mM Hepes buffer, pH 7.4, supplemented with 10 mM $MgCl_2$. To further delineate the cation sensitivity of TRA, it was investigated if monovalent cations or lower magnesium concentration might cause TRA´s loss of interaction with Erk2 in PBS buffer.

Filter retention assays were performed with α-^{32}P labeled TRA and increasing concentrations of inactive Erk2 in Hepes or PBS buffer with the varying Mg^{2+}, Na^+, or K^+ concentrations (Figure 5.5). The pH values of the buffers were tested and did not differ.

The amount of radioactively labeled RNA bound to Erk2 was detected and quantified. A four-parameter logistic fit was applied for K_D value determination. This fit allows for the determination of both the K_D value and the Hill coefficient. The Hill coefficient quantifies the steepness of a binding curve and may give information on the number of binding sites on a macromolecule. If one

molecule binds with positive cooperativeness to the target, the Hill coefficient should be close to a value of 1 (ideally between 0.8 and 1.5) [319].

First, it was investigated if the observed loss of affinity in PBS buffer was caused by the low magnesium concentration. To analyze this, the binding of TRA to inactive Erk2 was tested in Hepes buffer with distinct $MgCl_2$ concentrations (Figure 5.5).

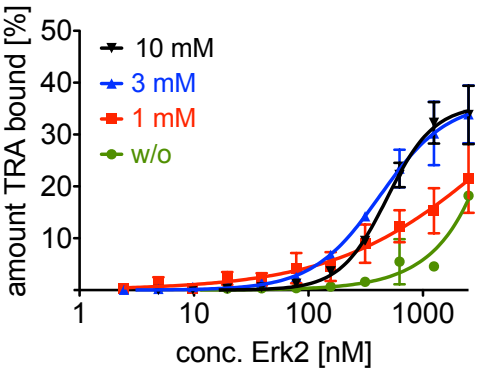

Figure 5.5: K_D value determination of TRA in Hepes buffer supplemented with indicated $MgCl_2$ concentrations. The amount of radioactively labeled TRA bound to inactive Erk2 is plotted against the Erk2 concentration. All experiments were performed at least twice (mean ± SEM). K_D values are listed in Table 5.4. w/o = without additional $MgCl_2$.

Table 5.4: K_D values [nM] and Hill coefficients of TRA binding to Erk2 in Hepes buffer with indicated $MgCl_2$ concentrations as determined from Figure 5.5.

$MgCl_2$	K_D [nM]	Hill coefficient
10 mM	487.6 ± 52.7	2.1 ± 0.4
3 mM	421.1 ± 82.5	1.5 ± 0.3
1 mM	> 1000	
0 mM	> 1000	

As can be seen in Figure 5.5 and Table 5.4, TRA binds with an affinity of 488 ± 52.7 nM to Erk2 in its selection buffer (10 mM Hepes, pH 7.4, supplemented with 10 mM $MgCl_2$). The observed K_D value is about 5-times higher than the reported K_D value of TRA´s progenitor, the family II aptamer [210]. This difference might be explained by different protein preparations.

The K_D value did not change when the $MgCl_2$ concentration in Hepes buffer was lowered from 10 to 3 mM (K_D 421.1 ± 82.5 nM). Therefore, the previously observed loss of affinity in PBS buffer was not caused by the lower magnesium concentration (3 mM) used for the binding assay but likely results from the presence of monovalent cations in PBS buffer.

The affinity of TRA for Erk2 in Hepes buffer decreased when the magnesium concentration was lowered to 1 mM or when magnesium was left out (Figure 5.5).

Strikingly, the Hill coefficients of TRA were observed to be higher than 1. This may indicate that more than one molecule binds with positive cooperativeness to Erk2 [319].

Next, the binding of TRA was analyzed for monovalent cation dependence. Thus, filter retention assays in Hepes buffer, supplemented with 10 mM $MgCl_2$, and with the addition of KCl or

NaCl concentrations identical to those present in PBS buffer, were performed (Figure 5.6).

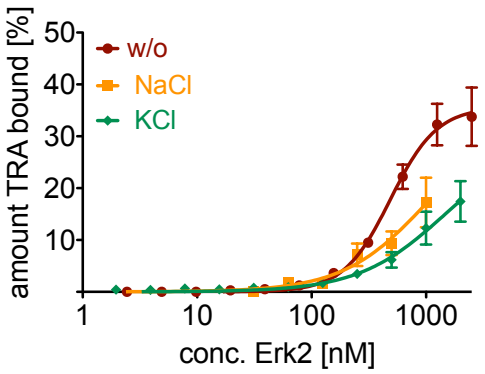

Figure 5.6: K_D value determination of TRA in Hepes buffer supplemented with 10 mM $MgCl_2$ and additional 130 mM NaCl or 2.7 mM KCl. The amount of radioactively labeled TRA bound to inactive Erk2 is plotted against the Erk2 concentration.The binding curve of TRA in the absence of monovalent cations is the same as in Figure 5.5. All experiments were performed at least three times (mean ± SEM). w/o = without additional KCl or NaCl.

Table 5.5: K_D values [nM] and Hill slopes of TRA binding to Erk2 in Hepes buffer, 10 mM $MgCl_2$, and NaCl or KCl as determined from Figure 5.6.

Salt	K_D [nM]	Hill coefficient
w/o	487.6 ± 52.7	2.1 ± 0.4
130 mM NaCl	> 1000	
2.7 mM KCl	> 1000	

w/o: without additional salt

TRA binds with an affinity of 488 ± 52.7 nM to Erk2 in 10 mM Hepes, pH 7.4, supplemented with 10 mM $MgCl_2$ (Figure 5.6, Table 5.5). The addition of either 130 mM NaCl or 2.7 mM KCl dropped the affinity of TRA for Erk2. Hence, TRA seems to be sensitive to the presence of monovalent cations tested (sodium, potassium).

Consequently, it was investigated how the presence of both potassium and sodium ions in PBS buffer affects the binding of TRA to Erk2 (Figure 5.7).

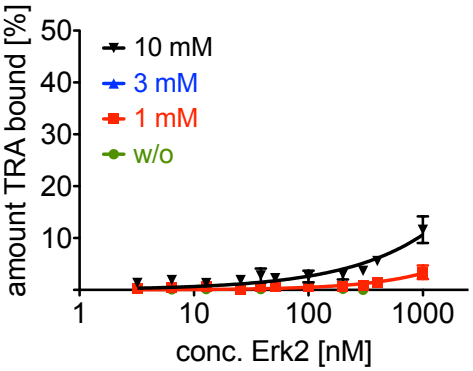

Figure 5.7: Binding assays with TRA in PBS buffer with indicated $MgCl_2$ concentrations. The amount of radioactively labeled TRA bound to inactive Erk2 is plotted against the Erk2 concentration. All experiments were performed at least twice (mean ± SEM). w/o = without additional $MgCl_2$.

Binding assays in PBS buffer further underline TRA´s sensitivity to ionic strength for Erk2 binding (Figure 5.5A, Table 5.4). The addition of 10 mM $MgCl_2$, the magnesium concentration which is identical to the concentration in TRA´s selection buffer (10 mM $MgCl_2$), could not rescue the interaction of TRA and Erk2. When the magnesium concentration was lowered further, no binding of TRA to Erk2 was detected.

Taken together, these data show that the binding of TRA to Erk2 is sensitive to the presence of monovalent cations tested (potassium and sodium). Furthermore, decreasing magnesium ion concentrations below 3 mM also affects the interaction of TRA and Erk2. Since the K^+ ion concentration is about 70-times higher in the cytoplasm and the concentration of free magnesium ions is reported to be approximately 1 mM [3], TRA could likely not be used within cells.

5.2.1.2 K_D value determination of aptamers C3 and C5

As mentioned before, two different selection strategies were performed to identify aptamers that would target Erk2 under more physiologicalyl relevant conditions (Section 3.4.2.5). PBS, supplemented with 3 mM $MgCl_2$, was chosen as the selection buffer. This buffer has been shown in previous experiments to give rise to aptamers that are adaptable to intracellular applications [182, 183].

A reselection of a doped library based on the sequence of the TRA aptamer was performed against **active** Erk2 and yielded the aptamer C5 (Figure 3.15B). To address an epitope that is present in inactive Erk2, a second selection was performed with a completely randomized library against **inactive** Erk2. This SELEX strategy yielded the aptamer C3 (Figure 3.15C).

The active conformation of Erk2 was bound by TRA with 10-fold higher affinity than inactive Erk2 [210]. Since it is very likely that C5 shares these properties, K_D values were determined for both active and inactive Erk2 (Figure 5.8A). In order to identify if C3 preferentially targets the active or inactive conformation of Erk2, filter retention assays were performed with both Erk2 proteins (Figure 5.8B). The K_D values of C3 and C5 were determined in selection buffer (PBS, 3 mM $MgCl_2$).

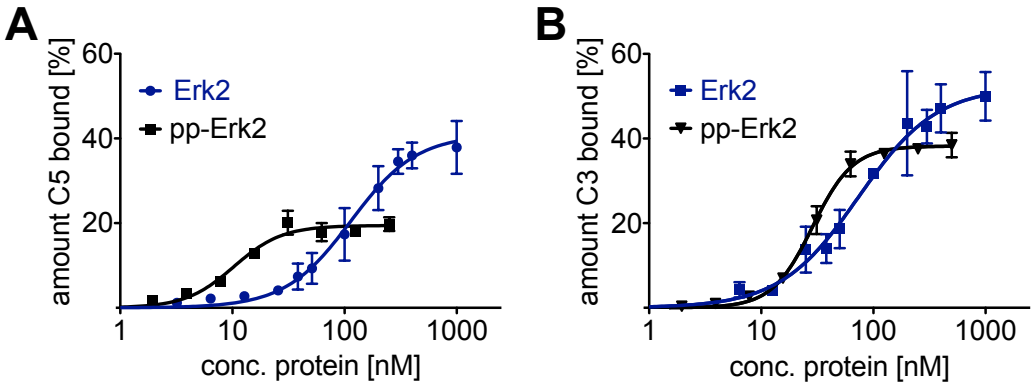

Figure 5.8: K_D value determination of C3 and C5. Binding curves of C5 (A) or C3 (B) for active and inactive Erk2. The amount of radioactively labeled RNA bound is plotted against the concentration of active (pp-Erk2) or inactive Erk2 (Erk2). K_D values are listed in Table 5.6. All experiments were performed in PBS buffer, supplemented with 3 mM $MgCl_2$ (n=2, mean ± SEM).

Table 5.6: K_D values and Hill coefficients (h) of C5 and C3 according to Figure 5.8.

Aptamer	K_D Erk2 [nM]	h Erk2	K_D pp-Erk2 [nM]	h pp-Erk2
C5	113.7 ± 26.1	1.5 ± 0.1	10.3 ± 1.1	2.1 ± 0.4
C3	73 ± 18.2	1.2 ± 0.3	28.6 ± 0.3	2.4 ± 0.3

Erk2: inactive Erk2, pp-Erk2: active Erk2

The results are summarized in Figure 5.8 and Table 5.6 and show that aptamer C5 binds with K_D values of 10.3 ± 1.1 nM to active Erk2 and 113.7 ± 26.1 nM to inactive Erk2, respectively. The 10-fold higher increase in affinity for active Erk2 is in accordance with the selection scheme and likely reflects the importance of the activation status of Erk2 recognitizing C5.

C3 binds with an affinity of 28.6 ± 0.3 nM to active Erk2 and 73.4 ± 18.2 nM to inactive Erk2 (Figure 5.8B, Table 5.6). The similar affinity of C3 for active and inactive Erk2 suggests that C3 targets an epitope that is present in both the active and inactive conformation of Erk2.

Notably, the saturation of the binding curves of C5 and C3 for Erk2 were lower that the saturation of the binding curves for inactive Erk2. These differences might result from distinct protein preparations. Inactive Erk2 was produced in-house whereas active Erk2 was purchased.

The Hill coefficients of C3 and C5 for inactive Erk2 were close to 1 (Table 5.6). This indicates that indeed a single aptamer binds to one Erk2 protein. Strikingly, the Hill coefficients of the aptamers binding curve for active Erk2 shifted above 2. The Hill slopes of the binding curves of C3 and C5 under the tested conditions indicate that more than one aptamer could bind to Erk2. However, this finding needs to be evaluated further because Hill slopes >> 1 may also arise if the protein concentrations used for the binding assays by far exceeds the K_D value [319].

5.2.1.3 Cation dependence of aptamers C3 and C5

The binding of C5´s progenitor TRA was shown to be greatly impaired in the presence of monovalent cations (Section 5.2.1.1). Since the long-term goal of this study was to apply the novel Erk2-binding aptamers C5 and C3 as inhibitors in a cell cultures studies, it was crucial to determine if the aptamers binding to Erk2 could be affected by ionic strength.

Consequently, the dependence of aptamer C3 and C5 on magnesium, sodium, or potassium ions for Erk2 binding was analyzed in distinct buffers. Since the aptamers were selected in PBS buffer, it is obvious that C3 and C5 would tolerate the presence of monovalent cations that are present in PBS buffer (130 mM MaCl, 2.7 mM KCl). Therefore, first it was investigated if binding of C3 and C5 could be sensitive to magnesium ions by supplementing PBS buffer with varying magnesium concentrations Figure 5.9).

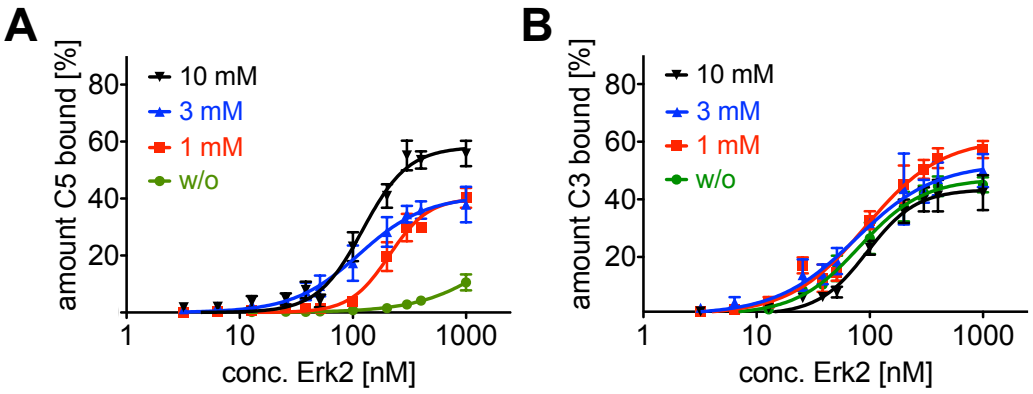

Figure 5.9: Binding assays in PBS buffer with varying $MgCl_2$ concentrations. The amount of radioactively labeled RNA bound to inactive Erk2 is plotted against the Erk2 concentration. Filter retention assays of C5 (A) or C3 (B) binding to Erk2 in PBS buffer supplemented with varying $MgCl_2$ concentrations. K_D values are listed in Table 5.7. Experiments were performed at least three times (mean ± SEM). w/o: without $MgCl_2$.

Table 5.7: K_D values [nM] and Hill coefficients (h) of C5 and C3 binding to Erk2 in PBS buffer with indicated $MgCl_2$ concentrations as determined from Figure 5.9.

$MgCl_2$	K_D C5 [nM]	h C5	K_D C3 [nM]	h C3
10 mM	122.2 ± 13.3	2.2 ± 0.3	94.6 ± 12.2	2.0 ± 0.4
3 mM	113.7 ± 27.2	1.5 ± 0.3	74.7 ± 19.6	1.2 ± 0.3
1 mM	210.1 ± 19	2.5 ± 0.5	91.9 ± 15.6	1.3 ± 0.2
0 mM	n.d.		81.2 ± 11.4	1.5 ± 0.2

n.d.: not detectable

As summarized in Figure 5.9A and Table 5.7, C5 revealed high tolerance to varying magnesium concentrations. The aptamer bound with similar K_D values to Erk2 when 1, 3, or 10 mM $MgCl_2$ were present in PBS buffer. In the absence of magnesium, the interaction of C5 and Erk2 was barely detectable at high Erk2 concentrations. Whether the loss of affinity of TRA or C5 at low magnesium concentration is due to effects on protein or aptamer folding or on the interaction of both needs to be investigated further.

The results of the experiments for C3 are summarized in Figure 5.9B and Table 5.7. Binding tests in PBS buffer with different $MgCl_2$ concentrations revealed that C3 exhibits similar affinities of about 90 nM in PBS buffer regardless of the magnesium concentration (Figure 5.9B). The lack of dependency on Mg^{2+} ions for Erk2-binding in PBS buffer is best reflected in the absence of magnesium. Most notably, C3 was still able to bind to Erk2 without alterations in affinity.

Next, it was evaluated if the aptamers would tolerate the absence of monovalent cations. Thus, binding assays were performed in Hepes buffer (Figure 5.10).

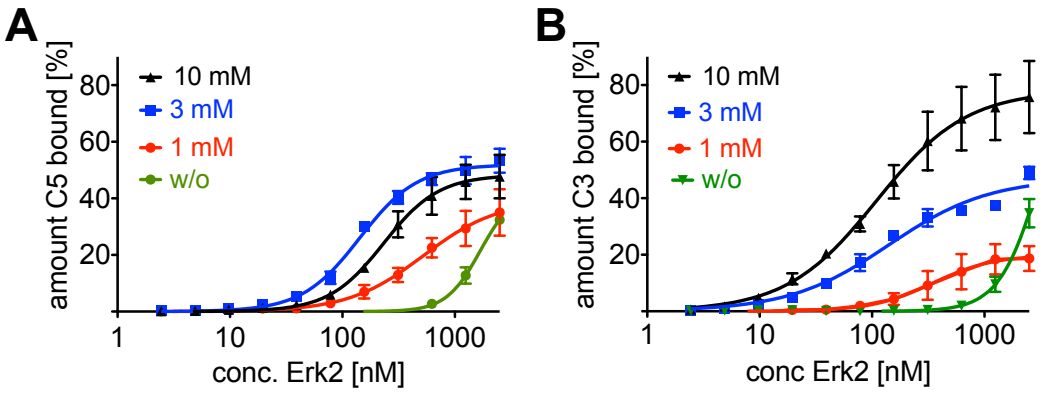

Figure 5.10: Binding assays in Hepes buffer with varying $MgCl_2$ concentrations. The amount of radioactively labeled RNA bound to Erk2 is plotted against the Erk2 concentration. Filter retention assays of C5 (A) or C3 (B) binding to inactive Erk2 in Hepes buffer supplemented with varying $MgCl_2$ concentrations. K_D values are listed in Table 5.8. Experiments were performed at least three times (mean ± SEM). w/o: without additional $MgCl_2$. The experiments shown in A) and B) were performed by D. Minich during a lab rotation.

Table 5.8: K_D values [nM] of C5 and C3 binding to Erk2 in Hepes buffer supplemented with indicated $MgCl_2$ concentrations as determined from Figure 5.10.

$MgCl_2$	K_D C5 [nM]	h C5	K_D C3 [nM]	h C3
10 mM	232.9 ± 29.5	1.8 ± 0.3	109.4 ± 25.3	1.1 ± 0.2
3 mM	142.4 ± 10.6	1.7 ± 0.2	141.7 ± 26.6	1.0 ± 0.1
1 mM	522.4 ± 194.9	1.3 ± 0.3	346 ± 117.9	1.6 ± 0.6
0 mM	> 1000		> 1000	

Figure 5.10A and Table 5.8 show that C5 binds to Erk2 with an affinity of 142.4 ± 10.6 nM in Hepes buffer, supplemented with 3 mM $MgCl_2$. The K_D values of C5 in Hepes buffer and PBS buffer (113.7 ± 27.4) are nearly identical. Moreover, aptamer C5 bound equally well to Erk2 when 3 or 10 mM $MgCl_2$ were present in Hepes buffer. This data indicate that C5 is able to tolerate the absence of monovalent cations (sodium and potassium) in the presence of certain magnesium ion concentrations.

However, the binding of C5 in Hepes buffer (Figure 5.10A, Table 5.8) displays higher constraints to magnesium than the interaction of C5 with Erk2 in PBS buffer (Figure 5.9A). Its K_D value decreased when the magnesium concentration was reduced below 3 mM.

In Hepes buffer, C3 bound with similar affinities in the presence of magnesium concentrations ranging from 3 to 10 mM (Figure 5.10A, Table 5.8). Similar K_D values were observed for PBS buffer (Figure 5.9B). Like C5, the interaction of C3 and Erk2 seems to tolerate the absence of monovalent cations in the presence of magnesium ions. However, the affinity of C3 decreased three-fold when the magnesium concentration was lowered to 1 mM. When magnesium was left out completely, the

affinity of C3 for Erk2 dropped even further. This sensitivity to magnesium ion concentrations was not observed in PBS buffer (Figure 5.9B) and indicates that the interaction of Erk2 and C3 is enhanced in the presence of monovalent cations.

Strikingly, the saturation of the binding curves C3 for Erk2 in Hepes buffer decreased when magnesium concentrations were reduced. This effect might result from distinct RNA preparations used for the assays.

In turn, the binding of C3 or C5 to Erk2 was further analyzed with binding studies in Hepes buffer, supplemented with 10 mM $MgCl_2$, and additional 2.7 mM KCl or 130 mM NaCl as supplied in PBS buffer (Figure 5.11, Table 5.9).

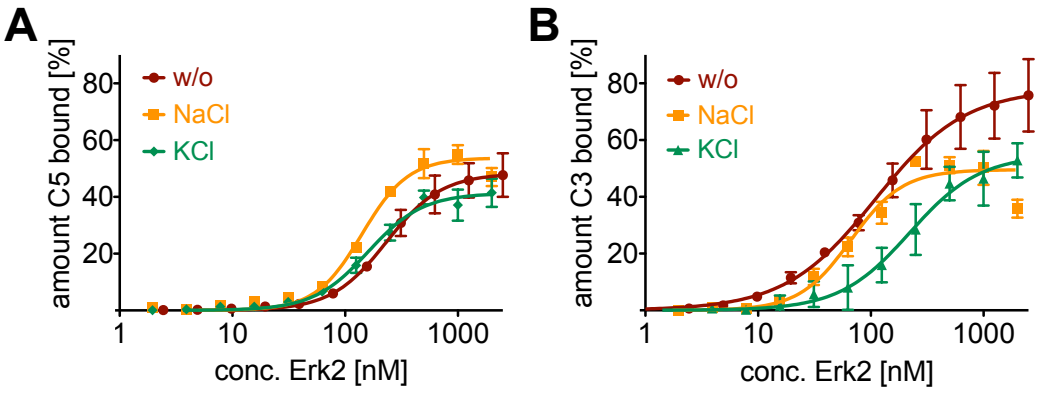

Figure 5.11: Binding assays in Hepes buffer, supplemented supplemented with 10 mM $MgCl_2$ and 2.7 mM KCl or 130 mM NaCl. The amount of radioactively labeled RNA bound to inactive Erk2 is plotted against the Erk2 concentration. Filter retention assays of C5 (A) or C3 (B) binding to inactive Erk2 in Hepes buffer supplemented with 10 mM $MgCl_2$ and 2.7 mM KCl or 130 mM NaCl. K_D values are listed in Table 5.9. Experiments were performed at least three times (mean ± SEM). w/o: without additional KCl or NaCl.

Table 5.9: K_D values [nM] of C5 and C3 binding to Erk2 in Hepes buffer, 10 mM $MgCl_2$, and additional KCl or NaCl as determined from Figure 5.10.

Salts	K_D C5 [nM]	h C5	K_D C3 [nM]	h C3
w/o	232.5 ± 31	1.8 ± 0.3	109.1 ± 23.9	1.1 ± 0.2
130 mM NaCl	140.8 ± 9.7	2.2 ± 0.3	66.6 ± 7.3	1.9 ± 0.3
2.7 mM KCl	159.8 ± 19	1.8 ± 0.3	221.6 ± 65.6	1.4 ± 0.4

w/o: without additional KCl or NaCl

In accordance with the selection scheme, the addition of NaCl or KCl to Hepes buffer did not affect the affinities of C5 or C3 for Erk2 in the presence of magnesium ions (Figure 5.11, Table 5.9).

Taken together, the SELEX strategy in high salt containing PBS buffer has given raise to aptamers that are adaptable to distinct ionic conditions. In summary, both C5 and C3 require monovalent cations and magnesium ions for Erk2 binding. They tolerate varying magnesium concentrations and the absence of monovalent cations under most tested conditions. Aptamer C5 requires at least 1 mM magnesium to bind to Erk2. Its interaction with Erk2 at low magnesium

concentrations is enhanced in the presence of monovalent cations. In contrast, the interaction of C3 and Erk2 seems to be less dependent on cation identity. C3 requires the presence of monovalent cations for Erk2 binding to tolerate the absence of magnesium ions. In the absence of monovalent cations, however, the binding of C3 can only be rescued by higher magnesium concentrations. Hence, the aptamers distinct properties to ionic strength indicates that cations play different roles to the interaction of C3 with Erk2 as compared to C5 and Erk2.

The Hill slopes of the binding curves of C3 and C5 under the tested conditions indicate that more than one aptamer could bind to Erk2. However, this finding needs to be evaluated further because Hill slopes >>1 may also arise if the protein concentrations used for the binding assays by far exceed the K_D value [319].

In the last step, it was investigated if the aptamers tolerance to ionic strength could also be assigned to a buffer system which mimics cytosolic cation concentrations to assess the potential for C3 and C5 for later cellular applications. Therefore, their affinities for Erk2 were determined in a phosphate buffer which mimics cytosolic cation concentrations (ICB: 16 mM KCl, 130 KCl and 1 mM $MgCl_2$, Figure 5.12) [320]. In this buffer, the sodium and potassium concentrations are reversed compared to PBS buffer.

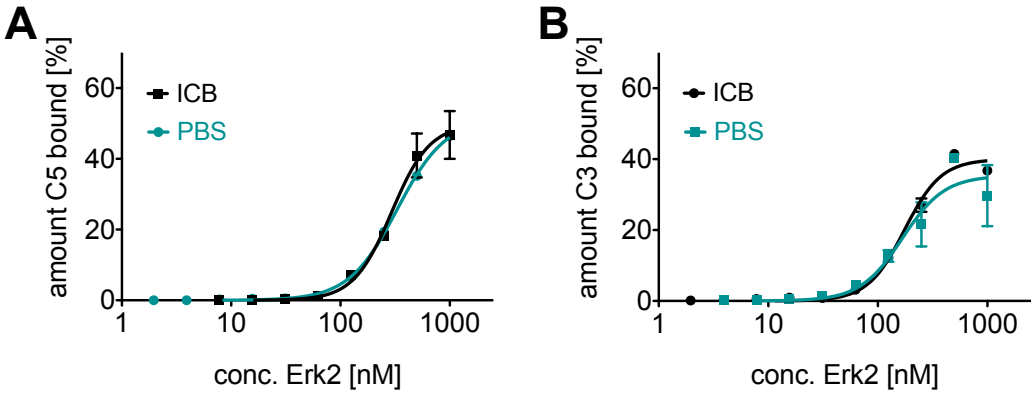

Figure 5.12: Binding assays in a cytosolic phosphate buffer. The amount of radioactively labeled RNA is plotted against the Erk2 concentration. Filter retention assays of C5 (A) or C3 (B) in phosphate buffer which mimics cytosolic cation concentrations (16 mM KCl, 130 KCl and 1 mM $MgCl_2$) or PBS buffer supplemented with 3 mM $MgCl_2$. Experiments were performed once in duplicates (mean ± SEM). ICB: cytosolic cation concentrations, PBS: PBS buffer with 3 mM $MgCl_2$.

Table 5.10: K_D values and Hill coefficients (h) of C5 and C3 according to Figure 5.12.

Buffer	**K_D C5 [nM]**	**h C5**	**K_D C3 [nM]**	**h C3**
ICB	175 ± 9.5	2.6 ± 0.3	167.5 ± 29.5	2.3 ± 0.7
PBS	330 ± 11.5	2 ± 0.1	300 ± 28	2.5 ± 0.5

Remarkably, both C5 and C3 bound with identical affinity to Erk2 in phosphate buffer with cytoplasmic-based cation concentrations and selection buffer (Figure 5.12, Table 5.10). Thus, the aptamers represent promising candidates for cellular assays.

5.2.2 Validation of non-binding point mutants of C5

Once determined, the secondary structure of an aptamer can be used to design a negative control sequence in the form of a non-binding point mutant. Since the precise secondary structure of aptamer C5 has not been determined yet, structural and mutational analysis based on TRA were utilized to identify non-binding point mutants of C5.

Seiwert *et al* performed extensive mutational analysis on TRA and identified point mutations that either reduced or diminished its inhibitory activity [210]. By slightly changing the sequence of one strand in the putative stem of TRA (mutation A1, Figure 5.13A), they demonstrated a complete loss of TRAs inhibitory activity. A mutation in the lower bulge of TRA was also shown to strongly affect TRA´s inhibitory activity (mutation B2, Figure 5.13A).

In C5, these nucleotides are conserved and can be found at the same position as in TRA, highlighting their importance for Erk2 binding (Figure 5.13B). Therefore, it was very likely that similar point mutations would affect the binding of aptamer C5. Thus, analog point mutants of aptamer C5 were designed. These point mutants, termed "C5 A1" and "C5 B2", contain two point mutations in either the stem or the lower bulge region of aptamer C5. The binding of the C5 point mutants to Erk2 was analyzed in selection buffer (PBS, 3 mM $MgCl_2$).

As can be seen in Figure 5.13B, no interaction of point mutants C5 A1 or C5 B2 with Erk2 was detected. Hence, this data indicates that similar structural properties might be shared by aptamer C5 and its parental aptamer TRA. Mutations at the same positions reduced both aptamers affinity or inhibitory properties.

The point mutants or a scrambled control RNA of C5 ("C5sc") were used as negative control sequences for C5. A scrambled control sequence was used as a negative control for C3, too. None of these sequences revealed any affinity for Erk2 (Section 10.1).

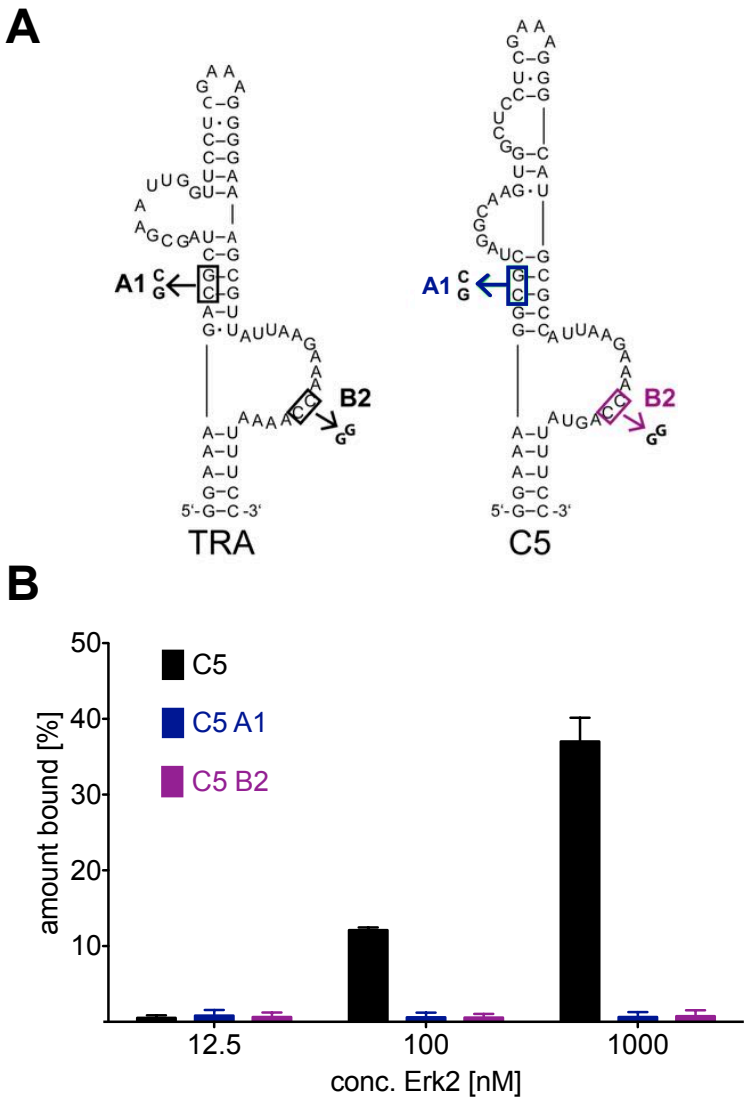

Figure 5.13: Validation of non-binding point mutants of aptamer C5. A) Proposed secondary structures of the RNA aptamers TRA and C5. Point mutations are annotated. B) Binding of aptamer C5 and point mutants C5 A1 and C5 B2 to inactive Erk2 in filter retention assays. Experiments were performed twice (mean ± SEM).

5.2.3 Specificity profile

Low molecular weight kinase inhibitors often interact with multiple members of a protein kinase family or target kinases from distinct subfamilies [91, 321]. The availability of more specific protein kinase inhibitors would be extremely useful in helping to delineate the physiological roles of these enzymes [87]. However, the identification of truly selective inhibitors has remained challenging since protein kinases represent a large family of approximately 520 enzymes that share high homology within their active site [7].

To investigate if the aptamers C3 and C5 interact with distinct members of the MAP kinase family, filter retention assays were performed with Erk1 (Erk1/2 MAPK family), p38α (p38 MAPK family), and JNK2α (JNK/SAPK MAPK family).

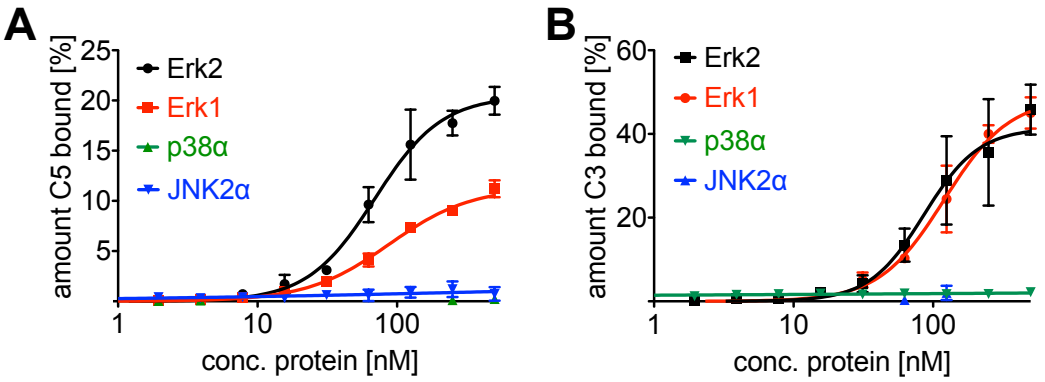

Figure 5.14: Specificity tests with different MAP kinases. Filter retention assays of A) C5 or B) C3 binding to different members of the Erk1/2, p38 or JNK MAP kinase families in PBS buffer, supplemented with 3 mM $MgCl_2$. The amount of radioactively labeled RNA is plotted against the protein concentration. K_D values are listed in Table 5.11. Experiments were performed at least twice (mean ± SEM). K_D values are listed in Table 5.11. Erk: extracellular signal-regulated kinase, JNK: c-Jun N-terminal kinases.

Table 5.11: K_D values and Hill coefficients (h) determined from Figure 5.14

MAPK	K_D C5 [nM]	h C5	K_D C3 [nM]	h C3
Erk2	69.3 ± 6.8	1.8 ± 0.3	86.1 ± 15.2	2.2 ± 0.7
Erk1	97.6 ± 8.3	1.5 ± 0.2	120.3 ± 12.6	1.9 ± 0.3
p38α	n.d.		n.d.	
JNK2α	n.d	.	n.d.	

n.d.: not detectable, MAPK: MAP kinase Erk: extracellular signal-regulated kinase, JNK: c-Jun N-terminal kinases.

Both aptamers demonstrated a remarkable ability to discriminate between different structurally similar MAP kinases (Figure 5.14). C3 and C5 revealed identical affinities for Erk2 and Erk1 (K_D values are listed in Table 5.11). This is not surprising because Erk1 and Erk2 share about 84% sequence identity (Figure 5.15) [257]. However, the saturation of binding curves of C5 for Erk1 and Erk2 differed by two-fold. This likely results from different protein preparations.

More importantly, no binding of C3 or C5 to p38α or JNK2α was detected which argues for a high degree of specificity (Figure 5.14). p38α and JNK2α MAP kinases share about 45% sequence

identity with Erk1/2 (Figure 5.15).

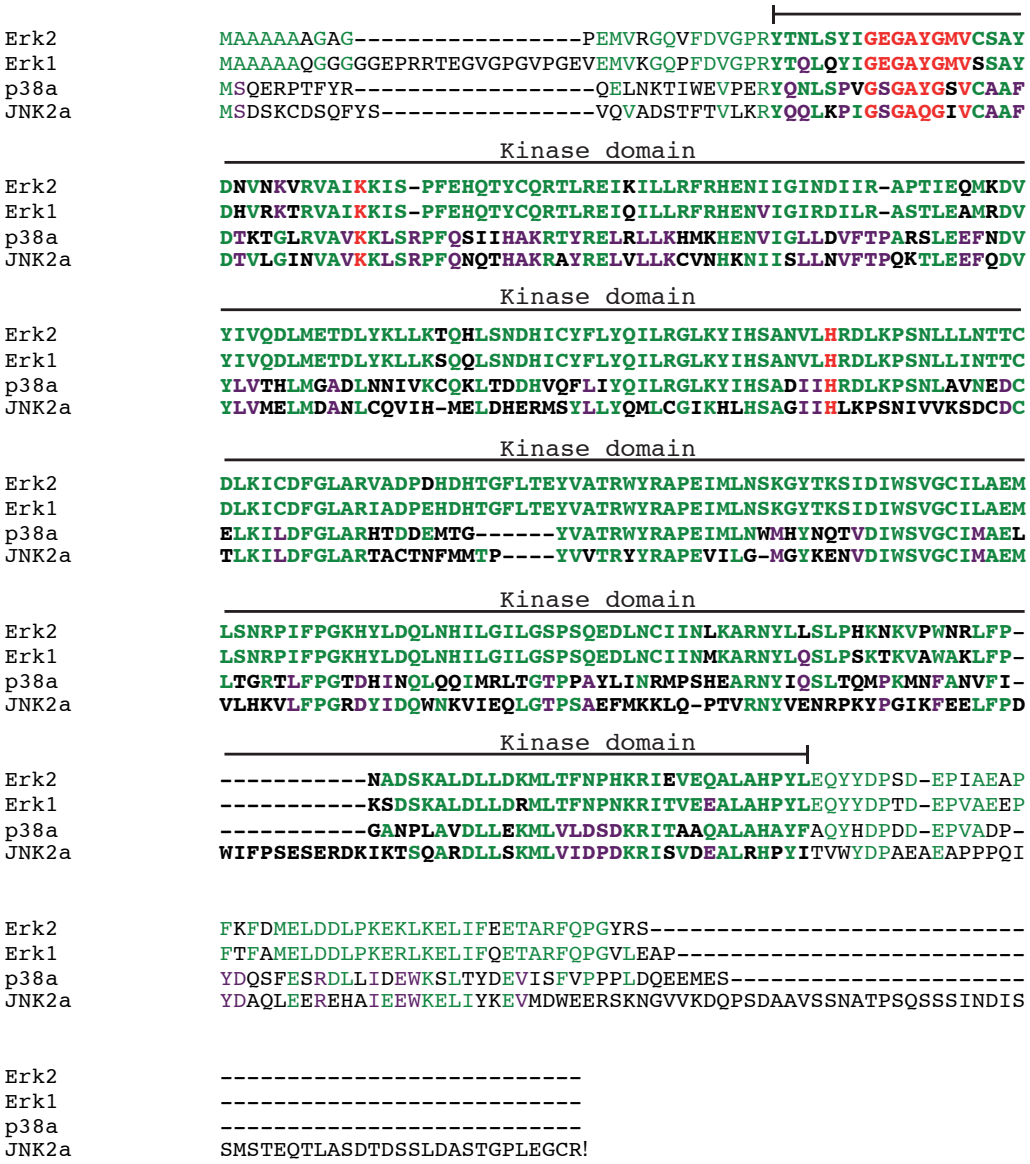

Figure 5.15: Amino acid sequences of Erk2, Erk1, p38α, and JNK2α. Identical amino acids are marked in green or purple. Conserved residues for ATP-binding are shown in red.

A further important point that was clearly shown in studies with small molecule kinase inhibitors was the fact that the specificity of a protein kinase inhibitor cannot be gauged simply by comparing its effects on the protein kinases to which it is most closely related [87]. For some kinase inhibitors, impressive selectivity against a panel of closely related kinases can suggest a high degree of specificity against the kinome [322, 323], whereas for other kinase inhibitors, specificity within a kinase subfamily does not necessarily predict overall selectivity [91]. Therefore, the specificity tests of the aptamers were extended towards other kinases belonging to distinct kinase groups as described by Manning *et al* [7].

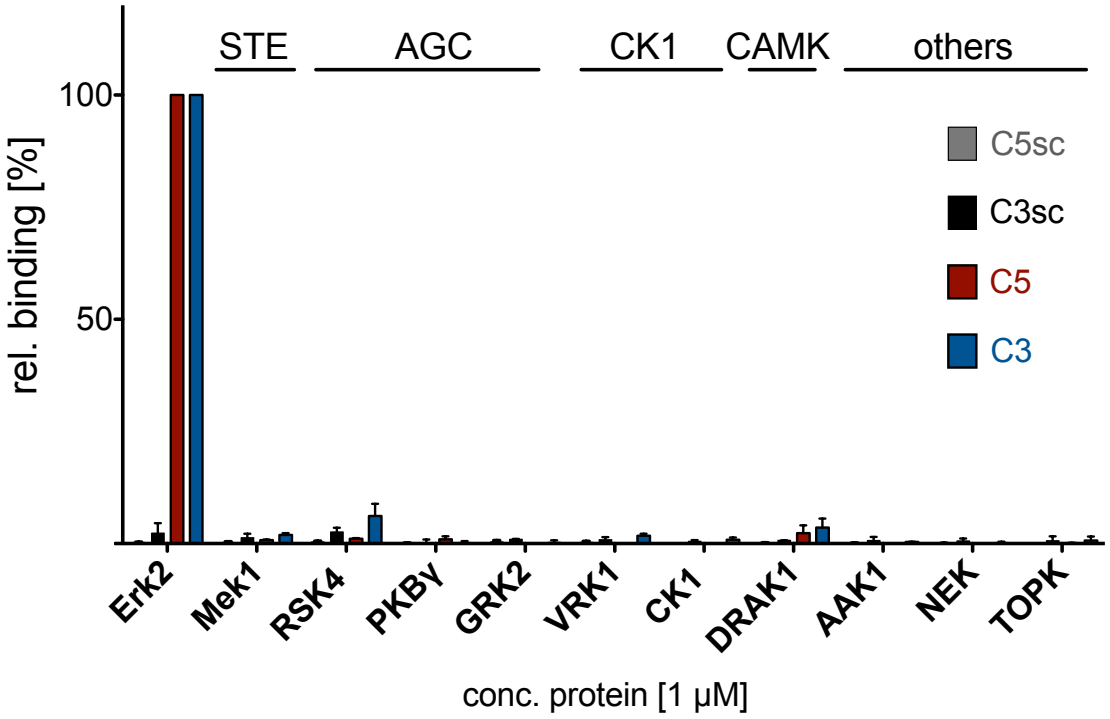

Figure 5.16: Specificity tests with a panel of 10 kinases belonging to distinct groups. Filter retention assay of C3 or C5 binding to Erk2 and distinct kinases belonging to different kinase superfamilies as described by Manning *et al* [7]. The amount of radioactively labeled RNA bound to inactive Erk2 was set to 100%. The amount of bound radioactively labeled RNA was normalized onto the amount of radioactively labeled C3 or C5 bound to Erk2. Assays were performed at least twice (mean ± SEM) in PBS buffer, supplemented with 3 mM $MgCl_2$. Erk2: extracellular signal-regulated kinase 2, MKK1: Mitogen-activated protein kinase kinase 1, RSK2: 90 kDa ribosomal S6 kinase, PKBγ: protein kinase Bγ, GRK2: G protein-coupled receptor kinase 2, VRK1: Vaccina-related kinase 1, CK1: casein kinase 1, DRAK1: DAP kinase-related apoptosis-inducing protein kinase 1, AAK1: AP2 associated protein kinase 1, NEK1: NimA related kinase 1, TOPK: Lymphokine-activated killer T-cell-originated protein kinase.

The results of these assays are summarized in Figure 5.16 and demonstrate that neither C3 nor C5 interacted with any other investigated kinases at concentrations 10-fold above the determined K_D-value with which Erk2 is bound. Taken together, these data indicate that aptamers C3 and C5 may be highly specific for Erk1/2 against the remainder of the kinome.

5.2.4 Investigation of the modes of action of C3 and C5

Subsequently, binding and functional assays were performed to assess the potential of the aptamers C3 and C5 as research tools.

5.2.4.1 ATP competition assays

The ancestor of C5, aptamer TRA, was described to compete with ATP for Erk2 binding [210]. Consequently, it was investigated if binding of C5 could be affected by ATP, too. Therefore, the binding of radioactively labeled C5 bound to 250 nM inactive Erk2 was measured in the presence of increasing concentrations of ATP and analyzed by filter retention analysis. UTP was used as negative control.

The equilibrium dissociation constant (Ki) of the complex was quantified by measuring the competition of ATP or UTP for C5 binding. To estimate the reliability of the Ki calculation, the 95 % confidence intervals (CI) are given. Confidence intervals indicate the concentration range that contains the true mean of the population with a likelihood of 95 %.

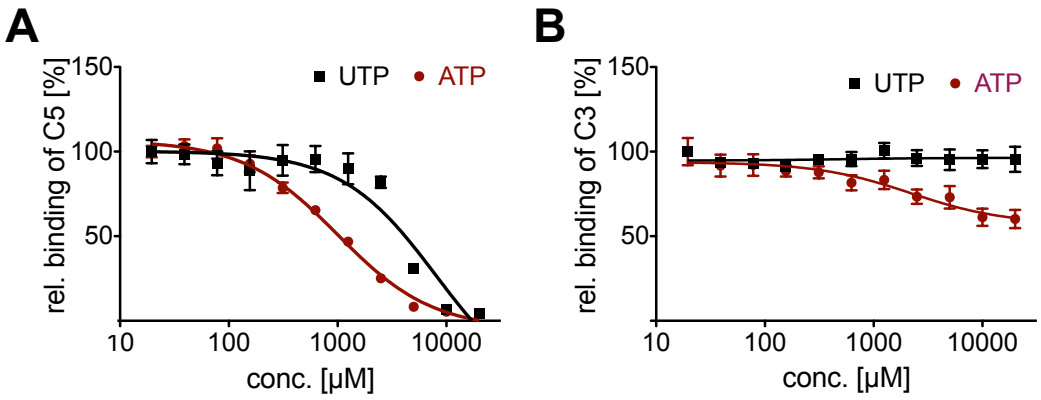

Figure 5.17: C5 competes with ATP for binding to Erk2. Filter retention analysis of radioactively labeled C5 (A) or C3 (B) binding to inactive Erk2 in the presence of 0 - 10,000 μM ATP or UTP in PBS buffer, supplemented with 3 mM $MgCl_2$. The amount of radioactively labeled RNA bound to inactive Erk2 without ATP was set to 100% (n = 4, mean ± SEM).

ATP strongly competed with the binding of aptamer C5 in a concentration dependent manner with an Ki of 980 μM (CI 753.6 to 1295, Figure 5.17A). In accordance with data from the literature, the determined Ki value lies in the same range as the K_D value of Erk2 for ATP (700 - 1600 μM) [245]. About 10 times higher concentrations of UTP also induced a reduction of C5 binding to Erk2, most likely through unspecific interactions with the ATP-binding site of Erk2 or the RNA itself. The Ki value of UTP is 7900 μM. However, a CI ranging from 2444 to 25545 indicates that this value is not accurate.

In order to find out if aptamer C3 also interferes with ATP for binding to Erk2, similar competitive binding experiments were performed. These experiments demonstrated that the binding of aptamer C3 to Erk2 is also affected by ATP (Figure 5.17B). In contrast to C5, a complete competition of the binding of aptamer C3 could not be monitored.

To validate that complete competition of C3 can indeed be observed in this experimental setup, the binding of radioactively labeled C3 RNA was analyzed in the presence of increasing concentration of unlabeled C3 or control RNA (Section 10.2). Complete reduction of C3 binding was observed by increasing concentrations of C3 RNA but not with control RNA.

This data indicates that the observed reduction in binding of C3 (Figure 5.17B) might result from electrostatic interactions between ATP and C3. Additionally, ATP could also affect C3 binding indirectly via an allosteric mechanism.

5.2.4.2 Erk2 activity assays

Aptamers that target the ATP-binding site were described to interfere with kinase activity [209, 210, 324]. In the next step, the aptamers impact on Erk2 kinase activity was evaluated. To achieve this, 60 nM active Erk2 was incubated with substrate proteins and increasing concentrations of C3, C5, control RNA or the commercially available ATP-competitive inhibitor FR180204. Erk2 activity was measured by transfer of γ-^{32}P from ATP to the artificial substrate protein myelin basic protein (MBP, 10 μM, Figure 5.18A,B).

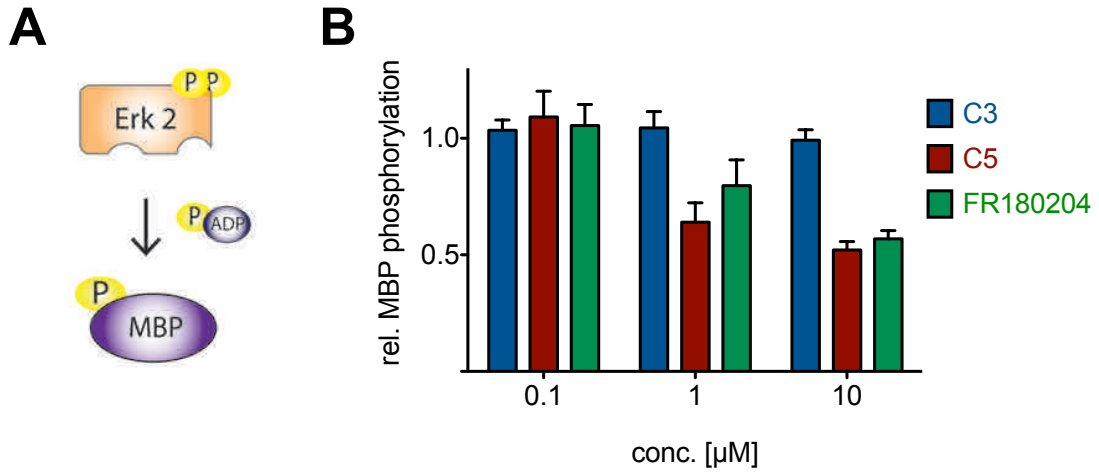

Figure 5.18: Erk2 activity assays. A) Schematic representation of the Erk2 activity assay. Erk2 is incubated with ATP and myelin basic protein as target protein. Inhibition of Erk2 activity results in a decrease in substrate phosphorylation. B) Erk2 activity assays with MBP as substrate. Data were normalized to the same concentration of control RNA. MBP assays were performed four times (mean ± SEM). MBP: Myelin basic protein, ADP+P: adenosine triphosphate (ATP).

Figure 5.18B shows that aptamer C5 inhibits Erk2 activity to a similar extent as the ATP-competitive inhibitor FR180204 [310]. However, the concentration of FR180204 needed to inhibit Erk2 activity in the kinase assay was 10 times higher than its reported IC_{50} value of 510 nM [325]. This difference likely results from lower ATP concentrations that were utilized by Ohori and co-workers (2.5μM in [325] vs. 100 μM in this assay).

Aptamer C3, on the other hand, did not show any inhibitory activity towards Erk2.

MBP was used as substrate for Erk2 during most of the kinase assays. However, all nucleic acids showed high background binding to MBP (Section 10.3.1). Most likely, this reflects MPB´s ability to sequester RNA through nonspecific electrostatic interactions due to its high isoelectric point (pI) of 11 [210].

In order to validate that the inhibition of substrate phosphorylation is solely assigned to direct inhibition of Erk2 by the aptamers, a GST-Elk1 fusion protein (1 μM) was used as a substrate for Erk2 (Figure 10.3). The fusion protein contains amino acids 307–428 of Elk1, which is a natural substrate for Erk2 [326]. No background interaction between GST-Elk1 and any RNA was observed (Section 10.3.1).

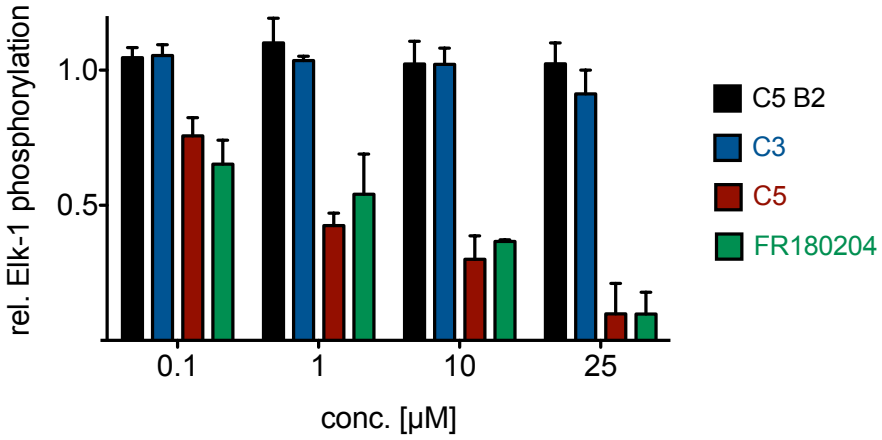

Figure 5.19: Erk2 activity assays. Erk2 activity assays with Elk-1 as substrate. Data were normalized to samples without RNA. Kinase assays were performed four times (mean ± SEM).

By using Elk1 as the substrate for Erk2 in the kinase assays, similar results were obtained as when MBP was used as substrate (Figure 5.19). Both aptamer C5 and FR180204 inhibited Erk2 activity. Aptamer C3, on the other hand, did not reveal any impact on kinase activity, even at concentrations of 25 μM.

The evidence given in this section demonstrate that aptamer C5 targets Erk2 in a similar mode of action as its ancestor TRA. C5 prevented ATP from binding to Erk2 and inhibited Erk2 activity. In summary, these data indicate that C5 may target the active site of Erk2. Aptamer C3 associated with Erk2 in the presence of ATP and did not have any impact on Erk2 kinase activity. Hence, it seems to recognize a different epitope on the kinase structure.

5.2.4.3 The putative binding site of C3 comprises the MAP kinase insert of Erk2

After having shown that C3 likely does not target the active site of Erk2, it was investigated if the putative binding site of the aptamer comprises another functional domain of Erk2 (Figure 5.20A). Erk2 contains several docking domains that have been shown to mediate the interaction with its substrate proteins, activating kinases and inactivating phosphatases [245].

One of these domains is the so-called "D-site recruitment site" (DRS). The DRS is located opposite to the catalytic cleft and consists of several negatively charged residues (Asp 316/319) and a hydrophobic groove [245].

Another functional domain is the MAP kinase insert, which is located in close proximity to the activation lip. The MAP kinase insert is a 31-amino acid insertion that can only be found in MAP kinases and cyclin dependent kinases. Its sequence is unique for one subfamily and provides additional functional specificity [245].

To elucidate whether the DRS or MAP kinase insert region are involved in mediating the binding of C3 or C5 to Erk2, the impact of Erk2 point mutations D319N (DRS) [327], or N236K, Y261N, and S264P42 (adjacent to or located within the MAP kinase insert) [328] were quantitatively analyzed on the aptamers binding with filter retention assays (Figure 5.20). Prior to any experiment, the purity of the recombinant proteins was determined to be >90% by SDS-PAGE analysis and Coomassie staining (Section 10.4).

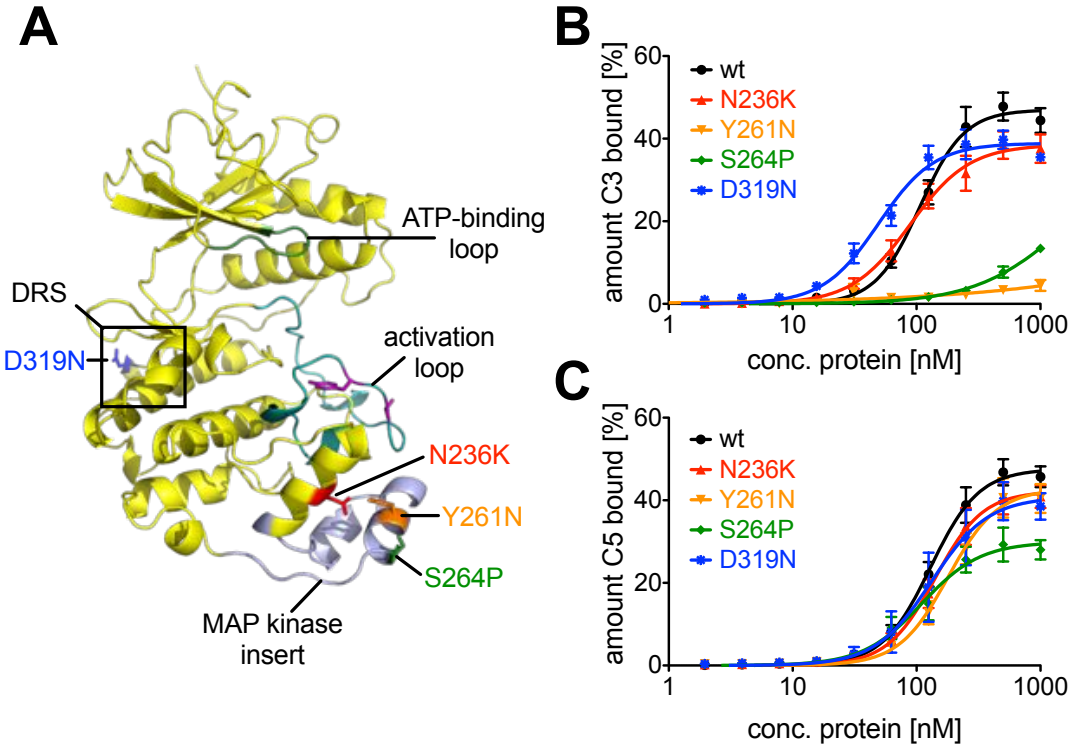

Figure 5.20: Aptamer C3 recognizes the MAP kinase insert of Erk2. A) Overall structure of inactive Erk2 (PDB 1ERK) depicted as cartoon ribbon. The ATP-binding loop, the activation loop and the MAP kinase insert region are shown in green, cyan and light purple, respectively. Mutated amino acids tested for aptamer binding are marked and colored. B) In this filter retention assay, the amount of radioactively labeled C3 RNA bound is plotted against the protein concentration. C) Binding of C5 to wildtype Erk2 ("wt") and Erk2 point mutants. K_D values are listed in Table 5.12. Data in B,C represent at least three independent measurements (mean ± SEM). Experiments were performed in selection buffer (PBS, 3 mM $MgCl_2$).

Table 5.12: K_D values and Hill coefficients (h) determined from Figure 5.20

Protein	K_D C5 [nM]	h C5	K_D C3 [nM]	h C3
wild-type	129.7 ± 9.4	2.2 ± 0.3	106.4 ± 7.5	2.4 ± 0.3
N236K	140.8 ± 13	2.2 ± 0.4	89.2 ± 10.4	1.8 ± 0.3
Y261N	179.4 ± 18.5	2.2 ± 0.4	>1000	
S264P	109.9 ± 15.4	1.8 ± 0.4	n.d.	
D319N	132.2 ±25.7	1.9 ± 0.6	49.4 ± 4.1	1.9 ± 0.3

n.d.: not detectable

As shown in Figure 5.20B and Table 5.12, the Erk2 DRS mutant D319N interacted with aptamer C3 with the same affinity as Erk2 wild-type protein, indicating that the DRS is mostly not involved in the Erk2-recognition by C3.

The Erk2 point mutation N236K is located adjacent to the MAP kinase insert region. A mutation at position N236 did not affect the binding of C3 at all (Figure 5.20B, Table 5.12). In contrast, the MAP kinase insert mutant S264P exhibited dramatically decreased interactions with C3 and the mutant Y261N completely failed to interact with C3 (Figure 5.20B, Table 5.12). Thus, the MAP kinase insert seems to be essential in the interaction of aptamer C3 and Erk2.

These binding experiments further support the notion that aptamer C3 recognizes a different epitope on the kinase structure than the ATP-competitive aptamer C5. Point mutations in the DRS or MAP kinase insert of Erk2 did not change the affinity of C5 to Erk2 (Figure 5.20BC, Table 5.12). This provides additional evidence that the binding site of C5 comprises the active site of Erk2.

5.2.4.4 Erk2 activation assays

The MAP kinase insert was described to contribute to diverse kinase-dependent and -independent functions of Erk2 [329]. However, most of these studies used overexpression or knockdown strategies. A domain-specific inhibitor, targeting only the MAP kinase insert region, would be invaluable as tool to study the precise function of this domain in cellular processes. At present, no small molecule inhibitor for the MAP kinase insert of Erk2 is available.

The MAP kinase insert region has been connected to the activation of Erk2 by its upstream kinase Mek1 [295]. Mek1 and the closely related kinase Mek2 are dual-specific kinases that phosphorylate a tyrosine (Y187) and a threonine (T185) residue in the activation loop of Erk1 or Erk2 [259, 330]. These phosphorylation events then induce a conformational change upon which Erk gains its full catalytic activity [290, 331].

To elucidate the potential of C3 as a domain-specific inhibitor, its impact on Erk2 activation and consecutive substrate phosphorylation was analyzed in an activation-based kinase assay (Figure 5.21A). For this assay, a constitutively active mutant of Mek1, named Mek1 G7B [332], was employed as the Erk2 activator and MBP as the substrate protein. By performing the kinase assay in the presence of γ-^{32}P-ATP, the impact of C3 and C5 on Erk2 activation and substrate phosphorylation could be monitored by γ -^{32}P incorporation into Erk2 and MBP. Subsequently, incorporation ofγ-^{32}P into Erk2 and MBP was quantified by SDS-PAGE gel analysis and autoradiography. For this kinase assay, 1 μM Mek1 G7B, 1 μM Erk2, and 10 μM MBP were used.

At concentrations used for this assay, C3 and C5 showed background binding to both MBP and Mek1 G7B (Section 10.3.1), but did not target Mek1 G7B activity directly (Section 10.3.2). Hence, any observed effects are likely not due to unspecific effects and reflect inhibited Erk2 kinase activity after impaired Erk2 activation.

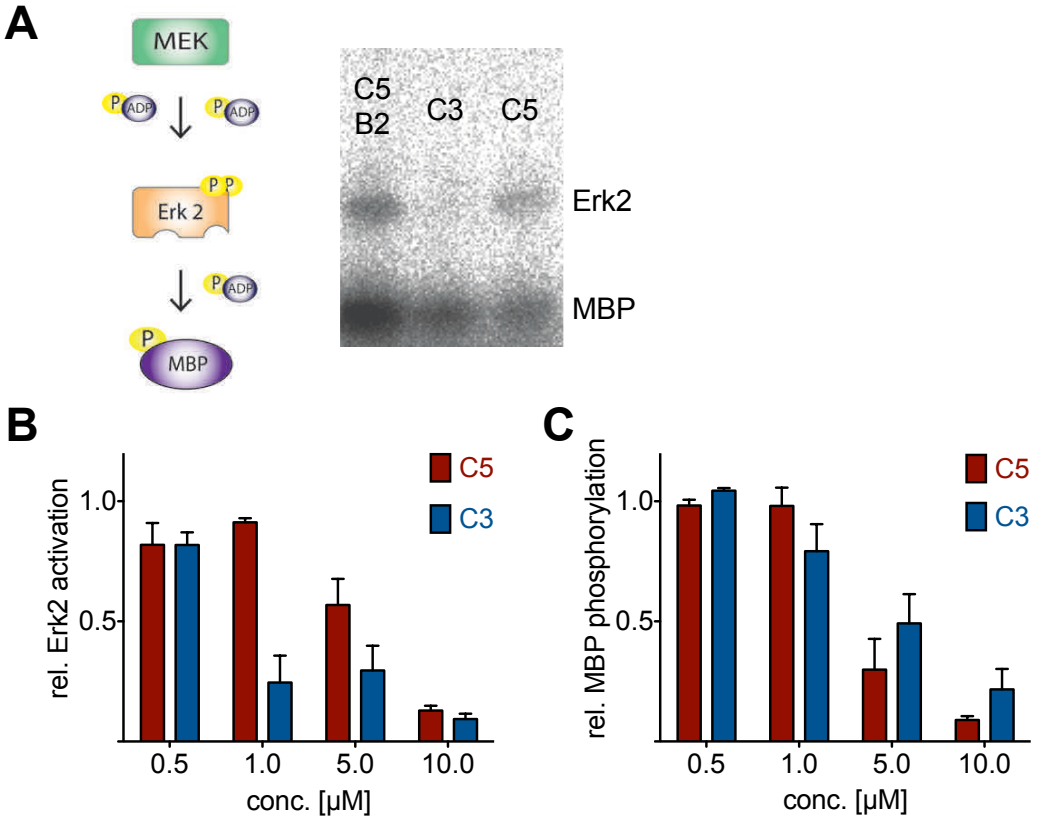

Figure 5.21: Erk2 activation assay. A) Schematic representation and autoradiography of a representative Erk2 activation assay. Incorporation of γ-^{32}P into Erk2 and MBP was monitored after addition of 5 μM RNA. A constitutively active Mek1 (Mek1 G7B) was employed as the Erk2 activator and MBP was used as the substrate. B) Erk2 activation quantified from the phosphorylation of Erk2. C) Erk2 activity quantified from the phosphorylation of MBP. Data were normalized onto control RNA. Experiments were performed at twice (mean ± SEM). MBP: Myelin basic protein, ADP+P: adenosine triphosphate (ATP).

The addition of increasing amounts of C3 resulted in strong inhibition of Erk2 phosphorylation and, thus, activation (Figure 5.21B). At a concentration of 1 μM, which reflects 10 times its K_D value for Erk2, aptamer C3 inhibited Erk2 activation completely. Furthermore, C3 reduced Erk2 substrate phosphorylation (Figure 5.21 C), albeit at elevated concentrations (Figure 5.21C). Hence, the inhibition of substrate phosphorylation likely reflects inhibited Erk2 kinase activity after impaired Erk2 activation.

Adding increasing concentrations of the ATP-competitive aptamer C5 also resulted in the inhibition of Erk2 activation. It required 10 μM C5 to completely inhibit the activation of Erk2 by Mek1 (Figure 5.21B). Moreover, C5 reduced Erk2 substrate phosphorylation (Figure 5.21C). It was observed that higher concentrations of C5 were needed to inhibit Erk2 activity than in the Erk2 activity assay (Section 5.2.4.2). This difference was likely caused by distinct kinase concentrations that were utilized (Erk2 activity assay: 60 nM Erk2; Erk2 activation assay: 1000 nM Erk2).

5.2.5 Summary

Taken together, the data presented in this section imply that the two aptamers bind to different sites on Erk2 and exhibit different modes of action in respect to kinase activity disturbance. Aptamer C5 recognizes Erk2 in an ATP-dependent manner and directly affects Erk2 kinase activity.

The putative binding site of C3 comprises the MAP kinase insert of Erk2. In contrast to C5, aptamer C3 does not target Erk2 activity itself. Instead, C3 demonstrated the ability to inhibit Erk2 kinase activity in an ATP- and substrate independent manner. This implicates that C3 could provide a valuable tool to study the function of the MAP kinase insert.

Both aptamers represent promising tools for the functional interference of Erk2 activity inside cells. Therefore, their effect on intracellular Erk1/2 MAP kinase signaling was investigated next.

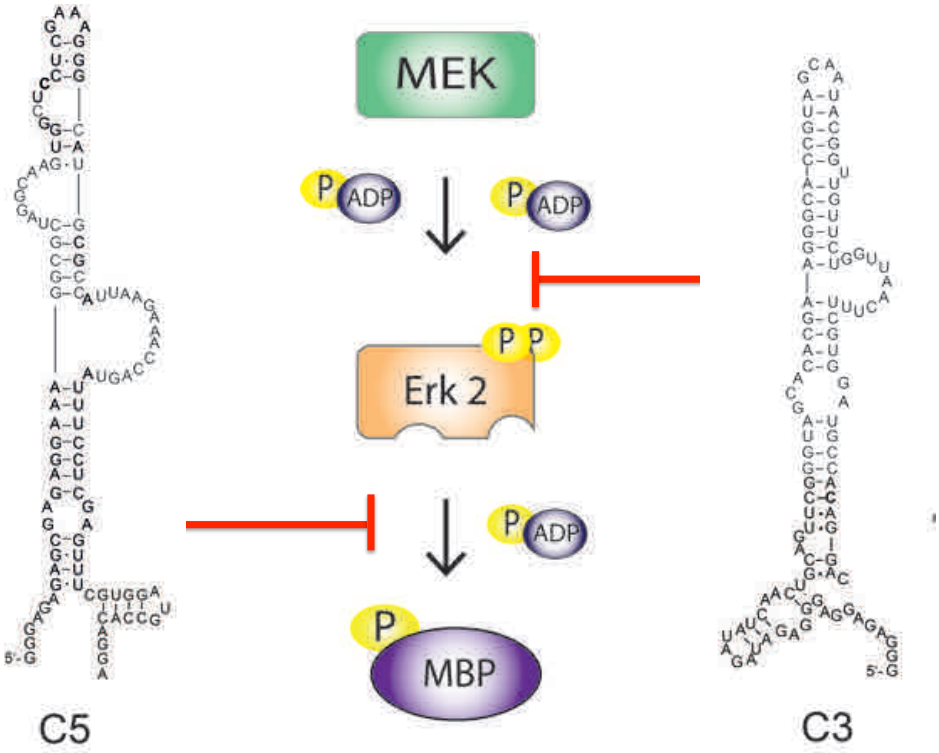

Figure 5.22: C3 and C5 exhibit different modes of action. Schematic representation of the different modes of action of C3 and C5.

5.3 Investigation of RNA aptamers as intracellular protein kinase inhibitors

Several lines of evidence support the conclusion that aptamers C3 and C5 might be applicable as Erk1/2 inhibitors in a cellular environment.
First, they bound to Erk2 under cytosolic ion conditions (Section 5.2.1.3). Second, C3 and C5 revealed remarkable specificity for Erk1/2 MAP kinases (Section 5.2.3). And lastly, C3 and C5 were able to interfere with distinct Erk2 functions *in vitro* (Section 5.2.4).

The following sections describe the elucidation of the aptamers putative inhibitory effects on Erk1/2 MAP kinase signaling. Therefore, the use of expression vectors and transfection or microinjection of *in vitro* transcribed RNA, was investigated to facilitate the delivery of the aptamers or control sequences into the cells.

5.3.1 C3 and C5 recognize endogenous Erk1/2

The selections of aptamers C3 and C5 were performed against recombinant Erk2 protein of rat origin [314]. Human and rat Erk2 differ in only two amino acids. Nevertheless, it had to be validated that C3 and C5 are able to interact with endogenous human Erk1/2 before applying them as inhibitors inside cells. Therefore, aptamer-protein pull-down assays were performed.

The scheme in Figure 5.23 explains the principle of this experiment. Briefly, biotinylated variants of C3, C5, or control RNA were coupled to Streptavidin-coated magnetic beads. These matrices were incubated with protein preparations from H460 cells. H460 cells are a human lung adeno carcinoma - derived cell line. After incubation, the affinity matrices were washed and bound proteins were detected by SDS-PAGE and immunoblot analysis.

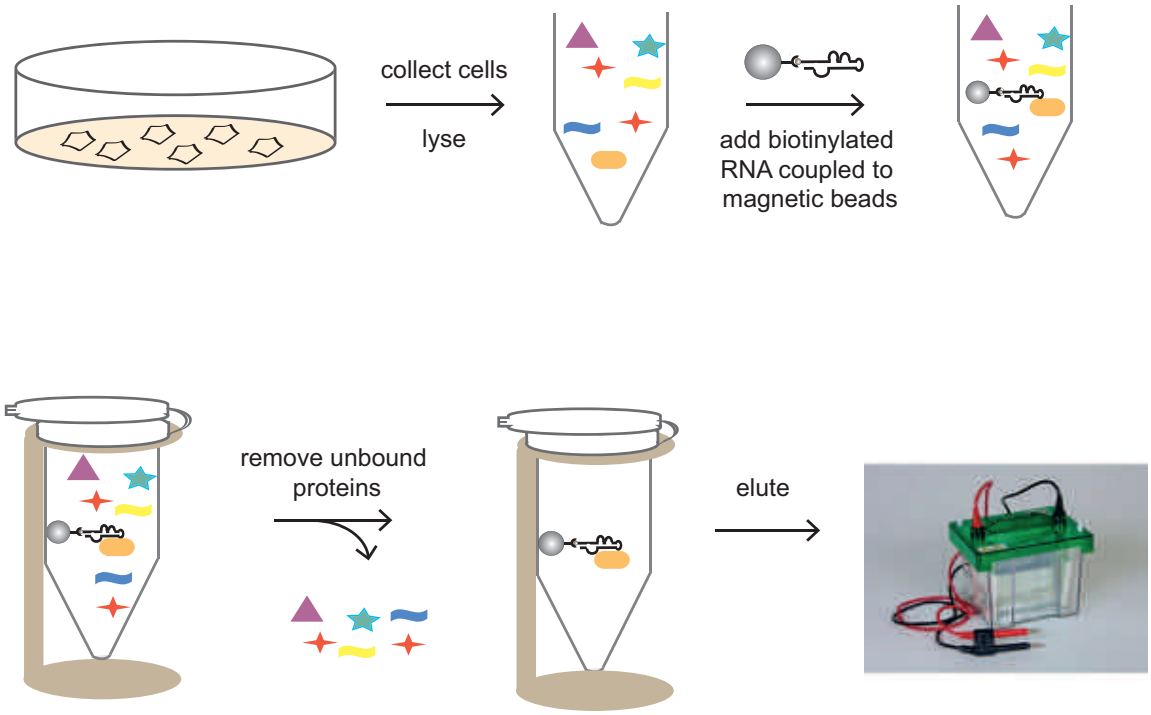

Figure 5.23: Pulldown Assay. Schematic representation of the RNA-protein pulldown assay. Picture of the SDS-PAGE chamber was taken from [333].

The interaction of C3 and C5 with endogenous proteins was elucidated for Erk1/2, p38α and JNK1α/β MAP kinases. The results are summarized in Figure 5.24 and show that both C3 and C5 interact with endogenous Erk1/2. Faint bands were observed for unloaded beads or control sequences. These bands might result from unspecifically bound Erk1/2 that were co-precipitated from cell lysate and subsequently detected with Erk1/2-specific antibodies.

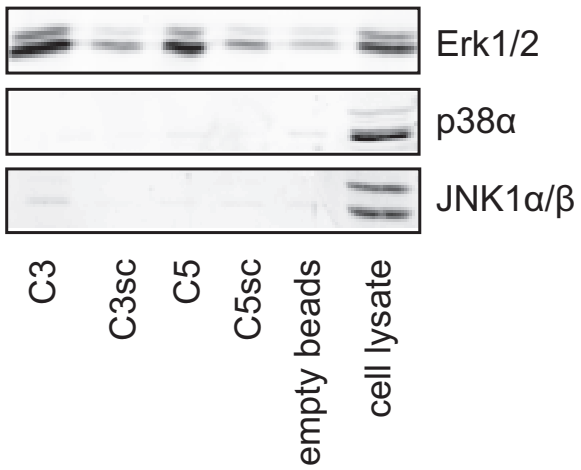

Figure 5.24: C3 and C5 interact with endogenous Erk1/2. Endogenous Erk1/2 were detected when C3 or C5 were used as an affinity matrix. Only background binding of Erk1/2 to control RNA and empty beads was observed. No binding of p38 or JNK1 to C3, C5 or controls were detected.

Moreover, no binding of C3 or C5 to endogenous p38α or JNK1α/β MAPK was detected. These experiments demonstrate that the derivation of aptamers with the potential to interact in a highly specific manner with endogenous proteins is feasible.

5.3.2 Intracellular expression of C3 and C5

The application of functional RNA intramers can be mediated through two types of molecules: *in vitro* transcribed aptamers or aptamer expression plasmids (Section 3.3.3). Plasmid expression is probably the most common approach to deliver RNA aptamers into cells [168]. Thereby, aptamers can be continuously synthesized by the host cell and inhibitory effects should prevail for a long period of time. Consequently, an intracellular expression system was employed to evaluate the aptamers potential as tools to modulate intracellular Erk1/2 activity.

5.3.2.1 Design of the aptamer expression vector

Inhibitory RNA aptamers have been expressed successfully inside eukaryotic cells, such as yeast and multi-cellular organisms, by using polymerase II or polymerase III based RNA expression vectors [181, 192, 334, 335]. A simple and reliable method for expressing RNA aptamers in mammalian cells was described by Mi and co-workers [181]. Briefly, they adopted a vector that delivers a H1 RNA polymerase III promoter for high levels of RNA expression [336]. The advantage of this approach is that RNA transcription starts accurately at the initial base of inserted sequences. Transcription terminates with the addition 6 thymidine residues and the RNA constructs contain two-four uridines (U) at the 3´- end.

A congruent strategy was employed to design an expression vector for expressing the Erk2-recogizing aptamers C3 and C5 inside eukaryotic cells (Figure 5.25). Since Erk1/2 concentrations are very high inside cells (1 μM, [337]), a vector was chosen that employed a U6 small nuclear (U6) RNA polymerase III promoter instead of a H1 promoter. Studies with shRNA have shown that U6 promoters often yield higher RNA expression levels that H1 promoters [338, 339].

Similar to the H1 Polymerase III vector, RNA transcription is supposed to start at the initial base of inserted sequences and terminates with the addition of two to four uridines at the 3‘- end. The ability of C3 and C5 to bind to Erk2 with three uridines at the 3‘- end was verified before cellular experiments were performed (Section 10.5).

In addition, the expression vector allowed the co-cistronic expression of Green Fluorescent Protein (GFP) under the control of a Polymerase II promoter. GFP expression from a RNA polymerase II promoter and RNA expression from a U6 polymerase III promoter enables the analysis and reliable correlation between observed signals and transfection efficiency.

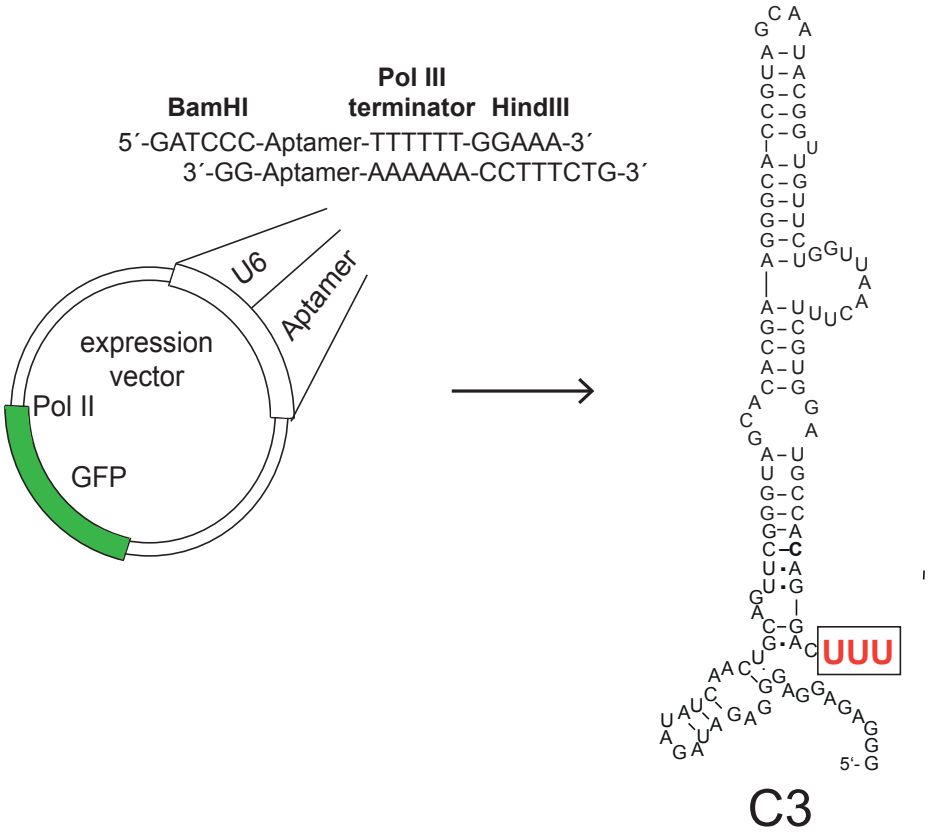

Figure 5.25: Design of the aptamer expression vector. Two complementary oligonucleotides containing full length C3, C5, or control sequences and six thymidines to terminate transcription were ligated into an expression vector downstream of a U6 gene-based RNA Polymerase III promoter. Upon transcription, three additional uridines are present at the 5´ end of the RNA. Furthermore, the expression vector contained a GFP gene under the control of a Polymerase II promoter. Modified from [181]. GFP: green fluorescent protein, Pol II: Polymerase II promoter, Pol III: Polymerase III promoter.

5.3.2.2 Effects of small molecule inhibitors on the SRE luciferase reporter gene assay

The experiments were conducted in HEK 293 cells. HEK cells are originally derived from human embryonic kidney cells grown in tissue culture. Since the transfection of efficiency of the RNA expression vectors was about 50% 24 hours after transfection (Section 10.5), putative inhibitory effects were not investigated by monitoring the effects on Erk1/2 target protein phosphorylation. Instead, it was chosen to co-transfect a plasmid encoding for a reporter gene to ensure that Erk1/2 signaling was quantified only in cells that were transfected with the RNA expression vectors. To this end, the SRE luciferase reporter gene assay was utilized (Figure 5.26) [188].

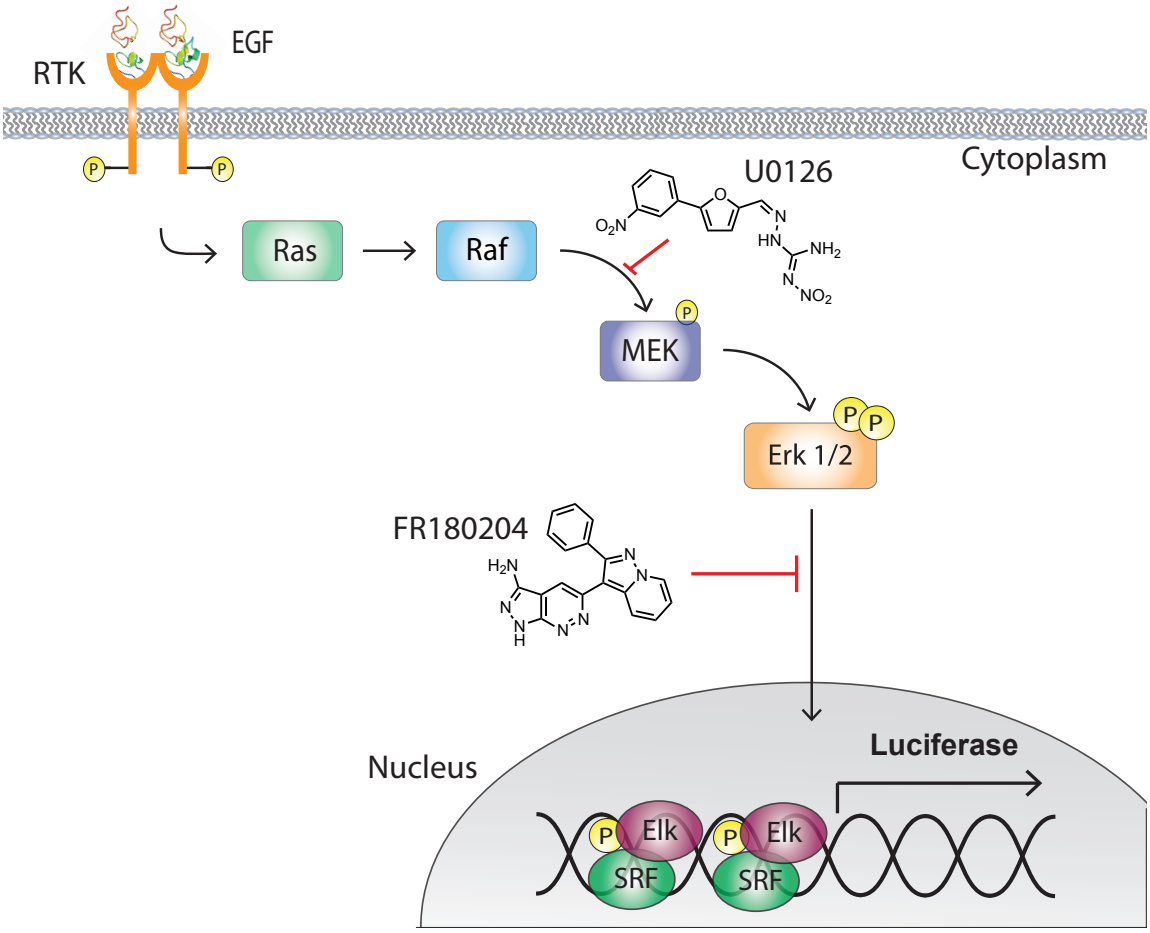

Figure 5.26: Schematic representation of the SRE luciferase reporter gene assay. Upon activation, Erk1/2 translocate into the nucleus and phosphorylate serum response transcription factors (SRFs [340]). Binding of SRF to the serum response element (SRE) then induces Luciferase expression. Firefly luciferase then catalyzes a light-emitting reaction which is proportional to Erk1/2 activity. The light-emitting reaction can be quantified in cell lysate. The small molecule U0126 blocks the activation of MEK by Raf whereas FR180204 blocks Erk1/2 activity in an ATP-dependent manner. Both inhibitors should decrease the luciferase signal. RTK: receptor tyrosine kinase, EGF: epidermal growth factor

This reporter gene assay enables the measurement and quantification of the firefly luciferase bioluminescence reaction respective to Erk1/2 activity (Figure 5.26): Upon activation, Erk1/2 translocate into the nucleus where they phosphorylate diverse targets, including the ternary complex transcription factor Elk-1 [341]. Elk-1 forms a complex with the serum response transcription factor (SRF) over the SRE and activates gene expression [342]. Elk-1 is phosphorylated by Erk1/2,

resulting in increased DNA binding, ternary complex formation, and transcriptional activation of the firefly luciferase gene [343, 344]. Firefly luciferase then catalyzes a light-emitting reaction [345]. This reaction is proportional to endogenous Erk1/2 activity and can be quantified in cell lysate.

First, it was investigated if direct inhibition of growth factor induced Erk1/2 signaling by the aptamers would be detectable with this reporter gene assay (Figure 5.26). To this end, two small molecule inhibitors were employed. FR180204 blocks Erk1/2 activity in an ATP-dependent manner [310]. U0126 is a non-ATP competitive Mek1/2 inhibitor that prevents the activation of MEK by Raf, and thus, inhibits Erk1/2 activation [346, 347]. Hence, the two inhibitors serve as references if inhibition of Erk1/2 activity by C5 or Erk1/2 activation by C3 could be observed.

To monitor inhibitory effects on Erk1/2 signaling, the SRE luciferase reporter plasmid and the RNA expression vectors were transfected at a ratio of 1:2.5 into HEK 293 cells. After transfection, the cells were incubated for 24 hours with the MEK1/2 inhibitor U0126 (2.5 μM), the Erk1/2 inhibitor FR180204 (10 μM), or solvent (0.4% DMSO). Afterwards, cells were starved for 4 hours (basal medium without fetal bovine serum) and stimulated with EGF for 2 hours. Then, cells were lysed and luciferase activity was detected. The GFP intensity was used to normalize the reporter gene activity.

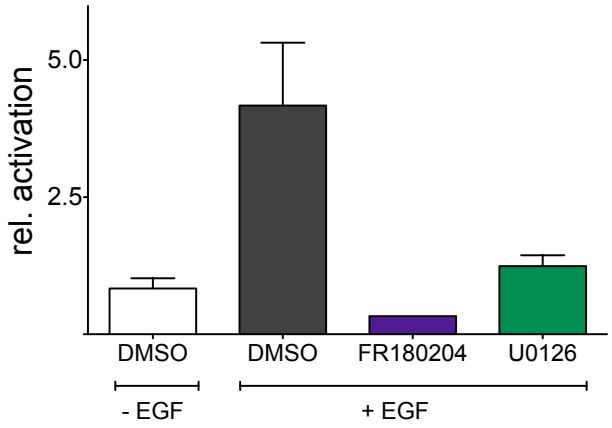

Figure 5.27: Effects of small molecule inhibitors on the SRE luciferase reporter gene assay in HEK 293 cells. This diagram shows the relative luciferase expession after co-transfection of the SRE luciferase reporter plasmid and the indicated vectors. After transfection, HEK 293 cells were treated with U0126 [2.5 μM], FR180204 [10 μM], or solvent [0.4% DMSO] for 24 hours, serum-starved and stimulated with EGF. The data are normalized with the unstimulated, empty vector transfected control cells set as 1 (mean ± SEM).

As shown in Figure 5.27, co-transfection of the SRE luciferase reporter plasmid and the empty control plasmid caused a readily detectable increase in luciferase activity. Incubation with the MEK1/2 inhibitor U0126 or Erk1/2 inhibitor FR180204 completely blocked luciferase expression. Hence, this reporter gene assay represents a suitable method to evaluate the putative inhibition of Erk1/2 activity by C5 or Erk1/2 activation by C3, respectively.

5.3.2.3 Effects of C3 and C5 on the SRE luciferase reporter gene assay

The effect of the RNA aptamers was investigated after co-transfection of the SRE luciferase reporter and the RNA expression vectors, which facilitated the expression of the aptamers C3 or C5, or the control sequences C5 B2, C3sc, or C5sc (Section 5.2.2). After transfection, HEK 293 cells were incubated for 24 hours and processed as described above.

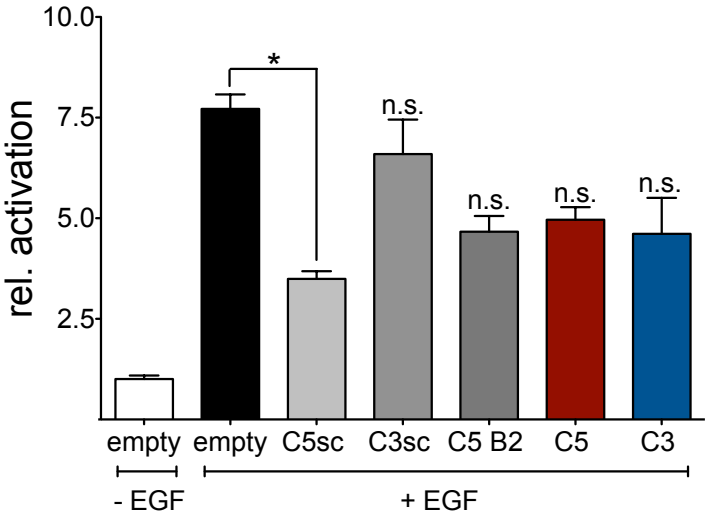

Figure 5.28: Effect of C3 and C5 on the SRE luciferase assay after 24 hours incubation. This diagram shows the relative luciferase expession after co-transfection of the SRE luciferase reporter plasmid and the indicated vectors. After transfection, HEK 293 cells were incubated for 24 hours, serum-starved, and stimulated with EGF. The data are normalized with the unstimulated, empty vector transfected control cells set as 1 (n =3, mean ± SEM). Expression of the control sequence C5sc induced a significant alteration of the luciferase signal whereas all other RNA expression vectors showed no inhibitory effects. Comparison was made by the use of the Kruskal-Wallis test with multiple comparison post-test. * indicates p-value < 0.05, n.s. not significant. Empty: empty control vector.

It was again possible to detect an increase in luciferase activity after transfection and EGF stimulation (Figure 5.28). Strikingly, the co-transfection of the control sequence C5sc resulted in a significant attenuation of the luciferase signal compared to the empty control vector ($p = 0.0183$, Kruskal-Wallis test with multiple comparison post-test).

Since C5sc does not bind to Erk1/2 (Section 10.1), these effects might be mediated either by a decrease in protein expression or off-target effects which interfere with Erk1/2 signaling. HEK 293 cells that were transfected with C5sc expression plasmids revealed a decrease in luciferase activity but did not show alterations in GFP expression levels (see Section 10.5 for a representative experiment). This implicates that the expression of C5sc affects the Erk1/2 MAP kinase pathway through off-target effects.

Notably, neither the expression of C3 nor C5 resulted in a decrease in luciferase expression after 24 hours (Figure 5.28). Thus, the incubation time of the RNA expression vectors was prolonged from 24 hours up to 72 hours. As can be seen in Figure 5.29, no inhibitory signal of C3 or C5 was observed after incubation periods of 36, 48, 60, or 72 hours. Surprisingly, no effects by C5sc were observed either.

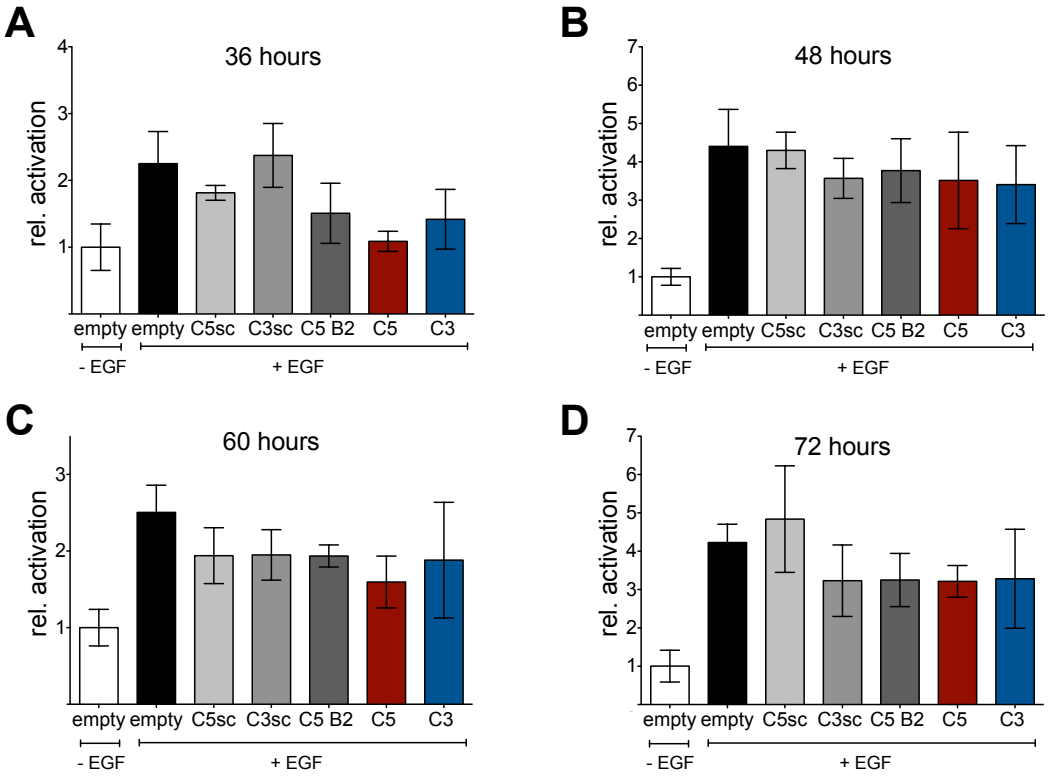

Figure 5.29: Luciferase assays 36-72 hours. These diagram show the relative luciferase activity after co-transfection of the SRE luciferase reporter plasmid with the indicated vectors. After transfection, HEK 293 cells were incubated for A) 36, B) 48, C) 60, or D) 72 hours, serum-starved and stimulated with EGF. The data are normalized with the unstimulated, empty vector transfected control cells set as 1. The RNA expression vectors showed no inhibitory effects on Erk1/2 signaling. Comparison (36 hours only) was made by the use of the Kruskal-Wallis test with multiple comparison post-test. Experiments were performed at least twice (mean ± SEM). Empty: empty control vector.

Taken together, these data demonstrate that C3 and C5 do not affect intracellular Erk1/2 activity under the tested conditions. Although the cellular RNA concentration and stability remain to be investigated, the fact that C5sc showed activity after 24 hours supports the notion that the RNA aptamers were indeed transcribed inside the cell. Therefore, two reason why the aptamers did not show inhibitory activity in this assays could have been a lack of stability as well as retention in cellular compartments. In turn, this could have prevented the aptamer´s access to Erk1/2.

5.3.3 Investigation of putative direct effects on Erk1/2 MAP kinase signaling after RNA transfection

In order to better control the cellular localization, the delivery strategy was changed in subsequent experiments to facilitate the modulation of Erk1/2 activity in the cytoplasm. Instead of utilizing a RNA expression vector, *in vitro* transcribed aptamers were directly transfected into the cells. This strategy has previously been applied to modulate Erk1/2 MAP kinase signaling with aptamer M69 in H460 cells [188, 189]. The target of aptamer M69 are cytohesin guanine nucleotide exchange factors, which are localized in the cytoplasm [183].

The transfection of exogenously synthesized aptamers offers several additional advantages: For

their synthesis, the RNAs do not rely on the host cells transcription machinery and can be tested for binding and functionality before application inside cells. Moreover, *in vitro* transcribed RNAs can easily be modified to improve stability, and to introduce chemical functionalities (Section 3.3.2).

5.3.3.1 Transfection efficiency of RNA aptamers

Since previous aptamer transfection experiments were conducted in H460 cells [188, 189], this cell line was chosen for subsequent experiments. H460 cells are a non-small cell lung cancer cell line. First, the transfection efficiency of this cell line was investigated. Thus, aptamers C3 or M69 were 5´-labeled with fluorescein and transfected for 5 hours. Transfection of the RNA aptamers took place in medium without serum to prevent degradation by nucleases.

Afterwards, the cells were treated with RNAse to remove RNAs that bound to the cell surface, and washed several times. The relative transfection efficiency was measured by detecting the fluorescence signal of the cells by flow cytometry.

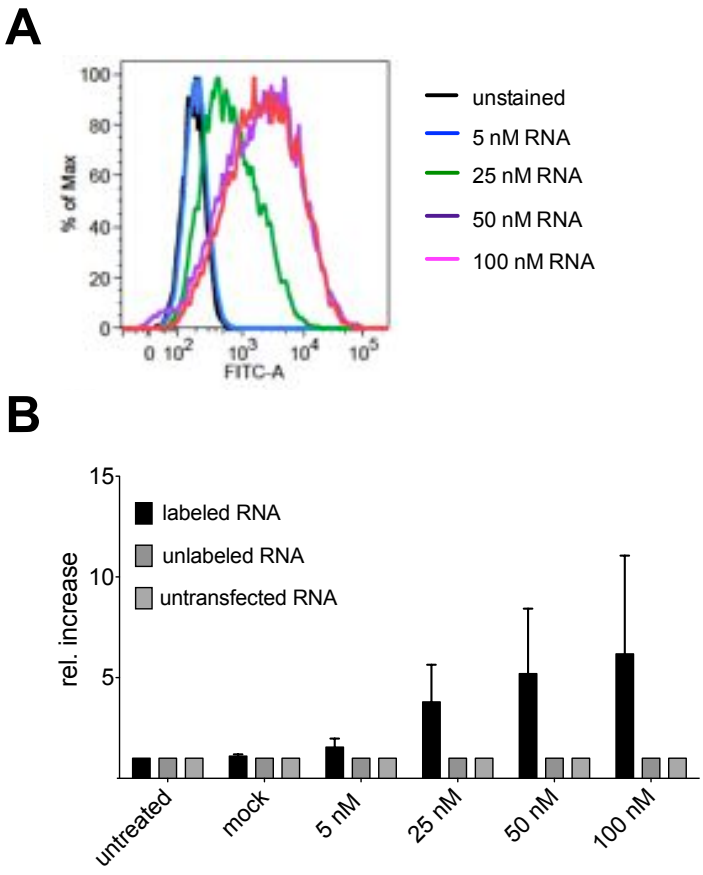

Figure 5.30: Transfection efficiency. Cells were transfected with fluorescein - labeled C3 or M69 (labeled RNA), unlabeled RNA or treated with fluorescein -labeled RNA in the absence of transfection reagent (untransfected RNA) for 5 hours. The relative transfection efficiency was measured by detecting the fluorescence signal of the cells by flow cytometry. A) Histogram showing a representative FACS experiment of H460 cells transfected with fluorescein labeled RNA. B) The bar diagram shows the detected fluorescence signal 5 hours after transfection. The signal was normalized with non-transfected control cells set as 1 (n = 2, mean ± SEM).

The results of these experiments are summarized in Figure 5.30 and show that H460 cells can be transfected with RNA aptamers in a concentration dependent manner. By utilizing RNA concentrations above 50 nM, all cells could be addressed by lipofection and revealed a detectable fluorescence signal (Figure 5.30B). The observed increase in the fluorescence signal results from internalized RNAs. No increase in fluorescence signal was observed in cells that were transfected with unlabeled RNA or incubated with fluorescein-labeled RNA without transfection reagent (Figure 5.30B).

Notably, the absolute intracellular RNA concentration was not quantified with this method. The following table gives an estimation of the intracellular RNA concentration that could be achieved by transfection.

Table 5.13: Estimation of the maximal intracellular RNA concentration that could be achieved by transfection of 250 nM RNA.

Absolute transfection efficiency [%]	Intracellular RNA concentration [nM]
15	5600
10	3750
5	1875
1	375
0.5	188

For the calculation, the following factors were taken into consideration: 75 pmol RNA in 300 μl reaction volume, cell number: 20,000, cell volume: 10^{-11} liter [188].

The estimated transfection efficiencies are in accordance with other studies, which quantified the total amount of transfected RNA in comparison to the original transfection mix for RNA aptamers to be 12% [188] or 6% for siRNA [348]. Hence, these concentration should be sufficient to monitor the inhibition of Erk2 activity by C5 and Erk1/2 activation by C3, respectively.

5.3.3.2 Effect of small molecule inhibitors on Erk1/2 signaling in H460 cells

Under the tested assay conditions, all cells could be transfected in a concentration-dependent manner with *in vitro* transcribed RNAs (see above). Therefore, putative effects of the aptamers were monitored by the quantification of intracellular Erk1/2 activation and downstream signaling via SDS-PAGE and western blot analysis.

Erk1/2 activation was quantified by detecting the phosphorylation of its activation loop with phosphospecific antibodies (Thr202/Tyr204, Thr 185/Tyr187). To analyze Erk1/2 activity in distinct cellular compartments, it was chosen to analyze the phosphorylation of two Erk1/2 substrates: Elk-1 (p-Ser383) and p-90-RSK1 (p90, p-Thr356/Ser360). Elk-1 is a nuclear transcription factor which becomes activated in the nucleus and p90-RSK1 is a kinase which becomes activated by Erk1/2 in the cytosol (Figure 5.31).

Consequently, it was investigated if direct inhibition of growth factor induced Erk1/2 signaling by the aptamers would be detectable in H460 cells. For this purpose, the two small molecule inhibitors FR180204 and U0126, were employed (Figure 5.31). Again, FR180204 and U0126 served as controls to verify if the inhibition of Erk1/2 activity by C5 or Erk1/2 activation of C3 would be detectable with this assay.

To monitor intracellular Erk1/2 activation and downstream signaling after inhibitor treatment, H460 cells were starved overnight (basal medium without fetal bovine serum). Cells were then treated with FR180204, U0126, or solvent (0.5% DMSO). Afterwards, the cells were stimulated

with EGF for 5 minutes, followed by cell lysis, SDS-PAGE, and immunoblot analysis. Actin served as loading control.

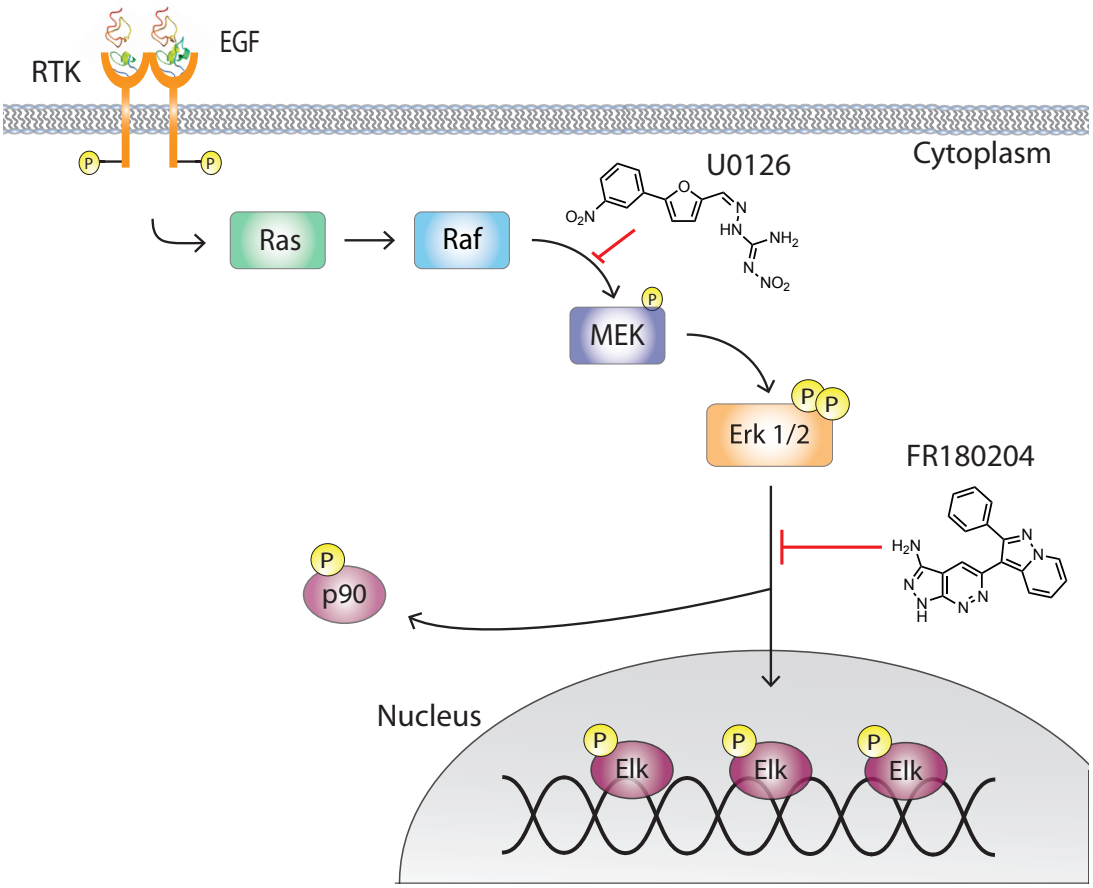

Figure 5.31: Erk1/2 signaling. The activation of intracellular Erk1/2 signaling is triggered by the binding of EGF to a receptor-tyrosine-kinase. Subsequently, the activation of the Erk1/2-MAPK-cascade is mediated by the small G-protein Ras. The activation of Erk1/2 results in the phosphorylation of diverse nuclear transcription factors (e.g. Elk-1) or targets in the cytosol (e.g. p-90-RSK1). The small molecule U0126 blocks the activation of MEK by Raf, whereas FR180204 blocks Erk1/2 activity in an ATP-dependent manner. RTK: receptor tyrosine kinase, p90: p-90-RSK1.
.

The results of the MEK inhibitor U0126 are depicted in Figure 5.32.

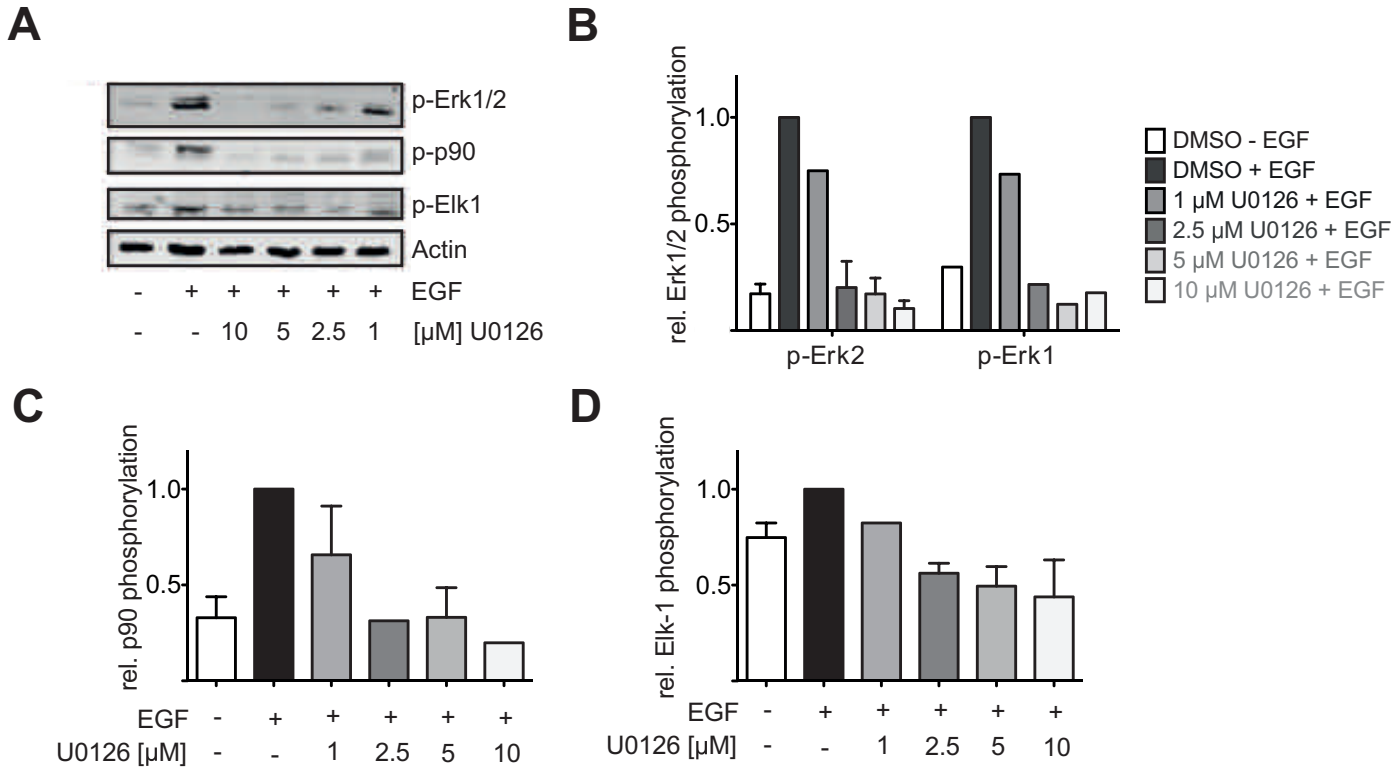

Figure 5.32: Effect of U0126 on Erk1/2 signaling in H460 cells. A) Representative immunoblot analysis of H460 cells treated with the control compound U0126 or solvent and stimulated with EGF. Phosphorylation of the indicated proteins was determined by immunodetection using phosphospecific antibodies. Actin served as loading control. B-D) These diagrams show relative phosphorylation levels of B) Erk1/2, C) p90 or D) Elk-1 after normalization for actin with EGF-stimulated cells set as 1 (n=3, mean ± SEM).

In H460 cells, it was possible to detect an increase in Erk1/2 signaling after EGF stimulation, which was found both in the level of Erk1/2 (Figure 5.32B) and of the substrate protein p90-RSK1 (Figure 5.32C). In contrast, Elk-1 activation was barely detectable (Figure 5.32D).

Treatment of H460 cells with the Mek inhibitor U0126 resulted in complete inhibition of Erk1/2 activation at a concentration of 2.5 μM (Figure 5.32B). This inhibitory effect was also found on the levels of the substrate proteins p90-RSK1 and Elk1 (Figure 5.32C,D).

When Erk1/2 activation was inhibited completely, phosphorylation of p90-RSK1 was reduced to the baseline level of unstimulated cells (Figure 5.32C). Interestingly, Elk-1 phosphorylation seemed to be more strongly reduced in U0126 treated cells that in unstimulated cells (Figure 5.32D). Since Elk-1 is phosphorylated by additional kinases besides Erk1/2 [349], this effect might be explained by off-target effects of the inhibitor.

These data indicate that inhibition of Erk1/2 activation and downstream signaling, in accordance with the mode of action of aptamer C3, could be detected with this assay.

Treatment with ATP-competitive Erk1/2 inhibitor FR180204 also resulted in the inhibition of substrate phosphorylation (Figure 5.33).

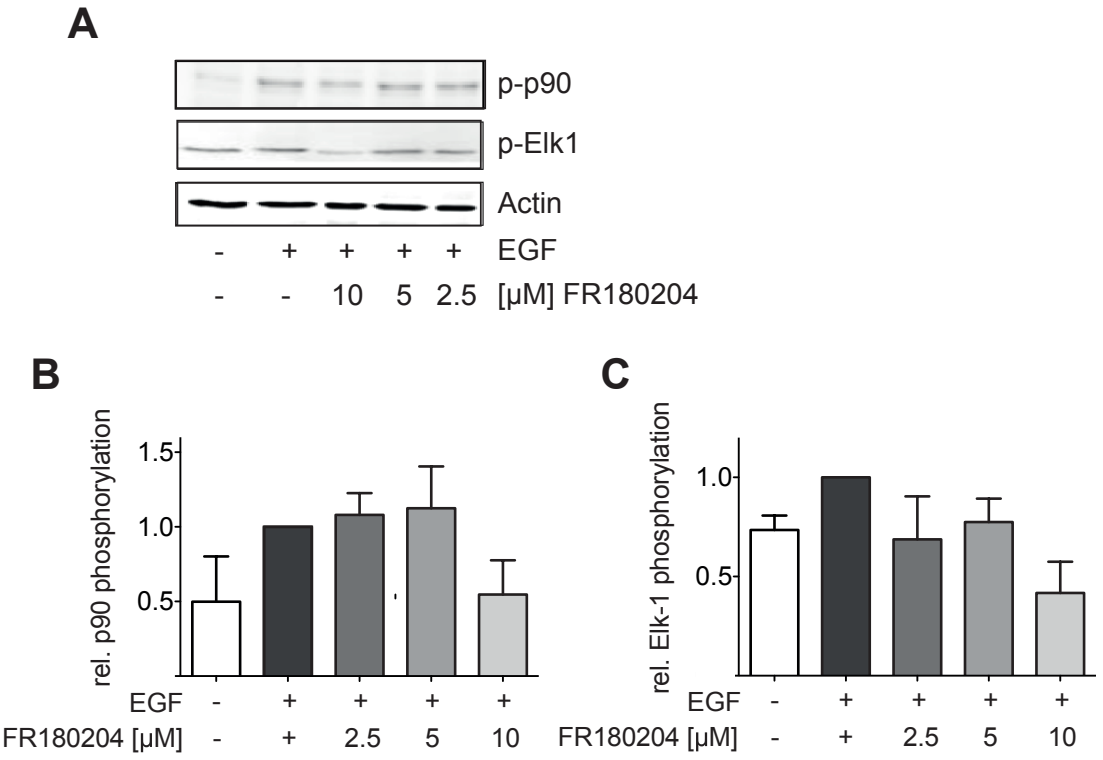

Figure 5.33: Effect of FR180204 on Erk1/2 signaling in H460 cells. A) Representative immunoblot analysis of H460 cells treated with FR180204 or solvent and stimulated with EGF. Phosphorylation of the indicated proteins was determined by immunodetection using phosphospecific antibodies. Actin served as loading control. B-C) These diagrams show relative phosphorylation levels of B) p90-RSK1 or C) Elk-1 after normalization for actin with the EGF-stimulated cells set as 1 (n=2, mean ± SEM).

At a concentration of 10 μM, p90-RSK1 phosphorylation was reduced to the same baseline level that is found in unstimulated cells (Figure 5.33B) and Elk-1 phosphorylation decreased even further than the phosphorylation level found in unstimulated cells (Figure 5.33B). This was also observed for the Mek inhibitor U0126 (Figure 5.32).

In total, the Erk1/2 inhibitor FR10204 seems to be less potent that U0126. Inhibition of Erk1/2 activity was observed at a high concentrations (10 μM) whereas the addition of U0126 blocked downstream signaling at a concentration of 2.5 μM (Figure 5.33B,C).

Taken together, these data suggest that the inhibition of the Erk1/2 pathway with C5 could be detectable by reduction of both Elk-1 and p90-RSK1 phosphorylation.

5.3.3.3 Effect of C3 and C5 on Erk1/2 signaling in H460 cells

In the next step, the aptamers effect on Erk1/2 MAPK signaling was investigated. To this end, 250 nM C3 or C5 aptamer were transfected into H460 cells and inhibition of cellular Erk1/2 activity was monitored. The transfection took place in the absence of serum to prevent both nuclease-mediated degradation and activation of the signal transduction pathway. To activate Erk1/2 signaling, the cells were stimulated with EGF for 5 minutes before cell-lysis.

By using these transfection conditions, intracellular RNA concentrations of up to 6 μM can be expected (Section 5.3.3.1). This concentration has been sufficient to monitor the inhibition of Erk2 activity by C5 (Section 5.2.4.2) and Erk1/2 activation by C3 (Section 5.2.4.4) *in vitro*.

C3sc was used as a control sequence for C3 and C5. In addition, the effects of TRA and C5sc on Erk1/2 MAP kinase signaling were also investigated.

TRA has previously been shown to lose its affinity for Erk2 in the presence of potassium ions (Section 5.2.1.1). Since potassium ions are highly abundant within the cytosol, it was tested if the predicted lack of activity *in vitro* could indeed be observed *in vivo*.

C5sc does not bind to Erk1/2 and revealed side effects on Erk1/2 signaling in the luciferase assay (Section 5.3.2.3), Subsequently, it was investigated which Erk1/2 targets could be affected by cross-talk as a response to the transfection of C5sc.

First, the RNA´s effect on Erk1/2 activation was detected with phosphospecific antibodies (Section 5.3.3.2). Heat shock cognate protein 70 (Hsc70) served as loading control.

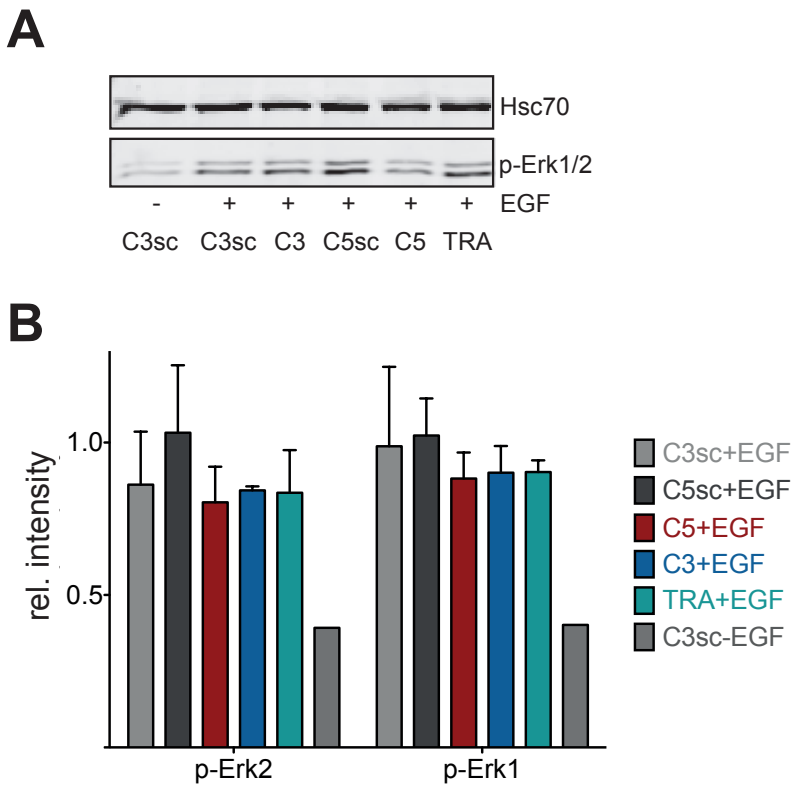

Figure 5.34: Effect of C3 and C5 on Erk1/2 activation in H460 cells. A) Representative immunoblot analysis of H460 cells transfected with the indicated RNAs and stimulated with EGF. Phosphorylation of the indicated proteins was determined by immunodetection using phosphospecific antibodies. Hsc70 served as loading control. B) This diagram shows relative phosphorylation levels of Erk1/2 after normalization for hsc70 (n=3, mean ± SEM).

The results of these experiments are depicted in Figure 5.34. Contrary to the inhibition of Erk1/2 activation by C3 which was detected *in vitro*, no inhibition of cellular Erk1/2 activation was observed (Figure 5.34). Moreover, neither C5 nor TRA revealed an inhibitory effect on Erk1/2 activation.

C5sc also did not affect Erk!/2 activation directly. This supports the notion that the observed effects in the luciferase assay might have arisen from cross-talk with another signal transduction pathway.

Subsequently Erk1/2 activity was monitored by substrate phosphorylation of p90-RSK1 (p-90, Thr356/ Ser360) and Elk-1 (p-Ser383) (Figure 5.35).

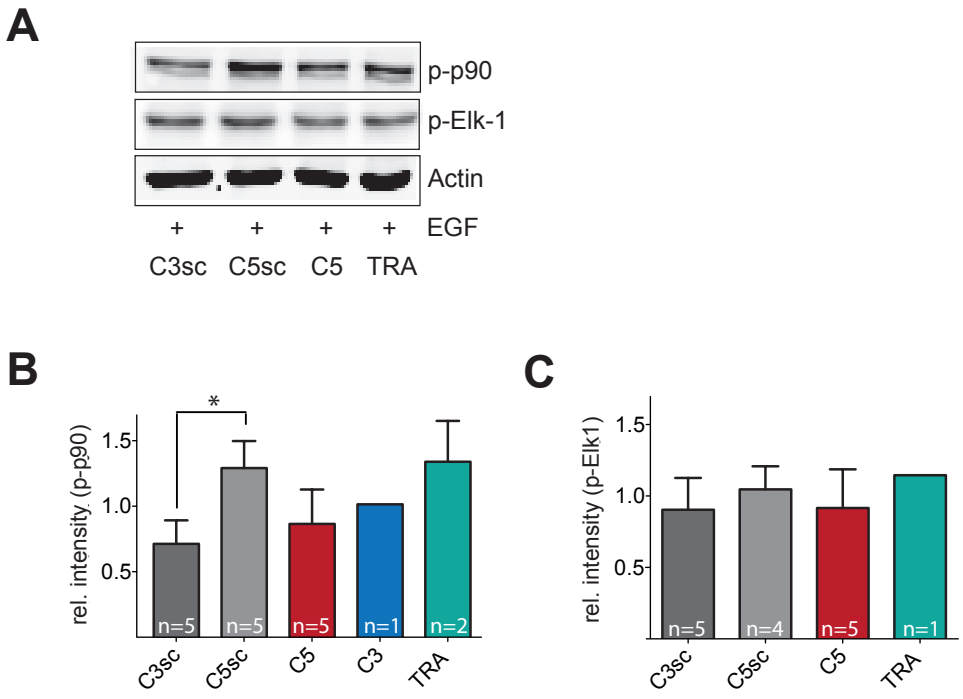

Figure 5.35: Effect of C3 and C5 on substrate phosphorylation in H460 cells. A) Representative immunoblot analysis of H460 cells transfected with 250 nM of the indicated RNAs and stimulation with EGF. Phosphorylation of the indicated proteins was determined by immunodetection using phosphospecific antibodies. Actin served as loading control. B-C) These diagrams show relative phosphorylation levels of B) p90-RSK1 or C) Elk-1 after normalization for actin (mean ± SEM). B) C5sc induces a significant upregulation of p90-RSK1 phosphorylation in comparison to C3sc. Comparison was made with the "Mann Whitney test. * indicates p value <0.05, n.s.: not significant.

Under these conditions, C3 and C5 transfected samples did not display any inhibitory effects on p90-RKS1 phosphorylation (Figure 5.35B).However, previous results have implicated that intracellular expression of C5sc induces a downregulation of the Erk1/2 MAP kinase pathway (Section 5.3.2.3). Here, it could be observed that transfection of C5sc increased phosphorylation levels by 45% compared to C3sc (p=0.0159, Mann Whitney test). Hence, p90-RSK1 seems to be one of the Erk1/2 targets affected by the secondary effects of C5sc.

TRA revealed sensitivity to the presence of monovalent cations *in vitro*). Surprisingly, transfection of TRA also induced an up-regulation of p90-RSK1 phosphorylation in comparison to C3sc, C3, or C5 (Figure 5.35A).

Moreover, none of the transfected aptamers have shown an inhibitory effect on Elk-1 phosphorylation. In contrast to their effect on p90-RSK1 phosphorylation, C5sc and TRA did not promote an increase in Elk-1 phosphorylation (Figure 5.35C).

In summary, neither C3 nor C5 induced a down-regulation of Erk1/2 activation or activity in H460 cells. In order to verify that the lack of inhibitory effect was not dependent on the cell line used, the transfection experiments were repeated in A431 cells. In contrast to H460 cells, A431 do not have an activating mutation in the *Ras* oncogene [350].

5.3.3.4 Effect on Erk1/2 signaling in A431 cells

The putative effect of the Erk2 aptamers was also investigated in A431 cells. A431 are human squamous carcinoma cells and have successfully been employed before to investigate MAP kinase signaling inhibitors [351, 352].

The cells were again transfected with 250 nM aptamers or control sequences and processed as described for H460 cells (Section 5.3.3.3). Erk1/2 activity was again measured by phosphorylation of the substrate proteins Elk-1 (p-Ser383) and p90-RSK1 (p-90, p-Thr356/Ser360). Actin served as loading control.

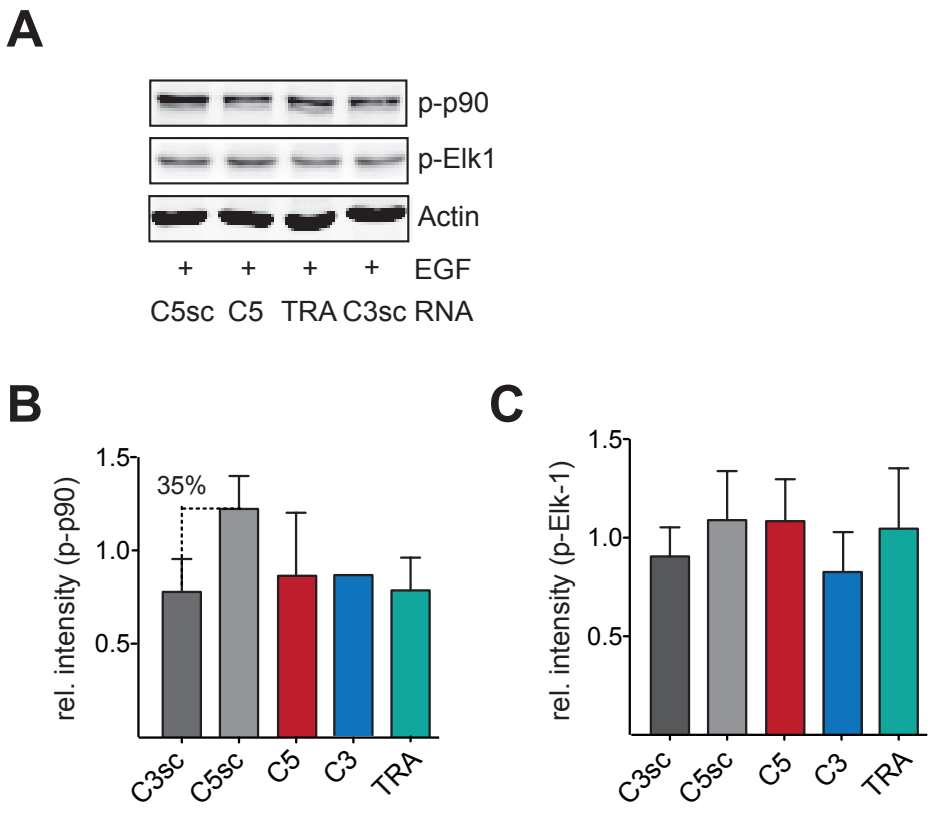

Figure 5.36: Effect of C3 and C5 in A431 cells. A) Representative immunoblot analysis of A431 cells transfected with the indicated RNAs and stimulated with EGF. Phosphorylation of the indicated proteins was determined by immunodetection using phosphospecific antibodies. Actin served as loading control. B-C) These diagrams show relative phosphorylation levels of B) p90-RSK1 or (C Elk-1 after normalization for actin (n=2, mean ± SEM).

Neither C3 nor C5 transfected samples displayed any inhibitory effect on p90 phosphorylation (Figure 5.36B). Again, C5sc induced an increase in p90 phosphorylation by approximately 35%. In H460 cells, this was also observed for TRA (Section 5.3.3.3).

None of the sequences interfered with Elk-1 phosphorylation (Figure 5.36C). This is again in accordance with the data from H460 cells that did not demonstrate any inhibitory or stimulatory effect of C3, C5, or the control RNAs on Elk-1 phosphorylation (Section 5.3.3.3).
To this end, no explicit inhibitory effect of C3 or C5 on Erk1/2 activity and, thus, substrate phos-

phorylation was observed after RNA transfection into A431 cells.

5.3.3.5 Transfection of *in vitro* transcribed RNAs impairs cell viability

The non-targeting control sequences C5sc and C3sc, as well as TRA, have exerted distinct effects on the phosphorylation of the Erk1/2 substrate p90-RSK1 in two cell lines (Sections 5.3.3.3, 5.3.3.4).

This raised the questions whether the lipofection of *in vitro* transcribed RNAs exhibits even more pronounced off-target effects, which could impair the use of this technique for research applications. In order to answer this question, the RNAs effects on cell proliferation was investigated.

The effect of the control RNA and the aptamers on cell proliferation was analyzed transfected H460 cells at different time-points (Figure 5.37). To achieve this, the transfection conditions were down-scaled from immunoblot experiments to a smaller volume in 96-well plates. 5 or 0.5 pmol RNA in this assay equal 250 or 25 nM transfected RNA during immunoblot experiments, respectively.

At the time point when cells were harvested for immunoblot experiments (4 hours after transfection), none of the aptamers or control RNAs showed any effects on cell viability (Figure 5.37A).

24 hours after transfection, a clear relationship existed between cell survival and lipid-mediated RNA delivery. Incubation with 5 pmol RNA led to a reduction of cell proliferation by 50%, regardless of the sequence (Figure 5.37B). This effect was not observed for mock transfected cells and, thus, seems to reflect RNA-mediated toxicity. This toxic phenotype seems to be concentration-dependent because no toxicity was observed at lower RNA concentrations (0.5 pmol).

Incubation with 5 pmol C3, C5, and C3sc led to identical levels of cell death as were observed after 24 hours (Figure 5.37C). Quite notably, cell proliferation was completely inhibited in C5sc and TRA transfected samples. The transfection of 0.5 pmol RNA did not affect cell proliferation after 72 hours (Figure 5.37C). Hence, toxic secondary effects can be abolished by using lower RNA concentrations.

In summary, there has been a strong correlation between cell survival and lipid-mediated RNA delivery under the assay conditions. These effects are both concentration - and time - dependent. Furthermore, it was shown that off-target effects of this assay are capable of inducing strong, quantifiable phenotypes that impact Erk1/2 substrate protein phosphorylation (Sections 5.3.3.3, 5.3.3.4).

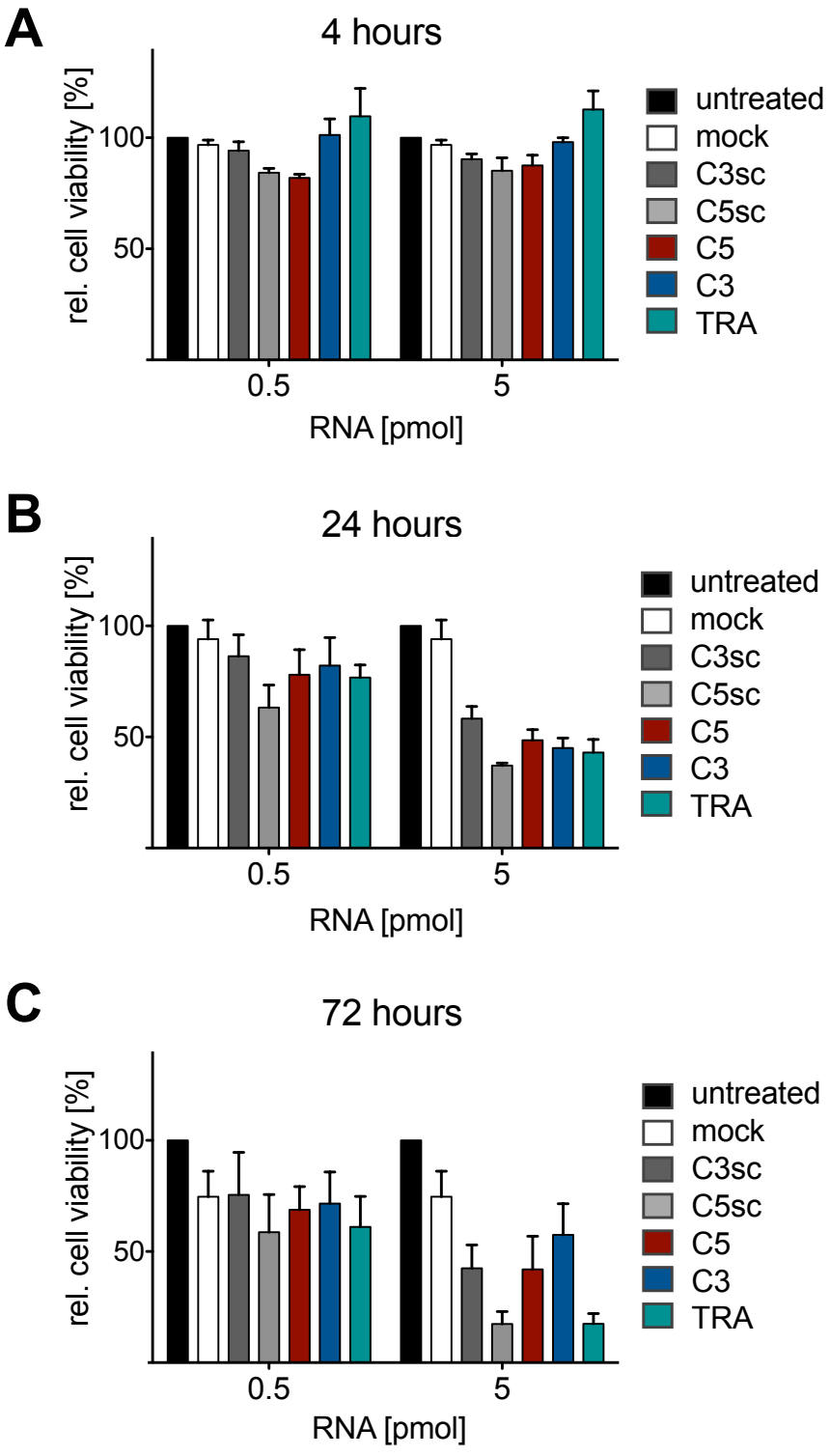

Figure 5.37: Transfection of *in vitro* transcribed RNAs impairs cell viability. The diagrams show the relative cell viability after transfection and incubation with the indicated RNAs (0.5 or 5 pmol) or transfection reagent (mock) at the indicated time-points. The relative cell viability was determined by using a MTT assay. The data are normalized with the untreated control cells set as 100% (n=4, mean ± SEM). mock: mock transfection.

5.4 Aptamer-based control of neuronal Erk1/2 signaling

So far, none of the transfection experiments have revealed any inhibition of Erk1/2 signaling. In contrast, only off-target effects, which occurred in a time - and concentration dependent manner, were monitored.

The lack of the inhibitory effects of the aptamers could be due to distinct features. For example, it might have been possible that the aptamers are located in a cellular compartment, which could have prevented their direct access to Erk1/2. In addition, it could have been possible that any putative effects on Erk1/2 activation or activity are masked by cross-talk with other signal transduction pathways.

Based on this hypothesis, I decided to use microinjection as a delivery method to introduce the aptamers into the cell. This technique enables to directly inject the aptamers into the cytosol and allows for direct access to Erk1/2. More importantly, the aptamers effects on Erk1/2 signaling can be monitored on single-cell level and in real-time within minutes after application. This could minimize cross-talk with other signal transduction pathways.

Contrary to the previous transfection experiments, the microinjection experiments were not performed with cultured cells. Our group is collaborating with Prof. Becks working group at the University Hospital on another project. Since Prof. Beck´s lab is widely renowned for electrophysiological recording techniques and has expertise in monitoring neuronal Erk1/2 activity [353], we developed an assay in which we could both introduce the aptamers into cells and monitor the aptamers effects on cellular Erk1/2 signaling in real-time. To this end, we introduced the aptamers into the soma of CA1 pyramidal neurons in murine brain slices and monitored their effect on neuronal Erk1/2 signaling with whole-cell patch clamp recordings (Figure 5.38). Erk2 is activated this area of the hippocampus following high-frequency stimulation that induce a certain form of long term potentiation [281].

Because this assay required expertise in electrophysiological recording and in-depth training in neurobiology in order to optimize the assay conditions, the whole-cell recordings were performed by Therese Alich (Beck lab) during her Master´s Thesis [354]. I performed all binding data.

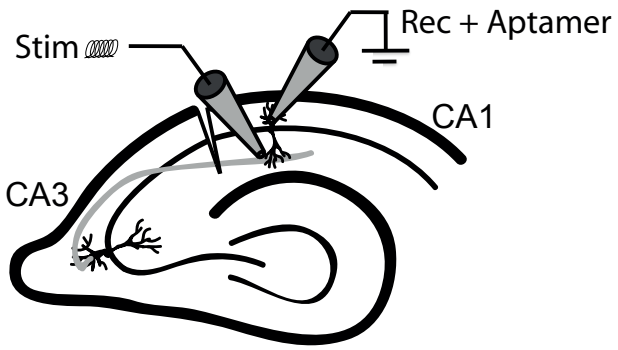

Figure 5.38: Whole-cell recording setup. Schematic representation of a hippocampus slice showing stimulating (Stim) and recording (Rec) sites. The aptamers were introduced into the soma of CA1 pyramidal neurons via the recording electrode.

5.4.1 Truncation of C3, C5, and C5 B2.

The tip diameter of the patch pipette is in the low μM range [355]. In order to facilitate the diffusion of the aptamers through the tip, C5 and C5 B2 were truncated from 112 to 71 nucleotides and C3 was truncated from 101 to 59 nucleotides by removing the primer-binding sites of the original aptamers. The resulting aptamers C5.71 and C3.59 are shown in Figure 5.39. C3.59 and C5.71 were tested for Erk2 binding with filter retention assays and revealed the same affinities as the full-length aptamers C3 and C5, respectively (Figure 5.39, Table 5.14).

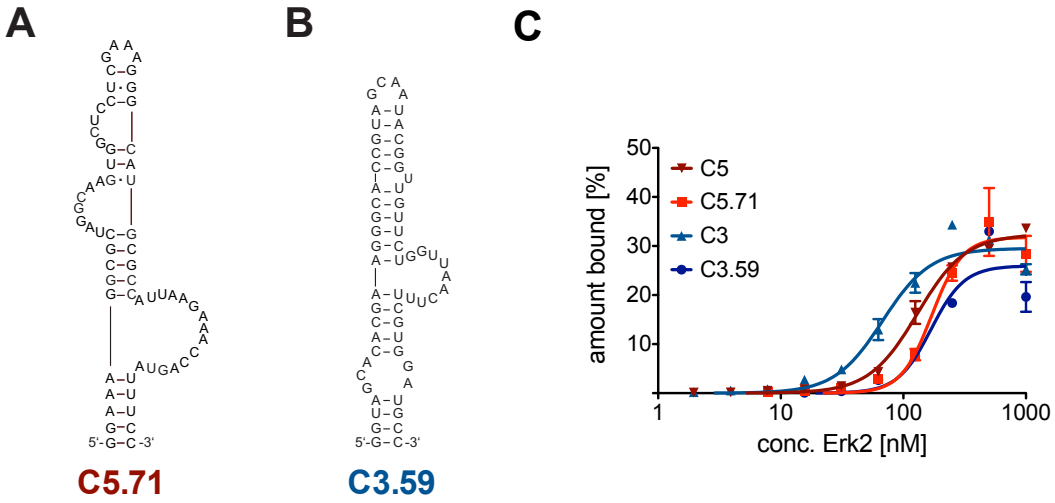

Figure 5.39: Truncated variants of C3 and C5. Proposed secondary structure of the truncated aptamers A) C5.71, and B) C3.59. C) Filter retention assay of full-length aptamers C3 and C5 and their truncated variants binding to Erk2 in 1x PBS, 3 mM $MgCl_2$. K_D values are listed in table 5.14.

Table 5.14: K_D values and Hill coefficients (h) according to Figure 5.39.

Aptamer	K_D [nM]	h
C5	130 ± 6.3	2.2 ± 0.2
C5.71	170.7 ± 15.8	3.5 ± 0.8
C3	67.8 ± 6.5	2.2 ± 0.4
C3.59	167.9± 22	3.2 ± 1.0

5.4.2 Distribution of aptamers within neurons

Next, the truncated aptamers were introduced into the soma of CA1 pyramidal neurons via the recording electrode and their spatio-temporal distribution was monitored by two-photon microscopy. Therefore, the aptamers the RNA sequences were 5´-labeled with fluorescein. In addition, cells were co-labelled with Alexa594 for better visualization of the neurons morphology.

The observed fluorescence signal of aptamer C5.71 could be detected in the soma after 5 minutes (Figure 5.40). Within the ensuing 15 minutes, the fluorescence signal of aptamer C5 increased in the distal dendrite. Hence, this data implicates that the introduction of the aptamers into the soma and dendrite with the whole-cell recording setup occurs rapidly.

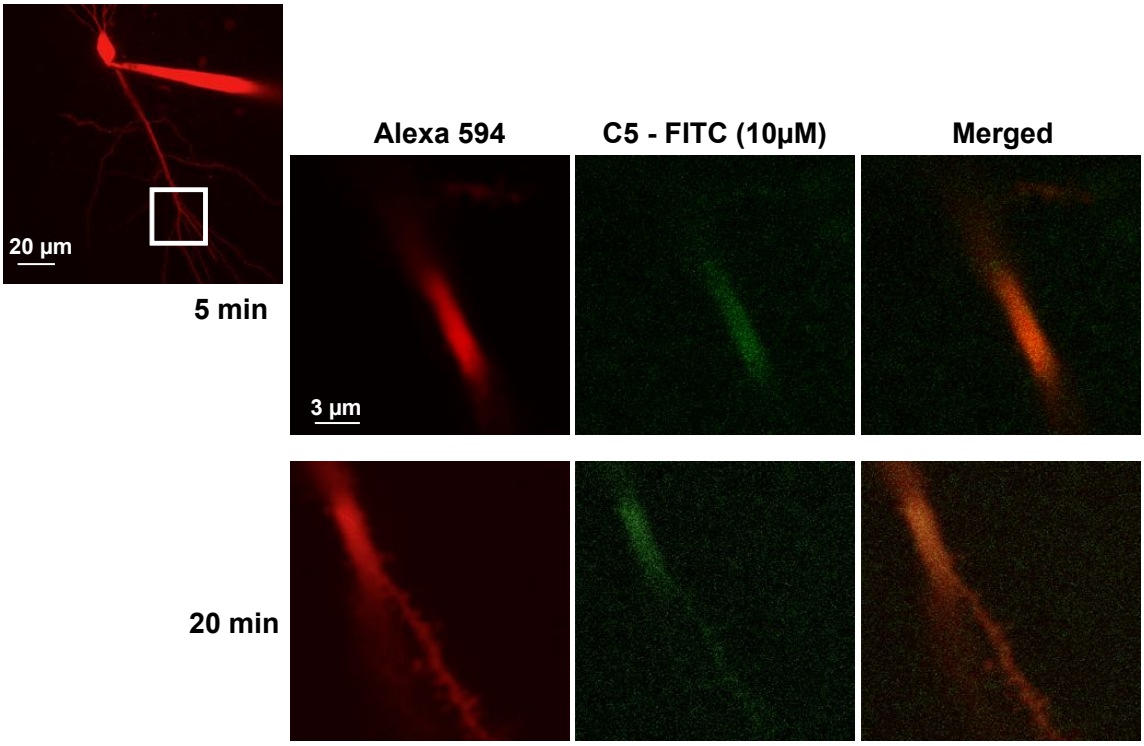

Figure 5.40: C5.71 diffuses into the distal dendrite. Images of a CA1 pyramidal neurons with fluorescein - labeled aptamer C5.71 (C5-FITC, green) and Alexa595 (red). The upper left panel shows the soma and apical dendrite of a CA1 pyramidal neuron and the recording pipette. The white box shows the distal dendrite, which is magnified on the right side.

5.4.3 U1026 inhibits neuronal Erk1/2 signaling

As mentioned in the introduction, Erk1/2 can be activated by certain electric stimulation patterns in the hippocampus. Among other substrates, activated Erk1/2 catalyze the phosphorylation of the $K_V4.2$ ion channel and thereby modulate the channels activity [281, 282]. Erk1/2 activity is also linked to decrease the channels outward K^+ current [283].

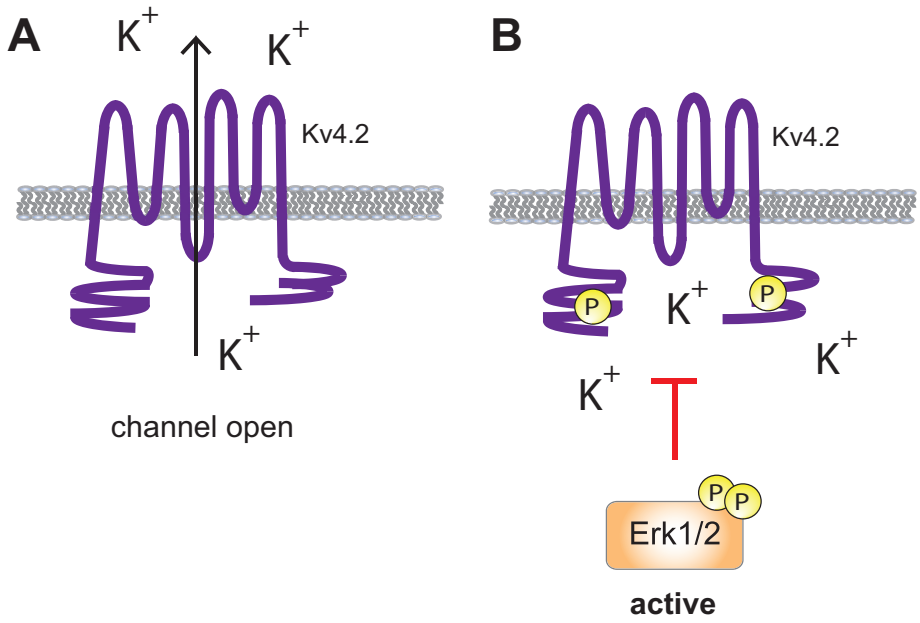

Figure 5.41: Model of neuronal Erk1/2 signaling. A) Dendritic excitability is modulated by ion channels, especially by A-type K^+ channels, such as the $K_V4.2$ potassium channel subunits [356]. B) Erk1/2 catalyze the phosphorylation of $K_V4.2$ [281]. In addition, phosphorylation by Erk1/2 was described to inhibit the channels activity [282] and to decrease the outward K^+ current [283].

First, it was tested if the inhibition of cellular Erk1/2 signaling in response to the Mek1/2 inhibitor could be monitored by effects on the voltage potential after stimulation (Figure 5.41). This has been previously been described in the literature [282, 357].

To monitor the effects of Erk1/2 inhibition on neuronal functions, 40 μM U0126 was dissolved in the recording solution and introduced into the soma. After a stable baseline was recorded for 10 minutes, Erk1/2 activity was induced [354].

A stable increase in voltage potential could be monitored within the first 15 minutes (Figure 5.42). Afterwards, the membrane potential reached a plateau. In turn, the Mek inhibitor U0126 blocked any alterations in membrane potential recordings. Hence, this readout is suitable to monitor inhibition of Erk1/2 activity in neurons.

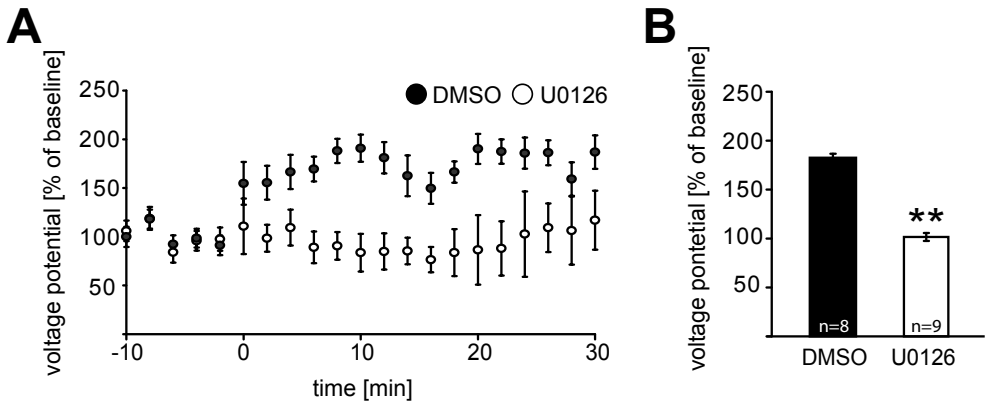

Figure 5.42: Effect of the Mek inhibitor U0126 on Erk1/2 signaling. A) This diagram shows membrane potential recordings during the experiments performed with 40 μM U0126 or solvent (0.4% DMSO). Stimulation started at the timepoint 0. Y axes depict membrane potential amplitudes normalized to the baseline amplitudes before stimulation. Experiments were performed at least eight times (mean ± SEM). B) For comparison, the recordings between 20 - 30 minutes of each slice were were averaged. Comparison were made with the Wilkinason rank-test. ** indicates significance between DMSO and U0126 (p-value <0.01).

5.4.4 Effect of C3.59 and C5.71 on neuronal Erk1/2 signaling

To monitor now the aptamers impact on neuronal Erk1/2 signaling, 1 μM C3.59, C5.71, or the control RNA C5 B2.71 were dissolved in the recording solution and introduced into CA1 pyramidal neurons via the patch pipette. Again, a stable baseline was monitored for 10 minutes before Erk1/2 activity was induced by high frequency stimulation.

The experiments are summarized in Figure 5.43. Recordings taken with the control sequence C5 B2.71 displayed an increase in membrane potential after 15 minutes (Figure 5.43A). In contrast, no alterations in voltage potential were monitored when C5.71 was introduced into the neuron ($p = 0.026$, Kruskall-Wallis test with non-parametric multi comparison post - test).

Importantly, these inhibitory effects are in accordance with previous biochemical assays that employed the Mek1/2 inhibitor U0126 [282, 357] and implicate that C5.71 modulates Erk1/2 activity.

In contrast, experiments performed with C3.59 revealed a rapid rise of the membrane potential directly after stimulation started (Figure 5.43B). However, at the concentration used in this assay, C3.59 did not significantly interfere with potentiation during the measurements.

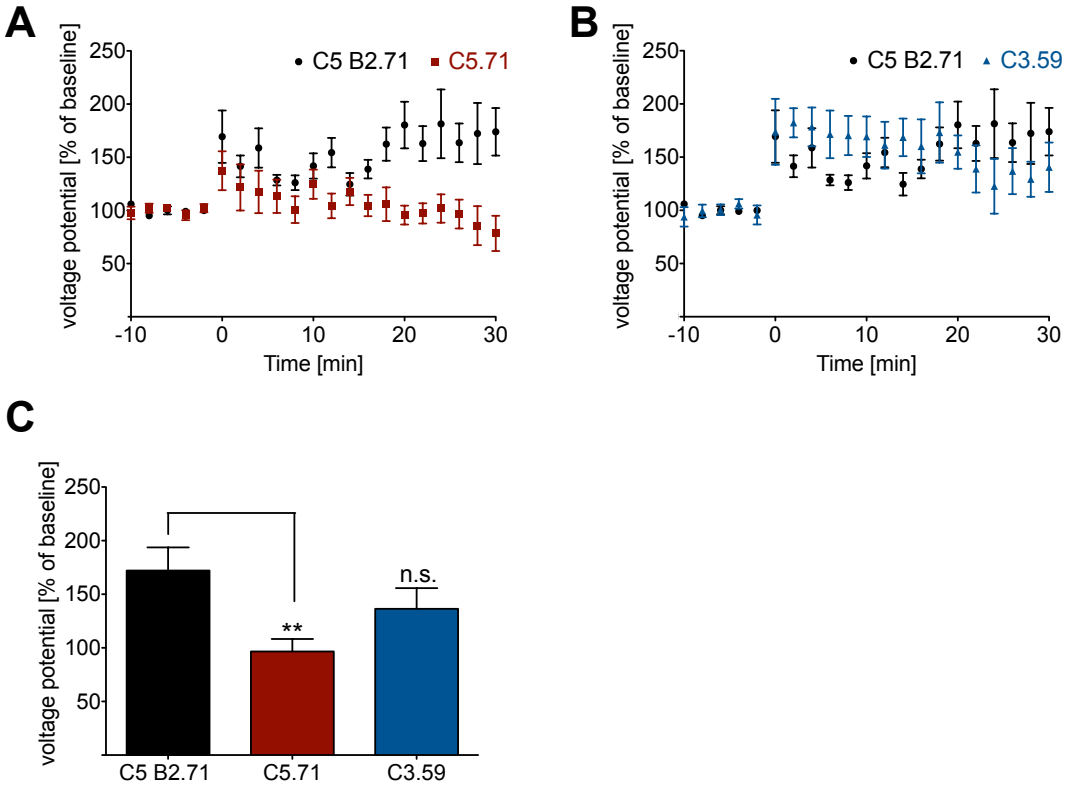

Figure 5.43: Effect of C3.59 and C5.71 on neuronal Erk1/2 signaling. A) These diagrams show membrane potential recordings during the experiments performed with 1 μM A) C5 B2.71, and C5.71, or B) B2.71 and C3.59. Stimulation started at the timepoint 0. Y axes depict membrane potential amplitudes normalized to the baseline amplitudes before stimulation. Experiments were performed at least six times (mean ± SEM). C) For comparison, the recordings between 20 - 30 minutes of each slice were were averaged. Comparison were made with the Kruskall-Wallis test with non-parametric multi - comparison post - test. ** indicates significance between C5 B2.71 and C5.71 (p-value <0.01), n.s. not significant.

5.4.5 C5.71 and C5 B2.71 do not affect neuronal Erk1/2-independent functions

In order to further validate that the effect of C5.71 on voltage potential recordings after stimulation was indeed dependent on the inhibition of Erk1/2 by C5.71, several control experiments were performed.

The alteration in voltage-potential in response to the induced electric stimulation pattern combines the activity and cross-talk of several kinases (PKA, PKC, CaM kinase II) and second messenger cascades in addition to Erk1/2 [358]. Hence, it was verified that the change in voltage potential observed after the addition of C5.71 is indeed dependent on Erk1/2. To achieve this, an Erk1/2-independent increase in voltage potential was induced [357].

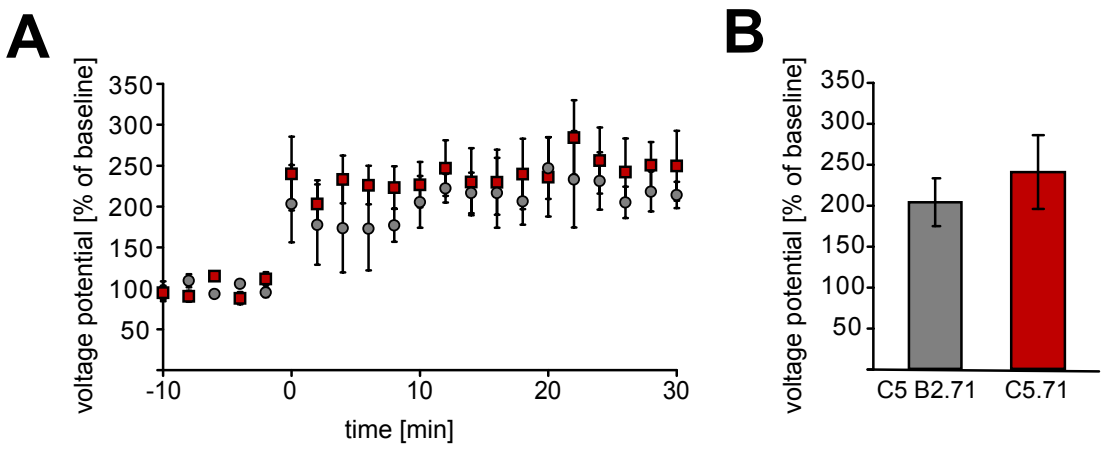

Figure 5.44: Effect of C5.71 and C5 B2.71 on neuronal Erk1/2-independent signaling. A) This diagram shows membrane potential recordings during the experiments performed with 1 μM C5 B2.71 and C5.71. Stimulation started at the timepoint 0. Y axes depict membrane potential amplitudes normalized to the baseline amplitudes before stimulation. Data are show mean ± SEM. B) For comparison, the recordings between 20 - 30 minutes of each slice were were averaged.

Stimulation with the Erk1/2-independent protocol resulted in an instant increase in voltage potential (Figure 5.44A). Thereby, no difference between the control sequence C5 B2.71 and the aptamer C5.71 was observed (Figure 5.44A, B), which further proves that the aptamer C5.71 indeed inhibits neuronal Erk1/2 activity.

Moreover, it was investigated if the introduction of C5.71 or the C5 B2.71 control sequence during recording had induced off-target effects that could interfere with neuronal functions. Since neither C5.71 and C5 B2.71 altered the passive or active properties of CA1 neurons [354], the effects observed by C5.71 also do not seem to be mediated by off-target effects.

Taken together, it was shown in this chapter that aptamer C5 effectively inhibits a neuronal function that requires Erk1/2 activity. The introduction of the aptamer directly into the cytosol of neurons during whole-cell patch-clamp recordings provided a novel and generally applicable strategy which allowed both to modulate and to monitor kinase activity on single-cell level and in real-time. These data implicate that RNA aptamers can provide a new class of potent tools to manipulate intracellular kinase activity and to study signal transduction pathways in neurons.

6 Discussion

Protein kinase inhibitors represent valuable tools for therapeutic applications and chemical biology research. In order to investigate if RNA aptamers might represent a promising class of molecular tools that overcomes the limitations of other types of pharmacological inhibitors, distinct strategies were followed in this study:

First, the co-crystal structure of aptamer C13 and its target GRK2 was determined to unravel the molecular determinants which constitute to an ATP-competitive aptamers specificity (Section 5.1).

Furthermore, two novel Erk2-recognizing aptamers were throughly characterized (Section 5.2). Remarkably, both aptamer C3 and C5 bound to their target with huge tolerance to ionic conditions (Section 5.2.1.2). C3 and C5 also revealed high specificity (Section 5.2.3) and addressed distinct sites on Erk2 (Sections 5.2.4.1, 5.2.4.3). Thus, C3 and C5 were able to inhibit distinct functions of Erk2 (Sections 5.2.4.2, 5.2.4.4), highlighting the potential of RNA aptamers as domain specific inhibitors.

Most importantly, this study revealed that aptamers can be applied as intracellular inhibitors of kinase activity (Section 5.4). When introduced into neurons, aptamer C5 inhibited a neuronal-function that is known to require Erk1/2 activity (Section 5.4.4).

6.1 The co-crystal structure of GRK2 and C13 variants

In order to be used as research tools, protein kinase inhibitors should exhibit high specificity. In contrast to many small molecule protein kinase inhibitors, RNA aptamers have been shown to inhibit the function of their respective kinases with high specificity [127, 209, 210]. However, the precise aspects how ATP-competitive aptamers derive their specificity were yet unknown. For the investigation of the molecular determinants of this interaction, the co-crystal structure of RNA aptamer C13 with GRK2 was determined [209].

Figure 6.1 shows the co-crystal structure of GRK2 with the C13.28 aptamer variant in comparison to the ATP-competitive small molecule inhibitor Paroxetine [359]. ATP-competitive small molecules form one to three hydrogen bonds with the amino acids located in the hinge region of the kinase [33]. Thereby, they mimic the hydrogen bonds that are normally formed by the adenine ring of [35, 360]. They usually do not exploit the ribose binding site or the triphosphate binding site of ATP [33]. Due to the high conservation of the active site, ATP-competitive inhibitors often lack specificity [87–91].

The co-crystal structure demonstrates that aptamer C13.18 targets about 1,100 A^2 of accessible surface area, which is about the same surface area size involved in mediating protein-protein interactions [115]. Additionally, the co-crystal structure also shows that C13.28 is sterically more demanding than the small molecule inhibitor. Thus, the aptamer exhibit a higher likelihood of blocking protein-protein interactions. In general, these attributes may contribute to the capability of aptamers to be highly specific research tools.

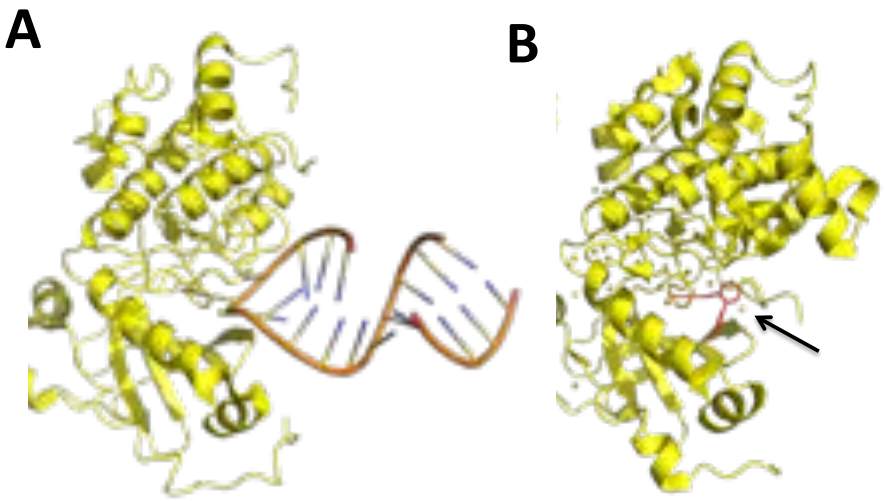

Figure 6.1: Interactions between the kinase domain of GRK2, C13.28 and a small molecule inhibitor. The interactions between C13.28 and the kinase domain of GRK2 (yellow, PDB entry 3UZS) comprise a bigger surface on the protein than the small molecule inhibitor Paroxetine (red, PDB entry 3V5W).

The co-crystal structure reveals the existence of a previously unknown conformation of GRK2 in which the axis of the kinase domain were rotated by 8° as compared to other ATP-bound GRK-complexes. Domain reorganization indicates that the aptamer not only binds to GRK2, but also induces a conformational shift in the protein structure. The reorganization of the kinase domain could prevent kinase activity and might be exploited by small molecule inhibitors that can be identified in C13 displacement assays.

Domain reorganization is not a unique feature of C13 but has also been demonstrated for the NF-KB- p50 aptamer complex [361]. A smaller degree of GRK2 kinase domain reorganization has previously been observed in structures of GRK2 bound to small molecule inhibitors [237, 239].

In summary, it could be demonstrated that C13 stabilizes a unique inactive conformation of GRK2 through multiple interactions, both within and outside of the kinase domain. It could be observed that a small part of the aptamer (nucleotides A49-C52) forms extensive interaction within the active site of GRK2 (Section 5.1.2). The most striking feature of the complex is the adenine nucleotide at position 51. Adenine 51 mimics the AMP moiety of ATP and is the key element of the aptamers interaction with GRK2. In this regard, C13 differs to ATP-competitive small molecule inhibitors, which usually do not exploit the ribose or the triphosphate binding sites [33]. Due to the low resolution of the complex, it was not possible to determine precise interactions at the atomic level. Nevertheless, it is very likely that A51 also forms a hydrogen bond to the hinge region of GRK2.

Outside of the active site, basic residues of the αF-αG-loop are also essential for aptamer binding (Section 5.1.4), likely because they form electrostatic interaction with the RNA backbone. Since all members of the GRK superfamily contain a basic αF-αG-loop but adopt different inactive conformation [315], the shape and size of the kinase domain seems to be important for the aptamer´s binding and specificity. In this regard, the aptamer differs from previously described GRK2 inhibitors, such as the rather unspecific inhibitor Balanol [362] or the Takeda compounds [238]. They achieve selectivity solely by conformational differences within the active site of a kinase domain [237, 239].

6.2 Sequence homology between ATP-competitive aptamers

Elucidating the precise determinants which contribute to aptamer C13´s high specificity has not only gained intriguing insights into the interaction of an ATP-competitive aptamers interaction with its target. This information has also aided in the identification of a novel inhibitor scaffold that might be applied to other aptamers.

Various ATP-competitive small molecule receptor tyrosine kinase inhibitors employ quinazoline moieties as scaffolds within their structure (Figure 6.2) [363, 364]. These scaffolds can serve as building blocks for kinase inhibitors in medicinal chemistry [365, 366].

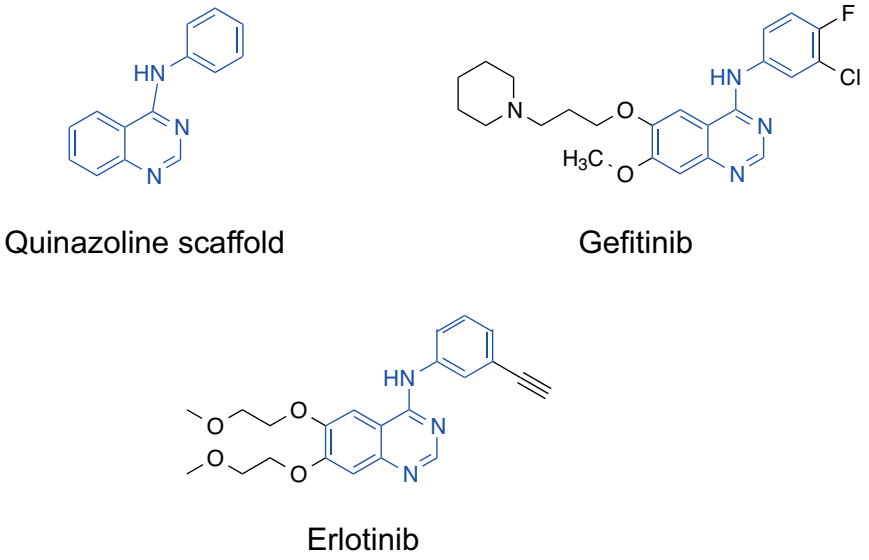

Figure 6.2: Quinazoline scaffolds in protein kinase inhibitors. The ATP-competitive small molecule cancer drugs Gefitinib and Erlotinib contain quinazoline scaffolds.

Nucleotides C47-C52 of the aptamer C13 have been shown to interact within the active site of GRK2 and could represent a nucleotide scaffold. A derivation of this motif was discovered in another RNA aptamer, termed K16 (Figure 6.3) [367]. K16 was selected against cyclin G-associated kinase (GAK) [367]. GAK belongs to the CMGC kinase family and not to the AGC family as GRK2. Except for this motif, aptamer K16 shows no overall sequence identity with C13. It is not clear yet if K16 also interacts with GRK2.

K16 GGGAGAGGAGGGAAGUCUACAUCUUAUCAGAAAGCGCCCAACUGAGAGCGUUGUUGC
C13 GGGAGAGGAGGGAGAUAGAUAUCAACUGCAGUUCGGGUAGCAC AGA

K16 GGCUGAUGCCACACGCAUAGUUUCUGGAGUUGACGAAGCU
C13 CCAUACGGGAGAGAAACUUGUGCAACCCGGGGCUACUUUCGUGGAUGCCACAGGAC

Figure 6.3: Sequence homology between C13 and K16. A variation of the ATP-mimicking motif of C13 was also found in the ATP-competitive aptamer K16.

K16 competes with ATP for binding to GAK. Thus, it is extremely likely that the motif also

mimics ATP-binding in the active site of cyclin G-associated kinase. The sequence of the motif in aptamer K16 is CCA**C**ACGG. The substitution of uracil for cytosine is in accordance with data from the co-crystal of C13 and GRK2, which revealed that the nucleotide at this position contributes its phosphate backbone for binding to the active site and not the nucleotide base (Section 5.1.2).

The existence of the ATP-mimicking motif of C13 in another aptamer may pave the way towards the development of other specific aptamers. For example, this motif might be included into a constrained library for the selection of novel aptamers with inhibitory properties. The specificity of these aptamers might be guided by unique epitopes outside of the active sites, or by shape, and/or size control.

Interestingly, the ATP-mimicking motif of C13 and K16 is absent in C5, TRA [210], or the PKC targeting aptamers [324]. Nevertheless, another putative ATP-mimicking motif can be found TRA and C5 (Figure 6.4).

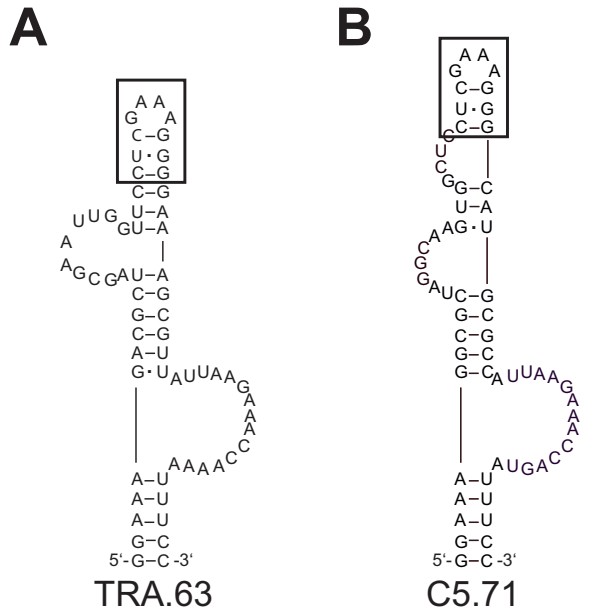

Figure 6.4: The putative ATP-binding scaffold of TRA and C5. Secondary structure prediction of A) TRA and B) C5. The putative ATP-binding motifs are annotated.

Hence, aptamers that inhibit kinase activity might employ versatile motifs for kinase recognition and specificity. Elucidating these motifs will not only clarify the aptamers mode of action, but may also reveal new, unresolved inhibitory entities that may serve as scaffolds for the identification of novel kinase inhibitors.

6.2.1 Identification of kinase inhibitors by aptamer displacement

Specific kinase inhibitors represent valuable tools for chemical biology research and therapeutic applications. Because of its excellent specificity, aptamer C13 represents a promising research tool to study GRK2 function. However, the lack of suitable techniques for systemic *in vivo* administration limits its potential as a drug in therapeutic settings [125]. For such purposes, small molecule inhibitors would be preferable [206]. Thal and co-workers used the C13.28 variant of aptamer C13 in a displacement assays for the identification of small molecule GRK2 inhibitors and identified Paroxetine as a direct inhibitor of GRK2 activity (Figure 6.5) [359].

Paroxetine also shares similar inhibitory properties as C13.28 and recognizes the ATP-binding site of GRK2 [359]. Paroxetine inhibits GRK2 activity within cells and increases cardiac contrac-

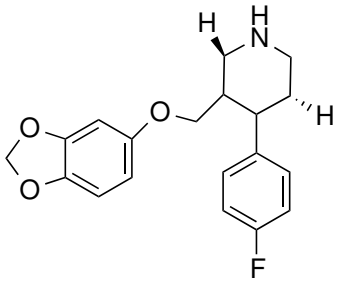

Figure 6.5: Chemical structure of Paroxetine. Chemical structure of Paroxetine. Paroxetine is a FDA-approved psychotropic drug for the treatment of mental disorders, e.g. major depression and anxiety disorders [368]. Paroxetine was also identified as a GRK2 inhibitor in a C13-28 aptamer displacement assay [359].

tility in isolated cardiomyocytes and myocardial β-adrenergic receptors inotrophic reserve in living mice. Strikingly, Paroxetine (DB00715) is actually a long known, FDA-approved psychotropic drug for the treatment of mental disorders, such as major depression, and anxiety disorders [368]. As such, Paroxetine is known to inhibit the human serotonin transporter (SERT) and to prevent the neuronal re-uptake of serotonin [369]. Furthermore, Paroxetine is described to inhibit the activities of the norepinephrine transporter (NET), cytochromes CYP2D6 and P450, and nitric oxide synthase [369, 370].

Not surprisingly, this lack of specificity limits the application of Paroxetine as a research tool. Like two sites of a coin, lack of specificity does not hamper the application of Paroxetine for mental disorders. However, at clinically relevant doses, Paroxetine has not been correlated with a large cardiovascular effect in adults [359], which limits its use for the treatment of heart failure. Subsequently, structure-activity relationship studies of Paroxetine were conducted to reduce the inhibitors activity towards the serotonin transporter [371]. The Paroxetine analogue designed exhibited a 20-fold decrease of activity towards serotonie uptake but also revealed an increase in the potency for inhibition of other AGC kinases.

The study by Thal and co-workers has shown that aptamer displacement assays offer a promising alternative to inhibitor identification with conventional strategies (Section 3.2.1.1). Many kinase inhibitors are obtained by the high-throughput screening of large compound libraries against a target kinase of interest [81, 82]. However, this approach is often based on *in vitro* kinase assays to detect hit compounds [372]. In cases where active kinase conformations or interaction partners are unknown, or when the identification of non ATP-competitive inhibitors is desired [373], it is challenging to identify a putative inhibitor.

In theory, aptamers might facilitate the identification of drug candidates for the complete disease-relevant kinome. They can be easily selected without any structural knowledge about the target protein or interaction partner [133]. Moreover, automated platforms nowadays enable the identification of highly affine and specific aptamers against hundreds of disease relevant targets in a short time [374, 375].

6.3 Characterization of the novel Erk2 aptamers C3 and C5

Aptamer C13 has proven that RNA aptamers can be powerful, selective protein kinase inhibitors that can even serve in the identification of novel aptamer- or small molecule-based kinase inhibitors. Next, the potential of aptamers as kinase inhibitors was investigated for the MAP kinases Erk1/2 (Section 5.2). Erk1/2 are particularly relevant targets because their pathway is deregulated in more

than 30% of all human cancers [304].

6.3.1 Sensitivity to ionic strength

Aptamers can easily be obtained from an iterative *in vitro* selection process, termed SELEX [131, 132]. This technique allows to pre-select for molecules that are stable and can bind to their target under desired conditions. TRA, the first Erk2-recognizing aptamer, was selected in the absence of monovalent cations [210]. However, the aptamer lost its ability to interact with Erk2 in the presence of monovalent cations. (Section 5.2.1.1).

Metal ions play a crucial role in determining the structure, stability, and biological properties of RNA [376]. Cations can accumulate near the RNA backbone and shield electrostatic interactions [377–379] or contact electronegative pockets within the RNA structure itself [376]. In addition to RNA folding, metal ions can also be critical for structural and functional aspects of proteins [380, 381]. The addition of monovalent cations could interfere with the recognition of Erk2 by destabilizing structural elements within the structure of TRA. A study by Lambert and co-workers has shown that some secondary and tertiary structures, such as a hairpin and a pseudoknot structure, were insensitive to ion identity, whereas other tertiary structures become more stable with decreasing ion size [382]. Smaller ions seem to be able to approach the RNA surface more closely and thereby affect stacking or electrostatic interactions. This, in turn, might affect the RNA fold.

Thus, new selections were performed to identify aptamers with the ability to bind to Erk2 in the presence of monovalent cations. Aptamer C3 and C5 were selected in an isotonic high salt buffer and revealed their remarkable ability to bind to Erk2 with high tolerance to distinct monovalent cations and magnesium ion concentrations (Section 5.2.1.3). However, this was quiet surprising because C3 and C5 were selected without any selection pressure towards ionic strength. This selection scheme could have also resulted in a loss of affinity for Erk2 in the absence of monovalent cations or presence of cytosolic ion concentrations.

Although C3 and C5 was not selected for binding to Erk2 under cytosolic conditions, their tolerance to ionic strength could have played an important role for the application of C5 as an intramer. Therefore, for future aptamers with the final goal of intracellular application, the presence of monovalent cations, cytosolic buffer conditions or selection pressure towards insensitivity to monovalent cations during the SELEX process, should be considered. Literature suggests that many intramers have been selected in the presence of monovalent cations and magnesium, either in PBS buffer [182, 183], or in Hepes but with $MgCl_2$ and with additional NaCl [195] or KCl [186, 202].

One reason why C3 and C5 are not affected by different monovalent cation concentration could be presence of secondary and tertiary structures, which are independent of cation identity [382]. C5 could be less sensitive to monovalent cations than TRA due to twelve mutations, which are located mainly in the central stem and upper bulged region (Figure 3.15). These mutations could lead to a stabilization of the central stem and allows the building of additional base pairs at the upper stem, rendering its overall fold less sensitive to cationic strength. Therefore, it should be investigated which mutation and structural differences between C5 and TRA affect their (in)sensitivity to monovalent cations.

As mentioned above, metal ions can also be critical for structural and function aspects of proteins [380, 381]. ATP-competition and kinase activity assays strongly suggest that C5 and TRA target the active site of Erk2. Most protein kinases, including Erk2, require Mg^{2+} ions within their active site for coordinating ATP and catalytic reactions [383]. Hence, it is not unlikely that the interaction of TRA or C5 within the active site is facilitated by a bridging magnesium ion, as was observed for C13 and GRK2. A decrease in magnesium concentrations could lead either to a decrease of bridging magnesium ions, rendering TRA and C5 unable to bind to Erk2.

6.3.2 Affinity and specificity

As was already shown for aptamer C13 (Section 5.1), this study confirms that affine and specific aptamers can be seleceted for by SELEX. A magnetic bead-based SELEX strategy (Section 3.4.2.5) led to the identification of aptamers C3 and C5, which bound with high affinities in the low nM range to Erk2 (Section 5.2.1.2). Their affinities are in the same range as the affinities of aptamers for other kinase targets [209, 210, 324]. The Hill coefficients of the interactions lay between 1.1-2.2, which argues that indeed only one aptamer binds to the target molecule.

A detailed comprehensive assessment of the specificity of C3 and C5 was performed across the kinome families. It revealed that aptamers C3 and C5 bind to the MAP kinase Erk1 and Erk2, which share sequence homology of 85%. The main difference between Erk1 and Erk2 is the presence of 19 additional amino acids in the N-terminus of Erk1. The N-terminus of Erk1 was shown to be responsible for the slower nuclear shuttling rate of Erk1 in comparison to Erk2 [384].
Moreover, no binding of C3 or C5 to other JNK and p38 MAP kinases, which share >40% overall homology within the kinase domain [385], could be detected. Additionally, C3 and C5 do not bind to other tested kinases from different subfamilies.

High specificity is an important requirement for the application of protein kinase inhibitors as research tools. There are on the order of 20,000 different types of proteins in the cell [323]. At high inhibitor concentrations, it becomes increasingly likely that an inhibitor will bind to unintended targets [386]. Even weak interactions with other kinases within cells, could bring out the so-called "albumin problem", which was described by Gold and co-workers for analyte detection [387]. For example, an inhibitor could bind with an affinity of 1 nM to a kinase target and with an affinity of 1 μM to a second, unintended kinase. If the unintended kinase is present at 1 μM, the inhibitor would bind to half to the intended and half to the unintended kinases, and thus, could induce secondary effects.

With an intracellular concentration of 1 μM [337], MAP kinases belong to the most abundantly expressed kinases in mammalian cells [388–390]. A study in yeast cells has shown that 63 % of the cellular protein kinases are expressed at a concentration between 1 and 50 nM, and only 11 kinases (13 %) are expressed at higher concentrations than 150 nM [391]. These values provide an estimation that the protein concentration used in the specificity panel (Section 5.2.3) was far higher than the intracellular concentration of most protein kinases. Hence, the lack of binding of C3 and C5 to other kinases suggests a high degree of specificity against the remainder of the kinome.

6.4 Modes of action

This study has shown that aptamers do not only bind with high affinity and specificity to their target. It could also been demonstrated that aptamers bind to distinct sites on one target and block kinase functions in ATP-competitive or non-ATP competitive manner (Sections 5.2.4.2, 5.2.4.4).

6.4.1 Aptamer C5

Aptamer C5 was identified by performing a reselection against active Erk2 with a partially constrained library based on the sequence of TRA (Section 3.4.2.5). Aptamer C5 competes with ATP for Erk2 binding and inhibits Erk2 activity (Section 5.2.4.2).

The potential of C5 to inhibit Erk2 activity was evaluated in two distinct kinase assays. In the first assay reported here, active Erk2 was employed and its ability to phosphorylate target proteins was measured (Section 5.2.4.2). The addition of C5 resulted in a marked reduction in

phosphorylated MBP and Elk-1. In this assay, C5 demonstrates similar potency as the ATP-competitive inhibitor FR180204 [310, 325].

The second assay utilized a kinase cascade in which inactive Erk2 becomes activated by a constitutive active Mek1 kinase [332]. Erk2 activity was measured by substrate phosphorylation (Section 5.2.4.3). C5 also inhibited Erk2 activity in this assay. However, it was observed that higher concentrations of C5 were needed to inhibit Erk2 activity than in the Erk2 activity assay. It should be kept in mind that the lowest IC_{50} value that can be measured equals half the kinase concentration in the assay [323]. Since higher kinase concentrations were utilized in the second assay (Erk2 activity assay: 60 nM Erk2, Erk2 activation assay: 1000 nM Erk2), higher concentrations of C5 were needed to inhibit Erk2 activity.

The ability of C5 to compete with ATP strongly suggests that C5 acts via the ATP-binding site of Erk2. In addition, the higher affinity of C5 to the active conformation of Erk2 also hints into the direction that C5 targets a structural aspect which is more prominent in active Erk2 than inactive Erk2. These structural features that discriminate active from inactive Erk2 include the activation loop, the MAP kinase insert and the L16 segment from the N-terminal domain [392]. Since the binding of C5 was not affected by mutations within the MAP kinase insert or D-site recruitment site (DRS) docking domain (Section 5.2.4.3), these domains likely do not contribute to the binding region of C5.

The precise inhibition mechanism of C5 remains to be investigated. The interaction of C5 with Erk2 could prevent ATP or substrates from binding to Erk2, and could induce conformational changes in the kinase domain that lock Erk2 into an inactive state, as was shown for C13 and GRK2 [315].

Given the high specificity of C5, the aptamer provides great advantages over other ATP-competitive Erk1/2 inhibitors to study signal transduction pathways. For example, Ohori and co-workers identified FR180204, an Erk2 inhibitor that recognizes the ATP-binding pocket of Erk2 [304, 389]. Its specificity was tested against only four kinases belonging to the MAP kinase family [389]. Another ATP-dependent inhibitor of Erk1/2, called FR148083, was identified by screening compounds generated from a fermentation culture broth [390]. This compound interacts with Mek1 and probably other kinases [390].

6.4.2 Aptamer C3

Aptamer C3 was selected against the inactive conformation of Erk2 (Section 3.4.2.5). C3 binds with similar affinities to active or inactive Erk2 (Section 5.2.1.2). In contrast to C5 or TRA, it does not compete with ATP for Erk2-binding and does not inhibit the catalytic activity of Erk2 (Sections 5.2.4.2, 5.2.4.4).

6.4.2.1 The putative binding site of C3 comprises the MAP kinase insert of Erk2

Binding studies with Erk2 docking domain mutant proteins were performed to investigate the putative binding site of C3 (Section 5.2.4.3).
These studies revealed a complete loss of affinity of C3 for point mutations at tyrosine 261 to asparagine (Y261N), and serine 264 to proline (S264P). A mutation of histidine 230 to arginine (H230R), or aspartate 319 to asparagine (D319N) did not affect the binding of C3 to Erk2. Tyrosine 261 and serine 264 are located in close proximity to the activation loop of Erk2 (Section 5.2.4.3).

As crystal structures of the Erk2-C3 complex are not available, it can only be estimated how the mutations described here might impair C3-Erk2 complex formation. It is possible that C3 might directly interact with both tyrosine 261 and serine 264 in Erk2-C3 complexes. This accentuates the fact that mere changes of amino acids can have great impact on the binding of C3 to Erk2. The substitution of tyrosine 261 to asparagine could prevent stacking interactions between the aromatic side-chain of tyrosine with the ribonucleic acid bases. Furthermore, the asparagine side-chain could

form hydrogen bond interactions with the aptamer that could affect its fold or interaction with other residues. The S264P mutation might impair hydrogen bond interactions that could be formed by serine 264.

More likely, the mutations Y261N or S264P might affect the binding of C3 indirectly, by altering the conformations of other Erk2 residues critical for aptamer binding.
The Erk2 point mutants H230R, Y261N and YS264P have been identified in a yeast two hybrid screen based on their inability to interact with Erk2 [295]. Some mutant proteins were described to have an adverse effect on protein kinase activity. The Y261N mutant protein showed a 3.5-fold increase in the apparent K_M for MBP (Erk2: 11 μM, Y261N: 38 μM) whereas the S264P and N236K mutants retained similar kinetic behavior as Erk2 wild-type [295].

The reduced catalytic activity of the tyrosine mutant raises the possibility that the conformation of the activation loop or other structural aspects of the C-terminus of Erk2 were affected by the point mutation Y261N [295, 393]. Tyrosine 261 is located in close proximity to other residues that form direct contacts with the activation loop [295]. In turn, local conformational changes could explain the more pronounced effect of the Y261N mutation on C3 binding as compared to the S264P mutation.

The mutation of tyrosine 261 to alanine has previously been reported to disrupt the interactions between Erk2 and Elk-1 in a GST-pulldown assays [293]. The finding that C3 was not able to inhibit Elk-1 phosphorylation (Section 5.2.4.2) supports the notion that the binding of C3 to Erk2 induces conformational changes in the Erk2 structure.

Serine 264 is not located in close proximity to amino acids that directly engage in interactions with the activation loop [295]. The substitution of serine to proline might induce smaller alterations within the local conformation of the MAP kinase insert which affects the aptamers binding. Prolines are known to disrupt protein secondary structures because they are unable to adopt a normal alpha-helix or beta-sheet conformation [394, 395].

Although the binding data obtained in this study provide strong hints about the putative binding region of aptamer C3, high-resolution crystal structures of the Erk2-C3 complex should be obtained in the future. Such structures will provide substantial insight into the recognition of Erk2 by C3 and will reveal how specific mutations disrupt this interaction.

The putative binding site of C3 on Erk2 was shown to be comprised of residues 261 and 264. It is also likely that C3 recognizes a positively charged amino acid cluster (bold letters, Erk2 residues 257-275: **K**A**R**NYLLSLP**HK**N**K**VPWN**R**) that surrounds tyrosine 261 and serine 264. This cluster was described to mediate the DNA binding activity of Erk2 and thus, might engage in the C3-Erk2 complex via electrostatic interactions [301].

Tyrosine 261 has been reported to belong to the F-site recruitment site (FRS) docking domain of Erk2 which interacts with many targets, including Elk-1, c-fos, SAP1 and the kinase suppressor of Ras (KSR) [57]. Tyrosine 261 and serine 264 are also located within the MAP kinase insert domain of Erk2. The MAP kinase insert has been associated with diverse functions, including transcriptional regulation or protein-protein interactions [329]. It is located at the C-terminus (Section 3.4.2.2), which would explain both the inability of C3 to compete with ATP-binding for Erk2 (Section 5.2.4.1), and to block kinase activity towards MBP (Section 5.2.4.2).

The MAP kinase insert domain is unique for MAP kinases, cyclin-dependent kinases and glycogen-synthase kinase 3 (GSK3) [396–398]. Hence, the aptamers high specificity might be derived from the inserts unique sequence composition. By targeting a unique region on Erk1/2, it is very likely that increased selectivity of aptamer C3 will be achieved compared to ATP-competitive Erk2 inhibitors.

6.4.2.2 C3 inhibits the activation of Erk2 by Mek1

Investigating the functions of individual protein domains is extremely challenging. A common method to study the function of a domain is the overexpression of a mutated variant of the protein [399]. However, this approach can affect protein folding, complex assembly and downstream regulation, and thereby provide inaccurate results [400].

Employing specific inhibitors that target a specific domain without affecting kinase activity, would avoid the problems associated with protein over-expression. There are only few domain-specific Erk2 inhibitors available for the D-site recruitment site (DRS), which include small molecule inhibitors [401, 402], or peptides that were derived from Mek kinases [403]. In addition, Kummer and colleagues described E40, a protein derived from ankyrin repeat proteins (DARPin), which targets the Thr-Glu-Tyr phosphorylation motif and the MAP kinase insert of inactive Erk2 [404]. However, this inhibitor cannot be used to study MAPK domain specific functions without targeting the activation loop at the same time.

At present, no small molecule inhibitor for the MAP kinase insert of Erk2 is available. In this study, it was investigated if C3 could block a specific function which is associated with the MAPK insert, namely the activation of Erk2 by its upstream kinase Mek1 [328]. In an *in vitro* kinase activation cascade assay, aptamer C3 inhibited the activation of Erk2 by a constitutive Mek1 mutant [332] and prevented downstream phosphorylation (Section 5.2.4.4). This indicates that C3 is indeed a domain-specific inhibitor.

The inhibitory concentration of C3 of 1 μM is in accordance with data from the literature. Similar kinase activation assays were used to monitor the potency of small molecule inhibitors that target the MAP kinase inserts of either JNK or p38 MAP kinases by Comess and co-workers [405]. Their most potent candidate inhibited the activation of JNK by its respective MAPK kinase with an IC_{50} value of 3.8 μM [405]. Additionally, C3 blocks Erk2 activation as potent as the Mek1-derived peptide inhibitors (2.5 μM, [403]).

DARPin E40 was also shown to inhibit the activation of Erk2 inside cells [404]. However, it was not investigated if this inhibition resulted from blockage of the Thr-Glu-Tyr phosphorylation motif alone or required the combination with the MAP kinase insert. The distinct affinities of C3 and E40 do not imply that C3 and DARPin E40 share the same molecular mechanism for the inhibition of Erk2 activation. DARPin E40 targets only the inactive Erk2 conformation and likely prevents the activation of Erk2 by Mek1 by shielding the Thr-Glu-Tyr phosphorylation motif [404]. In contrast, C3 binds with similar affinities to the active and inactive conformation of Erk2. Therefore, it is unlikely that C3 and DARPin E40 share the same modes of action.

More likely, however, would be an unique allosteric mode of action of C3, which was also postulated for the MAP kinase insert -specific inhibitors of JNK or p38 MAP kinases [405]. For example, C3 could impair Mek1-Erk2 complex formation by binding to tyrosine 261, serine 264, and other Erk2 residues. Another possibility would be that C3 induces a conformational change that does not necessarily prevent Mek1 from binding but inhibits the conformational rearrangement required for Erk2 activation. For example, binding of C3 might alter the conformation of the activation loop or enforce the conformation of the activation loop to a catalyticaly inactive state.

It has been described that Mek1 phosphorylates Erk2 on Tyr185 prior to phosphorylating Thr183 [406, 407]. Tyr185 is buried in unphosphorylated Erk2 and requires a conformational rearrangement in the activation loop for the hydroxyl of Tyr185 to enter the active site of Mek1 [408]. Hence, binding of C3 might block this conformational change. This notion is supported by the fact that the putative binding side residues of C3, serine 264 and tyrosine 261, are located in close proximity to the activation loop [295].

It could also be observed that C5 inhibits the activation of Erk2 by Mek1, albeit more than 10 times higher concentrations of C5 were needed than C3 to yield an inhibitory effect (Section 5.2.4.4). One reason for this could be that the aptamer interferes with Mek1 binding or blocks conformational changes.

In summary, this study implicates that C3 blocks Erk2 activity with a novel mode of action. The MAP kinase insert was described to contribute to diverse kinase-dependent and -independent functions of Erk2 [324]. C3 could provide a valuable tool to study them.

6.5 Investigation of aptamers as intracellular kinase inhibitors

Given their high specificity and ability to disrupt distinct kinase functions, aptamers may provide a novel class of molecular tools to dissect the function of particular protein kinases within complex signal transduction cascade. To estimate the capability of aptamers as protein kinase inhibitors within cells, several methods for their delivery into cells, cellular assays, and possible off-target effects, are discussed here. Taken together, these findings enabled the discovery that aptamers can be applied in neurons to elucidate the involvement of individual protein kinases in neuronal function.

6.5.1 Aptamer expression vector

In order to investigate if aptamers can be employed as intracellular kinase inhibitors, it was analyzed if expression of RNA aptamers within cells allows for targeting of intracellular protein kinase activity. In an initial approach, the aptamers or control sequences C5sc, C3sc, and C5 B2, were cloned into a Polymerase III-based expression vector, which is usually employed to facilitate the expression of high levels of shRNA via a U6 promoter [338]. An aptamer against the transcription factor NF-kappaB has been successfully transcribed and used with a similar expression system [181].

In the luciferase reporter gene assay, which was conducted in HEK 293 cells, no influence of the aptamers C3 or C5 was observed under the tested conditions (Section 5.3.2.3). Curiously, only the control sequence C5sc and small molecule inhibitors blocked luciferase activity after 24 hours.

The activity of C5sc in the luciferase assay argues to the fact that the RNAs were indeed transcribed inside the cell. Strikingly, C5sc does not bind to Erk2 or any other tested kinases *in vitro* (Section 5.2.3). Therefore, its effect on Erk1/2 MAP kinase signaling in the luciferase assay might result from interaction with one or more unintended proteins. This interaction might, in turn, induce off-target effects. The Erk1/2 signal pathway is frequently controlled by cross-talk with other signal transduction pathways [409–411]. Interference of C5sc with another signal transduction pathway, such as the stress-activated JNK MAPK pathway [412], can promote an decrease in Erk1/2 activity, which could be measured by a drop in luciferase activity.

Despite the biological activity of C5sc, it is not clear if sufficiently high concentrations of C3 and C5 RNAs were transcribed to block Erk1/2 activity. A study has shown that expression of anti-Rev aptamers via U6 constructs in cell culture yields 10^3 to 10^4 molecules per cell [170]. If similar RNA concentrations would be obtained by the expression system in this study, the intracellular RNA concentration may be too low to block Erk1/2 signaling.

Another plausible way to describe the discrepancy between the NF-kappa B aptamer and the Erk2 recognizing aptamers might be their affinities. The NF-kappa B aptamer was described to bind with a K_D value of 1 nM to its target *in vitro* [195]. In contrast, the Erk2 recognizing aptamers were more than 15-times less affine (Section 5.2.1.2), which might result in a lack of biological activity.

For intracellular expression, aptamer sequences are often expressed between flanking regions or as multivalent constructs [185]. To achieve this, the aptamers are fused to tRNAs, self-cleaving ribozymes, aberrantly spliced mRNAs, or embedded into U6 small nucleolar RNA [175, 184, 185]. For some aptamers, the addition of sequences from small RNA molecules, such as U6 snRNA, may lead to 10-fold higher expression levels and sometimes also to increased stability [170]. In turn, the design of expression constructs of C3 and C5 without any flanking sequences could have impaired their stability.

The expression constructs of C3 and C5 contain of about 110 nucleotides, which is four times the length of the NF-kappaB aptamer [181]. Speculations can be made if the longer constructs of C3 and C5 were more prone to misfolding or instability. The termination of transcription of the RNA constructs should stop at a defined stretch of 6 thymidines, which is located directly at the 3´-end of the coding DNA sequence [413]. It is supposed that the aptamers or control sequences contain 3 uridine residues, which have been shown not to affect their interaction with Erk2 *in vitro* (Section 10.5). Of course, it is possible that incorrect transcription occurs.

Additionally, the intracellular stability of C3 and C5 could be influenced by the endogenous ncRNA processing machinery. Cellular RNAs often undergo post-transcriptional modification during their maturation [414]. For example, mature U6 RNA, which is involved in splicing [415], undergoes site-specific pseudouridylation, 2´-O-methylation and acquires a gamma-monomethylphosphate cap structure [416]. It could be possible that modifications are introduced into C3 or C5. These modifications might affect their interaction with Erk1/2.

In turn, a lack of modifications could also target C3 and C5 as aberrant RNAs for degradation by RNA surveillance system. For polymerase III transcripts, this can occur via poly(A) addition by the TRAMP complex and 3´ degradation by the exosome [417]. Evidence for this mechanism was reported for 5S rRNA, U6 snRNA, the RNA component of signal recognition particle, and pre-tRNAs [418, 419].

Another regard has to be made about the intracellular localization of of C3 and C5. shRNAs are expressed in the nucleus and are recognized by the endogenous RNAi machinery, which facilitates further processing and export from the nucleus [420]. In contrast, U6 RNA is retained in the cytosol [421]. Due to a lack of obvious nuclear export or retention sequences, it is not clear if the aptamers are retained in the cytoplasm or nucleus. However, Erk1/2 is active in both cellular compartments [245]. Therefore, the aptamers should block Erk1/2 activity independently of its localization.

Aptamers have been transcribed through RNA polymerase II or III promoters in the expression cassette (Section 3.3.3). In turn, modulation of target protein function was achieved for distinct classes of proteins, such as transcription factors, or viral proteins [167, 168]. However, neither C3 nor C5 blocked Erk1/2 activity under the tested conditions. The intracellular RNA concentration, stability, and localization should be investigated in future studies in order to answer the question which expression system does allow to monitor aptamer-based control of intracellular Erk1/2 activity.

6.5.2 Effect of C3 and C5 on Erk1/2 signaling after transfection

Subsequently, it was tested if transfection of *in vitro* transcribed aptamers represents a suitable strategy to study the aptamers effect on Erk1/2 MAP kinase signaling. Exogenously synthesized aptamers do not rely on the host cells transcription machinery and can be tested for binding and functionality before their application inside cells. Moreover, *in vitro* transcribed RNAs can easily be modified to improve stability, and to introduce chemical functionalities (Section 3.3.2).

Several preliminarily experiments have validated the suitability of this experimental set-up. As can be seen in Section 5.3.1, both aptamers recognized not only recombinant Erk2, but also the endogenous protein. In addition, it was observed that fluorescein-labeled RNA aptamers can easily be transfected in a concentration-dependent manner (Section 5.3.3.1). In theory, intracellular RNA concentrations up to 6 μM could have been achieved. This concentration was high enough to block Erk2 activity and activation *in vitro*.

In comparison to the aptamers, the application of small molecule inhibitors induced a reduction of Erk1/2 signaling (Section 5.3.3.2), which is in line with previous observations [310, 422]. Thereby, the Mek1/2 inhibitor U0126 revealed higher potency than the Erk1/2 inhibitor FR180204 (Section 5.3.3.2). The lower potency of the ATP-competitive inhibitor FR18204 can be explained by the fact that the inhibitor must compete with high intracellular ATP levels [423].

The discrepancies between the Mek1/2 and Erk1/2 inhibitors might also result from lower cell-permeability of FR180204 or off-target effects which are mediated by U0126 [88, 89]. For example, U0126, which was identified as a Mek1/2 specific inhibitor, is known to inhibit the activation of Erk5 by Mek5 as potently as the activation of Erk1/2 [424, 425]. This, for example, could explain the stronger effects on p90-RSK1 phosphorylation, which is also mediated by Erk5 [426].

However, when C3 and C5 were transfected into H460 or A431 cells, no inhibitory effect on Erk1/2 activation or target protein phosphorylation was observed (Sections 5.3.3.3, 5.3.3.4). Strikingly, C5sc, which inhibited Erk1/2 signaling in the luciferase assay (Section 5.3.2.3), induced an increase in p90-RSK1 phosphorylation in distinct cells lines. Moreover, transfection of RNA into H460 impaired cell viability in a time- and concentration-dependent manner (Section 5.3.3.5).

Although nuclease-mediated degradation is a major concern when working with RNA aptamers, it is unlikely that the RNAs were completely degraded inside the cytoplasm because of the observed secondary effects. Theis *et al.* have also shown that a RNA aptamer and a random library were stable for 18 hours after transfection [188]. However, studies with siRNA showed that 4 hours after transfection, the majority of transfected siRNA remained in lipid vessels [427]. It might be possible that the aptamers were stuck in the endosomal/lysosomal compartment and the concentration of C3 and C5 might have been too low to block Erk1/2 signaling in the cytoplasm or nucleus.

Since the intracellular RNA localization and stability are unknown, it cannot be completely excluded that transfection of RNA aptamers represents a suitable method to study signal transduction pathways. Therefore, future studies should investigate the aptamers endosomal escape, cellular localization, and stability after transfection.

However, at one point, the cytosolic concentration was high enough to induce secondary effects. Only a few studies described the use of unmodified RNA aptamers to block intracellular signal transduction cascades but did not mention if off-target effects occurred [188, 189]. Studies with siRNA have shown that RNAs can elicit a variety of unintended responses in the cells [76, 77]. The cytotoxic effects of siRNAs or shRNAs can be associated with activation of RNA receptors [428], oversaturation of the endogenous microRNA processing machinery [429, 430], or sequence complementarity to other RNAs [431]. These effects can induce a reduction of cell viability similar to the effects observed in this study.

RNA receptors serve as an integral component of the human innate immune response to an invasion of RNA viruses [432]. Ultimately, RNA receptors can initiate pro-apoptotoc signaling cascades and up-regulate the expression of cytokine and chemokines, including type I interferons [433–435]. In non-immune cells, RNA receptors include double-stranded (ds)RNA-activated protein kinase (PKR) [436] and the retinoid acid-inducible gene (RIG)-I-like helicase (RLH) family members RIG-I and melanoma differentiation - associated protein 5 (MDA-5) [437–440].

The RNA aptamers contain several elements which makes them suitable targets for recognition by RNA receptors: Both RIG-1 and PKR are known to recognize *in vitro* transcribed RNA with 5´-triphosphate moieties as ligands [432, 441]. The 5´-triphosphate serves a hallmark to identify RNA as non-self and potentially pathogenic because cellular RNAs are typically capped by 7-methylguanosine at its 5´-end [432].

In addition to the presence of the 5´-triphosphate, structural aspects also play a role in RNA recognition by RIG-1 and PKR. RIG-1 requires the minimal combination of a double stranded stretch of 5-10 bases of RNA, together with a 5´-triphosphate end, to induce a response [442]. PKR can be activated by highly structured single-stranded RNAs with imperfect loops, bulges and single-strand tails [443–447] or unstructured ssRNA transcripts if a 5´-triphosphate is present [448].

Of course, it might be possible that the aptamers bind unspecifically to endogenous RNAs or are subjected to processing, as discussed before (Section 6.5.2).

In addition, this study shows that control sequences must be chosen with great care because

some RNA sequences elicit stronger secondary effects. Transfection of C5sc resulted in hyperphosphorylation of p90-RSK1 in C5sc transfected H460 cells (Section 5.3.3.3). A likely candidate that could mediate this phosphorylation might be Erk5, as it is known to phosphorylate p90-RSK on the same sites as Erk1/2 [426]. Erk5 activity has been found to increase in response to growth factors, serum, oxidative stress, and hyperosmolarity [449], and might also be activated due to the cytotoxic effects of C5sc.

The different effects of TRA on p90-RSK1 phosphorylation in H460 and A431 cells might be explained by differences in the genetic backgrounds of the cell lines. For example, both cell lines have different status of the tumor suppressor protein p53. A431 cells express mutated p53 whereas H460 cells contain wild-type p53 [450–452]. The p53 gene status, e.g. has been reported to modulate the chemosensitivity of non-small cell lung cancer cells by Lai and co-workers [452]. Their study suggests that an increase in chemosensitivity was attributable to wild-type p53 mediation of apoptosis. Hence, p53 gene status might also mediate distinct responses to cytotoxic RNA effects that could lead to variable side-effects.

Because of the secondary effects that were observed, assay conditions should be optimized to reduce these effects. Studies with siRNA and shRNA have shown that secondary effects can be prevented if lower concentrations of RNAs or chemical modified RNAs are used [453–456]. Thus, the selection for modified aptamers with higher affinity should be considered. By employing modified nucleotides [387], capillary electrophoresis (CE), or high-throughput sequencing–RNA affinity profiling [457] to SELEX, a vast improvement of selection efficiency and aptamer affinity for protein targets could be achieved [458].

6.5.3 Investigation of the aptamers effect on the Erk1/2 signal transduction pathway in neurons

In order to circumvent any problems which could be associated with cellular RNA localization and endosomal escape, the RNAs were directly injected into CA1 pyramidal neurons. By using fluorescent dyes, it was implicated that the aptamers diffuse within 20 minutes from the recording electrode into the distal dendrite (Sections 5.4.2).

Furthermore, this study has shown that C5 inhibits a rise in voltage potential, which is known to be dependent on Erk1/2 activity, and does not affect any of the tested neuronal Erk1/2 independent functions. These data are in accordance with previous studies, which utilized the Mek1/2 inhibitor U0126 [282, 357], and indicate that C5 inhibits a neuronal Erk1/2 function (Section 5.4.4).

In summary, the application of aptamers during whole-cell patch clamp-recordings has emerged as a unique and generally applicable strategy to monitor spatio-temporal effects on protein kinase inhibition during neuronal functions (Section 5.4). One main advantage of the microinjection measurements is that fact that the RNAs were injected directly into the cytosol and allowed to bypassed the endosomal/lysosomal compartment. The aptamers effects on kinase function could be monitored relatively rapidly, so that indirect or prolonged secondary effects on Erk1/2 signaling, such as decrease in cell viability or cross-talk with other signal transduction pathways, might have been minimized.

Since the cellular RNA concentration and stability after RNA transfection and expression are unknown, future studies should validate the aptamers ability or inability to block growth factor induced signaling on single-cell level after microinjection.

Another reason that could explain the aptamers effect on neuronal Erk1/2 signaling might result from high local Erk1/2 concentrations in the soma as opposed to putatively low local Ek1/2 concentrations within the dendrites. In cultured cells, Erk1/2 are known to translocated within 5 minutes into the nucleus after growth factor stimulation which leads to a decline in cytoplasmic

Erk1/2 [245]. The increase in nuclear Erk2 upon stimulation of dendritic spines takes at least 10 minutes [459]. However, it is yet unclear if the dendritic Erk1/2 pool depletes after stimulation and migrates from the dendrites into the nucleus [460] or if the pool of dendritic Erk1/2 is even lower than the pool of somatic Erk1/2.

The inability of C3 to inhibit neuronal Erk2 function might be considered as a further indication that intracellular activity of aptamers underlies functionality. C3 was neither capable of blocking a MAP kinase-independent function *in vitro* (Sections 5.2) nor in neurons (assuming that C5 affects K_V4.2 activity, Section 5.4.4).

The putative binding site of K_V4.2 for Erk2 contains a cluster of positively charged residues on the channels C-terminus channel [461]. This cluster argues for D-site mediated Erk1/2 - K_V4.2 - interaction [50]. Nevertheless, C3 revealed the ability to block both Erk2 activation and downstream signaling *in vitro* (Section 5.2.4.4). Hence, by blocking the activation of Erk1/2, it would have been likely that C3 is capable of altering the increase in voltage potential associated with Erk1/2 activity.

Notably, the effect of C3 on Erk2 activation was tested with both artificial activators and substrates under conditions that differ from the cytoplasm. Inside the cytoplasm, inactive Erk1/2 are either tethered to Mek1/2 or other anchor proteins [462] or exist with Mek1/2 and other upstream components in macrocomplexes with scaffold proteins [262]. Hence, the binding site of C3 would already be occupied within the cytoplasm. Since the interaction of the MAPKK-MAPK complex has been reported to be in the low nM range, e.g. 65 nM for Erk5 and Mek5 [463], it is very likely that higher concentrations of aptamer C3 will be needed to disrupt this interaction, block Erk1/2 activation, and neuronal functions.

In light of the observation that MAP kinase insert inhibitors of JNK were reported to be active at higher concentrations (10 μM) than a respective ATP-competitive inhibitor (1 μM) [405], C3s effect on neuronal MAP functions will be investigated at higher concentrations (10 μM).

6.6 Aptamers represent promising tools for chemical biology research

Protein kinases are key regulators of signal transduction pathways and control virtually all aspects of cellular life [66]. Protein kinases are so important for maintaining cellular homeostasis that deregulated kinase activity can cause or contribute to the progression of severe human diseases. For example, kinases have been identified to be the most frequently mutated proteins in cancer and are linked to cancer cell proliferation and survival [464, 465]. Over the last decades, a strong desire has emerged to unravel the precise biological role of the more than 500 human kinases during cellular homeostasis and disease biology [7, 24]. This knowledge can aid in the development of novel therapies [62].

Unfortunately, the comprehensive functional analysis of individual protein kinases within complex signal transduction cascades has remained one of the greatest challenges in molecular biology. Research into the biological role of single kinases has been hampered by a lack of specific tools [64, 65]. A key reason for the continued failure to produce specific inhibitors arises from the fact that the vast majority of kinase inhibitors are small molecules that target the ATP-binding site, which is highly conserved among the kinome [94]. ATP-competitive small molecule inhibitors are often found to exhibit undesirable off-target effects on multiple kinases or non-kinases, including ion channels [321, 466]. In fact, the side-effects have precluded these inhibitors from being useful research tools [467].

Aptamers are an emerging class of molecules that could represent a promising alternative to other types of pharmacological agents. Aptamers can be selected rapidly without the need for high-throughput screening facilities or even any structural information about the target protein or its interaction partners [468]. Like small molecules, aptamers can easily be synthesized, modified

in large scale, and can be administered in a dose-dependent manner [130, 167].

Importantly, the application of aptamers offers promising advantages over small organic molecules for diverse applications: aptamers can be linked with other RNA aptamers or functional entities to form multifunctional complexes, such as fluorescent biosensors for live-cell imaging. This has been demonstrated by using genetically encoded aptamer sensors for cellular metabolites [199, 200], proteins [201] or RNA [202–205]. Aptamers with one or more photolabile groups (so-called "caged aptamers") [469], whose activity can be turned on or off by light irradiation, can be utilized to study spatio-temporal effects on protein function.

This study has established the potential of aptamers as selective kinase inhibitors for chemical biology research. As was shown herein, aptamers can bind with high affinity and specificity in an ATP-competitive or non-ATP dependent manner to their target kinase (Sections 5.1, 5.2). The aptamers high specificity to even closely related protein kinases can be attributed to several elements, including the recognition of epitopes both within and outside of the kinase domain as well as the adaption to specific kinase conformations (Section 5.1) or the recognition of unique epitopes (Section 5.2.4.3).

It was also demonstrated that aptamers exhibit tremendous potential in inhibiting protein kinase functions (Sections 5.2.4.2, 5.2.4.4). This is mainly related to the ability of aptamers to address a functional surface epitope or domain, which enables them to competitively interfere with the binding of natural interaction partner, such as ATP (Section 5.2.4.1). The ability of aptamers to disrupt kinase activity or domain-specific functions makes them an attractive tool for research applications. Protein kinases are frequently controlled by protein interactions, which are mediated by docking domains [52, 53]. Since docking domain interactions are a key feature in mediating specificity during signal transduction, aptamers can become a valuable tools for extremely precise disruption of domain-specific functions.

So far, only a small fraction of the human kinome has been annotated with "specific" kinase inhibitors [64, 65]. Aptamers combine many features of chemical or biological kinase inhibitors and exhibit an intriguing potential for the interference with kinase activity inside cells. For example, the application of aptamer C5 in neurons could unravel further roles the Erk1/2 signal transduction pathway during different forms of long term potentiation and assist in the identification of direct targets during synaptic plasticity.

7 Outlook

The work described in this thesis contributes significantly to the development of aptamers as a novel molecular class of tools for chemical biology research. The high affinity, impressive specificity, ability to inhibit domain-specific functions or kinase activity by C3, C5, and C13 and, most importantly, the potential of C5 to block kinase-dependent neuronal functions opens the avenue towards the application of aptamers as tools to dissect intraneuronal signal transduction cascades. According to the findings of this study, several exiting questions have emerged.

7.1 Intracellular application of C13

Aptamer C13 and its target GRK2 have been used to identify the molecular determinants which contribute to an ATP-competitive aptamers high specificity for its target. However, reliable functional data about its cellular application and ability to block GRK2 signaling have not been obtained during this thesis. Since throughly characterized small molecule inhibitors of GRK2 are still rare, the application of C13 as an intramer could aid in the identification of disease-dependent and independent functions of GRK2.

The availability of appropriate delivery strategies and cellular assays offers exciting opportunities to elucidate the intracelular performance of C13.

GRK2 regulates many targets in the cytoplasm, including G protein-coupled receptors, receptor tyrosine kinases and cytoskeletal proteins [211]. In order for C13 to target GRK2 activity within the cytoplasm, a suitable delivery strategy should be chosen.
For instance, GRK2 can be transfected into the cytoplasm. Since this method can induce secondary effects (Section 5.3.3.5), any functional data should be verified by using the available non-binding point mutants of C13 as control sequences.

Additionally, C13 could be expressed in a construct that allows for delivery into the cytoplasm. To this end, a chimeric aptamer and ribozyme construct could be utilized, as was shown for the hepatitis delta virus (HDV) ribozyme and an aptamer against the NS3 protease domain of the hepatitis C virus [173]. The ribozyme processed the aptamer, which was then able to inhibit target function in the cytosol of mammalian cells. In this case, intracellular localization was mediated by employing a polymerase II promotor and cytoplasmic transport signal sequences.

Of course, it would also be possible to inject C13 into cells and monitor its effects on GRK2 activity on single-cell level.

A detailed investigation of the aptamers intracellular effect can be obtained by diverse cellular assays. GRK2 is known to phosphorylate many receptor and non-receptor substrates [211]. However, analysis of target protein phosphorylation is limited as specific antibodies for most targets, in particular GPCRs, are not available [470–472].

Another approach would be to study the interaction of GPCRs and arrestin which requires GRK2 activity. This interactions could be analyzed by FRET [473, 474] or fluorescence microscopy

[475]. Should C5 inhibit GRK2 activity, a decrease in FRET signal or reduced receptor internalization would be observed.

Single cell and microinjection experiments can be performed by monitoring the aptamers effect on β2-AR-mediated cardiomyocyte contractility *ex vivo* [476]. Contraction tracings of single ventricular cardiomyocytes should reveal an increase in cardiomyocyte contractility if GRK2 activity is inhibited. The blockage of GRK2 activity and its role on cardiomyocyte contractility has previously been validated by utilizing Paroxetine-treated mice [359] and a inhibitory peptide-expressing animal model of heart failure [477].

Future studies should also throughly investigate if C13 binds to GRK2 in a buffer that mimics cytosolic conditions as was shown for Erk2 and C3 or C5. Although buffer conditions represent an estimation and not a final proof of intracellular applicability, they could provide valuable information about the aptamers performance in cellular studies. As preliminary experiments have hinted into the direction that the interaction of C13 with GRK2 depends on the concentration of K^+ and Na^+ ions [209], the application of C13 in cellular studies might be hampered. Hence, it might be contrivable to perform a re-selection with a partially constrained library based on the sequence of C13 in a buffer that resembles intracellular conditions.

7.2 Sensitivity to ionic strength and secondary structure prediction

The Erk1/2-recognizing aptamers TRA, C3, and C5 were throughly characterized for cation dependency. This characterization revealed that the binding of TRA is affected by the presence of monovalent cations. In contrast, the binding of C5 (and C3) showed only little dependency for monovalent cations.

Since aptamer C5 and its progenitor TRA differ in only 12 nucleotides (Section 3.4.2.5), future studies should try to elucidate the reason for these differences. One explanation could be given when looking at the predicted secondary structures. The mutations could lead to a stabilization of both the central stem and the upper stem of C5 when compared to TRA. Hence, it is plausible that differences in sensitivity to cations might come from these secondary structural motifs. Point mutants of TRA and C5 should be designed to investigate this. For example, mutations that originate from the sequence of C5 can be introduced into TRA and its binding under different buffer conditions can be analyzed. Perhaps, this could allow for the identification of individual nucleotides that influence cation sensitivity by promoting conformational changes.

These point mutants could be employed for secondary structure prediction, such as chemical or enzymatic probing studies [478] or SHAPE (Selective 2'-hydroxyl acylation analyzed by primer extension) analysis [479], to define important secondary structural motifs that mediate or influence RNA fold in the presence of cations.

More importantly, secondary structure prediction of C3 and C5 should also be performed to investigate which nucleotides might directly engage in the interaction with Erk2. In turn, this can aid in the identification of novel point mutants or truncated variants of the aptamers.

7.3 Detailed investigation of the binding sites and modes of action of C3 and C5

Aptamer C5 was shown to recognize Erk2 in an ATP-competitive manner and to inhibit kinase activity whereas C3 was able to block the activation of Erk2 by Mek1 (Section 5.2). Of course, although *in vitro* data suggests that C5 targets the kinase domain and C3 the MAP kinase insert

of Erk2, this has yet to be proven. In order to achieve this, the crystal structure of the C5-Erk2 or C3-Erk2 complexes should be obtained.

Since C5 does not share the same sequence motif as the other ATP-competitive aptamers C13 and K16, it would be particularly interesting to observe if the aptamer positions an adenine residue to mimic ATP binding into the active site and derives specificity by charge and size complementarity as C13, or if C5 derives specificity by recognizing unique epitopes both within and outside of the active site.

By targeting a unique domain on Erk2, C3 could represent a valuable tool for chemical biology research. Hence, it will also be of utmost interest to define the complete binding surface of C3 on Erk2. Additionally, this information could provide valuable assets for studying the Mek-Erk interaction because no crystal structures of the Mek1-Erk2 complex are available yet. For instance, amino acid residues of Erk2 that comprise the binding site of C3 could also engage in direct interaction with Mek1 and could provide a novel druggable target. This could be extremely relevant because Mek1/2 are validated targets for cancer therapy [480, 481].

A putative epitope that could engage in the interaction of C3 and Erk2 is a cluster of positively charged amino acids that surrounds tyrosine 261 and serine 264 (Section 6.4.2.1). The interaction between this cluster and C3 could be investigated, e.g. by mutagenesis strategies or by using an assignment-free NMR approach that has recently been published for p38 MAP kinase [482].

In order to further elucidate the putative mode of action of C3, several strategies should be followed: First, it should be investigated if binding of C3 excludes the binding of Mek1. To achieve this, competition assays could be performed in which Mek1 would be titrated to a radioactively labeled C3 and Erk2. If binding of C3 blocks the binding of Mek1 either sterically or allosterically, a decrease in binding of C3 should be observed. Putative conformational changes could be monitored by obtaining the co-crystal complex of Erk2 and C3.

7.4 Specificity

Although the high specificity of C3 and C5 within the same kinase family and among distinct groups (Section 5.2.3) implicates high overall selectivity among the kinome, further examination is needed to evaluate the aptamers interaction with other kinases and non-kinases. The aptamers effects on other kinases could, in theory, be examined with large activity panels that include several hundred kinases. This service is commercially available and allows for efficient specificity profiling. However, as RNAse-free assay conditions can not be guaranteed, these specificity tests were not performed during this work

Nevertheless, it would also be possible to investigate the binding to endogenous proteins, including non-kinases, by conjugating the aptamer to a matrix and subsequently incubated with cell lysate [483–485]. After elution, the captured proteins can be subjected to mass spectrometry analysis [483]. Thereby, a biotinylated variant of C3 or C5 can be coupled to a Streptavidin-matrix, as was shown in the pulldown assays (Section 5.3.1).

Since C3, C5, or other aptamers could be useful as new tools to elucidate signal transduction pathways, adverse effects on other signal transduction pathways or interference with cell viability should be assessed early. If a decrease in cell viability or impact on other signal transduction pathway is observed, the readout or delivery method should be changed.

Aptamer C5 demonstrated the ability to inhibit a certain form of long term potentiation, which is known to require Erk1/2 activity (Section 5.4.4). In contrast to C5, the application of aptamer C3 did not block the increase in voltage potential but exhibited a shift of the action potential threshold to more depolarizated states [354]. Therefore, it should be examined if C3 targets the activity of voltage-gated potassium or sodium channels, which could be involved in regulating the action potential threshold. This can be achieved, for example, by examining the rise and decay time of the action potentials more closely. Furthermore, it would be exciting to investigate if any

changes in potassium or sodium channel activity by C3 could be mediated by blocking a hitherto unknown function of the MAP kinase insert of Erk1/2.

7.5 Cellular studies

Transfection of *in vitro* transcribed RNA and intracellular expression have been utilized to study the effect of C3 and C5 on growth factor - induced Erk1/2 signaling (Sections 5.3.3.3, 5.3.3.4, 5.3.2.3). It is yet unclear why the aptamers did not reveal inhibitory effects under the tested conditions.

Although the FACS experiments (Section 5.3.3.1) indicated that the aptamers had entered the cytoplasm, the intracellular stability, localization, and RNA concentrations should be examined. In order to determine the intracellular RNA concentration and stability, the total RNA of cells will have to be isolated after transfected with RNA or expression plasmids. The total RNA can then be reverse transcribed into cDNA and amplified by quantitative real-time PCR. The quantification of the absolute amount of RNA present in the cell will allow to assess if the intracellular aptamer concentration has been below the K_D value of C3 and C5. Subcellular fractionation by differential centrifugation will make it possible to examine the concentration and localization of the RNA aptamers in distinct cellular fractions, such as the nucleus [486].

In situ hybridization techniques based on antisense probes or fluorescently labeled aptamers could be used to explore the aptamer localization within the cells. These techniques could be coupled with super-resolution microscopy methods, such as STED, to further understand the aptamers distribution [487]. By staining for specific endosomal markers, such as distinct Rab proteins, the dynamics and complexity of endosomal escape could be investigated [488].

To this end, microinjection has emerged as a suitable strategy to monitor the aptamers effect on kinase function on single-cell level. Thus, it should be investigated if the aptamers would be able to block Erk1/2 signaling after growth factor stimulation by employing this delivery method. Perhaps the most promising strategy for monitoring changes in single-cell Erk1/2 activity after growth factor stimulation would be the use of a live-cell imaging FRET approach. By employing cells that co-express a FRET-based Erk1/2 kinase activity reporter construct and a mCherry-Erk2 fusion protein [489], changes in Erk1/2 activity could be monitored after or during injection of C3 and C5.

7.6 Identification and characterization of a putative novel Erk1/2 inhibitors

Aptamers that target unique epitopes and block domain-specific functions could provide an attractive starting point for the identification of non ATP-competitive kinase inhibitors by aptamer displacement screenings (Section 3.3.4).

Small molecule inhibitors that block kinase-domain independent functions may exhibit the same high specificity as their parental aptamers. Importantly, non ATP-competitive small molecule inhibitors may possess the key advantage of cell-permeability, which makes them attractive tools for elucidating signal transduction pathways. Displacement screening assays based on non ATP-competitive aptamers have the advantage that neither structural knowledge of a druggable spot nor the development of cumbersome target-independent assays for high-throughput screenings are required.

Aptamer C3, which targets the MAP kinase insert of Erk1/2, should be used in an aptamer displacement assay. These assays can be performed, for example, by using RiboGreen. a specific nucleic acid-binding dye, for the detection of C3 bound to immobilized Erk2. The putative small molecule inhibitor´s affinity for Erk2 can then be measured by microscale thermophoresis. This technique allows the determination of dissociation constants based on the movement of molecules

along a temperature gradient [490]). For this, one of the reaction partners has to be fluorescently labeled. This can be achieved, for example, by labeling the cysteine side chains of Erk2 with sulfhydryl-specific reagents.

Afterwards, the specificity of the compound should be assessed. Importantly, it should be evaluated if the compound can be utilized as a domain specific inhibitor. These experiments should be underlined by monitoring the compounds effects on Erk1/2 activation or other MAP kinase-specific functions within cells.

7.7 Identification of novel intramer candidates

So far, specific inhibitors for many kinases are still elusive and more than half of the human kinome is largely uncharacterized [64, 65]. Specific aptamers have only been identified against very few kinases, including PKC [324], GRK2 [209] and Erk2 [210]. Hence, many intriguing kinase targets are left to be explored.

7.7.1 Reduction of off-target effects

The greatest challenge of employing aptamers as protein kinase inhibitors inside cells is the avoidance of off-target effects (Section 5.3.3.5). Therefore, the use of lower RNA concentrations should be considered. For some siRNAs, this has been reported to reduce off-target effects [453–456]. To achieve this, aptamers with high affinities should be applied. Instead of bead-based selection strategies, aptamers should be selected with CE- [431] or high-throughput sequencing–RNA affinity profiling [457] - based selection strategies, which have previously given rise to aptamers with affinities in the picomolar range.

Being that they are ribonucleic acids with 5´-triphosphate moieties, RNA aptamers employ the intrinsic ability to activate RNA receptors that can distinguish non-self from self-RNA. Future aptamers might show improved cellular performance when side-effects are limited. In order to achieve this, several modifications should warrant consideration.

First, the removal of the 5´- triphosphate moiety of ssRNA may prevent 5´- triphosphate dependent activation of intracellular RNA receptors. The removal of the 5´- triphosphate has been reported to abrogate PKR activation in a study by Nallagatla and co-workers [448]. The role of the 5´- triphosphate has remained controversial for RIG-1 and seems to be dependent on the structural context. Many studies claimed the 5´- triphosphate to be essential for RIG-1 activation, whereas recent studies have demonstrated a 5´- triphosphate independent activation of RIG-1 by ssRNA aptamers [190].

In addition, nucleotide modifications might be introduced into RNA aptamers during or after the SELEX process [129]. Cellular RNAs often undergo post-transcriptional modification which might contribute to distinguishing cellular RNA from non-self RNA [491]. To date, more than 50 unique naturally occurring modified nucleosides have been identified in eukaryotes [492, 493]. It has recently been shown that nucleoside modifications can modulate RIG-1 [441, 494] or PKR activity [491, 495] in a RNA structure-specific manner. For example, in 5´- triphosphate-containing ssRNA, many base and sugar modifications, e.g. pseudouridine, 2´-thio-uridine (base) or 2´-O-methyl-uridine (backbone), abrogate PKR activation, although 2´-fluoro-modified ssRNA does not [190, 491, 495]. Chemical nucleotide modifications can also increase the thermodynamic stability of aptamers and prevent enzymatic degradation [496].

7.7.2 Identification of domain-specific inhibitors

The ability of aptamers to recognize kinases in an ATP-competitive or non ATP-competitive manner can easily be transferred onto other kinases. The identification of domain-specific aptamers can be achieved, e.g. by utilizing active or inactive kinase conformations that display the particular epitope [210], or by using individual sub-domains [133] during the SELEX process. Thereby, it is important that the epitope is surface exposed and highly conserved [114]. Additionally, the ATP-recognizing consensus motif that was found in aptamer C13 and K16 can be utilized in a doped library for the identification of a novel ATP-competitive aptamers.

7.7.3 Insensitivity to ionic strength

The lack of sensitivity to ionic strength of any aptamer could play an important role for the successful intracellular application of aptamers. In this regard, it could be possible that the presence of intracellular cationic strength, especially that of monovalent cations, during the SELEX process, will lead to successful performance of the aptamer within cells. However, although the ionic composition of the selection buffer is certainly important, there is no guideline which ionic strength during the SELEX process will give raise to functional intramers.

Literature suggests that functional intramers have been selected under many different conditions: Some intramers were selected in PBS buffer, which resembles extracellular ionic strength [182, 183]. The NF-kappaB aptamer was selected in a buffer consisting of Hepes and 0.1 mM NaCl [195] which also does not resemble intracellular monovalent cation concentrations, whereas other aptamers, e.g. the Spinach aptamer [202] or the E2F aptamer [186] were selected in Hepes buffer with cytosolic potassium concentrations.

Nevertheless, for aptamers with the final goal of intracellular application, the presence of monovalent cations, cytosolic buffer conditions or selection pressure towards insensitivity to monovalent cations during the SELEX process, will be beneficial.

8 Methods

8.1 Working with nucleic acids

8.1.1 Agarose gel electrophoresis

Usually, 2.5% agarose gels were used to monitor PCR products or *in vitro* transcribed RNAs. For a 2.5 % agarose gel, 2.5 g agarose was dissolved in 100 ml 1x TBE buffer and boiled for several minutes. After cooling down, 40 ml gels were purred and Ethidium bromide solution was added at a 1:10000 dilution. Samples were diluted with 2x DNA or 2x RNA loading buffer to a final concentration of 1x. For electrophoresis, gels were run in 1x TBE buffer at 150V for 15 minutes. Due to the intercalating Ethidium bromide, bands were visualized in a UV transilluminator (VWR) and compared to standard DNA ladders (Fermentas).

Table 8.1: Buffer for agarose gel electrophoresis

1x TBE	1x DNA loading dye	1x RNA loading dye
90 mM Tris, pH 8.0	25 mM Tris pH 8.0	50% Formamide
90 mM Borat	25% Glycerol (v/v)	0.013% SDS
2 mM EDTA	25 mM EDTA	0.25 mM EDTA
	Bromophenol Blue	Bromophenol Blue
	Xylenecyanol	Xylenecyanol

8.1.2 Polymerase chain reaction (PCR)

For the amplification of dsDNA that was later used as template for in vitro transcription, the following cycles were usually performed ten times.

Table 8.2: PCR programme

Step	Temperature [°C]	Time [min]
Denaturation	95	0.5
Annealing	55	0.5
Elongation	72	0.5

Table 8.3: Pipetting scheme for 1 PCR reaction

Reagent	Volume [μl]	Stock concentration	Final concentration
Pfu reaction buffer	10	10x	1x
$MgCl_2$	8	25 mM	2 mM
dNTPs	1	25 mM	0,25 mM
5´-primer	1	100 μM	1 μM
3´-primer	1	100 μM	1 μM
dsDNA template	1		1-20 nM
Pfu polymerase	1	2.5 U/μl	0.0225 U/μl
MilliQ water	ad 100μl		

8.1.3 PCR product purification

PCR products were purified with the commercially available "PCR and gel purification Kit" from Machery and Nagel according to the manufactorers protocol: Briefly, 2.5 PCRs were pooled for 1 column and eluted with 50 μl MilliQ water.

8.1.4 *In vitro* transcription (TK)

In vitro transcription of dsDNA containing a T7-RNA polymerase promotor sequence was performed as described in table 8.4. dsDNA resulting from approximately one purified PCR reaction was used as template per 100 μl transcription reaction. After over night incubation at 37°C, 0.5U DNAseI (Fermentas) was added per 1x TK. Afterwards incubation at 37°C for 30 minutes, RNA was precipitated as described in Section 8.1.9by polyacrylamide gel electrophoresis (Section 8.1.10) and subsequent RNA workup protocol (Section 8.1.11).

Table 8.4: Pipetting scheme for *in vitro* transcription reactions

Reagent	Volume [μl]	Stock	Final concentration
Hepes, pH 7.9	20	200 mM	40 mM
$MgCl_2$	1.6	1.5 M	25 mM
NTPs	10	25 mM	2.5 mM
DTT	5	100 mM	25 mM
Inorganic Pyrophosphatase	0.2	2 U/μl	0.02 U/μl
RNAsin	1.24	40 U/μl	0.5 U/μl
dsDNA template	10		150-300 pmol
T7 RNA polymerase	10	30 U/μl	1 U/μl
MilliQ water	ad 100 μl		

8.1.5 Radioactive transcription

For radioactive transcriptions using ^{32}P-GTP, 2 μl α-^{32}P-GTP was added to the reaction (Table 8.4). After incubation at 37°C for 2 hours, *tin vitro* transcribed RNA was purified using the "PCR and gel purification Kit" from Machery and Nagel according to the manufacturers instructions. Briefly, 200 μl buffer NTC was added to a 100 μl in vitro transcription reaction. Elution was performed with 50 μl MilliQ water.

8.1.6 GMPS transcription

For the generation of 5´-labeled RNA, in vitro transcription reactions were supplemented with 10 mM Guanosine-5´-Thiophosphate (GMPS, Genaxxon Biosciences). The GMPS moiety can later react with the Iodoacteyl-moiety via nucleophilic substitution.

Table 8.5: Pipetting scheme for GMPS transcription reactions

Reagent	Volume [μl]	Stock	Final
Hepes, pH 7.9	20	200 mM	40 mM
MgCl	1.6	1.5 M	25 mM
NTPs	10	25 mM	2.5 mM
DTT	5	100 mM	25 mM
Inorganic Pyrophosphatase	0.2	2 U/μl	0.02 U/μl
GMPS	6.7	150 mM	10 mM
RNAsin	1.24	40 U/μl	0.5 U/μl
dsDNA template	10		150-300 pmol
T7 RNA polymerase	10	30 U/μl	1 U/μl
MilliQ water	ad 100 μl		

After incubation for 6 hours at 37°C, the reaction mixture was Phenol-Chloroform extracted (Section 8.1.8) and precipitated (Section 8.1.9). The pellet was suspended in 10 μl MilliQ water/100μl TK and subsequently passed through G-25 Microspin columns (GE Healthcare) twice.

8.1.7 Generation of 5´- biotinylated or 5´-fluorescein-labeled RNA

A crump of 5-(Iodoacetamido)fluorescein (Sigma Aldrich) or EZ-link Iodoacetyl-PEG2-Biotin (Pierce) was dissolved in DMF. In the meantime, RNA was suspended in labeling buffer (1xTE pH 8.0, 2.3 M Urea, RNAsin 0.4 U/μl) and heated for 1 minute at 80°C. Afterwards, the mixture was cooled down on ice for 5 minutes. 40 μl Iodoacteyl- Biotin or –Fluorescein were added to 360 μl labeling mix. The reaction was allowed to proceed for 2 hours at 37°C. Afterwards, the RNA was precipitated (Section 8.1.9) and purified as described below.

Table 8.6: Pipetting scheme for labeling reactions

Reagent	Volume [μl]	Stock	Final
TE, pH 8.0	40	800 mM Tris, 500 mM EDTA	80 mM Tris, 50 mM EDTA
Urea	100	8.3 M	2.3 M
RNAsin	4	40 U/μl	0.4 U/μl
GMPS transcription	100		
MilliQ water	ad 360		

8.1.8 Phenol-Chloroform extraction and precipitation

One volume of Phenol (SIgma Aldrich) was added to one volume of nucleic acids solution. Samples were vortexed and centrifuged at 14000 rpm for 5 minutes. The upper, aqueous phase was then

transferred into a new 1.5 ml tube. Two volumes of Chloroform (AppliChem) were then added to the aqueous phase. Samples were mixed and centrifuged at 14000 rpm for 5 minutes. Again, the upper phase was transferred into a new 1.5 ml tubei. 1/10 volume 3M NaOAc, pH 5.4, and 3 volumes 100% Ethanol were added. The tube was inverted and centrifuged at 20000g for 30 minutes (4°C). The supernatant was discarded and the pellet was washed with 70% Ethanol and centrifuged for 5 minutes at 20000g (4°C). The pellets were air-dried and suspended in 10μl MilliQ water/100 μl transcription.

8.1.9 Ethanol precipitation

Ethanol precipitation is a common used technique for the de-salting and concentration of nucleic acids. Nucleic acids are polar and easily dissolve in water. The addition of monovalent cations (e.g. Na^+) neutralizes the negative charge of the phosphodiester backbone, making nucleic acids less soluble in water. Ethanol has a lower dielectric constant than water, making it easier for monovalent cations to interact with the negatively charged phosphodiester backbone, and causes the precipitation of nucleic acids.
Samples were split into 100 μl/1.5 ml tube. 1/10 Volume DNAseI 10x Buffer (Roche) and 0.5 U/μl DNAseI (Roche) were added to the mixture and incubated for 30 minutes at 37°C. Afterwards, 50 μl MilliQ water, 50 μl 0.5 M EDTA, pH 8.0, 100 μl 6 M NH40Ac and 1 ml ice-cold 1000% Ethanol were added. The tube was inverted and centrifuged at 20000g for 60 minutes (4°C). The supernatant was discarded and the pellet was washed with 700% Ethanol and centrifuged for 10 minutes at 20000g (4°C). The supernatant was discarded again. The pellets were air-dried and pooled in 140 μl PAA loading buffer.

Table 8.7: PAA loading buffer

PAA loading buffer
60% Formamide
5% SDS
0.25 mM EDTA
Bromophenol Blue
Xylenecyanol

8.1.10 Polyacrylamide gel electrophoresis (PAGE)

Polyacrylamide gel electrophoresis was employed to separate RNA molecules for analytical or preparative purposes.
The mixture for a 10% gel was prepared as described in (table 8.9) and poured between two glass plates. The gel was allowed to polymerize for at least 1 hour. The gel was placed into a running chamber and buffer reservoirs were filled with 1x TBE buffer. The gel was pre-run for 15 minutes at 350V. Before loading samples, the pockets were rinsed twice with 1x TBE. Samples were boiled for 3 minutes at 95°C and 70 % were loaded per lane. The gel was run for approximately 1.5-2 hours at 350 V.

Table 8.8: Pipetting scheme for one PA gel (10 %)

Solution	Volume [ml]
C (Rothiphorese sequencing gel concentrate)	28
D (8.3 M Urea)	35
B (8.3 M Urea in 10X TE)	7
APS (10%)	0.56
TEMED	0.028

8.1.11 RNA work-up

Once the Xylenxyanole band of the PAA loading buffer had reached the lower third of the PA gel, the gel was stopped. The glass plates were removed and the gel was wrapped in plastic foil. RNA bands could be detected by UV-shadowing at 254 nm. The right sized bands were then cut out with a sterile razor blade and transferred into a 1.5 ml tube. The gel slice was then crushed with a 1 ml pipette tip and suspended in 500 μl 0.3 M NaOAc, pH 5.4. The gel suspension was then frozen at -80°C for 30 minutes and incubated at 65°C for 1.5 hours under vigorous shaking (1300 rpm). Afterwards, gel suspension was filtered through a 5 ml syringe packed with silanized glass wool. The syringe was washed for three more times with 100 μl 0.3 M NaOAc, pH 5.4. The RNA was precipitated by the addition of 3 volumes 100% Ethanol and centrifugation at 20000g for 60 minutes (4°C). The supernatant was discarded and the pellet was washed with 70% Ethanol and centrifuged for 10 minutes at 20000g (4°C). The supernatant was discarded again. The pellets were air-dried and suspended in MilliQ water (10 μl water/100 μl TK).

8.1.12 Concentration measurements

The concentration of nucleic acids solutions was determined by employing a UV-spectrophotometer. A UV-spectrophotometer measures the absorption at a wavelength of 260 nm (A260) in a quartz cuvette. The concentration was calculated by using the following equitation:

$$c = \left[\frac{\text{mmol}}{\text{l}}\right] = \frac{\text{OD}_{260} \cdot k \cdot d}{\Sigma\text{nt} \cdot \text{Mw}}$$

d=dilution factor, k=absorption coefficient (ssRNA: 40 μg/ml), Mw=molecular weight (g/mol), nt=number of nucleotides

8.1.13 Determination of the labeling efficiency (5´-Biotin or 5´-FITC labeled RNA)

The yield and quality of biotinylated RNA was analyzed by gel shift assays. In this assay, equimolar concentrations of biotinylated RNA and Streptavidin were incubated in MilliQ water at 30°C for 30 minutes. Afterwards, the samples were suspended in RNA loading buffer and immediately loaded on a 2.5 % agarose gel. Control samples without Streptavidin or with non-biotinylated RNAs were run for validation. Biotinylation efficiency was determined by band quantification using GelDoc software (Biorad). Fluorescein-labeled RNA was run on a 2.5% agarose gel and detected using fluorescence reading option of the Phosphoimager (Fuji).

8.1.14 Coupling of biotinylated RNA to Streptavidin-coated Dynabeads

Usually 200 pmol biotinylated RNA was used to detect the interaction of aptamers or control RNA with endogenous proteins in pull-down experiments. The RNA was suspended in 200 μl 1x Binding and Wash (BW) buffer.
200 μl Streptavidin-coated Dynabeads (Invitrogen) were employed for the reaction. The supernatant of the beads was discarded. The beads were suspended in 200 μl 1x BuW buffer. Beads were separated from the mixture with a magnet and the supernatant was discarded again. Beads were washed 4 more times with 1200 μl 1x BW buffer. For labeling reactions, 200 μl RNA solution was added to the Dynabeads. The mixture was incubated at room-temperature on a over-head-tumbler for 45 minutes. Afterwards, beads were washed 4 times with 200 μl 1x PBS. Beads were suspended in 200 μl 1x PBS and kept on ice.

Table 8.9: Buffer recipe for the coupling of biotinylated RNA to Streptavidin-coated Dynabeads

1x BW buffer	**1x PBS**
5 mM Tris/HCl, pH 7.5	137 mM NaCl
0.5 mM EDTA	2.7 mM KCl
1 M NaCl	6.5 mM Na_2HPO_4
	1.47 mM NaH_2PO_4

8.2 Working with bacteria and bacterial plasmids

8.2.1 LB Medium and agar plates

For 10 10cm^2 dishes, 3.8 g agarose and 5 g LB broth (Sigma) were mixed in 250 ml MilliQ water and autoclaved for 15 minutes at 121°C. After cooling down, Ampicillin (AppliChem) was added to yield a final concentration of 100 μg/ml. Plates were kept at 4°C. LB medium was obtained by mixing 10 g LB broth with 500 ml water. LB medium was autoclaved for 15 minutes at 121°C and stored at room temperature.

8.2.2 Transformation of E.coli XLI blue or DE3

Chemically competent cells (Invitrogen) were thawed on ice for 3-5 minutes. 100 ng plasmid DNA or 5μl ligation mixture were added to 100μl competent cells. The cells were kept on ice for 30 minutes. Afterwards, bacteria were heat-shocked at 42°C for 45 seconds and immediately put back on ice. After 2 more minutes, 500μl pre-warmed SOC medium (Invitrogen) was added and cells were incubated at 37°C , 300 rpm. After 30 minutes, cells were centrifuged at 1000 rpm for 2 minutes. 500 μl medium was discarded and the pellet was suspended in the remaining 100μl medium. The bacteria were then plated on LB-Ampicillin plates and incubated over night at 37°C. Plated were stored for 1 month at 4°C.

8.2.3 Cultivation of E.coli XLI blue or DE3

The bacteria were cultivated in LB medium with the appropriated antibiotic (usually 100 μg/ml Ampicillin) at 37°C under vigorous shaking (150 rpm).

8.2.4 Preparation of Glycerol stocks

To store bacteria for a longer period at -80°C, 250 μl Bacteria were incubated with 500μl glycerin (AppliChem) for 30 minutes at room temperature. Afterwards, bacteria were transferred to the -80°C freezer.

8.2.5 Plasmid preparation from E.coli

For plasmid preparation in a small scale, 10 ml E.coli cultures were grown over night at 37°C, 150 rpm. Plasmids were extracted with the "NucleoSpin Plasmid" Kit from Machery and Nagel according to the manufacturers recommendation.
For plasmid preparation in a small scale, 200 ml E.coli cultures were grown over night at 37°C, 150 rpm. Plasmids were extracted with the "NucleoBond Midi" Kit from Machery and Nagel according to the manufacturers recommendation.

8.2.6 Plasmid preparation for sequencing

For sequencing reactions, DNA was quantified (Section 8.1.12) and diluted to a concentration of 30-100 ng/ml. Sequencing reactions were performed with the appropriative primer at GATC Biotech, Germany.

8.3 Working with proteins

8.3.1 Induction of protein expression

200 ml pre-cultures were inoculated with glycerol stocks and incubated with 100 μg/ml Ampicillin over night under vigorous shaking. 800 ml fresh LB-Amp medium was then poured to the pre-culture. Bacteria were grown until an OD_600= 0.6-0.7 was reached. Protein expression was induced with 1 mM Isopropyl-D-1-thiogalactopyranoside (IPTG, AppliChem) for 6 hours at 37°C.

8.3.2 Protein purification

Cells were harvested by centrifugation at 5000g for 20 minutes. The supernatant was discarded and pellets were stored at -80°C. The cell pellet was resuspended in 20 ml lysis buffer. The cells were disrupted with a French Press. For this, the bacterial suspension was sucked into the French Press and released with a definite pressure (1200 psi). The lysate was then cleared by centrifugation at 20000g at 4°C.
The Erk2 proteins are expressed as a His_6-tag fusion protein, which allows for the affinity purification with Ni-NTA-beads (Qiagen).The protein supernatant was then incubated with 2 ml Ni-NTA-beads in a head-top-tumbler for 30 minutes at 4°C. The beads were the transferred onto disposable columns (BioRad) and flow through (containing unbound proteins) was removed with a peristaltic pump. To elute the proteins bound to the Ni-NTA-matrix, 2 ml elution buffer was added and the flow through was collected. This step was repeated two more times. To purify recombinant proteins from Imidazole or protein aggregates, proteins were purified by size-exclusion or desalting columns using the Akta FPLC system. For size-exclusion, a Superdex200 column (GE healthcare) was equilibrated with 2 volumes of storage buffer . For desalting, a HiTrap5 columns (GE healthcare) was equilibrated with 2 volumes of storage buffer. Samples were injected and collected in 1 ml scale. Distinct protein fractions were pooled and stored at -80°C

Table 8.10: Buffers used for Erk2 purification

	lysis buffer/wash buffer	elution buffer	storage buffer
Tris/HCL	50 mM, pH 7.8	50 mM, pH 7.8	50 mM, pH 7.8
NaCl	300 mM	300 mM	300 mM
Imidazole	20 mM	500 mM	
Glycerin	5%	5%	5%

8.3.3 Determination of protein concentration: Bradford Assay

For quantification, the concentration of the protein samples is compared to a BSA standard curve (-3 mg/ml). The Coomassie Brilliant Blue G250 dye (Biorad) was diluted 1:10 and 150 μl were added to 2 μl protein sample. Absorbance was measured at 595 nm with the Varioscan platereader.

8.3.4 SDS-PAGE

For SDS-PAGE, protein samples were boiled for 3 minutes at 95°C in 1x SDS sample buffer (Lämmli buffer).
Seperating and stacking gel mixtures were cast between two thin glass slides. Either 5 μl recombinant protein, 40 μg cell lysate or 10μl precipitate from pulldown assays were loaded per lane. Page Ruler Pre-Stained Ladder (Fermentas, 5 μl /lane) served as size standard. Gels were run at 160 V for 60 minutes.

Table 8.11: Pipetting scheme for SDS-PAGE gels

	10% seperating gel	4% seperating gel
Acrylamide mix (30%	1667 μl l	213 μl l
water	2045 μl l	975 μl l
4x seperating buffer	1250 μl	
4x stacking buffer		400 μl
TEMED	30 μl	10.4 μl
APS (10% w/v)	8 μl	2 μl

8.3.5 Coomassie Staining

The recombinant proteins were subjected to SDS-PAGE gel analysis (Section 8.3.4) and Coomassie-Staining in order to analyze their purity. SDS-PAGE gels were incubated for 30 minutes in Coomassie Staining solution. Afterwards, the gel was destained until the protein bands became visible.

Table 8.12: Coomassie staining buffer

Coomassie staining (1l)	300 ml Methanol
	100 mll acetic acid
	600 ml water
	700 mg/ml Coomassie Brilliant Blue G250
Destaining solution (1l)	300 ml Methanol
	100 mll acetic acid
	600 ml water

8.4 In vitro RNA-protein interaction and kinase assays

8.4.1 Filter binding assay

The interaction of RNA with proteins was monitored by filter retention assays. In order to detect the affinity of the RNA-protein complex, 32^P-labeled RNA was incubated with increasing concentrations of proteins in 25 μl binding buffer (for Erk2, binding buffer usually contained PBS, 3 mM MgCl_2, for GRK2, binding buffer usually contained PBS, 3 mM MgCl_2, 1mg/ml Heparin) and incubated at 37°C for 30 minutes. In the meantime, the nitrocellulose membrane (0.45 μM, Schleicher and Schuell) was incubated in cathode buffer. After 25 minutes, the membrane was rinsed with MilliQ water and vacuum manifold was assembled. The membrane was equilibrated with 200 μl washing buffer (PBS, 3mM MgCl_2). 20 μl sample was loaded. Afterwards, the membrane was washed two more times with 200 μl washing buffer (PBS, 3 mM MgCl_2). 0.8 μl of 32^P-labeled RNA was spotted on the membrane to allow for the quantification of the percentage of RNA bound to the proteins. The amount of radioactively labeled RNA bound to proteins was then detected with a Fujifilm FLA-3000 (Fujifilm) and quantified using AIDA image software. Dissociation constant values (K_D) were determined by fitting data from at least two independent measurements to a one-site specific binding curve with a 4 parameter hill slope using GraphPad Prism 5.0.

Table 8.13: Buffers for filter retention assay

Cathode buffer	**Binding buffer**
25 mM Tris-HCl, pH 9.4	137 mM NaCl
40 mM Glycin	2.7 mM KCl
	6.5 mM Na_2HPO_4
	1.47 mM NaH_2PO_4
	2 mM $MgCl_2$

8.4.2 Competitive binding assays with ATP

In competition experiments employing inactive Erk2, 300 nM Erk (2x KD for C5) or 200 nM Erk (2x KD for C3) were incubated in binding buffer (PBS, 3 mM Mg$Cl_2$2) with radioactively labeled RNA and increasing concentrations of ATP or UTP (0-20000 μM, Larova). Erk2 was added last to the mixture. After incubation at 37°C for 30 minutes, samples were passed through a nitrocellulose membrane and quantified as described above.
In competition experiments employing active Erk2, 100 nM active Erk2 was incubated in binding

buffer (PBS, 3 mM $MgCl_2$) with radioactively labeled RNA and increasing concentrations of ATP or UTP (0-20000 μM). Erk2 was added last to the mixture. After incubation at 37°C for 30 minutes, samples were passed through a nitrocellulose membrane and quantified as above (Section 8.4.1). IC_{50} values were calculated from a dose-response curve and fitted using a three-parameter slope.

8.4.3 Competitive binding assays with aptamers in the recording solution

For experiments validating the functionality of C3, C5 or C5 B2 in recording solution, 300 nM Erk2 was incubated in 20 μl binding buffer (PBS, 3 mM $MgCl_2$). Indicated RNA concentrations were frozen in PBS or recording solution, thawed and 5 μl were used as competitors for radioactively labeled C3 or C5. The amount of radioactively labeled RNA bound to proteins was quantified as described as above.

8.4.4 Erk2 activity assays

Erk2 activity assays were performed in kinase assay buffer (20 mM Hepes, pH 7.4, 10 mM $MgCl_2$, 100 μM ATP and 0.1 μCi-P^{32}-ATP). 60 nM active Erk2 was incubated with indicated RNA concentrations and 10 μM MBP (Sigma Aldrich) or 1 μM GST-Elk1 (Cell Signaling Technology). The reaction was started with the addition of active Erk2 and was allowed to proceed for 15 minutes at 30°C. Afterwards, samples were passed through a nitrocellulose membrane and quantified as above (Section 8.4.1).

Table 8.14: Kinase assay buffer

Kinase assay buffer
20 mM Hepes, pH 7.4
10 mM $MgCl_2$
100 μM ATP
60 nM active Erk2
0.1 μCi-P^{32}-ATP
10 μM MBP or 1 μM GST-Elk1

8.4.5 Mek1-Erk2-activation assay

Erk2 activity assays were performed in kinase assay buffer. 1 μ Mek1 G7B, 1 μM Erk2 and 10 μM MBP were incubated with indicated RNA concentrations. Erk2 was added last. The reaction proceeded for 15 minutes at 30°C and was terminated by boiling the samples in Lämmli buffer (3 minutes, 95°C). Afterwards, samples were dissolved on a 10% SDS-PAGE gel (8.3.4) and phosphorylation of Erk2 and MBP was detected with a Fujifilm FLA-3000 (Fujifilm) and quantified using AIDA image software.

Table 8.15: Kinase activation assay buffer

Kinase activation assay buffer
20 mM Hepes, pH 7.4
10 mM $MgCl_2$
100 μM ATP
0.1 μCi-P^{32}-ATP
1 μM Erk2
1 μ Mek1 G7B 10 μM MBP

8.5 Working with eukaryotic cells

8.5.1 Cultivation

Cell lines were cultivated in the indicated media (PAA) supplemented with 10% FBS (Signa) at 37°C, 5% $C0_2$. Cells were cultivated until they reached a confluence of 80% and subsequently were splitted every 2-3 days.

Table 8.16: Cell lines and standard media

Cell line	medium	species	origin
H460	RPMI	human	NSCLC
Hek293	DMEM high glucose	human	Embryonic kidney
A431	RPMI	human	Epidermoid cancer

8.5.2 Freezing and thawing

Approx. 5x10^6 cells were collected per cryotube. The supernatant was discarded and cells were resuspended in 500 μl Medium (10% FCS) and 500 μl cryoprotective medium (Lonza). Cells were immediately transferred into the -80°C freezer and placed into the liquid nitrogen tank 24 hours later.
For thawing, one cryovial was placed into the waterbath (37°C) until the cell suspension was completely thawed. Cells were then transferred into a new 75-cm^2-flask. Medium was changed after 12 hours.

8.5.3 Mycoplams test

Mycoplasm tests were routinely performed according to the manufacturers protocol (Minerva Biosciences).

8.5.4 Transfection with RNA for Immunoblot analysis and Flow Cytometry

For RNA transfection by lipofection, indicated cell numbers were seeded 48 hours before transfection. Cells were cultivated for 24-30 hours in standard medium with FCS. On the second day, the standard medium was replaced with serum-free medium and cells were cultivated for further 16

hours. Before transfection, cells were washed with PBS once and fresh medium without FCS was added.

Table 8.17: Number of cells seeded for RNA transfection

Well format	Total volume	Cell line	no of cells	RNA [pmol/μl]
6-cm	3 ml	H460	600,000	750
6-cm	3 ml	A431	600,000	750
24 well	0.2 ml	H460	30,000	¡20
96-well	0.1 ml	H460	2000	¡2
96-well	0.1 ml	diverse	1000-3000	¡2

RNA was transfected at indicated concentrations of aptamer or control RNA. For this, the commercially available transfection reagent Lipofectamine LTX (Invitrogen) was mixed at a ration of 4:1 with Lipofectamine Plus and incubated with RNA in serum-freemedium for 30 minutes at room temperature. Afterwards, the mixture was added drop wise to the cells. After 5-6 hours, cells were stimulated with 50ng/ml EGF (AF-100-15, Peprotech) for 10 minutes.

Table 8.18: Pipetting scheme for RNA transfection

Well format	RNA [pmol/μl]	LTX [μl]	Plus [μl]	volume [μl]
6-cm	750	10	2.5	200
6-cm	750	10	2.5	200
24 well	¡20	2	0.5	50
96-well	¡2	0.1	0.025	100
96-well	¡2	0.1	0.025	100

8.5.5 Transfection with DNA plasmids

For plasmid transfection by lipofection, 20000-3000 cells were seeded in 24 well plates 18 hours prior to transfection in standard medium with FCS. On the second day, the standard medium was changed with 300 μl fresh medium and cells were transfected as described below.
The transfection mix was incubated for 30 minutes at room-temperature and added drop-wise to the cells. It was removed 12-24 hours after transfections and cells. Cells were incubated for 24-72 hours after transfection started.

Table 8.19: Pipetting scheme for RNA transfection

Transfection mix
300 ng Luciferase vector
700 ng expression vector
2 μl Lipofectamine LTX
0.7 μl Lipofectamine Plus
ad 50 μl OptiMEM

8.5.6 Inhibitor treatment

For treatment with inhibitors, cells were seeded as described above and allowed to grow for 24-30 hours in standard medium with FCS. Cells were then serum-starved and treated with inhibitors or DMSO over-night. Cells were stimulated with 50 ng/ml EGF for 5 minutes.

8.5.7 Cell lysis for SDS-PAGE and Immunoblot analysis

Before cell lysis, medium was discarded and cells were washed once with ice-cold PBS. Cells were harvested in cold PBS buffer on ice using a cell scraper. Subsequently, cells were centrifuged at 1000 rpm, 5 minutes, 4°C. Pellets were suspended in 25 μl 1x lysis buffer supplemented with protease-inhibitor mix. After incubation on ice for 20 minutes, cell debris was separated by centrifugation (20000g, 20 minutes, 4°C).
Protein concentration was determined by Bradford assay (Section 8.3.3). For SDS-PAGE and immunoblot analysis, 40 μg protein lysate was boiled in 1x Lämmli buffer (Section 8.3.4).

Table 8.20: Lysis Buffer

1x Lysis Buffer
20 mM Tris-HCl, pH 7.5
150 mM NaCl
1 mM EDTA
1 mM EGTA
2.5 mM sodium pyrophosphate
1 mM glycerophosphate
1 mM sodium vanadate
1% (v/v) Triton X-100

8.5.8 Pull-down of endogenous MAP kinases from cell lysate

Approximately 6x 10^6 H460 cells were washed three times with ice-cold PBS. Cells were detached on ice by using a cell scraper and collected by centrifugation (1000 g, 5 min, 4°C). The cell pellet was suspended in 1 ml 1x PBS (supplemented with 1% proteinase inhibitor mix, Serva) and homogenized (Polytron, Kinematica) at 4°C. Afterwards, the cell suspension was centrifuged at 20.000 g for 60 minutes. The supernatant was then supplemented wit $MgCl_2$ and Heparin (Sigma Aldrich) to final concentrations of 3 mM and 0.8 μg/μl, respectively.
RNA was biotinylated and coupled to magnetic beads as described previously (Section 8.1.14). After incubation, the cell lysate was added to the beads and incubated for 30 min at 37°C. Subsequently, the lysate was removed and the beads were washed 4x with 200 μl 1x PBS supplemented with 3 mM $MgCl_2$. Finally, the beads were suspended in 10 μl MilliQ water and 4x Lämmli buffer, boiled for 5 min at 95°C and subjected to SDS-Page gel analysis (Section 8.3.4).

8.5.9 Semi-dry blotting

Semi-dry blotting and Immunoblots were performed to detect proteins or phosphorylated proteins in cell lysates. Proteins were run on a SDS-PAGE gel and transferred onto a nitrocellulose membrane (0.45 μm, Schleicher and Schuell). The gel was stacked between different layers of paper that were

equilibrated in the annotated buffers. Transfer took place by applying 2 mA/cm^2 gel (here: 9x6cm, 108 mA) for 90 minutes.

Table 8.21: Schematic representation

Anode
2 filter paper in Anode buffer I
1 filter paper in Anode buffer II
nitrocellulose membrane in Anode buffer II
gel in cathode buffer
3 filterpaper in cathode buffer
Cathode

Table 8.22: Buffers used for semi-dry blotting

Anode buffer I	300 mM Tris-HCl, pH 10.5
Anode buffer II	25 mM Tris-HCl, pH 10.4
Cathode buffer	25 mM Tris-HCl, pH 9.4 40 mM Glycin

8.5.10 Immunoblot analysis

After transfer, membranes blocked under agitation with 5% BSA/1xTBS-T for 45 minutes at room-temperature. Afterwards, membranes were rinsed 3 times for 5 minutes with 1x TBS-T. Primary antibodies were diluted 1:500-1:10000 in 5 % BSA/1x TBS-T and incubated over-night at 4°C under agitation. Primary antibodies were used up to 4 times. Antibodies were removed and membranes were washed 3 times for 5 minutes with 1x TBS-T. Secondary antibodies coupled to Horseradish-Peroxidase (HRP) or IRDyes were diluted 1:10000 in 5% BSA/1x TBS-T and incubated for 45-60 minutes at room-temperature in the dark. Afterwards, membranes were washed 3 times for 5 minutes with 1x TBS-T. For HRP antibodies, visualization of the corresponding bands was achieved by enhanced Chemiluminescence and a VersaDoc Camera (Biorad). IRDye-labeled antibodies were detected by a Odyssey scanner (LiCor). Bands were quantified using the QuantityOne software from Biorad.

Table 8.23: Buffers for semi-dry blotting

10x TBS	**1x TBS-T**
200 mM Tris, pH 7.6 1.36 M NaCl	20 mM Tris, pH 7.6 136 mM NaCl 0.1 % (v/v) Tween-20

8.5.11 Proliferation assay

1500-6000 cells were seeded into a 96-well plate (PAA). Cells were cultivated in standard medium with 10 % FCS for 24 hours. On the second day, medium was discarded and cells were cultivated in

standard medium without FCS over night. For RNA transfection, cells were incubated for 6 hours with the reaction mixture. For inhibitor treatment, cells were incubated over night with inhibitors or solvent.
Afterwards, medium was discarded and cells were cultivated in standard medium with 1 % FCS. After 24-72 hours, 15 μl MTT dye solution was added to the cells. The cells were then incubated for 4 more hours at 37°C. Then, 100 μl MTT lysis buffer was added to the cells. After 1-2 hour incubation at 37°C, absorbance was measured at 570 nm in the Varioscan platereader.

Table 8.24: Buffers for MTT assays

MTT dye solution	**MTT lysis buffer**
5 mg/ml MTT dye in 1x PBS	250 ml DMF
	250 ml water
	100 g SDS
	10 ml acetic acid

8.5.12 Luciferase Assay

SRE-Luciferase assays were performed according to the Luciferae Glo assay protocol by Promega. Briefly, cells were stimulated with 50 ng/ml EGF for 6 hours prior to cell lysis. Afterwards, cells were washed twice with PBS and 400 μl 1x Reporter Lysis Buffer (Promega) was added to each well. The mixture was incubated for 30 minutes at 37°C.
In order to normalize the Luciferase signal onto the intrinsic GFP expression level, 100 μl cell lysate was transferred into black half-area plates (Firma) and fluorescence was detected at 488 nm using the ENspire platereade. 100 μl Luciferase assay substrate (Promega) was transferred into a half-area 96 well plate (Firma) and 15 μl l cell lysate (previously used to the detect GFP expression) was added. After incubation for 5 minutes in the dark, Luciferase signal was detected with the ENspire platereader. The luciferase signal was normalized onto the GFP signal for quantification. GFP and Luciferase measurements were performed in duplicates.

9 Materials

9.1 Oligos

Table 9.1: C13 aptamer and point mutants

Name	Type	Sequence
5´-Primer (C-47)	DNA	AATTCTAATACGACTCACTATAGGGAGAGGAGGGAGATA GATATCAA
3´-Primer (P20)	DNA	GTCCTGTGGCATCCACGAAA
C13	RNA	GGGAGAGGAGGGAGAUAGAUAUCAACUGCAGUUCGGGU AGCACAGACCAUACGGGAGAGAAACUUGUGCAACCCGGGG CUACUUUCGUGGAUGCCACAGGAC
C13 A49C	RNA	GGGAGAGGAGGGAGAUAGAUAUCAACUGCAGUUCGGGU AGCACAGACCCUACGGGAGAGAAACUUGUGCAACCCGGGG CUACUUUCGUGGAUGCCACAGGAC
C13 U50G	RNA	GGGAGAGGAGGGAGAUAGAUAUCAACUGCAGUUCGGGU AGCACAGACCAGACGGGAGAGAAACUUGUGCAACCCGGGG CUACUUUCGUGGAUGCCACAGGAC
C13 A51C	RNA	GGGAGAGGAGGGAGAUAGAUAUCAACUGCAGUUCGGGU AGCACAGACCAUCCGGGAGAGAAACUUGUGCAACCCGGGG CUACUUUCGUGGAUGCCACAGGAC
C13 C52A	RNA	GGGAGAGGAGGGAGAUAGAUAUCAACUGCAGUUCGGGU AGCACAGACCAUAAGGGAGAGAAACUUGUGCAACCCGGGG CUACUUUCGUGGAUGCCACAGGAC
C13 G53U	RNA	GGGAGAGGAGGGAGAUAGAUAUCAACUGCAGUUCGGGU AGCACAGACCAUACUGGAGAGAAACUUGUGCAACCCGGGG CUACUUUCGUGGAUGCCACAGGAC

Table 9.2: Erk2 aptamers and control sequences

Name	Type	Sequence
C3	5´-Primer (5´-C-47)	AATTCTAATACGACTCACTATAGGGAGAGGAGGGAGATAGA TATCAAGATATCAA
C3	3´-Primer (3´-C-20)	GTCCTGTGGCATCCACGAAA
C3	RNA	GGGAGAGGAGGGAGAUAGAUAUCAACUGCAGUUCGGGUA GCACACGAAGGGCACCGUAGCAAUACGGUUGUUCUGGUU AACUUUCGUGGAUGCCACAGGAC
C3sc	5´-Primer (5´-C-47)	AATTCTAATACGACTCACTATAGGGAGAGGAGGGAGATAGA TATCAAGATATCAA
C3sc	3´-Primer (3´-C-20)	GTCCTGTGGCATCCACGAAA
C3sc	RNA	GGGAGAGGAGGGAGAUAGAUAUCAAAGGAUCUAGGUCCG CGCUCUUGUUAAGCUACGUACGGAGGCCACACGAUUAGAU GGUUUCGUGGAUGCCACAGGAC
C5	5´-Primer (5´-P2-45)	AATTCTAATACGACTCACTATAGGGAGAGAGCGAGAGGTA ACTAA
C5	3´-Primer (3´-C-20)	GTCCTGTGGCATCCACGAAA
C5	RNA	GGGAGAGAGCGAGAGGUAACUAAGAGGAAAGGCGCUAGG CAAGUGGCUCCUCGAAAGGGCAUGCGCCAUUAAGAAACCA GUAUUUCCUCGAGUUUCGUGGAUGCCACAGGAC
C5sc	5´-Primer (5´-P2-45)	AATTCTAATACGACTCACTATAGGGAGAGAGCGAGAGGTA ACTAA
C5sc	3´-Primer (3´-C-20)	GTCCTGTGGCATCCACGAAA
C5sc	RNA	GGGAGAGAGCGAGAGGUAACUAAGACCGAGGACGGAUCGC AGAUGUCCGAGCUACACCAUACACAGGCGAAGGAGUGAUU AAUAGGUCUUGCUUUCGUGGAUGCCACAGGAC
C5 A1	5´-Primer (5´-P2-45)	AATTCTAATACGACTCACTATAGGGAGAGAGCGAGAGGTA ACTAA
C5 A1	3´-Primer (3´-C-20)	GTCCTGTGGCATCCACGAAA
C5 A1	RNA	GGGAGAGAGCGAGAGGUAACUAAGAGGAAAGGGCCUAGGC AAGUGGCUCCUCGAAAGGGCAUGCGCCAUUAAGAAACCAG UAUUUCCUCGAGUUUCGUGGAUGCCACAGGAC

Table 9.3: Erk2 aptamers and control sequences continued

Name	Type	Sequence
C5 B2	5´-Primer (5´-P2-45)	AATTCTAATACGACTCACTATAGGGAGAGAGCGAGAGGT AACTAA
C5 B2	3´-Primer (3´-C-20)	GTCCTGTGGCATCCACGAAA
C5 B2	RNA	GGGAGAGAGCGAGAGGUAACUAAGAGGAAAGGCGCUAG GCAAGUGGCUCCUCGAAAGGGCAUGCGCCAUUAAGAAA GGAGUAUUUCCUCGAGUUUCGUGGAUGCCACAGGAC
TRA	5´-Primer (5´-Tra4f)	AATTCTAATACGACTCACTATAGGGAGAGCCATACCTGGG AAAG
TRA	3´-Primer (3´-Tra4rev)	GGGATGCGTAACCTGGGA
TRA	RNA	GGGAGAGCCAUACCUGGGAAAGACGCUAGCGAAUUGG UUCCUCGAAAGGGGAAAGCGUUAUUAAGAAACCAAAA UUUCCCAGGUUACGCAUCCC

Table 9.4: Truncated Erk2 aptamers and control sequence used for whole-cell recordings

Name	Type	Sequence
C3.59	5´-Primer (5´-C3.59f)	AATTCTAATACGACTCACTATAGGTAGCACACGAAGGG CACCGTA
C3.59	3´-Primer (3´-C3.59r)	GGCATCCACGAAAGTTAACCA
C3.59	RNA	GGUAGCACACGAAGGGCACCGUAGCAAUACGGUUGUU CUGGUUAACUUUCGUGGAUGCC
C5.71	5´-Primer (5´-C5.71f)	AATTCTAATACGACTCACTATAGGAGGAAAGGCGCTAG GCAAGT
C5.71	3´-Primer (3´-C5.71r)	CGTCGAGGAAATACTGGTTTCTTAATGG
C5.71	RNA	GGAGGAAAGGCGCUAGGCAAGUGGCUCCUCGAAAGG GCAUGCGCCAUUAAGAAACCAGUAUUUCCUCGACG
C5.B2.71	5´-Primer (5´-C5.71f)	AATTCTAATACGACTCACTATAGGAGGAAAGGCGCTAG GCAAGT
C5.B2.71	3´-Primer (3´-B2.71r)	CGTCGAGGAAATACTCCTTTCTTAATGG
C5.B2.71	RNA	GGAGGAAAGGCGCUAGGCAAGUGGCUCCUCGAAAGG GCAUGCGCCAUUAAGAAAGGAGUAUUUCCUCGACG

9.2 Expression constructs

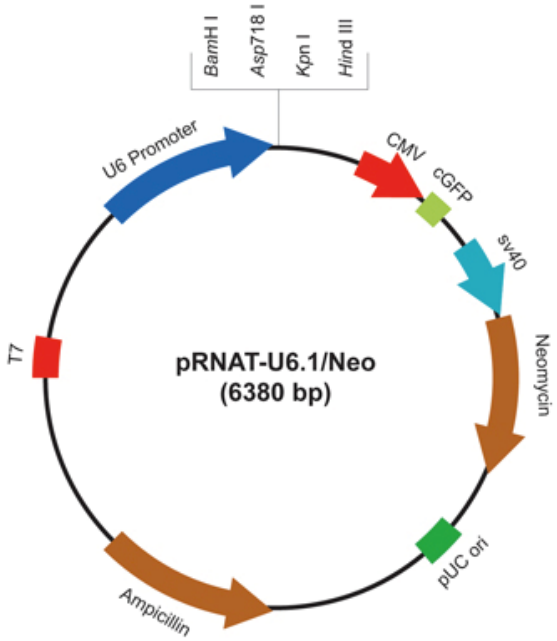

Figure 9.1: pRNAT U6.neo RNA expression vector. Full-length aptamers or control sequences were cloned with BamHI or HindIII into this vector.

9.2.1 Oligos

Table 9.5: Erk2 aptamers and control sequences used for intracellular expresion

Name	Sequence
C3	GGGAGAGGAGGGAGAUAGAUAUCAACUGCAGUUCGGGUAGCACACGAAGGGC ACCGUAGCAAUACGGUUGUUCUGGUUAACUUUCGUGGAUGCCACAGGACUUU
C3sc	GGGAGAGGAGGGAGAUAGAUAUCAAAGGAUCUAGGUCCGCGCUCUUGUUAAG CUACGUACGGAGGCCACACGAUUAGAUGGUUUCGUGGAUGCCACAGGACUUU
C5	GGGAGAGAGCGAGAGGUAACUAAGAGGAAAGGCGCUAGGCAAGUGGCUCCUC GAAAGGGCAUGCGCCAUUAAGAAACCAGUAUUUCCUCGAGUUUCGUGGAUGCC ACAGGACUUU

Table 9.6: Erk2 aptamers and control sequences used for intracellular expresion continued

Name	Sequence
C5sc	GGGAGAGAGCGAGAGGUAACUAAGACCGAGGACGGAUCGCAGAUGUCCG AGCUACACCAUACACAGGCGAAGGAGUGAUUAAUAGGUCUUGCUUUCGU GGAUGCCACAGGACUUU
C5 B2	GGGAGAGAGCGAGAGGUAACUAAGAGGAAAGGCGCUAGGCAAGUGGCUC CUCG AAAGGGCAUGCGCCAUUAAGAAAGGAGUAUUUCCUCGAGUUUCGU GGAUGCCACAGGACUUU

9.3 Proteins

Protein expressed during this thesis:

Erk2 wild-type
MAHHHHHHAMAAAAAGPEMVRGQVFDVGPRYTNLSYIGEGAYGMVCSAYDNLN
KVRVAIKKISPFEHQTYCQRTLREIKILLRFRHENIIGINDIIRAPTIEQMKDVYIVQDLM
ETDLYKLLKTQHLSNDHICYFLYQILRGLKYIHSANVLHRDLKPSNLLLNTTCDLKIC
DFGLARVADPDHDHTGFLTEYVATRWYRAPEIMLNSKGYTKSIDIWSVGCILAEMLS
NRPIFPGKHYLDQLNHILGILGSPSQEDLNCIINLKARNYLLSLPHKNKVPWNRLFPN
ADSKALDLLDKMLTFNPHKRIEVEQALAHPYLEQYYDPSDEPIAEAPFKFDMELDDL
PKEKLKELIFEETARFQPGYRS

Erk2 N236K
MAHHHHHHAMAAAAAGPEMVRGQVFDVGPRYTNLSYIGEGAYGMVCSAYDNLN
KVRVAIK KISPFEHQTYCQRTLREIKILLRFRHENIIGINDIIRAPTIEQMKDVYIVQDLM
ETDLYK LLKTQHLSNDHICYFLYQILRGLKYIHSANVLHRDLKPSNLLLNTTCDLKIC
DFGLARVADPDHDHTGFLTEYVATRWYRAPEIMLNSKGYTKSIDIWSVGCILAEMLS
NRPIFPGKHYLDQLKHILGILGSPSQEDLNCIINLKARNYLLSLPHKNKVPWNRLFPNA
DSKALDLLDKMLTFNPHKRIEVEQALAHPYLEQYYDPSDEPIAEAPFKFDMELDDLPK
EKLKELIFEETARFQPGYRS

Erk2 Y261N
MAHHHHHHAMAAAAAGPEMVRGQVFDVGPRYTNLSYIGEGAYGMVCSAYDNLN
KVRVAIKKISPFEHQTYCQRTLREIKILLRFRHENIIGINDIIRAPTIEQMKDVYIVQDLM
ETDLYKLLKTQHLSNDHICYFLYQILRGLKYIHSANVLHRDLKPSNLLLNTTCDLKIC
DFGLARVA DPDHDHTGFLTEYVATRWYRAPEIMLNSKGYTKSIDIWSVGCILAEML
SNRPIFPGKHYLDQLNHILGILGSPSQEDLNCIINLKARNNLLSLPHKNKVPWNRLF
PNADSKALDLLDKMLTFNPHKRIEVEQALAHPYLEQYYDPSDEPIAEAPFKFDME
LDDLPKEKLKELIFEETARFQPGYRS

Erk2 S264P
MAHHHHHHAMAAAAAGPEMVRGQVFDVGPRYTNLSYIGEGAYGMVCSAYDNLN
KVRVAIKKISPFEHQTYCQRTLREIKILLRFRHENIIGINDIIRAPTIEQMKDVYIVQDLM
ETDLYKLLKTQHLSNDHICYFLYQILRGLKYIHSANVLHRDLKPSNLLLNTTCDLKIC
DFGLARVADPDHDHTGFLTEYVATRWYRAPEIMLNSKGYTKSIDIWSVGCILAEMLS
NRPIFPGKHYLDQLNHILGILGSPSQEDLNCIINLKARNYLLPLPHKNKVPWNRLFPN
ADSKALDLLDKMLTFNPHKRIEVEQALAHPYLEQYYDPSDEPIAEAPFKFDMELDDL
PKEKLKELIFEETARFQPGYRS

Mek1 wild-type
HHHHHHGMASMTGGQQMGRDLYDDDDKDRWGSGGVGSALPGSKMPKKKPTPIQLN
PAPDGSAVNGTSSAETNLEALQKKLEELELDEQQRKRLEAFLTQKQKVGELKDDDFEKI
SELGAGNGGVVFKVSHKPSGLVMARKLIHLEIKPAIRNQIIRELQVLHECNSPYIVGFYGA
FYSDGEISICMEHMDGGSLDQVLKKAGRIPEQILGKVSIAVIKGLTYLREKHKIMHRDVKPS
NILVNSRGEIKLCDFGVSGQLIDSMANSFVGTRSYMSPERLQGTHYSVQSDIWSMGLSLV
EMAVGRYPIPPPDAKELELMFGCQVEGDAAETPPRPRTPGRPLSSYGMDSRPPMAIFELL
DYIVNEPPPKLPSGVFSLEFQDFVNKCLIKNPAERADLKQLMVHAFIKRSDAEEVDFAGW
LCSTIGLNQPSTPTHAAGV

Mek G7B
HHHHHHGMASMTGGQQMGRDLYDDDDKDRWGSGGVGSALPGSKMPKKKPTPIQLNPA
PDGSAVNGTSSAETNLEALQKKLEELELDAFLTQKQKVGELKDDDFEKISELGAGNGGVV
FK VSHKPSGLVMARKLIHLEIKPAIRNQIIRELQVLHECNSPYIVGFYGAFYSDGEISICMEH
MDGG SLDQVLKKAGRIPEQILGKVSIAVIKGLTYLREKHKIMHRDVKPSNILVNSRGEIKLC
DFGVSGQ LIDDD ADDFVGTRSYMSPERLQGTHYSVQSDIWSMGLSLVEMAVGRYPI PPPD
AKELELMFG CQVEGDAAETPPRPRTPGRPLSSY GMDSRPPMAIFELLDYIVNEPPPKLPSG
VFSLEFQDFVN KCLIKNPAERADLKQLMVHAFIKRSDAEEVDFAGWLCSTIGLNQ PST
PTHAAGV

Proteins from other sources:

Table 9.7: Proteins and suppliers

Name	**Supplier**
human Erk2, active	Proqinase, Germany
JNK2alpha2/SAPK1a, inactive	Merck Millipore, Germany
p38alpha MAPK, inactive	Marie-Sophie Raddatz, University of Bonn
GRK2	Prof. Dr. J. Tesmer, University of Michigan
RSK4	Prof. Dr. S. Knapp, University of Oxford
PKB?	Prof. Dr. S. Knapp, University of Oxford
VRK1	Prof. Dr. S. Knapp, University of Oxford
CK	Prof. Dr. S. Knapp, University of Oxford
DRAK1	Prof. Dr. S. Knapp, University of Oxford
AAK	Prof. Dr. S. Knapp, University of Oxford
NEK1	Prof. Dr. S. Knapp, University of Oxford
TOPK	Prof. Dr. S. Knapp, University of Oxford

9.4 Antibodies

Table 9.8: Antibodies

Antigen	Epitope	Company	Clone
Elk1	p-Ser383	Santa Cruz	B-4
p90-RSK1	p-T359/363	Epitomics/Biomol	E238
Erk1/2	p-T202/Y204	Cell Signalling	197G2
Erk1/2	subdomain XI	Santa Cruz	K-23
p38a	n.d.	Cell Signalling	9212
JNK1	amino acids 1-384	Santa Cruz	F-3
Actin	C-terminus	Santa Cruz	C-11
Hsc70	n.d	Stressgen/Biomol	N27F34
DyLight 700 Conjugated	Rabbit IgG (H+L)	Thermo Scientific	
DyLight 800 Conjugated	Mouse IgG (H+L)	Thermo Scientific	

9.5 Commercially available kits

Table 9.9: Commercially available kits

Application	Kit	Supplier
Luciferase	Luciferase Assay System E1501	Promega
Mycoplama tests	VenorGeM Classic Mycoplasma PCR Detection Kit	Minerva Biolabs
PCR purification	NucleoSpin Extract II Gel and PCR Clean-up	Macherey-Nagel
Plasmid purification (small scale)	NucleoSpin Plasmid	Macherey-Nagel
Plasmid purification (midi)	NucleoBond Xtra Midi	Macherey-Nagel

9.6 Reagents and chemicals

Table 9.10: Reagents

Reagent	Supplier
Agar	Sigma
Agarose Invitrogen	
Ampicillin sodium salt	AppliChem
Ammoniumacetate	Gruessing
Ammomiumperoxodisulfate (APS)	Roth
Bis-Acrylamid, Rotiphorese	Roth
Biotin	Sigma-Aldrich
Bovine Serum Albumin (BSA, nuclease and protease free)	Calbiochem
Bradford-reagent	BioRad
Bromphenol blue	Merck
Calf intestine alkaline phosphatase (CIAP)	Promega
Cell culture media	PAA
Chloroform	AppliChem
Coomassie Brilliant Blue G250	BioRad
Dimethylformamide (DMF)	Fischer Scientific
1,4-Dithiothreitol (DTT)	Roth
DPBS (1x), pH 7.4	PAA
di-Sodiumhydrogenphosphate-dihydrate	Merck
DNase	Roche
dNTPs	Larova
Dynabeads M-280 Streptavidin	Invitrogen
EGF; AF-100-15	Peprotech
Ethanol abs.	Sigma
Ethidium bromide	Roth
Ethylendiamintetraacetic acid (EDTA) p.A.	AppliChem
EZ-link PEO-iodoacetyl biotin	Genaxxon Biosciences
Fetal Bovine Serum (FBS), DE14-870F[1]	Lonza
FBS (Instant), F0685-3G, Lot 119K3396[2]	Sigma
Formaldehyde (36)	Fluka
GeneRuler 100 bp DNA Ladder	Thermoa

Table 9.11: Reagents

Reagent	**Supplier**
Glycine	Roth
Guanosine-5'-thiophosphate disodium salt	Emp Biotec
Hepes	Roth
HiTrap5 columns GE healthcare	
Hydrochloric acid (HCl)	Roth
Imidazole	AppliChem
Iodacetamido-fluorescein	Sigma
Iodacetamido-biotin (EZ-link PEG2)	Thermo Scientific
Isopropanol	Merck
Lennox Broth (LB)	Sigma
Lipofectamin LTX + Plus reagent	Invitrogen
Magnesiumchloride-hexahydrate	AppliChem
Methanol	VWR
MTT dye solution	AppliChem
Ni-NTA-beads	Qiagen
NTPs	Larova
Page Ruler Prestained Protein Ladder	Fermentas
Pfu polymerase	In house production
Potassium chloride (KCl)	Gruessing
RNasin	Promega
Rotiphorese Sequenziergel Konzentrat	Roth
Salt optimized carbon medium (SOC)	Sigma
Sodium Acetate	Gruessing
Sodium chloride p. A.	AppliChem
Sodium dodecylsulfate (SDS)	Roth
Sodium hydrogenphosphate	Sigma Aldrich
Sodium hydroxide	Gruessing
Sodium orthovanadate AppliChem	
Sodium pyrophosphate AppliChem	
Streptavidin	Sigma
Superdex200 column	GE Healthcare
T7 polymerase	In house production
N,N,N',N' -Tetramethylethylendiamide (TEMED) Roth	
Tris	Roth
Triton X-100	Merck
Trypsin/EDTA (10x)	PAA
Tween-20	Calbiochem
Urea	AppliChem
XL10 Gold Ultracompetent Cells	Invitrogen

9.7 Equipment

Table 9.12: Equipment

Equipment	Supplier
Agarose gel and equipment	in house construction
Analytical balance	Sartorius
Autoclave	Systec
Beaker	Schott
BioMate 3 Photometer	Thermo Spectronic
Cell culture media	PAA
Cell scraper	TPP
Centrifuges	Eppendorf
Culture dishes	TPP
Culture flask	TPP
Culture plates	TPP
Counter for radioactivity	Berthold
Cryo tubes	Roth
Disposable cuvettes	Roth
DPBS (1x), pH 7.4	PAA
Electrophoresis chambers	BioRad
Eppi vials	Sarstedt
Erlenmeyer flask	Schott
Fluorescence spectrometer	Enspire
G25 columns	GE Healthcare
Glass plates for PAGE	Baack
Glass bottles	Schott
Glasswool silanized	Serva
Gloves	Peske
Head-top-tumbler	Heidolph
Heating blocks	Bachofer
Hood (bacteria)	Antares
Hood (eukaryotic cell lines)	Hera
Incubator shaker	Innova
Incubator (37 °C-90 °C)	VWR
Incubator (cell culture)	Hera

Table 9.13: Equipment

Equipment	**Supplier**
Magnetic stirrer	IKA
Microwave	Bosch
Multichannel pipette	Eppendorf
Multipette	Eppendorf
NanoQuant infinite 200	Tecan
Nitrocellulose membrane (Protran 0.45 μM)	Schleicher and Schuell
Parafilm	Faust
PCR Thermocycler	Biometra
pH Paper	Macherey-Nagel
Phosphorimager screens and cassettes	Fuji
Phosphorimager FLA-3000	Fujifilm
Pipets	Eppendorf
Pipet tips	Sarstedt
Pipetboy Accu-Jet pro	Brand
Power supply for PAGE	Consort
Radioactivity protection gear (goggles, shields etc.)	Sigma
Reaction tubes (2 ml, 1.5 ml, 0.5 ml)	Sarstedt
Scalpel blades	Labomedic
Sterile filters (syringe filter)	Merck Millipore
Sunrise plate reader	Tecan
Tips for multipettes	Eppendorf
Thermomixer	Eppendorf
UV Transilluminator	VWR
VarioSkan	Thermo
Vortex mixer	Neolab
Vaccum manifold (filter binding assays)	Schleicher and Schuell
Water bath	GFL
Water purification system	Werner
96 well plates, half area, flat, black	Greiner Bio One
96 well plates, U-shape	Roth
Tecan Ultra reader	Tecan

10 Appendix

10.1 Negative control sequences

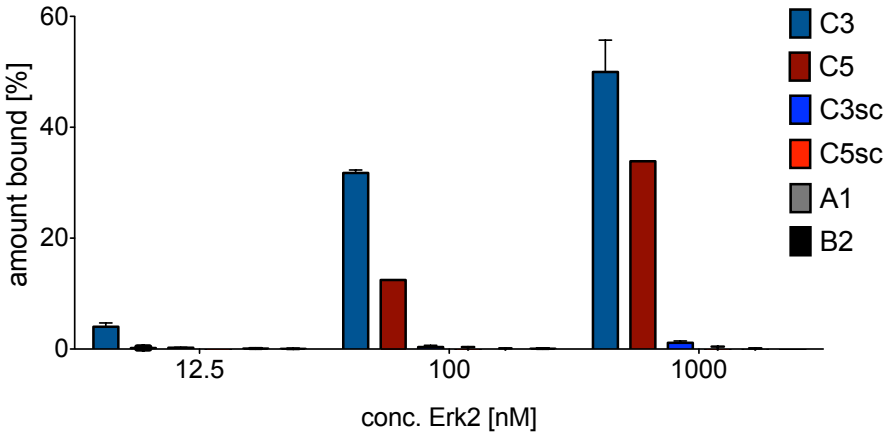

Figure 10.1: Binding assays with all negative control sequences. The amount of radioactively labeled RNA is plotted against the Erk2 concentration. Experiments were performed twice (mean ± SEM). None of the utilized negative control sequences for C3 or C5 revealed any affinity for Erk2.

10.2 Aptamer competition assays

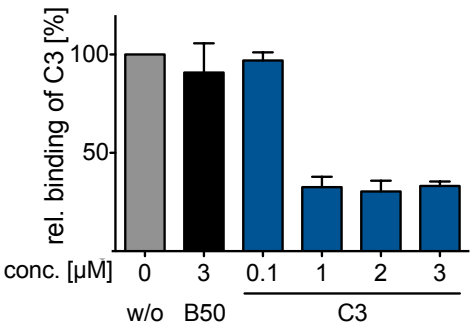

Figure 10.2: Aptamer competition assays. Binding of C3 to Erk2 in the presence of B50 library RNA or C3 in PBS buffer. The amount of radioactively lebeled C3 RNA without additional RNA was set to 1 (n=4, mean ± SEM). Data were obtained during my diploma thesis [497].

10.3 Kinase assays

10.3.1 Binding tests

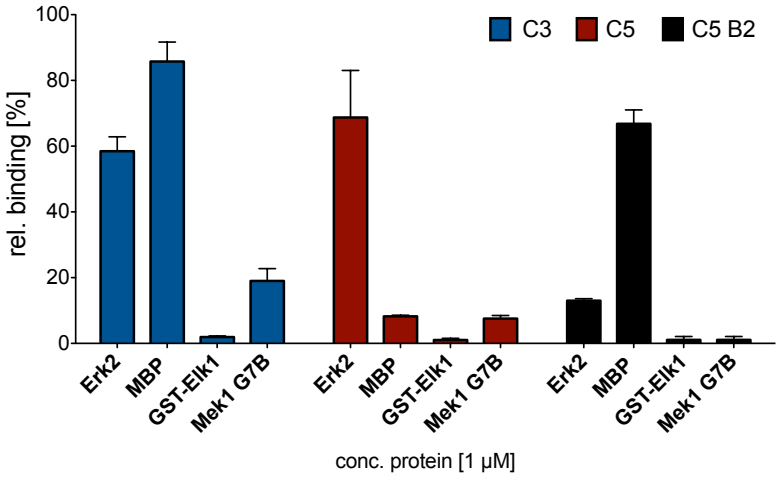

Figure 10.3: Binding assays. Binding assays with proteins utilized for kinase assays in Hepes buffer with 10 mM $MgCl_2$. The amount of radioactively labeled RNA bound to Erk2 is plotted against the protein concentration (n=2, mean ± SEM).

10.3.2 Activity towards Mek1 G7B

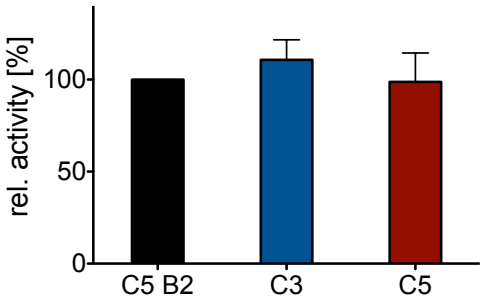

Figure 10.4: Effects on Mek1 catalytic activity. The aptamers effect on Mek1 activity was analyzed at a concentration of 12.5μM. As a readout, Mek1 autophosphorylation was measured. Data were normalized with the C5 B2 treated samples set as 100 %. Neither C3 nor C5 show any inhibitory activity towards Mek1 (n=3, mean ± SEM).

10.4 Recombinant Erk2 proteins

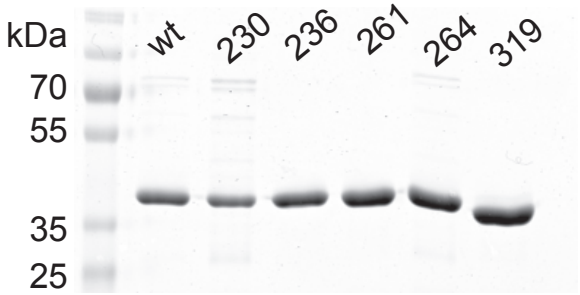

Figure 10.5: Recombinant Erk2 proteins. 5 ul recombinant proteins were utilized per lane of a 10 % SDS-PAGE gel. The molecular weight of Erk2 is approx. 42 kDa. Coomassie staining revealed high purity of the recombinant proteins utilized for point mutant studies. The mutant 230 was omitted from experiments.

10.5 Expression Vector

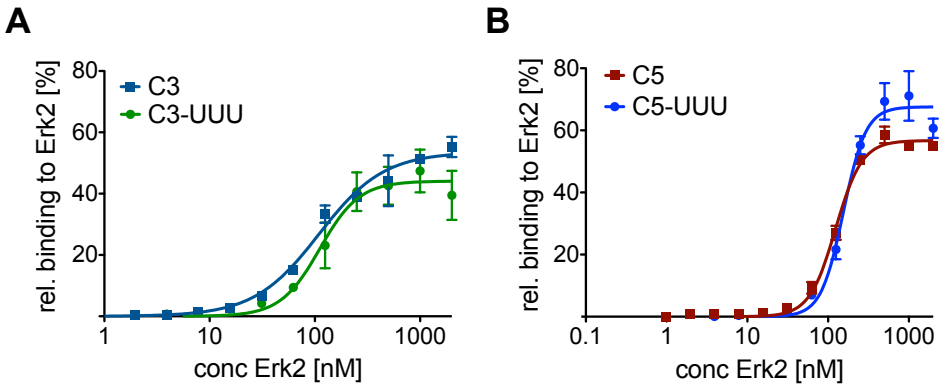

Figure 10.6: Binding assay of the aptamers with additional uracil residues. The amount or radioactively labeled A) C3 or B) C5 or its respective expression constructs bound to Erk2 is plotted against the Erk2 concentration (n=2, mean±SEM).

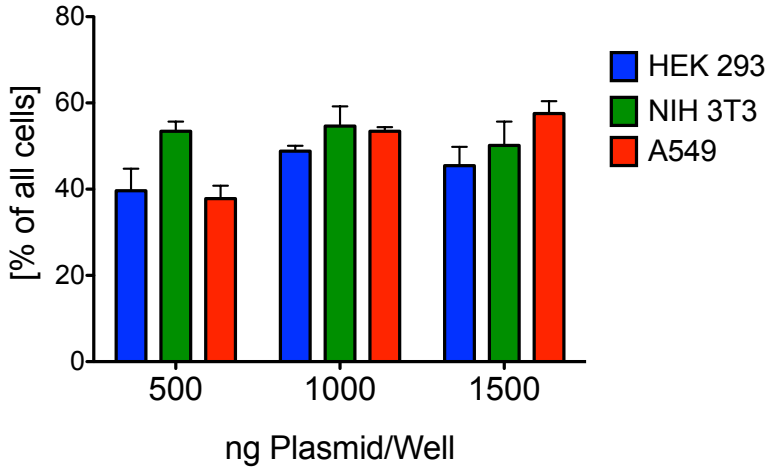

Figure 10.7: Transfection efficiency in distinct cell lines. Transfection efficiency was monitored 24 hours after transfection of the empty RNA expression vector at distinct plasmid concentrations. GFP expression was quantified by flow cytometry (n=2, mean±SEM).

10.6 Expression Vector 2

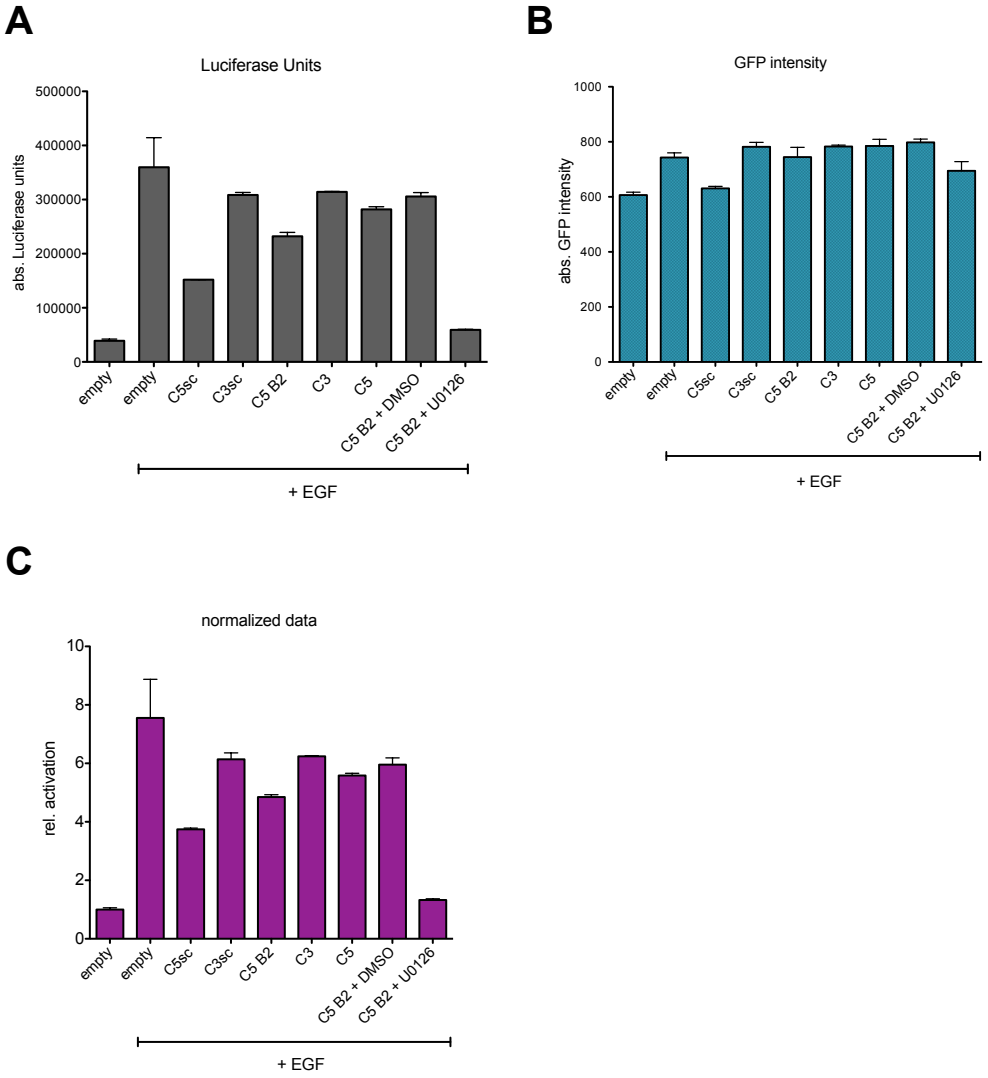

Figure 10.8: Representative luciferase assay. These diagrams show absolute A) GFP intesity and B) absolute luciferase units after transfection with the indicated vectors and stimulation with EGF. C) Luciferase data were normalized for GFP intensity with the unstimulated, empty vector control cells set as 1. This experiment was performed in duplicates.

10.7 Whole-cell recordings

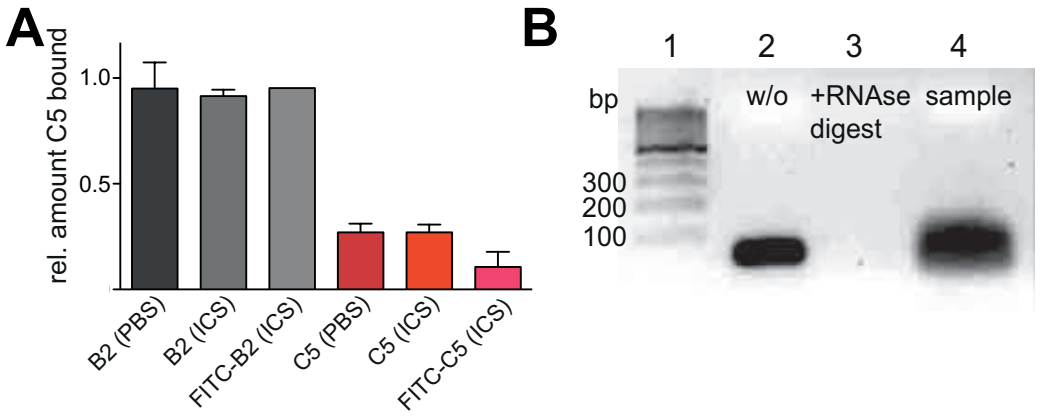

Figure 10.9: C5.71 is functional in recording solution. A) In order to validate the functionality of C5.71 for the assay conditions utilized during the electrophysiological measurement, indicated concentration of unlabeled or 5'-fluorescein-labeled C5.71 or C5 B2.71 control RNA were frozen in PBS or recording buffer (ICS), thawed and used to compete the binding of radioactively labeled C5 from Erk2. The amount of radioactively labeled C5.71 bound to Erk2 was normalized onto control samples without additional RNA added. Unlabeled RNAs were tested twice, fluorescein-labeled RNA was tested once (mean±SEM)). B) C5.71 RNA is not degraded during electrophysiological measurements. 25 pmol C5.71 RNA was incubated without (w/o, lane 2) or with spit as degradation control (+RNAse digest, lane 3). To validate the integrity of C5.71 for the assay conditions utilized during the electrophysiological measurement, C5.71 RNA was directly taken from the microinjection needle (sample, lane 4). No degradation could be observed after measurements.

Bibliography

[1] M. A. Lemmon and J. Schlessinger, "Cell signaling by receptor tyrosine kinases.," *Cell*, vol. 141, pp. 1117–1134, Jun 2010.

[2] J.-M. Beaulieu and R. R. Gainetdinov, "The physiology, signaling, and pharmacology of dopamine receptors.," *Pharmacol Rev*, vol. 63, pp. 182–217, Mar 2011.

[3] T. D. Pollard and W. C. Earnshaw, *Cell biology. Second edition.* Spektrum Akademischer Verlag, 2007.

[4] K. L. Pierce, R. T. Premont, and R. J. Lefkowitz, "Seven-transmembrane receptors.," *Nat Rev Mol Cell Biol*, vol. 3, pp. 639–650, Sep 2002.

[5] A. Christopoulos, "Allosteric binding sites on cell-surface receptors: novel targets for drug discovery.," *Nat Rev Drug Discov*, vol. 1, pp. 198–210, Mar 2002.

[6] L. N. Johnson, "The regulation of protein phosphorylation.," *Biochem Soc Trans*, vol. 37, pp. 627–641, Aug 2009.

[7] G. Manning, D. B. Whyte, R. Martinez, T. Hunter, and S. Sudarsanam, "The protein kinase complement of the human genome.," *Science*, vol. 298, pp. 1912–1934, Dec 2002.

[8] J. S. Fassler and A. H. West, "Histidine phosphotransfer proteins in fungal two-component signal transduction pathways.," *Eukaryot Cell*, vol. 12, pp. 1052–1060, Aug 2013.

[9] S. Klumpp and J. Krieglstein, "Reversible phosphorylation of histidine residues in vertebrate proteins.," *Biochim Biophys Acta*, vol. 1754, pp. 291–295, Dec 2005.

[10] S. Klumpp and J. Krieglstein, "Phosphorylation and dephosphorylation of histidine residues in proteins.," *Eur J Biochem*, vol. 269, pp. 1067–1071, Feb 2002.

[11] A. Kowluru, "Emerging roles for protein histidine phosphorylation in cellular signal transduction: lessons from the islet beta-cell.," *J Cell Mol Med*, vol. 12, pp. 1885–1908, Oct 2008.

[12] P. A. Schwartz and B. W. Murray, "Protein kinase biochemistry and drug discovery.," *Bioorg Chem*, vol. 39, pp. 192–210, Dec 2011.

[13] J. V. Olsen, B. Blagoev, F. Gnad, B. Macek, C. Kumar, P. Mortensen, and M. Mann, "Global, in vivo, and site-specific phosphorylation dynamics in signaling networks.," *Cell*, vol. 127, pp. 635–648, Nov 2006.

[14] E. S. Groban, A. Narayanan, and M. P. Jacobson, "Conformational changes in protein loops and helices induced by post-translational phosphorylation.," *PLoS Comput Biol*, vol. 2, p. e32, Apr 2006.

[15] H. Nishi, K. Hashimoto, and A. R. Panchenko, "Phosphorylation in protein-protein binding: effect on stability and function.," *Structure*, vol. 19, pp. 1807–1815, Dec 2011.

[16] H. Nishi, J. H. Fong, C. Chang, S. A. Teichmann, and A. R. Panchenko, "Regulation of protein-protein binding by coupling between phosphorylation and intrinsic disorder: analysis of human protein complexes.," *Mol Biosyst*, vol. 9, pp. 1620–1626, Jul 2013.

[17] T. Hunter, "Why nature chose phosphate to modify proteins.," *Philos Trans R Soc Lond B Biol Sci*, vol. 367, pp. 2513–2516, Sep 2012.

[18] D. G. Hardie, "Roles of protein kinases and phosphatases in signal transduction.," *Symp Soc Exp Biol*, vol. 44, pp. 241–255, 1990.

[19] E. H. Fischer and E. G. Krebs, "Conversion of phosphorylase b to phosphorylase a in muscle extracts.," *J Biol Chem*, vol. 216, pp. 121–132, Sep 1955.

[20] E. G. Krebs and E. H. Fischer, "The phosphorylase b to a converting enzyme of rabbit skeletal muscle. 1956.," *Biochim Biophys Acta*, vol. 1000, pp. 302–309, 1989.

[21] K. A. B. Krebs, E. G. and E. H. Fischer, "The muscle phosphorylase b kinase reaction.," *J Biol Chem*, vol. 231, pp. 73–83, Mar 1958.

[22] W. Eckhart, M. A. Hutchinson, and T. Hunter, "An activity phosphorylating tyrosine in polyoma t antigen immunoprecipitates.," *Cell*, vol. 18, pp. 925–933, Dec 1979.

[23] M. S. Collett and R. L. Erikson, "Protein kinase activity associated with the avian sarcoma virus src gene product.," *Proc Natl Acad Sci U S A*, vol. 75, pp. 2021–2024, Apr 1978.

[24] G. Manning, G. D. Plowman, T. Hunter, and S. Sudarsanam, "Evolution of protein kinase signaling from yeast to man.," *Trends Biochem Sci*, vol. 27, pp. 514–520, Oct 2002.

[25] R. Robinson, "Confirming the importance of the r-spine: new insights into protein kinase regulation.," *PLoS Biol*, vol. 11, p. e1001681, Oct 2013.

[26] N. Dhanasekaran and E. Premkumar Reddy, "Signaling by dual specificity kinases.," *Oncogene*, vol. 17, pp. 1447–1455, Sep 1998.

[27] J. Boudeau, D. Miranda-Saavedra, G. J. Barton, and D. R. Alessi, "Emerging roles of pseudokinases.," *Trends Cell Biol*, vol. 16, pp. 443–452, Sep 2006.

[28] A. Vulpetti and R. Bosotti, "Sequence and structural analysis of kinase atp pocket residues.," *Farmaco*, vol. 59, pp. 759–765, Oct 2004.

[29] J. D. R. Knight, T. Pawson, and A.-C. Gingras, "Profiling the kinome: current capabilities and future challenges.," *J Proteomics*, vol. 81, pp. 43–55, Apr 2013.

[30] S. K. Hanks, A. M. Quinn, and T. Hunter, "The protein kinase family: conserved features and deduced phylogeny of the catalytic domains.," *Science*, vol. 241, pp. 42–52, Jul 1988.

[31] H. S. Meharena, P. Chang, M. M. Keshwani, K. Oruganty, A. K. Nene, N. Kannan, S. S. Taylor, and A. P. Kornev, "Deciphering the structural basis of eukaryotic protein kinase regulation.," *PLoS Biol*, vol. 11, p. e1001680, Oct 2013.

[32] J. A. Endicott, M. E. M. Noble, and L. N. Johnson, "The structural basis for control of eukaryotic protein kinases.," *Annu Rev Biochem*, vol. 81, pp. 587–613, 2012.

[33] J. Zhang, P. L. Yang, and N. S. Gray, "Targeting cancer with small molecule kinase inhibitors.," *Nat Rev Cancer*, vol. 9, pp. 28–39, Jan 2009.

[34] L. N. Johnson, "Structural basis for substrate recognition and control in protein kinases.," *Ernst Schering Res Found Workshop*, no. 34, pp. 47–69, 2001.

[35] P. Traxler and P. Furet, "Strategies toward the design of novel and selective protein tyrosine kinase inhibitors.," *Pharmacol Ther*, vol. 82, no. 2-3, pp. 195–206, 1999.

[36] B. Nolen, S. Taylor, and G. Ghosh, "Regulation of protein kinases; controlling activity through activation segment conformation.," *Mol Cell*, vol. 15, pp. 661–675, Sep 2004.

[37] J. A. Adams, "Activation loop phosphorylation and catalysis in protein kinases: is there functional evidence for the autoinhibitor model?," *Biochemistry*, vol. 42, pp. 601–607, Jan 2003.

[38] J. Lew, "Map kinases and cdks: kinetic basis for catalytic activation.," *Biochemistry*, vol. 42, pp. 849–856, Feb 2003.

[39] M. Huse and J. Kuriyan, "The conformational plasticity of protein kinases.," *Cell*, vol. 109, pp. 275–282, May 2002.

[40] P. D. Jeffrey, A. A. Russo, K. Polyak, E. Gibbs, J. Hurwitz, J. MassaguÈ, and N. P. Pavletich, "Mechanism of cdk activation revealed by the structure of a cyclina-cdk2 complex.," *Nature*, vol. 376, pp. 313–320, Jul 1995.

[41] A. P. Kornev, N. M. Haste, S. S. Taylor, and L. F. T. Eyck, "Surface comparison of active and inactive protein kinases identifies a conserved activation mechanism.," *Proc Natl Acad Sci U S A*, vol. 103, pp. 17783–17788, Nov 2006.

[42] S. S. Taylor and A. P. Kornev, "Protein kinases: evolution of dynamic regulatory proteins.," *Trends Biochem Sci*, vol. 36, pp. 65–77, Feb 2011.

[43] A. C. Carrera, K. Alexandrov, and T. M. Roberts, "The conserved lysine of the catalytic domain of protein kinases is actively involved in the phosphotransfer reaction and not required for anchoring atp.," *Proc Natl Acad Sci U S A*, vol. 90, pp. 442–446, Jan 1993.

[44] J. A. Adams, "Kinetic and catalytic mechanisms of protein kinases.," *Chem Rev*, vol. 101, pp. 2271–2290, Aug 2001.

[45] N. Kannan and A. F. Neuwald, "Did protein kinase regulatory mechanisms evolve through elaboration of a simple structural component?," *J Mol Biol*, vol. 351, pp. 956–972, Sep 2005.

[46] A. Krupa, G. Preethi, and N. Srinivasan, "Structural modes of stabilization of permissive phosphorylation sites in protein kinases: distinct strategies in ser/thr and tyr kinases.," *J Mol Biol*, vol. 339, pp. 1025–1039, Jun 2004.

[47] J. D. R. Knight, T. Pawson, and A.-C. Gingras, "Profiling the kinome: current capabilities and future challenges.," *J Proteomics*, vol. 81, pp. 43–55, Apr 2013.

[48] S. S. Taylor, E. Radzio-Andzelm, and T. Hunter, "How do protein kinases discriminate between serine/threonine and tyrosine? structural insights from the insulin receptor protein-tyrosine kinase.," *FASEB J*, vol. 9, pp. 1255–1266, Oct 1995.

[49] J. A. Ubersax and J. E. Ferrell, Jr, "Mechanisms of specificity in protein phosphorylation.," *Nat Rev Mol Cell Biol*, vol. 8, pp. 530–541, Jul 2007.

[50] A. D. Sharrocks, S. H. Yang, and A. Galanis, "Docking domains and substrate-specificity determination for map kinases.," *Trends Biochem Sci*, vol. 25, pp. 448–453, Sep 2000.

[51] T. Tanoue and E. Nishida, "Molecular recognitions in the map kinase cascades.," *Cell Signal*, vol. 15, pp. 455–462, May 2003.

[52] A. Remenyi, M. C. Good, and W. A. Lim, "Docking interactions in protein kinase and phosphatase networks.," *Curr Opin Struct Biol*, vol. 16, pp. 676–685, Dec 2006.

[53] A. Remenyi, M. C. Good, R. P. Bhattacharyya, and W. A. Lim, "The role of docking interactions in mediating signaling input, output, and discrimination in the yeast mapk network.," *Mol Cell*, vol. 20, pp. 951–962, Dec 2005.

[54] B. A. Schulman, D. L. Lindstrom, and E. Harlow, "Substrate recruitment to cyclin-dependent kinase 2 by a multipurpose docking site on cyclin a.," *Proc Natl Acad Sci U S A*, vol. 95, pp. 10453–10458, Sep 1998.

[55] D. Vaudry, P. J. S. Stork, P. Lazarovici, and L. E. Eiden, "Signaling pathways for pc12 cell differentiation: making the right connections.," *Science*, vol. 296, pp. 1648–1649, May 2002.

[56] M. J. Robinson, S. A. Stippec, E. Goldsmith, M. A. White, and M. H. Cobb, "A constitutively active and nuclear form of the map kinase erk2 is sufficient for neurite outgrowth and cell transformation.," *Curr Biol*, vol. 8, pp. 1141–1150, Oct 1998.

[57] T. Lee, A. N. Hoofnagle, Y. Kabuyama, J. Stroud, X. Min, E. J. Goldsmith, L. Chen, K. A. Resing, and N. G. Ahn, "Docking motif interactions in map kinases revealed by hydrogen exchange mass spectrometry.," *Mol Cell*, vol. 14, pp. 43–55, Apr 2004.

[58] C. I. Chang, B.-e. Xu, R. Akella, M. H. Cobb, and E. J. Goldsmith, "Crystal structures of map kinase p38 complexed to the docking sites on its nuclear substrate mef2a and activator mkk3b.," *Mol Cell*, vol. 9, pp. 1241–1249, Jun 2002.

[59] Y.-S. Heo, S.-K. Kim, C. I. Seo, Y. K. Kim, B.-J. Sung, H. S. Lee, J. I. Lee, S.-Y. Park, J. H. Kim, K. Y. Hwang, Y.-L. Hyun, Y. H. Jeon, S. Ro, J. M. Cho, T. G. Lee, and C.-H. Yang, "Structural basis for the selective inhibition of jnk1 by the scaffolding protein jip1 and sp600125.," *EMBO J*, vol. 23, pp. 2185–2195, Jun 2004.

[60] P. Cohen, "The role of protein phosphorylation in human health and disease. the sir hans krebs medal lecture.," *Eur J Biochem*, vol. 268, pp. 5001–5010, Oct 2001.

[61] P. Cohen, "Protein kinases–the major drug targets of the twenty-first century?," *Nat Rev Drug Discov*, vol. 1, pp. 309–315, Apr 2002.

[62] A. Leary and S. R. D. Johnston, "Small molecule signal transduction inhibitors for the treatment of solid tumors.," *Cancer Invest*, vol. 25, pp. 347–365, Aug 2007.

[63] C. Kumar, A. V. Purandare, F. Y. Lee, and M. V. Lorenzi, "Kinase drug discovery approaches in chronic myeloproliferative disorders.," *Oncogene*, vol. 28, pp. 2305–2313, Jun 2009.

[64] O. Fedorov, S. Mueller, and S. Knapp, "The (un)targeted cancer kinome.," *Nat Chem Biol*, vol. 6, pp. 166–169, Mar 2010.

[65] S. Knapp, P. Arruda, J. Blagg, S. Burley, D. H. Drewry, A. Edwards, D. Fabbro, P. Gillespie, N. S. Gray, B. Kuster, K. E. Lackey, P. Mazzafera, N. C. O. Tomkinson, T. M. Willson, P. Workman, and W. J. Zuercher, "A public-private partnership to unlock the untargeted kinome.," *Nat Chem Biol*, vol. 9, pp. 3–6, Jan 2013.

[66] L. M. Graves, J. S. Duncan, M. C. Whittle, and G. L. Johnson, "The dynamic nature of the kinome.," *Biochem J*, vol. 450, pp. 1–8, Feb 2013.

[67] "Signal transduction as a drug-discovery platform.," *Nat Biotechnol*, vol. 18 Suppl, pp. IT37–IT39, Oct 2000.

[68] K.-H. Cho and O. Wolkenhauer, "Analysis and modelling of signal transduction pathways in systems biology.," *Biochem Soc Trans*, vol. 31, pp. 1503–1509, Dec 2003.

[69] J. New, W. Kendall, J. Huang, and E. Chesler, "Dynamic visualization of coexpression in systems genetics data.," *IEEE Trans Vis Comput Graph*, vol. 14, no. 5, pp. 1081–1094, 2008.

[70] M. Kawasumi and P. Nghiem, "Chemical genetics: elucidating biological systems with small-molecule compounds.," *J Invest Dermatol*, vol. 127, pp. 1577–1584, Jul 2007.

[71] P. J. Alaimo, M. A. Shogren-Knaak, and K. M. Shokat, "Chemical genetic approaches for the elucidation of signaling pathways.," *Curr Opin Chem Biol*, vol. 5, pp. 360–367, Aug 2001.

[72] K. Hu, C. Lee, D. Qiu, A. Fotovati, A. Davies, S. Abu-Ali, D. Wai, E. R. Lawlor, T. J. Triche, C. J. Pallen, and S. E. Dunn, "Small interfering rna library screen of human kinases and phosphatases identifies polo-like kinase 1 as a promising new target for the treatment of pediatric rhabdomyosarcomas.," *Mol Cancer Ther*, vol. 8, pp. 3024–3035, Nov 2009.

[73] D. Gilot, N. Le Meur, F. Giudicelli, M. Le Vee, D. Lagadic-Gossmann, N. ThÈret, and O. Fardel, "Rnai-based screening identifies kinases interfering with dioxin-mediated up-regulation of cyp1a1 activity.," *PLoS One*, vol. 6, no. 3, p. e18261, 2011.

[74] J. Brognard and T. Hunter, "Protein kinase signaling networks in cancer.," *Curr Opin Genet Dev*, vol. 21, pp. 4–11, Feb 2011.

[75] S. Bartz and A. L. Jackson, "How will rnai facilitate drug development?," *Sci STKE*, vol. 2005, p. pe39, Aug 2005.

[76] Y. Fedorov, E. M. Anderson, A. Birmingham, A. Reynolds, J. Karpilow, K. Robinson, D. Leake, W. S. Marshall, and A. Khvorova, "Off-target effects by sirna can induce toxic phenotype.," *RNA*, vol. 12, pp. 1188–1196, Jul 2006.

[77] A. L. Jackson and P. S. Linsley, "Recognizing and avoiding sirna off-target effects for target identification and therapeutic application.," *Nat Rev Drug Discov*, vol. 9, pp. 57–67, Jan 2010.

[78] W. A. Weiss, S. S. Taylor, and K. M. Shokat, "Recognizing and exploiting differences between rnai and small-molecule inhibitors.," *Nat Chem Biol*, vol. 3, pp. 739–744, Dec 2007.

[79] B. R. Stockwell, "Exploring biology with small organic molecules.," *Nature*, vol. 432, pp. 846–854, Dec 2004.

[80] P. R. Patel, H. Sun, S. Q. Li, M. Shen, J. Khan, C. J. Thomas, and M. I. Davis, "Identification of potent yes1 kinase inhibitors using a library screening approach.," *Bioorg Med Chem Lett*, vol. 23, pp. 4398–4403, Aug 2013.

[81] O. von Ahsen and U. Boemer, "High-throughput screening for kinase inhibitors.," *Chembiochem*, vol. 6, pp. 481–490, Mar 2005.

[82] H. Wesche, S.-H. Xiao, and S. W. Young, "High throughput screening for protein kinase inhibitors.," *Comb Chem High Throughput Screen*, vol. 8, pp. 181–195, Mar 2005.

[83] A. K. Ghose, T. Herbertz, D. A. Pippin, J. M. Salvino, and J. P. Mallamo, "Knowledge based prediction of ligand binding modes and rational inhibitor design for kinase drug discovery.," *J Med Chem*, vol. 51, pp. 5149–5171, Sep 2008.

[84] L. Q. M. Chow and S. G. Eckhardt, "Sunitinib: from rational design to clinical efficacy.," *J Clin Oncol*, vol. 25, pp. 884–896, Mar 2007.

[85] K. Imai and A. Takaoka, "Comparing antibody and small-molecule therapies for cancer.," *Nat Rev Cancer*, vol. 6, pp. 714–727, Sep 2006.

[86] M. A. Fabian, W. H. Biggs, 3rd, D. K. Treiber, C. E. Atteridge, M. D. Azimioara, M. G. Benedetti, T. A. Carter, P. Ciceri, P. T. Edeen, M. Floyd, J. M. Ford, M. Galvin, J. L. Gerlach, R. M. Grotzfeld, S. Herrgard, D. E. Insko, M. A. Insko, A. G. Lai, J.-M. LÈlias, S. A. Mehta, Z. V. Milanov, A. M. Velasco, L. M. Wodicka, H. K. Patel, P. P. Zarrinkar, and D. J. Lockhart, "A small molecule-kinase interaction map for clinical kinase inhibitors.," *Nat Biotechnol*, vol. 23, pp. 329–336, Mar 2005.

[87] S. P. Davies, H. Reddy, M. Caivano, and P. Cohen, "Specificity and mechanism of action of some commonly used protein kinase inhibitors.," *Biochem J*, vol. 351, pp. 95–105, Oct 2000.

[88] J. Bain, H. McLauchlan, M. Elliott, and P. Cohen, "The specificities of protein kinase inhibitors: an update.," *Biochem J*, vol. 371, pp. 199–204, Apr 2003.

[89] J. Bain, L. Plater, M. Elliott, N. Shpiro, C. J. Hastie, H. McLauchlan, I. Klevernic, J. S. C. Arthur, D. R. Alessi, and P. Cohen, "The selectivity of protein kinase inhibitors: a further update.," *Biochem J*, vol. 408, pp. 297–315, Dec 2007.

[90] T. Anastassiadis, S. W. Deacon, K. Devarajan, H. Ma, and J. R. Peterson, "Comprehensive assay of kinase catalytic activity reveals features of kinase inhibitor selectivity.," *Nat Biotechnol*, vol. 29, pp. 1039–1045, Nov 2011.

[91] M. I. Davis, J. P. Hunt, S. Herrgard, P. Ciceri, L. M. Wodicka, G. Pallares, M. Hocker, D. K. Treiber, and P. P. Zarrinkar, "Comprehensive analysis of kinase inhibitor selectivity.," *Nat Biotechnol*, vol. 29, pp. 1046–1051, Nov 2011.

[92] P. Dent, "Multi-kinase inhibition in ovarian cancer.," *Cancer Biol Ther*, vol. 15, Oct 2013.

[93] D. R. Duckett and M. D. Cameron, "Metabolism considerations for kinase inhibitors in cancer treatment.," *Expert Opin Drug Metab Toxicol*, vol. 6, pp. 1175–1193, Oct 2010.

[94] T. Force and K. L. Kolaja, "Cardiotoxicity of kinase inhibitors: the prediction and translation of preclinical models to clinical outcomes.," *Nat Rev Drug Discov*, vol. 10, pp. 111–126, Feb 2011.

[95] T. U. Mayer, "Chemical genetics: tailoring tools for cell biology.," *Trends Cell Biol*, vol. 13, pp. 270–277, May 2003.

[96] K. J. Cox, C. D. Shomin, and I. Ghosh, "Tinkering outside the kinase atp box: allosteric (type iv) and bivalent (type v) inhibitors of protein kinases.," *Future Med Chem*, vol. 3, pp. 29–43, Jan 2011.

[97] M. A. Bogoyevitch and D. P. Fairlie, "A new paradigm for protein kinase inhibition: blocking phosphorylation without directly targeting atp binding.," *Drug Discov Today*, vol. 12, pp. 622–633, Aug 2007.

[98] V. Lamba and I. Ghosh, "New directions in targeting protein kinases: focusing upon true allosteric and bivalent inhibitors.," *Curr Pharm Des*, vol. 18, no. 20, pp. 2936–2945, 2012.

[99] Z. Fang, C. Gruetter, and D. Rauh, "Strategies for the selective regulation of kinases with allosteric modulators: exploiting exclusive structural features.," *ACS Chem Biol*, vol. 8, pp. 58–70, Jan 2013.

[100] R. Eglen and T. Reisine, "Drug discovery and the human kinome: recent trends.," *Pharmacol Ther*, vol. 130, pp. 144–156, May 2011.

[101] A. A. Ivanov, F. R. Khuri, and H. Fu, "Targeting protein-protein interactions as an anticancer strategy.," *Trends Pharmacol Sci*, vol. 34, pp. 393–400, Jul 2013.

[102] A. Mullard, "Protein-protein interaction inhibitors get into the groove.," *Nat Rev Drug Discov*, vol. 11, pp. 173–175, Mar 2012.

[103] P. T. M. W. Charles A Janeway, Jr and M. J. Shlomchik., *Immunobiology: The Immune System in Health and Disease. 5th edition.* Garland Science, 2001.

[104] J.-L. Teillaud, "Engineering of monoclonal antibodies and antibody-based fusion proteins: successes and challenges.," *Expert Opin Biol Ther*, vol. 5 Suppl 1, pp. S15–S27, Sep 2005.

[105] G. Fuh, "Synthetic antibodies as therapeutics.," *Expert Opin Biol Ther*, vol. 7, pp. 73–87, Jan 2007.

[106] S. Miersch and S. S. Sidhu, "Synthetic antibodies: concepts, potential and practical considerations.," *Methods*, vol. 57, pp. 486–498, Aug 2012.

[107] C. A. Hudis, "Trastuzumab–mechanism of action and use in clinical practice.," *N Engl J Med*, vol. 357, pp. 39–51, Jul 2007.

[108] S. D. Jayasena, "Aptamers: an emerging class of molecules that rival antibodies in diagnostics.," *Clin Chem*, vol. 45, pp. 1628–1650, Sep 1999.

[109] D. Perez-Martinez, T. Tanaka, and T. H. Rabbitts, "Intracellular antibodies and cancer: new technologies offer therapeutic opportunities.," *Bioessays*, vol. 32, pp. 589–598, Jul 2010.

[110] U. H. Weidle, D. Maisel, U. Brinkmann, and G. Tiefenthaler, "The translational potential for target validation and therapy using intracellular antibodies in oncology.," *Cancer Genomics Proteomics*, vol. 10, no. 6, pp. 239–250, 2013.

[111] F. M. Cunha, D. A. Berti, Z. S. Ferreira, C. F. Klitzke, R. P. Markus, and E. S. Ferro, "Intracellular peptides as natural regulators of cell signaling.," *J Biol Chem*, vol. 283, pp. 24448–24459, Sep 2008.

[112] Y. Zhang, C. Eigenbrot, L. Zhou, S. Shia, W. Li, C. Quan, J. Tom, P. Moran, P. Di Lello, N. J. Skelton, M. Kong-Beltran, A. Peterson, and D. Kirchhofer, "Identification of a small peptide that inhibits pcsk9 protein binding to the low density lipoprotein receptor.," *J Biol Chem*, vol. 289, pp. 942–955, Jan 2014.

[113] H. Eldar-Finkelman and M. Eisenstein, "Peptide inhibitors targeting protein kinases.," *Curr Pharm Des*, vol. 15, no. 21, pp. 2463–2470, 2009.

[114] O. Kaidanovich-Beilin and H. Eldar-Finkelman, "Peptides targeting protein kinases: strategies and implications.," *Physiology (Bethesda)*, vol. 21, pp. 411–418, Dec 2006.

[115] A. W. White, A. D. Westwell, and G. Brahemi, "Protein-protein interactions as targets for small-molecule therapeutics in cancer.," *Expert Rev Mol Med*, vol. 10, p. e8, 2008.

[116] Y. Z. Lin, S. Y. Yao, R. A. Veach, T. R. Torgerson, and J. Hawiger, "Inhibition of nuclear translocation of transcription factor nf-kappa b by a synthetic peptide containing a cell membrane-permeable motif and nuclear localization sequence.," *J Biol Chem*, vol. 270, pp. 14255–14258, Jun 1995.

[117] J. Hawiger, "Noninvasive intracellular delivery of functional peptides and proteins.," *Curr Opin Chem Biol*, vol. 3, pp. 89–94, Feb 1999.

[118] J. Liu, M. You, Y. Pu, H. Liu, M. Ye, and W. Tan, "Recent developments in protein and cell-targeted aptamer selection and applications.," *Curr Med Chem*, vol. 18, no. 27, pp. 4117–4125, 2011.

[119] L. A. Holeman, S. L. Robinson, J. W. Szostak, and C. Wilson, "Isolation and characterization of fluorophore-binding rna aptamers.," *Fold Des*, vol. 3, no. 6, pp. 423–431, 1998.

[120] K. Harada and A. D. Frankel, "Identification of two novel arginine binding dnas.," *EMBO J*, vol. 14, pp. 5798–5811, Dec 1995.

[121] S. D. Mendonsa and M. T. Bowser, "In vitro selection of aptamers with affinity for neuropeptide y using capillary electrophoresis.," *J Am Chem Soc*, vol. 127, pp. 9382–9383, Jul 2005.

[122] S. E. Lupold, B. J. Hicke, Y. Lin, and D. S. Coffey, "Identification and characterization of nuclease-stabilized rna molecules that bind human prostate cancer cells via the prostate-specific membrane antigen.," *Cancer Res*, vol. 62, pp. 4029–4033, Jul 2002.

[123] Z. Balogh, G. Lautner, V. BardÛczy, B. Komorowska, R. E. Gyurcs·nyi, and T. MÈsz·ros, "Selection and versatile application of virus-specific aptamers.," *FASEB J*, vol. 24, pp. 4187–4195, Nov 2010.

[124] M.-S. L. Raddatz, A. Dolf, E. Endl, P. Knolle, M. Famulok, and G. Mayer, "Enrichment of cell-targeting and population-specific aptamers by fluorescence-activated cell sorting.," *Angew Chem Int Ed Engl*, vol. 47, no. 28, pp. 5190–5193, 2008.

[125] C. Meyer, U. Hahn, and A. Rentmeister, "Cell-specific aptamers as emerging therapeutics.," *J Nucleic Acids*, vol. 2011, p. 904750, 2011.

[126] G. R. Zimmermann, C. L. Wick, T. P. Shields, R. D. Jenison, and A. Pardi, "Molecular interactions and metal binding in the theophylline-binding core of an rna aptamer.," *RNA*, vol. 6, pp. 659–667, May 2000.

[127] R. Conrad and A. D. Ellington, "Detecting immobilized protein kinase c isozymes with rna aptamers.," *Anal Biochem*, vol. 242, pp. 261–265, Nov 1996.

[128] T. Hermann and D. J. Patel, "Adaptive recognition by nucleic acid aptamers.," *Science*, vol. 287, pp. 820–825, Feb 2000.

[129] A. D. Keefe, S. Pai, and A. Ellington, "Aptamers as therapeutics.," *Nat Rev Drug Discov*, vol. 9, pp. 537–550, Jul 2010.

[130] P. S. Pendergrast, H. N. Marsh, D. Grate, J. M. Healy, and M. Stanton, "Nucleic acid aptamers for target validation and therapeutic applications.," *J Biomol Tech*, vol. 16, pp. 224–234, Sep 2005.

[131] A. D. Ellington and J. W. Szostak, "In vitro selection of rna molecules that bind specific ligands.," *Nature*, vol. 346, pp. 818–822, Aug 1990.

[132] C. Tuerk and L. Gold, "Systematic evolution of ligands by exponential enrichment: Rna ligands to bacteriophage t4 dna polymerase.," *Science*, vol. 249, pp. 505–510, Aug 1990.

[133] R. Stoltenburg, C. Reinemann, and B. Strehlitz, "Selex–a (r)evolutionary method to generate high-affinity nucleic acid ligands.," *Biomol Eng*, vol. 24, pp. 381–403, Oct 2007.

[134] P. Majumder, K. N. Gomes, and H. Ulrich, "Aptamers: from bench side research towards patented molecules with therapeutic applications.," *Expert Opin Ther Pat*, vol. 19, pp. 1603–1613, Nov 2009.

[135] X. Ni, M. Castanares, A. Mukherjee, and S. E. Lupold, "Nucleic acid aptamers: clinical applications and promising new horizons.," *Curr Med Chem*, vol. 18, no. 27, pp. 4206–4214, 2011.

[136] J. L. Diener, H. A. Daniel Lagasse, D. Duerschmied, Y. Merhi, J.-F. Tanguay, R. Hutabarat, J. Gilbert, D. D. Wagner, and R. Schaub, "Inhibition of von willebrand factor-mediated platelet activation and thrombosis by the anti-von willebrand factor a1-domain aptamer arc1779.," *J Thromb Haemost*, vol. 7, pp. 1155–1162, Jul 2009.

[137] Y. Yang, D. Yang, H. J. Schluesener, and Z. Zhang, "Advances in selex and application of aptamers in the central nervous system.," *Biomol Eng*, vol. 24, pp. 583–592, Dec 2007.

[138] S. Ohuchi, "Cell-selex technology.," *Biores Open Access*, vol. 1, pp. 265–272, Dec 2012.

[139] J. Mi, Y. Liu, Z. N. Rabbani, Z. Yang, J. H. Urban, B. A. Sullenger, and B. M. Clary, "In vivo selection of tumor-targeting rna motifs.," *Nat Chem Biol*, vol. 6, pp. 22–24, Jan 2010.

[140] C. Cheng, Y. H. Chen, K. A. Lennox, M. A. Behlke, and B. L. Davidson, "In vivo selex for identification of brain-penetrating aptamers.," *Mol Ther Nucleic Acids*, vol. 2, p. e67, 2013.

[141] J. Gloekler, T. Schuetze, and Z. Konthur, "Automation in the high-throughput selection of random combinatorial libraries–different approaches for select applications.," *Molecules*, vol. 15, pp. 2478–2490, Apr 2010.

[142] R. Ostroff, T. Foreman, T. R. Keeney, S. Stratford, J. J. Walker, and D. Zichi, "The stability of the circulating human proteome to variations in sample collection and handling procedures measured with an aptamer-based proteomics array.," *J Proteomics*, vol. 73, pp. 649–666, Jan 2010.

[143] L. H. Lauridsen, J. A. Rothnagel, and R. N. Veedu, "Enzymatic recognition of 2'-modified ribonucleoside 5'-triphosphates: towards the evolution of versatile aptamers.," *Chembiochem*, vol. 13, pp. 19–25, Jan 2012.

[144] B. E. Eaton, L. Gold, B. J. Hicke, N. JanjiÊ, F. M. Jucker, D. P. Sebesta, T. M. Tarasow, M. C. Willis, and D. A. Zichi, "Post-selex combinatorial optimization of aptamers.," *Bioorg Med Chem*, vol. 5, pp. 1087–1096, Jun 1997.

[145] A. Adler, N. Forster, M. Homann, and H. U. Gˆringer, "Post-selex chemical optimization of a trypanosome-specific rna aptamer.," *Comb Chem High Throughput Screen*, vol. 11, pp. 16–23, Jan 2008.

[146] K. S. Schmidt, S. Borkowski, J. Kurreck, A. W. Stephens, R. Bald, M. Hecht, M. Friebe, L. Dinkelborg, and V. A. Erdmann, "Application of locked nucleic acids to improve aptamer in vivo stability and targeting function.," *Nucleic Acids Res*, vol. 32, no. 19, pp. 5757–5765, 2004.

[147] D. Jellinek, L. S. Green, C. Bell, C. K. Lynott, N. Gill, C. Vargeese, G. Kirschenheuter, D. P. McGee, P. Abesinghe, and W. A. Pieken, "Potent 2'-amino-2'-deoxypyrimidine rna inhibitors of basic fibroblast growth factor.," *Biochemistry*, vol. 34, pp. 11363–11372, Sep 1995.

[148] Y. Lin, D. Nieuwlandt, A. Magallanez, B. Feistner, and S. D. Jayasena, "High-affinity and specific recognition of human thyroid stimulating hormone (htsh) by in vitro-selected 2'-amino-modified rna.," *Nucleic Acids Res*, vol. 24, pp. 3407–3414, Sep 1996.

[149] Y. Lin, Q. Qiu, S. C. Gill, and S. D. Jayasena, "Modified rna sequence pools for in vitro selection.," *Nucleic Acids Res*, vol. 22, pp. 5229–5234, Dec 1994.

[150] G. Biesecker, L. Dihel, K. Enney, and R. A. Bendele, "Derivation of rna aptamer inhibitors of human complement c5.," *Immunopharmacology*, vol. 42, pp. 219–230, May 1999.

[151] C. P. Rusconi, E. Scardino, J. Layzer, G. A. Pitoc, T. L. Ortel, D. Monroe, and B. A. Sullenger, "Rna aptamers as reversible antagonists of coagulation factor ixa.," *Nature*, vol. 419, pp. 90–94, Sep 2002.

[152] P. E. Burmeister, S. D. Lewis, R. F. Silva, J. R. Preiss, L. R. Horwitz, P. S. Pendergrast, T. G. McCauley, J. C. Kurz, D. M. Epstein, C. Wilson, and A. D. Keefe, "Direct in vitro selection of a 2'-o-methyl aptamer to vegf.," *Chem Biol*, vol. 12, pp. 25–33, Jan 2005.

[153] F. Tolle and G. Mayer, "Dressed for success ñ applying chemistry to modulate aptamer functionality," *Chemical Science*, vol. 4, p. 60, 2013.

[154] S. Shigdar, J. Macdonald, M. O'Connor, T. Wang, D. Xiang, H. Al Shamaileh, L. Qiao, M. Wei, S.-F. Zhou, Y. Zhu, L. Kong, S. Bhattacharya, C. Li, and W. Duan, "Aptamers as theranostic agents: modifications, serum stability and functionalisation.," *Sensors (Basel)*, vol. 13, no. 10, pp. 13624–13637, 2013.

[155] G. Sengle, A. Jenne, P. S. Arora, B. Seelig, J. S. Nowick, A. Jaeschke, and M. Famulok, "Synthesis, incorporation efficiency, and stability of disulfide bridged functional groups at rna 5'-ends.," *Bioorg Med Chem*, vol. 8, pp. 1317–1329, Jun 2000.

[156] H. Y. Kong and J. Byun, "Nucleic acid aptamers: New methods for selection, stabilization, and application in biomedical science.," *Biomol Ther (Seoul)*, vol. 21, pp. 423–434, Nov 2013.

[157] P. Zhang, N. Zhao, Z. Zeng, C.-C. Chang, and Y. Zu, "Combination of an aptamer probe to cd4 and antibodies for multicolored cell phenotyping.," *Am J Clin Pathol*, vol. 134, pp. 586–593, Oct 2010.

[158] G. Mayer, "The chemical biology of aptamers.," *Angew Chem Int Ed Engl*, vol. 48, no. 15, pp. 2672–2689, 2009.

[159] S. M. Shamah, J. M. Healy, and S. T. Cload, "Complex target selex.," *Acc Chem Res*, vol. 41, pp. 130–138, Jan 2008.

[160] M. Famulok, J. S. Hartig, and G. Mayer, "Functional aptamers and aptazymes in biotechnology, diagnostics, and therapy.," *Chem Rev*, vol. 107, pp. 3715–3743, Sep 2007.

[161] M. Famulok and S. Verma, "In vivo-applied functional rnas as tools in proteomics and genomics research.," *Trends Biotechnol*, vol. 20, pp. 462–466, Nov 2002.

[162] L. Cerchia, P. H. Giangrande, J. O. McNamara, and V. de Franciscis, "Cell-specific aptamers for targeted therapies.," *Methods Mol Biol*, vol. 535, pp. 59–78, 2009.

[163] J. Zhou and J. J. Rossi, "Cell-specific aptamer-mediated targeted drug delivery.," *Oligonucleotides*, vol. 21, pp. 1–10, Feb 2011.

[164] C. S. M. Ferreira, M. C. Cheung, S. Missailidis, S. Bisland, and J. GariÈpy, "Phototoxic aptamers selectively enter and kill epithelial cancer cells.," *Nucleic Acids Res*, vol. 37, pp. 866–876, Feb 2009.

[165] J. Wang, G. Zhu, M. You, E. Song, M. I. Shukoor, K. Zhang, M. B. Altman, Y. Chen, Z. Zhu, C. Z. Huang, and W. Tan, "Assembly of aptamer switch probes and photosensitizer on gold nanorods for targeted photothermal and photodynamic cancer therapy.," *ACS Nano*, vol. 6, pp. 5070–5077, Jun 2012.

[166] S. Kruspe, C. Meyer, and U. Hahn, "Chlorin e6 conjugated interleukin-6 receptor aptamers selectively kill target cells upon irradiation.," *Mol Ther Nucleic Acids*, vol. 3, p. e143, 2014.

[167] M. Famulok, M. Blind, and G. Mayer, "Intramers as promising new tools in functional proteomics.," *Chem Biol*, vol. 8, pp. 931–939, Oct 2001.

[168] M. Famulok and G. Mayer, "Intramers and aptamers: applications in protein-function analyses and potential for drug screening.," *Chembiochem*, vol. 6, pp. 19–26, Jan 2005.

[169] B. A. Sullenger, H. F. Gallardo, G. E. Ungers, and E. Gilboa, "Overexpression of tar sequences renders cells resistant to human immunodeficiency virus replication.," *Cell*, vol. 63, pp. 601–608, Nov 1990.

[170] P. D. Good, A. J. Krikos, S. X. Li, E. Bertrand, N. S. Lee, L. Giver, A. Ellington, J. A. Zaia, J. J. Rossi, and D. R. Engelke, "Expression of small, therapeutic rnas in human cell nuclei.," *Gene Ther*, vol. 4, pp. 45–54, Jan 1997.

[171] R. E. Martell, J. R. Nevins, and B. A. Sullenger, "Optimizing aptamer activity for gene therapy applications using expression cassette selex.," *Mol Ther*, vol. 6, pp. 30–34, Jul 2002.

[172] L. Chaloin, M. J. Lehmann, G. Sczakiel, and T. Restle, "Endogenous expression of a high-affinity pseudoknot rna aptamer suppresses replication of hiv-1.," *Nucleic Acids Res*, vol. 30, pp. 4001–4008, Sep 2002.

[173] F. Nishikawa, N. Kakiuchi, K. Funaji, K. Fukuda, S. Sekiya, and S. Nishikawa, "Inhibition of hcv ns3 protease by rna aptamers in cells.," *Nucleic Acids Res*, vol. 31, pp. 1935–1943, Apr 2003.

[174] M. Y. Kim and S. Jeong, "Inhibition of the functions of the nucleocapsid protein of human immunodeficiency virus-1 by an rna aptamer.," *Biochem Biophys Res Commun*, vol. 320, pp. 1181–1186, Aug 2004.

[175] K. H. Choi, M. W. Park, S. Y. Lee, M.-Y. Jeon, M. Y. Kim, H. K. Lee, J. Yu, H.-J. Kim, K. Han, H. Lee, K. Park, W. J. Park, and S. Jeong, "Intracellular expression of the t-cell factor-1 rna aptamer as an intramer.," *Mol Cancer Ther*, vol. 5, pp. 2428–2434, Sep 2006.

[176] R. Chan, M. Gilbert, K. M. Thompson, H. N. Marsh, D. M. Epstein, and P. S. Pendergrast, "Co-expression of anti-nfkappab rna aptamers and sirnas leads to maximal suppression of nfkappab activity in mammalian cells.," *Nucleic Acids Res*, vol. 34, no. 5, p. e36, 2006.

[177] G. Kolb, S. Reigadas, D. Castanotto, A. Faure, M. Ventura, J. J. Rossi, and J.-J. ToulmÈ, "Endogenous expression of an anti-tar aptamer reduces hiv-1 replication.," *RNA Biol*, vol. 3, pp. 150–156, Oct 2006.

[178] Y. S. Choi, J. Hur, H. K. Lee, and S. Jeong, "The rna aptamer disrupts protein-protein interaction between beta-catenin and nuclear factor-kappab p50 and regulates the expression of c-reactive protein.," *FEBS Lett*, vol. 583, pp. 1415–1421, May 2009.

[179] D. Auslaender, M. Wieland, S. Auslaender, M. Tigges, and M. Fussenegger, "Rational design of a small molecule-responsive intramer controlling transgene expression in mammalian cells.," *Nucleic Acids Res*, vol. 39, p. e155, Dec 2011.

[180] J. Mi, X. Zhang, Z. N. Rabbani, Y. Liu, S. K. Reddy, Z. Su, F. K. Salahuddin, K. Viles, P. H. Giangrande, M. W. Dewhirst, B. A. Sullenger, C. D. Kontos, and B. M. Clary, "Rna aptamer-targeted inhibition of nf-kappa b suppresses non-small cell lung cancer resistance to doxorubicin.," *Mol Ther*, vol. 16, pp. 66–73, Jan 2008.

[181] J. Mi, X. Zhang, Z. N. Rabbani, Y. Liu, Z. Su, Z. Vujaskovic, C. D. Kontos, B. A. Sullenger, and B. M. Clary, "H1 rna polymerase iii promoter-driven expression of an rna aptamer leads to high-level inhibition of intracellular protein activity.," *Nucleic Acids Res*, vol. 34, no. 12, pp. 3577–3584, 2006.

[182] M. Blind, W. Kolanus, and M. Famulok, "Cytoplasmic rna modulators of an inside-out signal-transduction cascade.," *Proc Natl Acad Sci U S A*, vol. 96, pp. 3606–3610, Mar 1999.

[183] G. Mayer, M. Blind, W. Nagel, T. Bˆhm, T. Knorr, C. L. Jackson, W. Kolanus, and M. Famulok, "Controlling small guanine-nucleotide-exchange factor function through cytoplasmic rna intramers.," *Proc Natl Acad Sci U S A*, vol. 98, pp. 4961–4965, Apr 2001.

[184] M.-J. Li, G. Bauer, A. Michienzi, J.-K. Yee, N.-S. Lee, J. Kim, S. Li, D. Castanotto, J. Zaia, and J. J. Rossi, "Inhibition of hiv-1 infection by lentiviral vectors expressing pol iii-promoted anti-hiv rnas.," *Mol Ther*, vol. 8, pp. 196–206, Aug 2003.

[185] D. M. Held, J. D. Kissel, J. T. Patterson, D. G. Nickens, and D. H. Burke, "Hiv-1 inactivation by nucleic acid aptamers.," *Front Biosci*, vol. 11, pp. 89–112, 2006.

[186] J. Ishizaki, J. R. Nevins, and B. A. Sullenger, "Inhibition of cell proliferation by an rna ligand that selectively blocks e2f function.," *Nat Med*, vol. 2, pp. 1386–1389, Dec 1996.

[187] K. Konopka, N. Duezguenes, J. Rossi, and N. S. Lee, "Receptor ligand-facilitated cationic liposome delivery of anti-hiv-1 rev-binding aptamer and ribozyme dnas.," *J Drug Target*, vol. 5, no. 4, pp. 247–259, 1998.

[188] M. G. Theis, A. Knorre, B. Kellersch, J. Moelleken, F. Wieland, W. Kolanus, and M. Famulok, "Discriminatory aptamer reveals serum response element transcription regulated by cytohesin-2.," *Proc Natl Acad Sci U S A*, vol. 101, pp. 11221–11226, Aug 2004.

[189] A. Bill, A. Schmitz, B. Albertoni, J.-N. Song, L. C. Heukamp, D. Walrafen, F. Thorwirth, P. J. Verveer, S. Zimmer, L. Meffert, A. Schreiber, S. Chatterjee, R. K. Thomas, R. T. Ullrich, T. Lang, and M. Famulok, "Cytohesins are cytoplasmic erbb receptor activators.," *Cell*, vol. 143, pp. 201–211, Oct 2010.

[190] S.-Y. Hwang, H.-Y. Sun, K.-H. Lee, B.-H. Oh, Y. J. Cha, B. H. Kim, and J.-Y. Yoo, "5'-triphosphate-rna-independent activation of rig-i via rna aptamer with enhanced antiviral activity.," *Nucleic Acids Res*, vol. 40, pp. 2724–2733, Mar 2012.

[191] S.-M. Ryou, J.-M. Kim, J.-H. Yeom, S. Hyun, S. Kim, M. S. Han, S. W. Kim, J. Bae, S. Rhee, and K. Lee, "Gold nanoparticle-assisted delivery of small, highly structured rna into the nuclei of human cells.," *Biochem Biophys Res Commun*, vol. 416, pp. 178–183, Dec 2011.

[192] H. Shi, B. E. Hoffman, and J. T. Lis, "Rna aptamers as effective protein antagonists in a multicellular organism.," *Proc Natl Acad Sci U S A*, vol. 96, pp. 10033–10038, Aug 1999.

[193] M. Gabut, J. Dejardin, J. Tazi, and J. Soret, "The sr family proteins b52 and dasf/sf2 modulate development of the drosophila visual system by regulating specific rna targets.," *Mol Cell Biol*, vol. 27, pp. 3087–3097, Apr 2007.

[194] V. I. Rasheva, D. Knight, P. Bozko, K. Marsh, and M. V. Frolov, "Specific role of the sr protein splicing factor b52 in cell cycle control in drosophila.," *Mol Cell Biol*, vol. 26, pp. 3468–3477, May 2006.

[195] L. L. Lebruska and L. Maher, 3rd, "Selection and characterization of an rna decoy for transcription factor nf-kappa b.," *Biochemistry*, vol. 38, pp. 3168–3174, Mar 1999.

[196] B. Hoesel and J. A. Schmid, "The complexity of nf-?b signaling in inflammation and cancer.," *Mol Cancer*, vol. 12, p. 86, 2013.

[197] W. Kolanus, "Guanine nucleotide exchange factors of the cytohesin family and their roles in signal transduction.," *Immunol Rev*, vol. 218, pp. 102–113, Aug 2007.

[198] A. G. Papavassiliou, "The role of regulated phosphorylation in the biological activity of transcription factors srf and elk-1/sap-1.," *Anticancer Res*, vol. 14, no. 5A, pp. 1923–1926, 1994.

[199] J. S. Paige, T. Nguyen-Duc, W. Song, and S. R. Jaffrey, "Fluorescence imaging of cellular metabolites with rna.," *Science*, vol. 335, p. 1194, Mar 2012.

[200] C. A. Kellenberger, S. C. Wilson, J. Sales-Lee, and M. C. Hammond, "Rna-based fluorescent biosensors for live cell imaging of second messengers cyclic di-gmp and cyclic amp-gmp.," *J Am Chem Soc*, vol. 135, pp. 4906–4909, Apr 2013.

[201] W. Song, R. L. Strack, and S. R. Jaffrey, "Imaging bacterial protein expression using genetically encoded rna sensors.," *Nat Methods*, vol. 10, pp. 873–875, Sep 2013.

[202] J. S. Paige, K. Y. Wu, and S. R. Jaffrey, "Rna mimics of green fluorescent protein.," *Science*, vol. 333, pp. 642–646, Jul 2011.

[203] R. L. Strack, M. D. Disney, and S. R. Jaffrey, "A superfolding spinach2 reveals the dynamic nature of trinucleotide repeat-containing rna.," *Nat Methods*, vol. 10, pp. 1219–1224, Dec 2013.

[204] G. Pothoulakis, F. Ceroni, B. Reeve, and T. Ellis, "The spinach rna aptamer as a characterization tool for synthetic biology.," *ACS Synth Biol*, Sep 2013.

[205] W. Song, R. L. Strack, N. Svensen, and S. R. Jaffrey, "Plug-and-play fluorophores extend the spectral properties of spinach.," *J Am Chem Soc*, vol. 136, pp. 1198–1201, Jan 2014.

[206] M. Hafner, E. Vianini, B. Albertoni, L. Marchetti, I. Gruene, C. Gloeckner, and M. Famulok, "Displacement of protein-bound aptamers with small molecules screened by fluorescence polarization.," *Nat Protoc*, vol. 3, no. 4, pp. 579–587, 2008.

[207] M. Hafner, A. Schmitz, I. Gruene, S. G. Srivatsan, B. Paul, W. Kolanus, T. Quast, E. Kremmer, I. Bauer, and M. Famulok, "Inhibition of cytohesins by secinh3 leads to hepatic insulin resistance.," *Nature*, vol. 444, pp. 941–944, Dec 2006.

[208] N. Li, H. H. Nguyen, M. Byrom, and A. D. Ellington, "Inhibition of cell proliferation by an anti-egfr aptamer.," *PLoS One*, vol. 6, no. 6, p. e20299, 2011.

[209] G. Mayer, B. Wulffen, C. Huber, J. Brockmann, B. Flicke, L. Neumann, D. Hafenbradl, B. M. Klebl, M. J. Lohse, C. Krasel, and M. Blind, "An rna molecule that specifically inhibits g-protein-coupled receptor kinase 2 in vitro.," *RNA*, vol. 14, pp. 524–534, Mar 2008.

[210] S. D. Seiwert, T. Stines Nahreini, S. Aigner, N. G. Ahn, and O. C. Uhlenbeck, "Rna aptamers as pathway-specific map kinase inhibitors.," *Chem Biol*, vol. 7, pp. 833–843, Nov 2000.

[211] P. Penela, C. Murga, C. Ribas, V. Lafarga, and F. Mayor, Jr, "The complex g protein-coupled receptor kinase 2 (grk2) interactome unveils new physiopathological targets.," *Br J Pharmacol*, vol. 160, pp. 821–832, Jun 2010.

[212] A. Cannavo, D. Liccardo, and W. J. Koch, "Targeting cardiac ?-adrenergic signaling via grk2 inhibition for heart failure therapy.," *Front Physiol*, vol. 4, p. 264, 2013.

[213] Z. M. Huang, J. I. Gold, and W. J. Koch, "G protein-coupled receptor kinases in normal and failing myocardium.," *Front Biosci (Landmark Ed)*, vol. 16, pp. 3047–3060, 2011.

[214] S. T. Pleger, M. Boucher, P. Most, and W. J. Koch, "Targeting myocardial beta-adrenergic receptor signaling and calcium cycling for heart failure gene therapy.," *J Card Fail*, vol. 13, pp. 401–414, Jun 2007.

[215] M. R. Bristow, R. E. Hershberger, J. D. Port, E. M. Gilbert, A. Sandoval, R. Rasmussen, A. E. Cates, and A. M. Feldman, "Beta-adrenergic pathways in nonfailing and failing human ventricular myocardium.," *Circulation*, vol. 82, pp. I12–I25, Aug 1990.

[216] J. A. Pitcher, J. Inglese, J. B. Higgins, J. L. Arriza, P. J. Casey, C. Kim, J. L. Benovic, M. M. Kwatra, M. G. Caron, and R. J. Lefkowitz, "Role of beta gamma subunits of g proteins in targeting the beta-adrenergic receptor kinase to membrane-bound receptors.," *Science*, vol. 257, pp. 1264–1267, Aug 1992.

[217] J. A. Pitcher, K. Touhara, E. S. Payne, and R. J. Lefkowitz, "Pleckstrin homology domain-mediated membrane association and activation of the beta-adrenergic receptor kinase requires coordinate interaction with g beta gamma subunits and lipid.," *J Biol Chem*, vol. 270, pp. 11707–11710, May 1995.

[218] R. Fredriksson, M. C. Lagerstroem, L.-G. Lundin, and H. B. Schioeth, "The g-protein-coupled receptors in the human genome form five main families. phylogenetic analysis, paralogon groups, and fingerprints.," *Mol Pharmacol*, vol. 63, pp. 1256–1272, Jun 2003.

[219] T. Bojic, E. Sudar, D. Mikhailidis, D. Alavantic, and E. Isenovic, "The role of g protein coupled receptor kinases in neurocardiovascular pathophysiology.," *Arch Med Sci*, vol. 8, pp. 970–977, Dec 2012.

[220] T. Metayee, H. Gibelin, R. Perdrisot, and J.-L. Kraimps, "Pathophysiological roles of g-protein-coupled receptor kinases.," *Cell Signal*, vol. 17, pp. 917–928, Aug 2005.

[221] R. B. Penn, A. N. Pronin, and J. L. Benovic, "Regulation of g protein-coupled receptor kinases.," *Trends Cardiovasc Med*, vol. 10, pp. 81–89, Feb 2000.

[222] H. Brinks and W. J. Koch, "Targeting g protein-coupled receptor kinases (grks) in heart failure.," *Drug Discov Today Dis Mech*, vol. 7, no. 2, pp. e129–e134, 2010.

[223] A. Lymperopoulos, G. Rengo, and W. J. Koch, "Grk2 inhibition in heart failure: something old, something new.," *Curr Pharm Des*, vol. 18, no. 2, pp. 186–191, 2012.

[224] M. C. Cho, M. Rao, W. J. Koch, S. A. Thomas, R. D. Palmiter, and H. A. Rockman, "Enhanced contractility and decreased beta-adrenergic receptor kinase-1 in mice lacking endogenous norepinephrine and epinephrine.," *Circulation*, vol. 99, pp. 2702–2707, May 1999.

[225] K. M. Anderson, A. D. Eckhart, R. N. Willette, and W. J. Koch, "The myocardial beta-adrenergic system in spontaneously hypertensive heart failure (shhf) rats.," *Hypertension*, vol. 33, pp. 402–407, Jan 1999.

[226] C. A. Harris, T. T. Chuang, and C. A. Scorer, "Expression of grk2 is increased in the left ventricles of cardiomyopathic hamsters.," *Basic Res Cardiol*, vol. 96, pp. 364–368, Jul 2001.

[227] J. A. Petrofski and W. J. Koch, "The beta-adrenergic receptor kinase in heart failure.," *J Mol Cell Cardiol*, vol. 35, pp. 1167–1174, Oct 2003.

[228] H. A. Rockman, K. R. Chien, D. J. Choi, G. Iaccarino, J. J. Hunter, J. Ross, Jr, R. J. Lefkowitz, and W. J. Koch, "Expression of a beta-adrenergic receptor kinase 1 inhibitor prevents the development of myocardial failure in gene-targeted mice.," *Proc Natl Acad Sci U S A*, vol. 95, pp. 7000–7005, Jun 1998.

[229] M. L. Williams and W. J. Koch, "Viral-based myocardial gene therapy approaches to alter cardiac function.," *Annu Rev Physiol*, vol. 66, pp. 49–75, 2004.

[230] L. E. Vinge, P. W. Raake, and W. J. Koch, "Gene therapy in heart failure.," *Circ Res*, vol. 102, pp. 1458–1470, Jun 2008.

[231] P. W. J. Raake, P. Schlegel, J. Ksienzyk, J. Reinkober, J. Barthelmes, S. Schinkel, S. Pleger, W. Mier, U. Haberkorn, W. J. Koch, H. A. Katus, P. Most, and O. J. Mueller, "Aav6.barkct cardiac gene therapy ameliorates cardiac function and normalizes the catecholaminergic axis in a clinically relevant large animal heart failure model.," *Eur Heart J*, vol. 34, pp. 1437–1447, May 2013.

[232] W. Z. Suo and L. Li, "Dysfunction of g protein-coupled receptor kinases in alzheimer's disease.," *ScientificWorldJournal*, vol. 10, pp. 1667–1678, 2010.

[233] D. W. King, R. Steinmetz, H. A. Wagoner, T. S. Hannon, L. Y. Chen, E. A. Eugster, and O. H. Pescovitz, "Differential expression of grk isoforms in nonmalignant and malignant human granulosa cells.," *Endocrine*, vol. 22, pp. 135–142, Nov 2003.

[234] D. Sorriento, A. Fusco, M. Ciccarelli, A. Rungi, A. Anastasio, A. Carillo, G. Dorn, 2nd, B. Trimarco, and G. Iaccarino, "Mitochondrial g protein coupled receptor kinase 2 regulates proinflammatory responses in macrophages.," *FEBS Lett*, vol. 587, pp. 3487–3494, Nov 2013.

[235] N. E. Ward and C. A. O'Brian, "Kinetic analysis of protein kinase c inhibition by staurosporine: evidence that inhibition entails inhibitor binding at a conserved region of the catalytic domain but not competition with substrates.," *Mol Pharmacol*, vol. 41, pp. 387–392, Feb 1992.

[236] C. R. Loomis and R. M. Bell, "Sangivamycin, a nucleoside analogue, is a potent inhibitor of protein kinase c.," *J Biol Chem*, vol. 263, pp. 1682–1692, Feb 1988.

[237] J. J. G. Tesmer, V. M. Tesmer, D. T. Lodowski, H. Steinhagen, and J. Huber, "Structure of human g protein-coupled receptor kinase 2 in complex with the kinase inhibitor balanol.," *J Med Chem*, vol. 53, pp. 1867–1870, Feb 2010.

[238] S. Fujiwara, S. Ikeda, and M. Kaneko, "Cardiotonic agent comprising grk inhibitor," Mar. 29 2007. WO Patent App. PCT/JP2006/318,666.

[239] D. M. Thal, R. Y. Yeow, C. Schoenau, J. Huber, and J. J. G. Tesmer, "Molecular mechanism of selectivity among g protein-coupled receptor kinase 2 inhibitors.," *Mol Pharmacol*, vol. 80, pp. 294–303, Aug 2011.

[240] C. M. Kim, S. B. Dion, J. J. Onorato, and J. L. Benovic, "Expression and characterization of two beta-adrenergic receptor kinase isoforms using the baculovirus expression system.," *Receptor*, vol. 3, no. 1, pp. 39–55, 1993.

[241] A. Hasbi, S. Allouche, F. Sichel, L. Stanasila, D. Massotte, G. Landemore, J. Polastron, and P. Jauzac, "Internalization and recycling of delta-opioid receptor are dependent on a phosphorylation-dephosphorylation mechanism.," *J Pharmacol Exp Ther*, vol. 293, pp. 237–247, Apr 2000.

[242] M. U. Kassack, P. Hoegger, D. A. Gschwend, K. Kameyama, T. Haga, R. C. Graul, and W. Sadee, "Molecular modeling of g-protein coupled receptor kinase 2: docking and biochemical evaluation of inhibitors.," *AAPS PharmSci*, vol. 2, no. 1, p. E2, 2000.

[243] R. Winstel, H.-G. Ihlenfeldt, G. Jung, C. Krasel, and M. J. Lohse, "Peptide inhibitors of g protein-coupled receptor kinases.," *Biochem Pharmacol*, vol. 70, pp. 1001–1008, Oct 2005.

[244] M. J. Lohse, R. J. Lefkowitz, M. G. Caron, and J. L. Benovic, "Inhibition of beta-adrenergic receptor kinase prevents rapid homologous desensitization of beta 2-adrenergic receptors.," *Proc Natl Acad Sci U S A*, vol. 86, pp. 3011–3015, May 1989.

[245] R. Roskoski, Jr, "Erk1/2 map kinases: structure, function, and regulation.," *Pharmacol Res*, vol. 66, pp. 105–143, Aug 2012.

[246] S. Nishimoto and E. Nishida, "Mapk signalling: Erk5 versus erk1/2.," *EMBO Rep*, vol. 7, pp. 782–786, Aug 2006.

[247] L. Santarpia, S. M. Lippman, and A. K. El-Naggar, "Targeting the mapk-ras-raf signaling pathway in cancer therapy.," *Expert Opin Ther Targets*, vol. 16, pp. 103–119, Jan 2012.

[248] M. H. Cobb, T. G. Boulton, and D. J. Robbins, "Extracellular signal-regulated kinases: Erks in progress.," *Cell Regul*, vol. 2, pp. 965–978, Dec 1991.

[249] L. B. Rosen, D. D. Ginty, M. J. Weber, and M. E. Greenberg, "Membrane depolarization and calcium influx stimulate mek and map kinase via activation of ras.," *Neuron*, vol. 12, pp. 1207–1221, Jun 1994.

[250] D. M. Owens and S. M. Keyse, "Differential regulation of map kinase signalling by dual-specificity protein phosphatases.," *Oncogene*, vol. 26, pp. 3203–3213, May 2007.

[251] J. Schlessinger, "Cell signaling by receptor tyrosine kinases.," *Cell*, vol. 103, pp. 211–225, Oct 2000.

[252] M. M. McKay and D. K. Morrison, "Integrating signals from rtks to erk/mapk.," *Oncogene*, vol. 26, pp. 3113–3121, May 2007.

[253] A. G. Batzer, D. Rotin, J. M. Urea, E. Y. Skolnik, and J. Schlessinger, "Hierarchy of binding sites for grb2 and shc on the epidermal growth factor receptor.," *Mol Cell Biol*, vol. 14, pp. 5192–5201, Aug 1994.

[254] M. Innocenti, P. Tenca, E. Frittoli, M. Faretta, A. Tocchetti, P. P. Di Fiore, and G. Scita, "Mechanisms through which sos-1 coordinates the activation of ras and rac.," *J Cell Biol*, vol. 156, pp. 125–136, Jan 2002.

[255] J. Avruch, A. Khokhlatchev, J. M. Kyriakis, Z. Luo, G. Tzivion, D. Vavvas, and X. F. Zhang, "Ras activation of the raf kinase: tyrosine kinase recruitment of the map kinase cascade.," *Recent Prog Horm Res*, vol. 56, pp. 127–155, 2001.

[256] M. A. Bogoyevitch and N. W. Court, "Counting on mitogen-activated protein kinases–erks 3, 4, 5, 6, 7 and 8.," *Cell Signal*, vol. 16, pp. 1345–1354, Dec 2004.

[257] A. C. Lloyd, "Distinct functions for erks?," *J Biol*, vol. 5, no. 5, p. 13, 2006.

[258] R. Lefloch, J. Pouyssegur, and P. Lenormand, "Total erk1/2 activity regulates cell proliferation.," *Cell Cycle*, vol. 8, pp. 705–711, Mar 2009.

[259] D. J. Robbins, E. Zhen, H. Owaki, C. A. Vanderbilt, D. Ebert, T. D. Geppert, and M. H. Cobb, "Regulation and properties of extracellular signal-regulated protein kinases 1 and 2 in vitro.," *J Biol Chem*, vol. 268, pp. 5097–5106, Mar 1993.

[260] M. H. Cobb, S. Xu, M. Cheng, D. Ebert, D. Robbins, E. Goldsmith, and M. Robinson, "Structural analysis of the map kinase erk2 and studies of map kinase regulatory pathways.," *Adv Pharmacol*, vol. 36, pp. 49–65, 1996.

[261] S. Yoon and R. Seger, "The extracellular signal-regulated kinase: multiple substrates regulate diverse cellular functions.," *Growth Factors*, vol. 24, pp. 21–44, Mar 2006.

[262] Z. Yao and R. Seger, "The erk signaling cascade–views from different subcellular compartments.," *Biofactors*, vol. 35, no. 5, pp. 407–416, 2009.

[263] I. Wortzel and R. Seger, "The erk cascade: Distinct functions within various subcellular organelles.," *Genes Cancer*, vol. 2, pp. 195–209, Mar 2011.

[264] M. C. Mendoza, E. E. Er, and J. Blenis, "The ras-erk and pi3k-mtor pathways: cross-talk and compensation.," *Trends Biochem Sci*, vol. 36, pp. 320–328, Jun 2011.

[265] J. Zuber, O. I. Tchernitsa, B. Hinzmann, A. C. Schmitz, M. Grips, M. Hellriegel, C. Sers, A. Rosenthal, and R. Schaefer, "A genome-wide survey of ras transformation targets.," *Nat Genet*, vol. 24, pp. 144–152, Feb 2000.

[266] A. Schulze, B. Nicke, P. H. Warne, S. Tomlinson, and J. Downward, "The transcriptional response to raf activation is almost completely dependent on mitogen-activated protein kinase kinase activity and shows a major autocrine component.," *Mol Biol Cell*, vol. 15, pp. 3450–3463, Jul 2004.

[267] A. Plotnikov, E. Zehorai, S. Procaccia, and R. Seger, "The mapk cascades: signaling components, nuclear roles and mechanisms of nuclear translocation.," *Biochim Biophys Acta*, vol. 1813, pp. 1619–1633, Sep 2011.

[268] S. Peng, Y. Zhang, J. Zhang, H. Wang, and B. Ren, "Erk in learning and memory: a review of recent research.," *Int J Mol Sci*, vol. 11, no. 1, pp. 222–232, 2010.

[269] G. M. Thomas and R. L. Huganir, "Mapk cascade signalling and synaptic plasticity.," *Nat Rev Neurosci*, vol. 5, pp. 173–183, Mar 2004.

[270] G. Wu, R. Malinow, and H. T. Cline, "Maturation of a central glutamatergic synapse.," *Science*, vol. 274, pp. 972–976, Nov 1996.

[271] I. Ehrlich and R. Malinow, "Postsynaptic density 95 controls ampa receptor incorporation during long-term potentiation and experience-driven synaptic plasticity.," *J Neurosci*, vol. 24, pp. 916–927, Jan 2004.

[272] L. S. Lerea, L. S. Butler, and J. O. McNamara, "Nmda and non-nmda receptor-mediated increase of c-fos mrna in dentate gyrus neurons involves calcium influx via different routes.," *J Neurosci*, vol. 12, pp. 2973–2981, Aug 1992.

[273] H. Bading, D. D. Ginty, and M. E. Greenberg, "Regulation of gene expression in hippocampal neurons by distinct calcium signaling pathways.," *Science*, vol. 260, pp. 181–186, Apr 1993.

[274] J. J. Zhu, Y. Qin, M. Zhao, L. Van Aelst, and R. Malinow, "Ras and rap control ampa receptor trafficking during synaptic plasticity.," *Cell*, vol. 110, pp. 443–455, Aug 2002.

[275] M. J. Kim, A. W. Dunah, Y. T. Wang, and M. Sheng, "Differential roles of nr2a- and nr2b-containing nmda receptors in ras-erk signaling and ampa receptor trafficking.," *Neuron*, vol. 46, pp. 745–760, Jun 2005.

[276] M. A. Patterson, E. M. Szatmari, and R. Yasuda, "Ampa receptors are exocytosed in stimulated spines and adjacent dendrites in a ras-erk-dependent manner during long-term potentiation.," *Proc Natl Acad Sci U S A*, vol. 107, pp. 15951–15956, Sep 2010.

[277] D. Dinev, B. W. Jordan, B. Neufeld, J. D. Lee, D. Lindemann, U. R. Rapp, and S. Ludwig, "Extracellular signal regulated kinase 5 (erk5) is required for the differentiation of muscle cells.," *EMBO Rep*, vol. 2, pp. 829–834, Sep 2001.

[278] F. Huang, J. K. Chotiner, and O. Steward, "Actin polymerization and erk phosphorylation are required for arc/arg3.1 mrna targeting to activated synaptic sites on dendrites.," *J Neurosci*, vol. 27, pp. 9054–9067, Aug 2007.

[279] P. Tsokas, T. Ma, R. Iyengar, E. M. Landau, and R. D. Blitzer, "Mitogen-activated protein kinase upregulates the dendritic translation machinery in long-term potentiation by controlling the mammalian target of rapamycin pathway.," *J Neurosci*, vol. 27, pp. 5885–5894, May 2007.

[280] P. R. Westmark, C. J. Westmark, S. Wang, J. Levenson, K. J. O'Riordan, C. Burger, and J. S. Malter, "Pin1 and pkmzeta sequentially control dendritic protein synthesis.," *Sci Signal*, vol. 3, no. 112, p. ra18, 2010.

[281] J. P. Adams, A. E. Anderson, A. W. Varga, K. T. Dineley, R. G. Cook, P. J. Pfaffinger, and J. D. Sweatt, "The a-type potassium channel kv4.2 is a substrate for the mitogen-activated protein kinase erk.," *J Neurochem*, vol. 75, pp. 2277–2287, Dec 2000.

[282] S. Watanabe, D. A. Hoffman, M. Migliore, and D. Johnston, "Dendritic k+ channels contribute to spike-timing dependent long-term potentiation in hippocampal pyramidal neurons.," *Proc Natl Acad Sci U S A*, vol. 99, pp. 8366–8371, Jun 2002.

[283] L. A. Schrader, S. G. Birnbaum, B. M. Nadin, Y. Ren, D. Bui, A. E. Anderson, and J. D. Sweatt, "Erk/mapk regulates the kv4.2 potassium channel by direct phosphorylation of the pore-forming subunit.," *Am J Physiol Cell Physiol*, vol. 290, pp. C852–C861, Mar 2006.

[284] S. Davis, P. Vanhoutte, C. Pages, J. Caboche, and S. Laroche, "The mapk/erk cascade targets both elk-1 and camp response element-binding protein to control long-term potentiation-dependent gene expression in the dentate gyrus in vivo.," *J Neurosci*, vol. 20, pp. 4563–4572, Jun 2000.

[285] J. F. Guzowski, G. L. Lyford, G. D. Stevenson, F. P. Houston, J. L. McGaugh, P. F. Worley, and C. A. Barnes, "Inhibition of activity-dependent arc protein expression in the rat hippocampus impairs the maintenance of long-term potentiation and the consolidation of long-term memory.," *J Neurosci*, vol. 20, pp. 3993–4001, Jun 2000.

[286] R. Waltereit, B. Dammermann, P. Wulff, J. Scafidi, U. Staubli, G. Kauselmann, M. Bundman, and D. Kuhl, "Arg3.1/arc mrna induction by ca2+ and camp requires protein kinase a and mitogen-activated protein kinase/extracellular regulated kinase activation.," *J Neurosci*, vol. 21, pp. 5484–5493, Aug 2001.

[287] K. Rosenblum, M. Futter, K. Voss, M. Erent, P. A. Skehel, P. French, L. Obosi, M. W. Jones, and T. V. P. Bliss, "The role of extracellular regulated kinases i/ii in late-phase long-term potentiation.," *J Neurosci*, vol. 22, pp. 5432–5441, Jul 2002.

[288] S.-W. Ying, M. Futter, K. Rosenblum, M. J. Webber, S. P. Hunt, T. V. P. Bliss, and C. R. Bramham, "Brain-derived neurotrophic factor induces long-term potentiation in intact adult hippocampus: requirement for erk activation coupled to creb and upregulation of arc synthesis.," *J Neurosci*, vol. 22, pp. 1532–1540, Mar 2002.

[289] D. A. Frank and M. E. Greenberg, "Creb: a mediator of long-term memory from mollusks to mammals.," *Cell*, vol. 79, pp. 5–8, Oct 1994.

[290] B. J. Canagarajah, A. Khokhlatchev, M. H. Cobb, and E. J. Goldsmith, "Activation mechanism of the map kinase erk2 by dual phosphorylation.," *Cell*, vol. 90, pp. 859–869, Sep 1997.

[291] D. A. Johnson, P. Akamine, E. Radzio-Andzelm, M. Madhusudan, and S. S. Taylor, "Dynamics of camp-dependent protein kinase.," *Chem Rev*, vol. 101, pp. 2243–2270, Aug 2001.

[292] D. Jacobs, D. Glossip, H. Xing, A. J. Muslin, and K. Kornfeld, "Multiple docking sites on substrate proteins form a modular system that mediates recognition by erk map kinase.," *Genes Dev*, vol. 13, pp. 163–175, Jan 1999.

[293] C. A. Dimitri, W. Dowdle, J. P. MacKeigan, J. Blenis, and L. O. Murphy, "Spatially separate docking sites on erk2 regulate distinct signaling events in vivo.," *Curr Biol*, vol. 15, pp. 1319–1324, Jul 2005.

[294] J. A. Smith, C. E. Poteet-Smith, K. Malarkey, and T. W. Sturgill, "Identification of an extracellular signal-regulated kinase (erk) docking site in ribosomal s6 kinase, a sequence critical for activation by erk in vivo.," *J Biol Chem*, vol. 274, pp. 2893–2898, Jan 1999.

[295] F. L. Robinson, A. W. Whitehurst, M. Raman, and M. H. Cobb, "Identification of novel point mutations in erk2 that selectively disrupt binding to mek1.," *J Biol Chem*, vol. 277, pp. 14844–14852, Apr 2002.

[296] B. Zhou, J. Zhang, S. Liu, S. Reddy, F. Wang, and Z.-Y. Zhang, "Mapping erk2-mkp3 binding interfaces by hydrogen/deuterium exchange mass spectrometry.," *J Biol Chem*, vol. 281, pp. 38834–38844, Dec 2006.

[297] A. W. Whitehurst, F. L. Robinson, M. S. Moore, and M. H. Cobb, "The death effector domain protein pea-15 prevents nuclear entry of erk2 by inhibiting required interactions.," *J Biol Chem*, vol. 279, pp. 12840–12847, Mar 2004.

[298] J. Rodriguez, F. Calvo, J. M. Gonz·lez, B. Casar, V. Andres, and P. Crespo, "Erk1/2 map kinases promote cell cycle entry by rapid, kinase-independent disruption of retinoblastoma-lamin a complexes.," *J Cell Biol*, vol. 191, pp. 967–979, Nov 2010.

[299] D. Chuderland, A. Konson, and R. Seger, "Identification and characterization of a general nuclear translocation signal in signaling proteins.," *Mol Cell*, vol. 31, pp. 850–861, Sep 2008.

[300] E. Zehorai, Z. Yao, A. Plotnikov, and R. Seger, "The subcellular localization of mek and erk–a novel nuclear translocation signal (nts) paves a way to the nucleus.," *Mol Cell Endocrinol*, vol. 314, pp. 213–220, Jan 2010.

[301] S. Hu, Z. Xie, A. Onishi, X. Yu, L. Jiang, J. Lin, H.-s. Rho, C. Woodard, H. Wang, J.-S. Jeong, S. Long, X. He, H. Wade, S. Blackshaw, J. Qian, and H. Zhu, "Profiling the human protein-dna interactome reveals erk2 as a transcriptional repressor of interferon signaling.," *Cell*, vol. 139, pp. 610–622, Oct 2009.

[302] L. Colucci-D'Amato, C. Perrone-Capano, and U. di Porzio, "Chronic activation of erk and neurodegenerative diseases.," *Bioessays*, vol. 25, pp. 1085–1095, Nov 2003.

[303] M. Hetman and A. Gozdz, "Role of extracellular signal regulated kinases 1 and 2 in neuronal survival.," *Eur J Biochem*, vol. 271, pp. 2050–2055, Jun 2004.

[304] P. J. Roberts and C. J. Der, "Targeting the raf-mek-erk mitogen-activated protein kinase cascade for the treatment of cancer.," *Oncogene*, vol. 26, pp. 3291–3310, May 2007.

[305] B. B. Friday and A. A. Adjei, "Advances in targeting the ras/raf/mek/erk mitogen-activated protein kinase cascade with mek inhibitors for cancer therapy.," *Clin Cancer Res*, vol. 14, pp. 342–346, Jan 2008.

[306] J. S. Sebolt-Leopold, "Advances in the development of cancer therapeutics directed against the ras-mitogen-activated protein kinase pathway.," *Clin Cancer Res*, vol. 14, pp. 3651–3656, Jun 2008.

[307] K. Burkhard, S. Smith, R. Deshmukh, A. D. MacKerell, Jr, and P. Shapiro, "Development of extracellular signal-regulated kinase inhibitors.," *Curr Top Med Chem*, vol. 9, no. 8, pp. 678–689, 2009.

[308] F. Chen, A. D. Mackerell, Jr, Y. Luo, and P. Shapiro, "Using caenorhabditis elegans as a model organism for evaluating extracellular signal-regulated kinase docking domain inhibitors.," *J Cell Commun Signal*, vol. 2, pp. 81–92, Dec 2008.

[309] B. Dai, X. F. Zhao, K. Mazan-Mamczarz, P. Hagner, S. Corl, E. M. Bahassi, S. Lu, P. J. Stambrook, P. Shapiro, and R. B. Gartenhaus, "Functional and molecular interactions between erk and chk2 in diffuse large b-cell lymphoma.," *Nat Commun*, vol. 2, p. 402, 2011.

[310] M. Ohori, T. Kinoshita, M. Okubo, K. Sato, A. Yamazaki, H. Arakawa, S. Nishimura, N. Inamura, H. Nakajima, M. Neya, H. Miyake, and T. Fujii, "Identification of a selective erk inhibitor and structural determination of the inhibitor-erk2 complex.," *Biochem Biophys Res Commun*, vol. 336, pp. 357–363, Oct 2005.

[311] N. K. Vaish, F. Dong, L. Andrews, R. E. Schweppe, N. G. Ahn, L. Blatt, and S. D. Seiwert, "Monitoring post-translational modification of proteins with allosteric ribozymes.," *Nat Biotechnol*, vol. 20, pp. 810–815, Aug 2002.

[312] J. Tang and R. R. Breaker, "Mechanism for allosteric inhibition of an atp-sensitive ribozyme.," *Nucleic Acids Res*, vol. 26, pp. 4214–4221, Sep 1998.

[313] J. Tang and R. R. Breaker, "Rational design of allosteric ribozymes.," *Chem Biol*, vol. 4, pp. 453–459, Jun 1997.

[314] G. Mayer, "personal communication.".

[315] V. M. Tesmer, S. Lennarz, G. Mayer, and J. J. G. Tesmer, "Molecular mechanism for inhibition of g protein-coupled receptor kinase 2 by a selective rna aptamer.," *Structure*, vol. 20, pp. 1300–1309, Aug 2012.

[316] T. Maeda, Y. Imanishi, and K. Palczewski, "Rhodopsin phosphorylation: 30 years later.," *Prog Retin Eye Res*, vol. 22, pp. 417–434, Jul 2003.

[317] D. T. Lodowski, J. A. Pitcher, W. D. Capel, R. J. Lefkowitz, and J. J. G. Tesmer, "Keeping g proteins at bay: a complex between g protein-coupled receptor kinase 2 and gbetagamma.," *Science*, vol. 300, pp. 1256–1262, May 2003.

[318] V. M. Tesmer, T. Kawano, A. Shankaranarayanan, T. Kozasa, and J. J. G. Tesmer, "Snapshot of activated g proteins at the membrane: the galphaq-grk2-gbetagamma complex.," *Science*, vol. 310, pp. 1686–1690, Dec 2005.

[319] B. K. Shoichet, "Interpreting steep dose-response curves in early inhibitor discovery.," *J Med Chem*, vol. 49, pp. 7274–7277, Dec 2006.

[320] H. F. Lodish, *Molecular cell biology.* New York: Scientific American Books., 1999.

[321] M. L. Wynn, A. C. Ventura, J. A. Sepulchre, H. J. Garcia, and S. D. Merajver, "Kinase inhibitors can produce off-target effects and activate linked pathways by retroactivity.," *BMC Syst Biol*, vol. 5, p. 156, 2011.

[322] M. Vieth, R. E. Higgs, D. H. Robertson, M. Shapiro, E. A. Gragg, and H. Hemmerle, "Kinomics-structural biology and chemogenomics of kinase inhibitors and targets.," *Biochim Biophys Acta*, vol. 1697, pp. 243–257, Mar 2004.

[323] Z. A. Knight and K. M. Shokat, "Features of selective kinase inhibitors.," *Chem Biol*, vol. 12, pp. 621–637, Jun 2005.

[324] R. Conrad, L. M. Keranen, A. D. Ellington, and A. C. Newton, "Isozyme-specific inhibition of protein kinase c by rna aptamers.," *J Biol Chem*, vol. 269, pp. 32051–32054, Dec 1994.

[325] M. Ohori, "Erk inhibitors as a potential new therapy for rheumatoid arthritis.," *Drug News Perspect*, vol. 21, pp. 245–250, Jun 2008.

[326] F. H. Cruzalegui, E. Cano, and R. Treisman, "Erk activation induces phosphorylation of elk-1 at multiple s/t-p motifs to high stoichiometry.," *Oncogene*, vol. 18, pp. 7948–7957, Dec 1999.

[327] K. A. Burkhard, F. Chen, and P. Shapiro, "Quantitative analysis of erk2 interactions with substrate proteins: roles for kinase docking domains and activity in determining binding affinity.," *J Biol Chem*, vol. 286, pp. 2477–2485, Jan 2011.

[328] F. L. Robinson, A. W. Whitehurst, M. Raman, and M. H. Cobb, "Identification of novel point mutations in erk2 that selectively disrupt binding to mek1.," *J Biol Chem*, vol. 277, pp. 14844–14852, Apr 2002.

[329] J. Rodriguez and P. Crespo, "Working without kinase activity: phosphotransfer-independent functions of extracellular signal-regulated kinases.," *Sci Signal*, vol. 4, no. 196, p. re3, 2011.

[330] D. J. Robbins, E. Zhen, M. Cheng, S. Xu, C. A. Vanderbilt, D. Ebert, C. Garcia, A. Dang, and M. H. Cobb, "Regulation and properties of extracellular signal-regulated protein kinases 1, 2, and 3.," *J Am Soc Nephrol*, vol. 4, pp. 1104–1110, Nov 1993.

[331] C. N. Prowse and J. Lew, "Mechanism of activation of erk2 by dual phosphorylation.," *J Biol Chem*, vol. 276, pp. 99–103, Jan 2001.

[332] S. J. Mansour, J. M. Candia, J. E. Matsuura, M. C. Manning, and N. G. Ahn, "Interdependent domains controlling the enzymatic activity of mitogen-activated protein kinase kinase 1.," *Biochemistry*, vol. 35, pp. 15529–15536, Dec 1996.

[333] http://biophoretics.com/212-290-large/vgme02-mini-elpho-electrophoresis system.jpg.

[334] M. Thomas, S. Chedin, C. Carles, M. Riva, M. Famulok, and A. Sentenac, "Selective targeting and inhibition of yeast rna polymerase ii by rna aptamers.," *J Biol Chem*, vol. 272, pp. 27980–27986, Oct 1997.

[335] G. Werstuck and M. R. Green, "Controlling gene expression in living cells through small molecule-rna interactions.," *Science*, vol. 282, pp. 296–298, Oct 1998.

[336] E. Myslinski, J. C. AmÈ, A. Krol, and P. Carbon, "An unusually compact external promoter for rna polymerase iii transcription of the human h1rna gene.," *Nucleic Acids Res*, vol. 29, pp. 2502–2509, Jun 2001.

[337] A. Fujioka, K. Terai, R. E. Itoh, K. Aoki, T. Nakamura, S. Kuroda, E. Nishida, and M. Matsuda, "Dynamics of the ras/erk mapk cascade as monitored by fluorescent probes.," *J Biol Chem*, vol. 281, pp. 8917–8926, Mar 2006.

[338] P. I. Maekinen, J. K. Koponen, A.-M. Kaerkkaeinen, T. M. Malm, K. H. Pulkkinen, J. Koistinaho, M. P. Turunen, and S. Ylae-Herttuala, "Stable rna interference: comparison of u6 and h1 promoters in endothelial cells and in mouse brain.," *J Gene Med*, vol. 8, pp. 433–441, Apr 2006.

[339] D. M. Cummins, S. G. Tyack, and T. J. Doran, "Characterisation and comparison of the chicken h1 rna polymerase iii promoter for short hairpin rna expression.," *Biochem Biophys Res Commun*, vol. 416, pp. 194–198, Dec 2011.

[340] P. Shore and A. D. Sharrocks, "The transcription factors elk-1 and serum response factor interact by direct protein-protein contacts mediated by a short region of elk-1.," *Mol Cell Biol*, vol. 14, pp. 3283–3291, May 1994.

[341] G. Buchwalter, C. Gross, and B. Wasylyk, "Ets ternary complex transcription factors.," *Gene*, vol. 324, pp. 1–14, Jan 2004.

[342] C. S. Hill, R. Marais, S. John, J. Wynne, S. Dalton, and R. Treisman, "Functional analysis of a growth factor-responsive transcription factor complex.," *Cell*, vol. 73, pp. 395–406, Apr 1993.

[343] H. Gille, A. D. Sharrocks, and P. E. Shaw, "Phosphorylation of transcription factor p62tcf by map kinase stimulates ternary complex formation at c-fos promoter.," *Nature*, vol. 358, pp. 414–417, Jul 1992.

[344] H. Gille, M. Kortenjann, O. Thomae, C. Moomaw, C. Slaughter, M. H. Cobb, and P. E. Shaw, "Erk phosphorylation potentiates elk-1-mediated ternary complex formation and transactivation.," *EMBO J*, vol. 14, pp. 951–962, Mar 1995.

[345] L. Pinto da Silva and J. C. G. Esteves da Silva, "Firefly chemiluminescence and bioluminescence: efficient generation of excited states.," *Chemphyschem*, vol. 13, pp. 2257–2262, Jun 2012.

[346] M. F. Favata, K. Y. Horiuchi, E. J. Manos, A. J. Daulerio, D. A. Stradley, W. S. Feeser, D. E. Van Dyk, W. J. Pitts, R. A. Earl, F. Hobbs, R. A. Copeland, R. L. Magolda, P. A. Scherle, and J. M. Trzaskos, "Identification of a novel inhibitor of mitogen-activated protein kinase kinase.," *J Biol Chem*, vol. 273, pp. 18623–18632, Jul 1998.

[347] J. V. Duncia, J. Santella, 3rd, C. A. Higley, W. J. Pitts, J. Wityak, W. E. Frietze, F. W. Rankin, J. H. Sun, R. A. Earl, A. C. Tabaka, C. A. Teleha, K. F. Blom, M. F. Favata, E. J. Manos, A. J. Daulerio, D. A. Stradley, K. Horiuchi, R. A. Copeland, P. A. Scherle, J. M. Trzaskos, R. L. Magolda, G. L. Trainor, R. R. Wexler, F. W. Hobbs, and R. E. Olson, "Mek inhibitors: the chemistry and biological activity of u0126, its analogs, and cyclization products.," *Bioorg Med Chem Lett*, vol. 8, pp. 2839–2844, Oct 1998.

[348] S. Veldhoen, S. D. Laufer, A. Trampe, and T. Restle, "Cellular delivery of small interfering rna by a non-covalently attached cell-penetrating peptide: quantitative analysis of uptake and biological effect.," *Nucleic Acids Res*, vol. 34, no. 22, pp. 6561–6573, 2006.

[349] A. J. Whitmarsh, S. H. Yang, M. S. Su, A. D. Sharrocks, and R. J. Davis, "Role of p38 and jnk mitogen-activated protein kinases in the activation of ternary complex factors.," *Mol Cell Biol*, vol. 17, pp. 2360–2371, May 1997.

[350] Y. Ma, F.-C. Guo, W. Wang, H.-S. Shi, D. Li, and Y.-S. Wang, "K?ras gene mutation as a predictor of cancer cell responsiveness to metformin.," *Mol Med Rep*, vol. 8, pp. 763–768, Sep 2013.

[351] M. L. Janmaat, F. A. E. Kruyt, J. A. Rodriguez, and G. Giaccone, "Response to epidermal growth factor receptor inhibitors in non-small cell lung cancer cells: limited antiproliferative effects and absence of apoptosis associated with persistent activity of extracellular signal-regulated kinase or akt kinase pathways.," *Clin Cancer Res*, vol. 9, pp. 2316–2326, Jun 2003.

[352] E. B. Burova, I. S. Smirnova, I. V. Gonchar, A. N. Shatrova, and N. N. Nikolsky, "Inhibition of the egf receptor and erk1/2 signaling pathways rescues the human epidermoid carcinoma a431 cells from ifn?-induced apoptosis.," *Cell Cycle*, vol. 10, pp. 2197–2205, Jul 2011.

[353] C. Bernard, A. Anderson, A. Becker, N. P. Poolos, H. Beck, and D. Johnston, "Acquired dendritic channelopathy in temporal lobe epilepsy.," *Science*, vol. 305, pp. 532–535, Jul 2004.

[354] T. Alich, "Aptamer-based disruption of spike-timing plasticity," Master's thesis, Faculty of Neurosciences at the University of Bonn, 2014.

[355] N. Fertig, R. H. Blick, and J. C. Behrends, "Whole cell patch clamp recording performed on a planar glass chip.," *Biophys J*, vol. 82, pp. 3056–3062, Jun 2002.

[356] X. Chen, L.-L. Yuan, C. Zhao, S. G. Birnbaum, A. Frick, W. E. Jung, T. L. Schwarz, J. D. Sweatt, and D. Johnston, "Deletion of kv4.2 gene eliminates dendritic a-type k+ current and enhances induction of long-term potentiation in hippocampal ca1 pyramidal neurons.," *J Neurosci*, vol. 26, pp. 12143–12151, Nov 2006.

[357] J. A. Rosenkranz, A. Frick, and D. Johnston, "Kinase-dependent modification of dendritic excitability after long-term potentiation.," *J Physiol*, vol. 587, pp. 115–125, Jan 2009.

[358] P. Smolen, D. A. Baxter, and J. H. Byrne, "A model of the roles of essential kinases in the induction and expression of late long-term potentiation.," *Biophys J*, vol. 90, pp. 2760–2775, Apr 2006.

[359] D. M. Thal, K. T. Homan, J. Chen, E. K. Wu, P. M. Hinkle, Z. M. Huang, J. K. Chuprun, J. Song, E. Gao, J. Y. Cheung, L. A. Sklar, W. J. Koch, and J. J. G. Tesmer, "Paroxetine is a direct inhibitor of g protein-coupled receptor kinase 2 and increases myocardial contractility.," *ACS Chem Biol*, vol. 7, pp. 1830–1839, Nov 2012.

[360] Y. Liu and N. S. Gray, "Rational design of inhibitors that bind to inactive kinase conformations.," *Nat Chem Biol*, vol. 2, pp. 358–364, Jul 2006.

[361] D.-B. Huang, D. Vu, L. A. Cassiday, J. M. Zimmerman, L. J. Maher, 3rd, and G. Ghosh, "Crystal structure of nf-kappab (p50)2 complexed to a high-affinity rna aptamer.," *Proc Natl Acad Sci U S A*, vol. 100, pp. 9268–9273, Aug 2003.

[362] J. Setyawan, K. Koide, T. C. Diller, M. E. Bunnage, S. S. Taylor, K. C. Nicolaou, and L. L. Brunton, "Inhibition of protein kinases by balanol: specificity within the serine/threonine protein kinase subfamily.," *Mol Pharmacol*, vol. 56, pp. 370–376, Aug 1999.

[363] M. Gonzalez and H. Cerecetto, "Quinoxaline derivatives: a patent review (2006–present).," *Expert Opin Ther Pat*, vol. 22, pp. 1289–1302, Nov 2012.

[364] M. T. Conconi, G. Marzaro, L. Urbani, I. Zanusso, R. Di Liddo, I. Castagliuolo, P. Brun, F. Tonus, A. Ferrarese, A. Guiotto, and A. Chilin, "Quinazoline-based multi-tyrosine kinase inhibitors: synthesis, modeling, antitumor and antiangiogenic properties.," *Eur J Med Chem*, vol. 67, pp. 373–383, Sep 2013.

[365] V. Desplat, A. Geneste, M.-A. Begorre, S. B. Fabre, S. Brajot, S. Massip, D. Thiolat, D. Mossalayi, C. Jarry, and J. Guillon, "Synthesis of new pyrrolo[1,2-a]quinoxaline derivatives as potential inhibitors of akt kinase.," *J Enzyme Inhib Med Chem*, vol. 23, pp. 648–658, Oct 2008.

[366] J. Porter, S. Lumb, F. Lecomte, J. Reuberson, A. Foley, M. Calmiano, K. le Riche, H. Edwards, J. Delgado, R. J. Franklin, J. M. Gascon-Simorte, A. Maloney, C. Meier, and M. Batchelor, "Discovery of a novel series of quinoxalines as inhibitors of c-met kinase.," *Bioorg Med Chem Lett*, vol. 19, pp. 397–400, Jan 2009.

[367] N. Florin, "Unpublished data.".

[368] M. Bourin, P. Chue, and Y. Guillon, "Paroxetine: a review.," *CNS Drug Rev*, vol. 7, no. 1, pp. 25–47, 2001.

[369] C. B. Nemeroff and M. J. Owens, "Neuropharmacology of paroxetine.," *Psychopharmacol Bull*, vol. 37 Suppl 1, pp. 8–18, 2003.

[370] M. S. Finkel, F. Laghrissi-Thode, B. G. Pollock, and J. Rong, "Paroxetine is a novel nitric oxide synthase inhibitor.," *Psychopharmacol Bull*, vol. 32, no. 4, pp. 653–658, 1996.

[371] K. T. Homan, E. Wu, M. W. Wilson, P. Singh, S. D. Larsen, and J. J. G. Tesmer, "Structural and functional analysis of g protein-coupled receptor kinase inhibition by paroxetine and a rationally designed analog.," *Mol Pharmacol*, vol. 85, pp. 237–248, Feb 2014.

[372] H. Ma, S. Deacon, and K. Horiuchi, "The challenge of selecting protein kinase assays for lead discovery optimization.," *Expert Opin Drug Discov*, vol. 3, pp. 607–621, Jun 2008.

[373] P. Chene, "Challenges in design of biochemical assays for the identification of small molecules to target multiple conformations of protein kinases.," *Drug Discov Today*, vol. 13, pp. 522–529, Jun 2008.

[374] P. Nahid, E. Bliven-Sizemore, L. G. Jarlsberg, M. A. De Groote, J. L. Johnson, G. Muzanyi, M. Engle, M. Weiner, N. Janjic, D. G. Sterling, and U. A. Ochsner, "Aptamer-based proteomic signature of intensive phase treatment response in pulmonary tuberculosis.," *Tuberculosis (Edinb)*, Feb 2014.

[375] L. Gold, D. Ayers, J. Bertino, C. Bock, A. Bock, E. N. Brody, J. Carter, A. B. Dalby, B. E. Eaton, T. Fitzwater, D. Flather, A. Forbes, T. Foreman, C. Fowler, B. Gawande, M. Goss, M. Gunn, S. Gupta, D. Halladay, J. Heil, J. Heilig, B. Hicke, G. Husar, N. Janjic, T. Jarvis, S. Jennings, E. Katilius, T. R. Keeney, N. Kim, T. H. Koch, S. Kraemer, L. Kroiss, N. Le, D. Levine, W. Lindsey, B. Lollo, W. Mayfield, M. Mehan, R. Mehler, S. K. Nelson, M. Nelson, D. Nieuwlandt, M. Nikrad, U. Ochsner, R. M. Ostroff, M. Otis, T. Parker, S. Pietrasiewicz, D. I. Resnicow, J. Rohloff, G. Sanders, S. Sattin, D. Schneider, B. Singer, M. Stanton, A. Sterkel, A. Stewart, S. Stratford, J. D. Vaught, M. Vrkljan, J. J. Walker, M. Watrobka, S. Waugh, A. Weiss, S. K. Wilcox, A. Wolfson, S. K. Wolk, C. Zhang, and D. Zichi, "Aptamer-based multiplexed proteomic technology for biomarker discovery.," *PLoS One*, vol. 5, no. 12, p. e15004, 2010.

[376] D. E. Draper, "A guide to ions and rna structure.," *RNA*, vol. 10, pp. 335–343, Mar 2004.

[377] S. E. Butcher and A. M. Pyle, "The molecular interactions that stabilize rna tertiary structure: Rna motifs, patterns, and networks.," *Acc Chem Res*, vol. 44, pp. 1302–1311, Dec 2011.

[378] Z.-J. Tan and S.-J. Chen, "Salt contribution to rna tertiary structure folding stability.," *Biophys J*, vol. 101, pp. 176–187, Jul 2011.

[379] M. Girardot, H.-Y. Li, S. Descroix, and A. Varenne, "Determination of binding parameters between lysozyme and its aptamer by frontal analysis continuous microchip electrophoresis (facmce).," *J Chromatogr A*, vol. 1218, pp. 4052–4058, Jul 2011.

[380] X. Arias-Moreno, O. Abian, S. Vega, J. Sancho, and A. Velazquez-Campoy, "Protein-cation interactions: structural and thermodynamic aspects.," *Curr Protein Pept Sci*, vol. 12, pp. 325–338, Jun 2011.

[381] C. Baldauf, K. Pagel, S. Warnke, G. von Helden, B. Koksch, V. Blum, and M. Scheffler, "How cations change peptide structure.," *Chemistry*, vol. 19, pp. 11224–11234, Aug 2013.

[382] D. Lambert, D. Leipply, R. Shiman, and D. E. Draper, "The influence of monovalent cation size on the stability of rna tertiary structures.," *J Mol Biol*, vol. 390, pp. 791–804, Jul 2009.

[383] W. F. Waas, M. A. Rainey, A. E. Szafranska, K. Cox, and K. N. Dalby, "A kinetic approach towards understanding substrate interactions and the catalytic mechanism of the serine/threonine protein kinase erk2: identifying a potential regulatory role for divalent magnesium.," *Biochim Biophys Acta*, vol. 1697, pp. 81–87, Mar 2004.

[384] M. Marchi, A. D'Antoni, I. Formentini, R. Parra, R. Brambilla, G. M. Ratto, and M. Costa, "The n-terminal domain of erk1 accounts for the functional differences with erk2.," *PLoS One*, vol. 3, no. 12, p. e3873, 2008.

[385] Y. Jiang, Z. Li, E. M. Schwarz, A. Lin, K. Guan, R. J. Ulevitch, and J. Han, "Structure-function studies of p38 mitogen-activated protein kinase. loop 12 influences substrate specificity and autophosphorylation, but not upstream kinase selection.," *J Biol Chem*, vol. 272, pp. 11096–11102, Apr 1997.

[386] S. V. Frye, "Structure-activity relationship homology (sarah): a conceptual framework for drug discovery in the genomic era.," *Chem Biol*, vol. 6, pp. R3–R7, Jan 1999.

[387] L. Gold, N. Janjic, T. Jarvis, D. Schneider, J. J. Walker, S. K. Wilcox, and D. Zichi, "Aptamers and the rna world, past and present.," *Cold Spring Harb Perspect Biol*, vol. 4, Mar 2012.

[388] J. Ferrell, Jr, "Tripping the switch fantastic: how a protein kinase cascade can convert graded inputs into switch-like outputs.," *Trends Biochem Sci*, vol. 21, pp. 460–466, Dec 1996.

[389] R. R. Bhatt and J. Ferrell, Jr, "Cloning and characterization of xenopus rsk2, the predominant p90 rsk isozyme in oocytes and eggs.," *J Biol Chem*, vol. 275, pp. 32983–32990, Oct 2000.

[390] T. Arooz, C. H. Yam, W. Y. Siu, A. Lau, K. K. Li, and R. Y. Poon, "On the concentrations of cyclins and cyclin-dependent kinases in extracts of cultured human cells.," *Biochemistry*, vol. 39, pp. 9494–9501, Aug 2000.

[391] F. Sherman, *Guide to Yeast Genetics and Molecular Biology*. San Diego: Academic Press, 1991.

[392] A. N. Hoofnagle, K. A. Resing, E. J. Goldsmith, and N. G. Ahn, "Changes in protein conformational mobility upon activation of extracellular regulated protein kinase-2 as detected by hydrogen exchange.," *Proc Natl Acad Sci U S A*, vol. 98, pp. 956–961, Jan 2001.

[393] J. L. Wilsbacher, E. J. Goldsmith, and M. H. Cobb, "Phosphorylation of map kinases by map/erk involves multiple regions of map kinases.," *J Biol Chem*, vol. 274, pp. 16988–16994, Jun 1999.

[394] B. K. Kay, M. P. Williamson, and M. Sudol, "The importance of being proline: the interaction of proline-rich motifs in signaling proteins with their cognate domains.," *FASEB J*, vol. 14, pp. 231–241, Feb 2000.

[395] A. A. Morgan and E. Rubenstein, "Proline: the distribution, frequency, positioning, and common functional roles of proline and polyproline sequences in the human proteome.," *PLoS One*, vol. 8, no. 1, p. e53785, 2013.

[396] H. L. De Bondt, J. Rosenblatt, J. Jancarik, H. D. Jones, D. O. Morgan, and S. H. Kim, "Crystal structure of cyclin-dependent kinase 2.," *Nature*, vol. 363, pp. 595–602, Jun 1993.

[397] D. H. Brotherton, V. Dhanaraj, S. Wick, L. Brizuela, P. J. Domaille, E. Volyanik, X. Xu, E. Parisini, B. O. Smith, S. J. Archer, M. Serrano, S. L. Brenner, T. L. Blundell, and E. D. Laue, "Crystal structure of the complex of the cyclin d-dependent kinase cdk6 bound to the cell-cycle inhibitor p19ink4d.," *Nature*, vol. 395, pp. 244–250, Sep 1998.

[398] A. A. Russo, L. Tong, J. O. Lee, P. D. Jeffrey, and N. P. Pavletich, "Structural basis for inhibition of the cyclin-dependent kinase cdk6 by the tumour suppressor p16ink4a.," *Nature*, vol. 395, pp. 237–243, Sep 1998.

[399] S.-K. Hong, S. Yoon, C. Moelling, D. Arthan, and J.-I. Park, "Noncatalytic function of erk1/2 can promote raf/mek/erk-mediated growth arrest signaling.," *J Biol Chem*, vol. 284, pp. 33006–33018, Nov 2009.

[400] T. J. Gibson, M. Seiler, and R. A. Veitia, "The transience of transient overexpression.," *Nat Methods*, vol. 10, pp. 715–721, Aug 2013.

[401] C. N. Hancock, A. Macias, E. K. Lee, S. Y. Yu, A. D. Mackerell, Jr, and P. Shapiro, "Identification of novel extracellular signal-regulated kinase docking domain inhibitors.," *J Med Chem*, vol. 48, pp. 4586–4595, Jul 2005.

[402] F. Chen, C. N. Hancock, A. T. Macias, J. Joh, K. Still, S. Zhong, A. D. MacKerell, Jr, and P. Shapiro, "Characterization of atp-independent erk inhibitors identified through in silico analysis of the active erk2 structure.," *Bioorg Med Chem Lett*, vol. 16, pp. 6281–6287, Dec 2006.

[403] B. R. Kelemen, K. Hsiao, and S. A. Goueli, "Selective in vivo inhibition of mitogen-activated protein kinase activation using cell-permeable peptides.," *J Biol Chem*, vol. 277, pp. 8741–8748, Mar 2002.

[404] L. Kummer, P. Parizek, P. Rube, B. Millgramm, A. Prinz, P. R. E. Mittl, M. Kaufholz, B. Zimmermann, F. W. Herberg, and A. Pl¸ckthun, "Structural and functional analysis of phosphorylation-specific binders of the kinase erk from designed ankyrin repeat protein libraries.," *Proc Natl Acad Sci U S A*, vol. 109, pp. E2248–E2257, Aug 2012.

[405] K. M. Comess, C. Sun, C. Abad-Zapatero, E. R. Goedken, R. J. Gum, D. W. Borhani, M. Argiriadi, D. R. Groebe, Y. Jia, J. E. Clampit, D. L. Haasch, H. T. Smith, S. Wang, D. Song, M. L. Coen, T. E. Cloutier, H. Tang, X. Cheng, C. Quinn, B. Liu, Z. Xin, G. Liu, E. H. Fry, V. Stoll, T. I. Ng, D. Banach, D. Marcotte, D. J. Burns, D. J. Calderwood, and P. J. Hajduk, "Discovery and characterization of non-atp site inhibitors of the mitogen activated protein (map) kinases.," *ACS Chem Biol*, vol. 6, pp. 234–244, Mar 2011.

[406] D. J. Robbins and M. H. Cobb, "Extracellular signal-regulated kinases 2 autophosphorylates on a subset of peptides phosphorylated in intact cells in response to insulin and nerve growth factor: analysis by peptide mapping.," *Mol Biol Cell*, vol. 3, pp. 299–308, Mar 1992.

[407] J. Ferrell, Jr and R. R. Bhatt, "Mechanistic studies of the dual phosphorylation of mitogen-activated protein kinase.," *J Biol Chem*, vol. 272, pp. 19008–19016, Jul 1997.

[408] F. Zhang, A. Strand, D. Robbins, M. H. Cobb, and E. J. Goldsmith, "Atomic structure of the map kinase erk2 at 2.3 a resolution.," *Nature*, vol. 367, pp. 704–711, Feb 1994.

[409] D. Fey, D. R. Croucher, W. Kolch, and B. N. Kholodenko, "Crosstalk and signaling switches in mitogen-activated protein kinase cascades.," *Front Physiol*, vol. 3, p. 355, 2012.

[410] E. Aksamitiene, A. Kiyatkin, and B. N. Kholodenko, "Cross-talk between mitogenic ras/mapk and survival pi3k/akt pathways: a fine balance.," *Biochem Soc Trans*, vol. 40, pp. 139–146, Feb 2012.

[411] C. Wang, A. Cigliano, S. Delogu, J. Armbruster, F. Dombrowski, M. Evert, X. Chen, and D. F. Calvisi, "Functional crosstalk between akt/mtor and ras/mapk pathways in hepatocarcinogenesis: implications for the treatment of human liver cancer.," *Cell Cycle*, vol. 12, pp. 1999–2010, Jul 2013.

[412] Y. H. Shen, J. Godlewski, J. Zhu, P. Sathyanarayana, V. Leaner, M. J. Birrer, A. Rana, and G. Tzivion, "Cross-talk between jnk/sapk and erk/mapk pathways: sustained activation of jnk blocks erk activation by mitogenic factors.," *J Biol Chem*, vol. 278, pp. 26715–26721, Jul 2003.

[413] P. Richard and J. L. Manley, "Transcription termination by nuclear rna polymerases.," *Genes Dev*, vol. 23, pp. 1247–1269, Jun 2009.

[414] M. Helm, "Post-transcriptional nucleotide modification and alternative folding of rna.," *Nucleic Acids Res*, vol. 34, no. 2, pp. 721–733, 2006.

[415] H. D. Madhani, R. BordonnÈ, and C. Guthrie, "Multiple roles for u6 snrna in the splicing pathway.," *Genes Dev*, vol. 4, pp. 2264–2277, Dec 1990.

[416] T. Kiss, "Biogenesis of small nuclear rnps.," *J Cell Sci*, vol. 117, pp. 5949–5951, Dec 2004.

[417] J. Houseley and D. Tollervey, "The many pathways of rna degradation.," *Cell*, vol. 136, pp. 763–776, Feb 2009.

[418] S. Kadaba, X. Wang, and J. T. Anderson, "Nuclear rna surveillance in saccharomyces cerevisiae: Trf4p-dependent polyadenylation of nascent hypomethylated trna and an aberrant form of 5s rrna.," *RNA*, vol. 12, pp. 508–521, Mar 2006.

[419] L. A. Copela, C. F. Fernandez, R. L. Sherrer, and S. L. Wolin, "Competition between the rex1 exonuclease and the la protein affects both trf4p-mediated rna quality control and pre-trna maturation.," *RNA*, vol. 14, pp. 1214–1227, Jun 2008.

[420] D. D. Rao, J. S. Vorhies, N. Senzer, and J. Nemunaitis, "sirna vs. shrna: similarities and differences.," *Adv Drug Deliv Rev*, vol. 61, pp. 746–759, Jul 2009.

[421] M. P. Terns, E. Lund, and J. E. Dahlberg, "3'-end-dependent formation of u6 small nuclear ribonucleoprotein particles in xenopus laevis oocyte nuclei.," *Mol Cell Biol*, vol. 12, pp. 3032–3040, Jul 1992.

[422] Y. Hu, M. Bally, W. H. Dragowska, and L. Mayer, "Inhibition of mitogen-activated protein kinase/extracellular signal-regulated kinase kinase enhances chemotherapeutic effects on h460 human non-small cell lung cancer cells through activation of apoptosis.," *Mol Cancer Ther*, vol. 2, pp. 641–649, Jul 2003.

[423] L. Garuti, M. Roberti, and G. Bottegoni, "Non-atp competitive protein kinase inhibitors.," *Curr Med Chem*, vol. 17, no. 25, pp. 2804–2821, 2010.

[424] S. Kamakura, T. Moriguchi, and E. Nishida, "Activation of the protein kinase erk5/bmk1 by receptor tyrosine kinases. identification and characterization of a signaling pathway to the nucleus.," *J Biol Chem*, vol. 274, pp. 26563–26571, Sep 1999.

[425] N. Mody, J. Leitch, C. Armstrong, J. Dixon, and P. Cohen, "Effects of map kinase cascade inhibitors on the mkk5/erk5 pathway.," *FEBS Lett*, vol. 502, pp. 21–24, Jul 2001.

[426] A. Ranganathan, G. W. Pearson, C. A. Chrestensen, T. W. Sturgill, and M. H. Cobb, "The map kinase erk5 binds to and phosphorylates p90 rsk.," *Arch Biochem Biophys*, vol. 449, pp. 8–16, May 2006.

[427] D. B. Mike Byrom, Vince Pallotta and L. Ford, "Fluorescence analysis of the rnai effect." online.

[428] M. Olejniczak, K. Polak, P. Galka-Marciniak, and W. J. Krzyzosiak, "Recent advances in understanding of the immunological off-target effects of sirna.," *Curr Gene Ther*, vol. 11, pp. 532–543, Dec 2011.

[429] D. Grimm, "The dose can make the poison: lessons learned from adverse in vivo toxicities caused by rnai overexpression.," *Silence*, vol. 2, p. 8, 2011.

[430] J. N. Martin, N. Wolken, T. Brown, W. T. Dauer, M. E. Ehrlich, and P. Gonzalez-Alegre, "Lethal toxicity caused by expression of shrna in the mouse striatum: implications for therapeutic design.," *Gene Ther*, vol. 18, pp. 666–673, Jul 2011.

[431] A. L. Jackson, J. Burchard, J. Schelter, B. N. Chau, M. Cleary, L. Lim, and P. S. Linsley, "Widespread sirna off-target transcript silencing mediated by seed region sequence complementarity.," *RNA*, vol. 12, pp. 1179–1187, Jul 2006.

[432] R. Toroney, C. M. Hull, J. E. Sokoloski, and P. C. Bevilacqua, "Mechanistic characterization of the 5'-triphosphate-dependent activation of pkr: lack of 5'-end nucleobase specificity, evidence for a distinct triphosphate binding site, and a critical role for the dsrbd.," *RNA*, vol. 18, pp. 1862–1874, Oct 2012.

[433] R. Besch, H. Poeck, T. Hohenauer, D. Senft, G. Haecker, C. Berking, V. Hornung, S. Endres, T. Ruzicka, S. Rothenfusser, and G. Hartmann, "Proapoptotic signaling induced by rig-i and mda-5 results in type i interferon-independent apoptosis in human melanoma cells.," *J Clin Invest*, vol. 119, pp. 2399–2411, Aug 2009.

[434] H. Kato, K. Takahasi, and T. Fujita, "Rig-i-like receptors: cytoplasmic sensors for non-self rna.," *Immunol Rev*, vol. 243, pp. 91–98, Sep 2011.

[435] S. A. Beckham, J. Brouwer, A. Roth, D. Wang, A. J. Sadler, M. John, K. Jahn-Hofmann, B. R. G. Williams, J. A. Wilce, and M. C. J. Wilce, "Conformational rearrangements of rig-i receptor on formation of a multiprotein:dsrna assembly.," *Nucleic Acids Res*, vol. 41, pp. 3436–3445, Mar 2013.

[436] L. R. Saunders and G. N. Barber, "The dsrna binding protein family: critical roles, diverse cellular functions.," *FASEB J*, vol. 17, pp. 961–983, Jun 2003.

[437] H. Kato, S. Sato, M. Yoneyama, M. Yamamoto, S. Uematsu, K. Matsui, T. Tsujimura, K. Takeda, T. Fujita, O. Takeuchi, and S. Akira, "Cell type-specific involvement of rig-i in antiviral response.," *Immunity*, vol. 23, pp. 19–28, Jul 2005.

[438] H. Kato, O. Takeuchi, S. Sato, M. Yoneyama, M. Yamamoto, K. Matsui, S. Uematsu, A. Jung, T. Kawai, K. J. Ishii, O. Yamaguchi, K. Otsu, T. Tsujimura, C.-S. Koh, C. Reis e Sousa, Y. Matsuura, T. Fujita, and S. Akira, "Differential roles of mda5 and rig-i helicases in the recognition of rna viruses.," *Nature*, vol. 441, pp. 101–105, May 2006.

[439] Y.-M. Loo, J. Fornek, N. Crochet, G. Bajwa, O. Perwitasari, L. Martinez-Sobrido, S. Akira, M. A. Gill, A. GarcÌa-Sastre, M. G. Katze, and M. Gale, Jr, "Distinct rig-i and mda5 signaling by rna viruses in innate immunity.," *J Virol*, vol. 82, pp. 335–345, Jan 2008.

[440] S. Jensen and A. R. Thomsen, "Sensing of rna viruses: a review of innate immune receptors involved in recognizing rna virus invasion.," *J Virol*, vol. 86, pp. 2900–2910, Mar 2012.

[441] V. Hornung, J. Ellegast, S. Kim, K. BrzÛzka, A. Jung, H. Kato, H. Poeck, S. Akira, K.-K. Conzelmann, M. Schlee, S. Endres, and G. Hartmann, "5'-triphosphate rna is the ligand for rig-i.," *Science*, vol. 314, pp. 994–997, Nov 2006.

[442] A. Schmidt, T. Schwerd, W. Hamm, J. C. Hellmuth, S. Cui, M. Wenzel, F. S. Hoffmann, M.-C. Michallet, R. Besch, K.-P. Hopfner, S. Endres, and S. Rothenfusser, "5'-triphosphate rna requires base-paired structures to activate antiviral signaling via rig-i.," *Proc Natl Acad Sci U S A*, vol. 106, pp. 12067–12072, Jul 2009.

[443] S. Davis and J. C. Watson, "In vitro activation of the interferon-induced, double-stranded rna-dependent protein kinase pkr by rna from the 3' untranslated regions of human alpha-tropomyosin.," *Proc Natl Acad Sci U S A*, vol. 93, pp. 508–513, Jan 1996.

[444] P. C. Bevilacqua, C. X. George, C. E. Samuel, and T. R. Cech, "Binding of the protein kinase pkr to rnas with secondary structure defects: role of the tandem a-g mismatch and noncontiguous helixes.," *Biochemistry*, vol. 37, pp. 6303–6316, May 1998.

[445] Y. Ben-Asouli, Y. Banai, Y. Pel-Or, A. Shir, and R. Kaempfer, "Human interferon-gamma mrna autoregulates its translation through a pseudoknot that activates the interferon-inducible protein kinase pkr.," *Cell*, vol. 108, pp. 221–232, Jan 2002.

[446] U.-A. Bommer, A. V. Borovjagin, M. A. Greagg, I. W. Jeffrey, P. Russell, K. G. Laing, M. Lee, and M. J. Clemens, "The mrna of the translationally controlled tumor protein p23/tctp is a highly structured rna, which activates the dsrna-dependent protein kinase pkr.," *RNA*, vol. 8, pp. 478–496, Apr 2002.

[447] X. Zheng and P. C. Bevilacqua, "Activation of the protein kinase pkr by short double-stranded rnas with single-stranded tails.," *RNA*, vol. 10, pp. 1934–1945, Dec 2004.

[448] S. R. Nallagatla, J. Hwang, R. Toroney, X. Zheng, C. E. Cameron, and P. C. Bevilacqua, "5'-triphosphate-dependent activation of pkr by rnas with short stem-loops.," *Science*, vol. 318, pp. 1455–1458, Nov 2007.

[449] X. Wang, K. G. Finegan, A. C. Robinson, L. Knowles, R. Khosravi-Far, K. A. Hinchliffe, R. P. Boot-Handford, and C. Tournier, "Activation of extracellular signal-regulated protein kinase 5 downregulates fasl upon osmotic stress.," *Cell Death Differ*, vol. 13, pp. 2099–2108, Dec 2006.

[450] D. J. Park, S. P. Wilczynski, R. L. Paquette, C. W. Miller, and H. P. Koeffler, "p53 mutations in hpv-negative cervical carcinoma.," *Oncogene*, vol. 9, pp. 205–210, Jan 1994.

[451] W. A. Yeudall, I. C. Paterson, V. Patel, and S. S. Prime, "Presence of human papillomavirus sequences in tumour-derived human oral keratinocytes expressing mutant p53.," *Eur J Cancer B Oral Oncol*, vol. 31B, pp. 136–143, Mar 1995.

[452] S. L. Lai, R. P. Perng, and J. Hwang, "p53 gene status modulates the chemosensitivity of non-small cell lung cancer cells.," *J Biomed Sci*, vol. 7, no. 1, pp. 64–70, 2000.

[453] D. Semizarov, P. Kroeger, and S. Fesik, "sirna-mediated gene silencing: a global genome view.," *Nucleic Acids Res*, vol. 32, no. 13, pp. 3836–3845, 2004.

[454] S. P. Persengiev, X. Zhu, and M. R. Green, "Nonspecific, concentration-dependent stimulation and repression of mammalian gene expression by small interfering rnas (sirnas).," *RNA*, vol. 10, pp. 12–18, Jan 2004.

[455] A. L. Jackson, S. R. Bartz, J. Schelter, S. V. Kobayashi, J. Burchard, M. Mao, B. Li, G. Cavet, and P. S. Linsley, "Expression profiling reveals off-target gene regulation by rnai.," *Nat Biotechnol*, vol. 21, pp. 635–637, Jun 2003.

[456] X. Lin, X. Ruan, M. G. Anderson, J. A. McDowell, P. E. Kroeger, S. W. Fesik, and Y. Shen, "sirna-mediated off-target gene silencing triggered by a 7 nt complementation.," *Nucleic Acids Res*, vol. 33, no. 14, pp. 4527–4535, 2005.

[457] J. M. Tome, A. Ozer, J. M. Pagano, D. Gheba, G. P. Schroth, and J. T. Lis, "Comprehensive analysis of rna-protein interactions by high-throughput sequencing-rna affinity profiling.," *Nat Methods*, vol. 11, pp. 683–688, Jun 2014.

[458] S. D. Mendonsa and M. T. Bowser, "In vitro evolution of functional dna using capillary electrophoresis.," *J Am Chem Soc*, vol. 126, pp. 20–21, Jan 2004.

[459] B. I. Kanterewicz, N. N. Urban, D. B. McMahon, E. D. Norman, L. J. Giffen, M. F. Favata, P. A. Scherle, J. M. Trzskos, G. Barrionuevo, and E. Klann, "The extracellular signal-regulated kinase cascade is required for nmda receptor-independent ltp in area ca1 but not area ca3 of the hippocampus.," *J Neurosci*, vol. 20, pp. 3057–3066, May 2000.

[460] J. S. Wiegert and H. Bading, "Activity-dependent calcium signaling and erk-map kinases in neurons: a link to structural plasticity of the nucleus and gene transcription regulation.," *Cell Calcium*, vol. 49, pp. 296–305, May 2011.

[461] L. A. Schrader, Y. Ren, F. Cheng, D. Bui, J. D. Sweatt, and A. E. Anderson, "Kv4.2 is a locus for pkc and erk/mapk cross-talk.," *Biochem J*, vol. 417, pp. 705–715, Feb 2009.

[462] M. Fukuda, Y. Gotoh, and E. Nishida, "Interaction of map kinase with map kinase kinase: its possible role in the control of nucleocytoplasmic transport of map kinase.," *EMBO J*, vol. 16, pp. 1901–1908, Apr 1997.

[463] G. Glatz, G. Gogl, A. Alexa, and A. Remenyi, "Structural mechanism for the specific assembly and activation of the extracellular signal regulated kinase 5 (erk5) module.," *J Biol Chem*, vol. 288, pp. 8596–8609, Mar 2013.

[464] L. D. Wood, D. W. Parsons, S. Jones, J. Lin, T. Sjˆblom, R. J. Leary, D. Shen, S. M. Boca, T. Barber, J. Ptak, N. Silliman, S. Szabo, Z. Dezso, V. Ustyanksky, T. Nikolskaya, Y. Nikolsky, R. Karchin, P. A. Wilson, J. S. Kaminker, Z. Zhang, R. Croshaw, J. Willis, D. Dawson, M. Shipitsin, J. K. V. Willson, S. Sukumar, K. Polyak, B. H. Park, C. L. Pethiyagoda, P. V. K. Pant, D. G. Ballinger, A. B. Sparks, J. Hartigan, D. R. Smith, E. Suh, N. Papadopoulos, P. Buckhaults, S. D. Markowitz, G. Parmigiani, K. W. Kinzler, V. E. Velculescu, and B. Vogelstein, "The genomic landscapes of human breast and colorectal cancers.," *Science*, vol. 318, pp. 1108–1113, Nov 2007.

[465] J. Lin, C. M. Gan, X. Zhang, S. Jones, T. Sjˆblom, L. D. Wood, D. W. Parsons, N. Papadopoulos, K. W. Kinzler, B. Vogelstein, G. Parmigiani, and V. E. Velculescu, "A multidimensional analysis of genes mutated in breast and colorectal cancers.," *Genome Res*, vol. 17, pp. 1304–1318, Sep 2007.

[466] Y. K. Son, H. Park, A. L. Firth, and W. S. Park, "Side-effects of protein kinase inhibitors on ion channels.," *J Biosci*, vol. 38, pp. 937–949, Dec 2013.

[467] J. C. M. Uitdehaag, F. Verkaar, H. Alwan, J. de Man, R. C. Buijsman, and G. J. R. Zaman, "A guide to picking the most selective kinase inhibitor tool compounds for pharmacological validation of drug targets.," *Br J Pharmacol*, vol. 166, pp. 858–876, Jun 2012.

[468] F. Hoppe-Seyler, I. Crnkovic-Mertens, E. Tomai, and K. Butz, "Peptide aptamers: specific inhibitors of protein function.," *Curr Mol Med*, vol. 4, pp. 529–538, Aug 2004.

[469] A. Pinto, S. Lennarz, A. Rodrigues-Correia, A. Heckel, C. K. O'Sullivan, and G. Mayer, "Functional detection of proteins by caged aptamers.," *ACS Chem Biol*, vol. 7, pp. 360–366, Feb 2012.

[470] M. C. Michel, T. Wieland, and G. Tsujimoto, "How reliable are g-protein-coupled receptor antibodies?," *Naunyn Schmiedebergs Arch Pharmacol*, vol. 379, pp. 385–388, Apr 2009.

[471] B. C. Jensen, P. M. Swigart, and P. C. Simpson, "Ten commercial antibodies for alpha-1-adrenergic receptor subtypes are nonspecific.," *Naunyn Schmiedebergs Arch Pharmacol*, vol. 379, pp. 409–412, Apr 2009.

[472] N. Hamdani and J. van der Velden, "Lack of specificity of antibodies directed against human beta-adrenergic receptors.," *Naunyn Schmiedebergs Arch Pharmacol*, vol. 379, pp. 403–407, Apr 2009.

[473] J. D. Violin, X.-R. Ren, and R. J. Lefkowitz, "G-protein-coupled receptor kinase specificity for beta-arrestin recruitment to the beta2-adrenergic receptor revealed by fluorescence resonance energy transfer.," *J Biol Chem*, vol. 281, pp. 20577–20588, Jul 2006.

[474] M. J. Lohse, S. Nuber, and C. Hoffmann, "Fluorescence/bioluminescence resonance energy transfer techniques to study g-protein-coupled receptor activation and signaling.," *Pharmacol Rev*, vol. 64, pp. 299–336, Apr 2012.

[475] C. Walther, S. Nagel, L. E. Gimenez, K. Moerl, V. V. Gurevich, and A. G. Beck-Sickinger, "Ligand-induced internalization and recycling of the human neuropeptide y2 receptor is regulated by its carboxyl-terminal tail.," *J Biol Chem*, vol. 285, pp. 41578–41590, Dec 2010.

[476] J. Song, X.-Q. Zhang, J. Wang, E. Cheskis, T. O. Chan, A. M. Feldman, A. L. Tucker, and J. Y. Cheung, "Regulation of cardiac myocyte contractility by phospholemman: Na+/ca2+ exchange versus na+ -k+ -atpase.," *Am J Physiol Heart Circ Physiol*, vol. 295, pp. H1615–H1625, Oct 2008.

[477] N. C. Salazar, X. Vallejos, A. Siryk, G. Rengo, A. Cannavo, D. Liccardo, C. De Lucia, E. Gao, D. Leosco, W. J. Koch, and A. Lymperopoulos, "Grk2 blockade with ?arkct is essential for cardiac ?2-adrenergic receptor signaling towards increased contractility.," *Cell Commun Signal*, vol. 11, p. 64, 2013.

[478] Z. Xu and G. M. Culver, "Chemical probing of rna and rna/protein complexes.," *Methods Enzymol*, vol. 468, pp. 147–165, 2009.

[479] K. A. Wilkinson, E. J. Merino, and K. M. Weeks, "Selective 2'-hydroxyl acylation analyzed by primer extension (shape): quantitative rna structure analysis at single nucleotide resolution.," *Nat Protoc*, vol. 1, no. 3, pp. 1610–1616, 2006.

[480] J. Martin-Liberal, L. Lagares-Tena, and J. Larkin, "Prospects for mek inhibitors for treating cancer.," *Expert Opin Drug Saf*, Mar 2014.

[481] M. R. Lackner, "Prospects for personalized medicine with inhibitors targeting the ras and pi3k pathways.," *Expert Rev Mol Diagn*, vol. 10, pp. 75–87, Jan 2010.

[482] Y. Kodama, K. Takeuchi, N. Shimba, K. Ishikawa, E.-i. Suzuki, I. Shimada, and H. Takahashi, "Rapid identification of ligand-binding sites by using an assignment-free nmr approach.," *J Med Chem*, vol. 56, pp. 9342–9350, Nov 2013.

[483] Y. Futamura, M. Muroi, and H. Osada, "Target identification of small molecules based on chemical biology approaches.," *Mol Biosyst*, vol. 9, pp. 897–914, May 2013.

[484] U. Rix and G. Superti-Furga, "Target profiling of small molecules by chemical proteomics.," *Nat Chem Biol*, vol. 5, pp. 616–624, Sep 2009.

[485] L. S. Lerman, "A biochemically specific method for enzyme isolation.," *Proc Natl Acad Sci U S A*, vol. 39, pp. 232–236, Apr 1953.

[486] M. S. Taha, K. Nouri, L. G. Milroy, J. M. Moll, C. Herrmann, L. Brunsveld, R. P. Piekorz, and M. R. Ahmadian, "Subcellular fractionation and localization studies reveal a direct interaction of the fragile x mental retardation protein (fmrp) with nucleolin.," *PLoS One*, vol. 9, no. 3, p. e91465, 2014.

[487] T. T. Weil, R. M. Parton, and I. Davis, "Making the message clear: visualizing mrna localization.," *Trends Cell Biol*, vol. 20, pp. 380–390, Jul 2010.

[488] A. Sorkin and M. von Zastrow, "Endocytosis and signalling: intertwining molecular networks.," *Nat Rev Mol Cell Biol*, vol. 10, pp. 609–622, Sep 2009.

[489] S. Ahmed, K. G. Grant, L. E. Edwards, A. Rahman, M. Cirit, M. B. Goshe, and J. M. Haugh, "Data-driven modeling reconciles kinetics of erk phosphorylation, localization, and activity states.," *Mol Syst Biol*, vol. 10, p. 718, 2014.

[490] C. J. Wienken, P. Baaske, U. Rothbauer, D. Braun, and S. Duhr, "Protein-binding assays in biological liquids using microscale thermophoresis.," *Nat Commun*, vol. 1, p. 100, 2010.

[491] S. R. Nallagatla and P. C. Bevilacqua, "Nucleoside modifications modulate activation of the protein kinase pkr in an rna structure-specific manner.," *RNA*, vol. 14, pp. 1201–1213, Jun 2008.

[492] P. A. Limbach, P. F. Crain, and J. A. McCloskey, "Summary: the modified nucleosides of rna.," *Nucleic Acids Res*, vol. 22, pp. 2183–2196, Jun 1994.

[493] J. Rozenski, P. F. Crain, and J. A. McCloskey, "The rna modification database: 1999 update.," *Nucleic Acids Res*, vol. 27, pp. 196–197, Jan 1999.

[494] D. Uzri and L. Gehrke, "Nucleotide sequences and modifications that determine rig-i/rna binding and signaling activities.," *J Virol*, vol. 83, pp. 4174–4184, May 2009.

[495] S. R. Nallagatla, C. N. Jones, S. K. B. Ghosh, S. D. Sharma, C. E. Cameron, L. L. Spremulli, and P. C. Bevilacqua, "Native tertiary structure and nucleoside modifications suppress trna's intrinsic ability to activate the innate immune sensor pkr.," *PLoS One*, vol. 8, no. 3, p. e57905, 2013.

[496] R. E. Wang, H. Wu, Y. Niu, and J. Cai, "Improving the stability of aptamers by chemical modification.," *Curr Med Chem*, vol. 18, no. 27, pp. 4126–4138, 2011.

[497] S. Lennarz, "Charakterisierung von intrameren als neuartige, spezifische inhibitoren der map kinasen erk1 und erk2," Master's thesis, Mathematisch-Naturwissenschaftlichen Fakultaet, LIMES Institut, Universitaet Bonn, 2010.